

THE  
**IIOAB**  
**JOURNAL**

VOLUME 10 : NO 2 : AUGUST 2019 : ISSN 0976-3104

**SUPPLEMENT ISSUE**

Institute of Integrative Omics and  
Applied Biotechnology Journal

Dear Esteemed Readers, Authors, and Colleagues,

I hope this letter finds you in good health and high spirits. It is my distinct pleasure to address you as the Editor-in-Chief of Integrative Omics and Applied Biotechnology (IIOAB) Journal, a multidisciplinary scientific journal that has always placed a profound emphasis on nurturing the involvement of young scientists and championing the significance of an interdisciplinary approach.

At Integrative Omics and Applied Biotechnology (IIOAB) Journal, we firmly believe in the transformative power of science and innovation, and we recognize that it is the vigor and enthusiasm of young minds that often drive the most groundbreaking discoveries. We actively encourage students, early-career researchers, and scientists to submit their work and engage in meaningful discourse within the pages of our journal. We take pride in providing a platform for these emerging researchers to share their novel ideas and findings with the broader scientific community.

In today's rapidly evolving scientific landscape, it is increasingly evident that the challenges we face require a collaborative and interdisciplinary approach. The most complex problems demand a diverse set of perspectives and expertise. Integrative Omics and Applied Biotechnology (IIOAB) Journal has consistently promoted and celebrated this multidisciplinary ethos. We believe that by crossing traditional disciplinary boundaries, we can unlock new avenues for discovery, innovation, and progress. This philosophy has been at the heart of our journal's mission, and we remain dedicated to publishing research that exemplifies the power of interdisciplinary collaboration.

Our journal continues to serve as a hub for knowledge exchange, providing a platform for researchers from various fields to come together and share their insights, experiences, and research outcomes. The collaborative spirit within our community is truly inspiring, and I am immensely proud of the role that IIOAB journal plays in fostering such partnerships.

As we move forward, I encourage each and every one of you to continue supporting our mission. Whether you are a seasoned researcher, a young scientist embarking on your career, or a reader with a thirst for knowledge, your involvement in our journal is invaluable. By working together and embracing interdisciplinary perspectives, we can address the most pressing challenges facing humanity, from climate change and public health to technological advancements and social issues.

I would like to extend my gratitude to our authors, reviewers, editorial board members, and readers for their unwavering support. Your dedication is what makes IIOAB Journal the thriving scientific community it is today. Together, we will continue to explore the frontiers of knowledge and pioneer new approaches to solving the world's most complex problems.

Thank you for being a part of our journey, and for your commitment to advancing science through the pages of IIOAB Journal.



Yours sincerely,

*Vasco Azevedo*

**Vasco Azevedo**, Editor-in-Chief  
Integrative Omics and Applied Biotechnology  
(IIOAB) Journal





**Prof. Vasco Azevedo**  
*Federal University of Minas Gerais*  
Brazil

## Editor-in-Chief

### *Integrative Omics and Applied Biotechnology (IIOAB) Journal Editorial Board:*



**Nina Yiannakopoulou**  
*Technological Educational Institute of Athens*  
Greece



**Jyoti Mandlik**  
*Bharati Vidyapeeth University*  
India



**Rajneesh K. Gaur**  
*Department of Biotechnology, Ministry of Science and Technology*  
India



**Swarnalatha P**  
*VIT University*  
India



**Vinay Aroskar**  
*Sterling Biotech Limited*  
Mumbai, India



**Sanjay Kumar Gupta**  
*Indian Institute of Technology*  
New Delhi, India



**Arun Kumar Sangaiah**  
*VIT University*  
Vellore, India



**Sumathi Suresh**  
*Indian Institute of Technology*  
Bombay, India



**Bui Huy Khoi**  
*Industrial University of Ho Chi Minh City*  
Vietnam



**Tetsuji Yamada**  
*Rutgers University*  
New Jersey, USA



**Moustafa Mohamed Sabry Bakry**  
*Plant Protection Research Institute*  
Giza, Egypt



**Rohan Rajapakse**  
*University of Ruhuna*  
Sri Lanka



**Atun RoyChoudhury**  
*Ramky Advanced Centre for Environmental Research*  
India



**N. Arun Kumar**  
*SASTRA University*  
Thanjavur, India



**Bui Phu Nam Anh**  
*Ho Chi Minh Open University*  
Vietnam



**Steven Fernandes**  
*Sahyadri College of Engineering & Management*  
India



## ARTICLE

# THE USE OF DYNAMIC GEOMETRY SYSTEMS AS A MEANS OF VISUAL THINKING ACTIVATION FOR STUDENTS WHO STUDY MATHEMATICAL ANALYSIS

T.Yu. Gainutdinova\*, M.Yu. Denisova, A.V. Smirnova, Z.F. Shakirova, O.A. Shirokova

*N.I. Lobachevsky Institute of Mathematics and Mechanics, Kazan Federal University, Kazan, RUSSIAN FEDERATION*

## ABSTRACT

At present, software products are increasingly being used in universities for teaching various disciplines for both professional and educational purposes. The Federal State Educational Standard of Higher Education in the Russian Federation presents new requirements related to the application of modern information technologies to learning outcomes. In this regard, Russian higher education enters a qualitatively new level: the task of widespread use of information technologies in general and vocational education is being solved, which contributes to the modernization of the educational process, activating the thinking activity of the students, contributing to the development of the creativity of teachers, thereby increasing the effectiveness of the educational process. The goal of informatization is the global intensification of intellectual activity through the use of new information technologies, such as: computer, multimedia and interactive. This is especially relevant in the teaching of mathematical disciplines. The paper proposes a technique related to the systematic use of mathematical packages in the process of teaching mathematical analysis. This technique allows the use of dynamic geometry software systems (Dynamic Geometry System) to overcome the difficulties associated with spatial representation, which arise when studying applications of definite integrals. The suggested teaching methodology based on the use of Dynamic Geometry System Geo Gebra and multimedia technologies includes: presentation of theoretical material, step-by-step construction of the required object, calculation of body volume as consisting of parallel sections. The article presents solutions on the topic "Defined Integral" using the Geo gebra package implementing the proposed technique.

## INTRODUCTION

**KEY WORDS**  
Definite integral,  
mathematical software,  
principle of visualization

The federal state educational standard of higher education, approved by the order of the Ministry of Education and Science of Russia, imparts to the learning outcomes new requirements related to the use of modern computer systems [1]. In connection with this, at present Russian higher education gets a qualitatively new level: the task of mass use of computer and information technologies in general and professional education is being solved.

The teaching of mathematics under modern conditions has begun to undergo major changes towards in terms of decreasing the number of hours given, since the development of science makes it necessary to introduce new disciplines into the learning process. This leads to a reduction and a more superficial presentation of the material of the basic mathematical courses. At the same time, educational facilities in mathematics practically do not change. The problem arises: how to make mathematical education more effective. To solve it, it is necessary to pay serious attention to the methodology of teaching mathematical disciplines using information technologies [2].

"In the field of teaching mathematics, there is the problem of integrating fundamental mathematical education and the very methodology of teaching mathematics, taking into account the current trends in the growth of the influence of information technologies" [3].

The solution of this problem is realized in the papers, where issues of mathematical - computer modeling and also geometric modelling are covered [4,5].

The use of multimedia technologies and systems of computer mathematics (SCM) makes it possible to include a wide visual series in the educational process, thereby activating the figurative thinking of students and helping them to perceive the proposed material in a holistic manner. The teacher has the opportunity to combine the presentation of theoretical information with showing the visual material. The use of multimedia technologies allows the teacher to manage the demonstration of visual material much more effectively, "opening new opportunities in the organization of the learning process, and also in developing the creative abilities of the students" [6].

Particularly topical was the use in the higher school of specialized software packages in the study of various disciplines [7,8,9,10], which are based on the principle of visibility. In accordance with this principle, specific geometric constructions are used in teaching, visualization of which makes it possible to easily solve the problems posed. The ability to visually represent geometric objects is a key feature of systems of dynamic geometry.

Many qualitative studies have been carried out both in software [11] of dynamic geometry systems and in the effective use of these systems in educational process.

For example, it has been shown in [12,13,14] that one of the effective ways to solve a number of problems in modern mathematical education is the use of the Geo Gebra dynamic geometry system.

Received: 12 Oct 2018  
Accepted: 16 Dec 2018  
Published: 2 Jan 2019

\*Corresponding Author  
Email:  
tgainut@mail.ru

## MATERIALS AND METHODS

### Statement of the problem

In this paper, we propose a methodology for teaching a section of mathematical analysis related to applications of certain integrals in calculating body volumes using information technologies.

The perception of this material is simplified with a reasonable use of visual opportunities provided by information technologies. The researched objects are demonstrated using multimedia technologies and computer mathematics systems, which allows the teacher to combine the material with a dynamic video sequence. This is a simple and logical explanation - the means that the computer provides for displaying information, surpass any printed matters. In no textbook, you cannot represent the object in dynamics. With such opportunities, the question arises related with the use of video materials.

### Methodology

The complexity of the spatial representation and the absence of illustrative elements makes it impossible to see the objects researched entirely and makes it difficult to study applications of certain integrals. It is known that Dynamic Geometry (DGS) software systems can be useful tools in the study of this section, for example, DGSGeoGebra [15, 16] presents the possibility of step-by-step view of the solution of the problem and visualization of the theorems proofs.

In connection with the above, the teaching methodology based on the use of DGS Geo Gebra and multimedia technologies may include:

- presentation of theoretical material;
- step-by-step construction of the desired body;
- Calculation of body volume over areas of parallel sections.

The presentation of theoretical material [17] can be based on the use of presentations, video clips, dynamic video sequences, etc [Fig. 1].


<p align="center"><b>Calculation of body volume over areas of parallel sections</b></p> <p>Find the volume <math>V</math> of the body <math>T</math> if we know the areas <math>S</math> of any section of the given body by planes perpendicular to the axis <math>OZ</math>. The area depends on the position of the cutting plane, i.e. is a function of <math>x</math>: <math>S=S(x)</math>.</p> <p><b>!</b> <math>S(x)</math> – continuous function</p> <p>Draw the planes</p> <p><b>!</b> <math>x = x_0 = a, x = x_1, \dots, x = x_{i-1}, x = x_i, \dots, x = x_n = b</math></p> <p>Let us construct a cylindrical body. Cylinder capacity:</p> <p><b>!</b> <math>V_n = \sum_{i=1}^n S(\xi_i)</math></p>	<p>The limit of this sum under <math>\max \Delta x_i \rightarrow 0</math> is called the body volume</p> <div style="border: 1px solid black; padding: 5px; margin: 5px;"> <math display="block">V = \lim_{\max \Delta x_i \rightarrow 0} \sum_{i=1}^n S(\xi_i) \Delta x_i</math> </div> <p><math>V_n</math> is an integral sum for a continuum function <math>S(x)</math> on the stretch <math>[a, b]</math>, and the limit exists and is expressed by the definite integral:</p> <div style="border: 1px solid black; padding: 5px; margin: 5px;"> <math display="block">V = \int_a^b S(x) dx</math> </div> 
--	--

Fig. 1: The example of presentation of theoretical material.

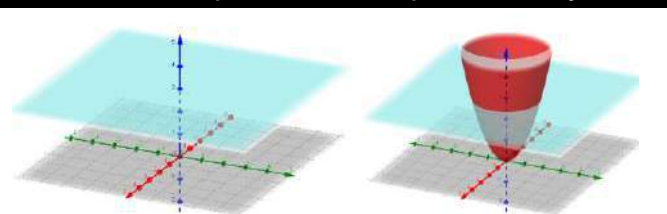
Step-by-step construction of the desired body involves the use of computer mathematics systems that allow a dynamic review of the problem solution. Consider the application of this methodology on the basis of the example of solving the following problems [3].

**Example 1.** Find the volume of the body bounded by the paraboloids surface  $x^2+y^2=z$  and the plane  $z=3$ .

In [Table 1], in points 1–3, the steps for constructing the target body in DGS Geo Gebra are presented.

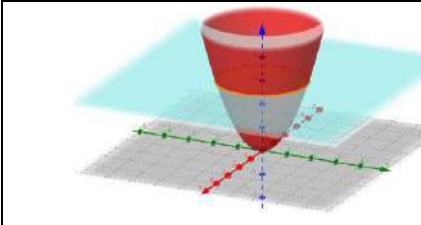
**Table 1:** The example of step-by-step construction

**1. We construct the plane  $z = 3$  and the paraboloid  $x^2 + y^2 = z$**



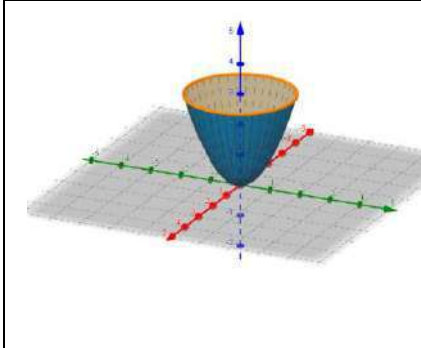
- Paraboloid
  - a:  $x^2 + y^2 + 0z^2 - z = 0$
- Plane
  - b:  $z = 3$

2. Find their intersection using the tool



- Conic
  - c:  $X = (0, 0, 3) + (1.73 \cos(t), 1.73 \sin(t), 0)$

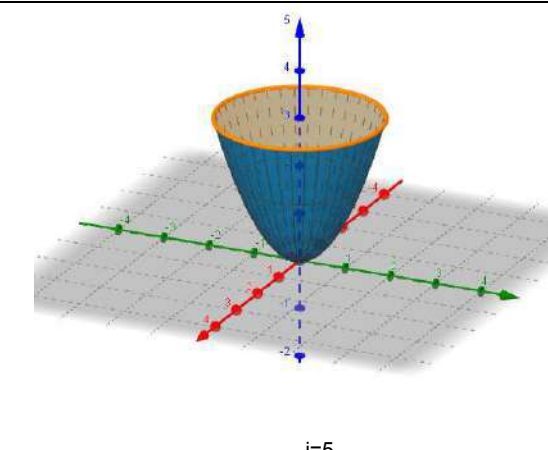
3. We describe the body, the volume of which must be found.



- Surface
  - $e(c, t) = \begin{pmatrix} t \cos(c) \\ t \sin(c) \\ t^2 \end{pmatrix}$
- Parametric curve
  - d:  $\left. \begin{matrix} y = \sqrt{3} \sin(t) \\ z = 3 \end{matrix} \right\} - 3.14 \leq t \leq \pi$

We note that for step-by-step viewing of the solution of the problem and dynamic visualization of the construction of the desired body, it is necessary to create a slider and determine the conditions for displaying body components for objects with different values of the slider. For example, create the slider  $i$  with an interval from 0 to 6 (step 1) [Table 2].

**Table 2:** Settings of slider



$i=5$

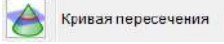
In the "Object Properties" slider dialog box, set the animation behavior: speed -1; repeat - increase (once). The objects of the desired body (point 3) are displayed at  $4 \leq i \leq 6$ , and the previous constructions (points 1-2) correspond to the values  $0 \leq i \leq 3$ .

Using the results of the construction, we find the volume by means of the integral:

$$V = 4 \cdot \int_0^{\sqrt{3}} dx \int_0^{\sqrt{3-x^2}} (3-x^2-y^2) dy = \frac{9\pi}{2}$$

**Example 2.** Find the volume of the body bounded by the cylindrical surface  $x^2 + y^2 = 5$  and the planes:  $z=0$  and  $y+z=3$ .

When calculating body volume over areas of parallel sections, we use dynamic visualization, which is realized by introducing the slider  $t$  with an interval from  $-\sqrt{5}$  to  $\sqrt{5}$  in steps of 0.1.

To move the section along the  $Ox$  axis, you need to join the  $x$  coordinate with the value of the slider  $t$ . Set the section using the tool  .

In this example, the section is a polygon, so it is convenient to construct it by specifying the coordinates of the vertices parametrically:

$$\begin{aligned} A(t, \sqrt{5-t^2}, 0); & B(t, -\sqrt{5-t^2}, 0); \\ C(t, -\sqrt{5-t^2}, 3 + \sqrt{5-t^2}); & \\ D(t, \sqrt{5-t^2}, 3 - \sqrt{5-t^2}) & \end{aligned}$$

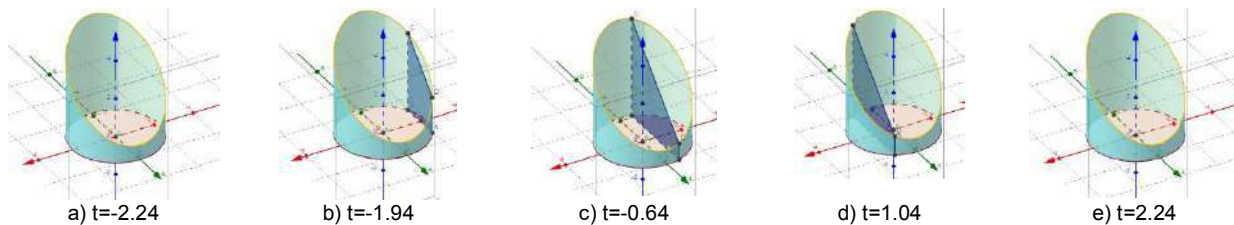


**Fig. 2(a-e):** The dynamic visualization of sections.

Using the results of the construction, we find the volume by means of the integral.

$$V = 4 \int dx \int (3-y) dy = 15\pi$$

## RESULTS AND DISCUSSION

Perception of the teaching material depends on the way how the educational process is organized, what is aimed at. That is why it is necessary to pay serious attention to the teaching methods of mathematical disciplines using information technology.

The presented method is based on the systematic usage of information technology during teaching process of higher mathematics. Mathematical packages, including a dynamic geometric environment - the Dynamic Geometry (DGS) software systems are successful approaches for a teacher. They combine both multimedia and programming tools, thereby providing informatization of the educational process.

The following results were obtained during the research:

- using of multimedia technologies assists to improve the level of understanding of complex sections of higher mathematics;
- dynamic Geometry Systems allows to make geometric constructions of the explored objects visualization of which help to solve tasks and view them in dynamics;
- using of multimedia technologies and systems of computer mathematics helps to optimize the educational process, using time at different stages of teaching more rationally;
- a method based on the systematic using of IT contributes to a deep understanding of the subject and the development of interest in its study.

Using of information and communication technologies has a great influence on the content, forms and methods of teaching. New educational technologies which are used during the learning process improves the teaching methods, allows using the visual possibilities provided by computer mathematics systems along with traditional methods, techniques and methods.

The article proposes a technique for teaching a section of mathematical analysis related to applications of definite integrals during calculating of volume of shapes using multimedia technologies and graphical capabilities of dynamic geometry systems. The usage of the proposed method of teaching showed that



DGS Geo Gebra is a necessary tool to build geometric constructions of the explored objects, the visualization of which help to solve tasks for calculating volume of shapes.

## CONCLUSION

The introduction of this technique is recommended due to the current level of development of information technology, as well as problems associated with the using of visualization of spatial modeling of objects. Using of multimedia technologies allows a teacher to diversify the study material with new activities, enrich it with visual information, increase the motivation of students and their interest to the subject. Students actively participate in the learning process, are trained to think independently, to protect their own points of view, to model real mathematical objects.

The creation and development of methods based on the systematic using of information technology is a necessary step towards increasing the effectiveness of mathematical education.

## CONFLICT OF INTEREST

There is no conflict of interest.

## ACKNOWLEDGEMENTS

The work is performed according to the Russian Government Program of Competitive Growth of Kazan Federal University.

## FINANCIAL DISCLOSURE

None

## REFERENCES

- [1] Agoston M. [2005] Computer Graphics and Geometric Modeling. Implementation and Algorithms. Springer.
- [2] Allen Leung, Arthur Man Sang Lee. [2013] Students' geometrical perception on a task-based dynamic geometry platform. Educational Studies in Mathematics. 82:361–377.
- [3] Berman GN. [2005] Collection of problems on the course of mathematical analysis. Moscow: Science.
- [4] Denisova M. [2016] Application of the Geo Gebra interactive environment in the study of a definite integral. VI International Scientific-Practical Conference Mathematics education in school and university: theory and practice. 218-220.
- [5] Gainutdinova T, Denisova M, Shirokova O. [2016] Innovative Teaching Methods in Formation of Professional Competencies of Future Mathematics Teachers. International Forum on Teacher Education Collection of IFTE 2017, The European Proceedings of Social & Behavioral Sciences EpSBS. 197-205.
- [6] Gainutdinova T, Shirokova O. [2016] Features of Professional Teachers Training of Informatics in a Programming Course. International Forum on Teacher Education Collection of IFTE. The European Proceedings of Social & Behavioral Sciences EpSBS. 12:30-37.
- [7] Hohenwarter M, Hohenwarter Ju. Introduction to GeoGebra. <http://www.geogebra.org/book/intro-en>.
- [8] Knyazeva G. [2010] Application of multimedia technologies in educational institutions. Vestnik VUIT. URL: <http://cyberleninka.ru/article/n/primeneniie-multimediynyh-tehnologiy-v-obrazovatelnyh-uchrezhdeniyah>.
- [9] Larin S. [2015] Computer animation in the environment of GeoGebra in the lessons of mathematics: a textbook.
- [10] Piskunov N. [1978] Differential and Integral Calculus. Moscow: Science.
- [11] Salomon D. [2006] Transformations and Projections in Computer Graphics Springer.
- [12] Sozcu Omer F, Ziatdinov R, Ipek I. [2013] The effects of computer-assisted and distance learning of geometric modeling. European Journal of Contemporary Education. 1-2(39):175-181.
- [13] The State Program of the Russian Federation Development of Education for 2013-2020 [2014]. Government of the Russian Federation.
- [14] Voevodin V, Voevodin VI. [2003] Electronic educational tools: new ideas. Mathematics in Higher Education. 1:11-20.
- [15] Zaripov F. [2016] Development and introduction of a system for the preparation of a teacher of mathematics and computer science on the basis of methods of mathematical, didactic modeling and interdisciplinary connections Materials of the International Scientific and Practical Conference ITES. 33-40.
- [16] Ziatdinov R, Rakuta V. [2012] Dynamic geometry environments as a tool for computer modeling in the system of modern mathematics education. European Journal of Contemporary Education. 1(1):93-100.
- [17] <http://www.geogebra.org/cms/rn/institutes>

## ARTICLE

# STUDY OF ASPHALTENE SUBSTANCES TO DETERMINE THE OPTIMAL METHOD OF DEALING WITH DEFERRED

Alim F. Kemalov, Dinar Z. Valiev\*, Ruslan A. Kemalov

*Institute of Geology and Petroleum Technologies, Kazan Federal University, Kazan, RUSSIA*

## ABSTRACT

*In the work, a comparative analysis of asphaltene substances deposits (ASP-B) from pipelines of two oil enterprises was carried out. The similarity of the group components of the ASP-B data is revealed. To determine the optimal method for controlling sediments, a classification was made and the most effective solvent was selected. 3 deposits ASP-B (PJSC Tatneft) belong to the paraffin type, therefore, the most effective solvent will be solvents on a paraffinic, naphthenic or unsaturated basis. Since the main mass of the deposit is paraffin hydrocarbons, the removal of these deposits will be more effective when dissolving the paraffinic part of the sediments. 2 deposits of ASP-B (JSC Tatneftprom-Zyuzeyevneft) belong to the asphaltene type. For ASP-B asphaltene type, the most effective solvent is an aromatic solvent. These solvents have a good dissolving power with respect to asphalt-resinous substances. The solutions of each component of the sediments were analyzed by the conductometric method of dispersion analysis with the help of the particle size analyzer Coulter Counter in order to determine the particle size, the comparative evaluation of the sizes and ratios in sediments of various oils. It has been revealed that in the investigated sediments, despite the different origin and differences in the group composition, the components of the ASP-B do not differ in their characteristics from each other, the group components have a similar molecular mass and structure.*

## INTRODUCTION

The problems associated with oil transportation occupy an equal position with the problems of oil preparation. When transporting highly paraffinic oils, the problem of occurrence of deposits of asphalt-resin-paraffin (ASP-B) is sharply raised [1]. The occurrence of these deposits leads to a sharp deterioration in the conditions for the transport of oil, a reduction in capacity, an increase in the hydraulic resistance of the pipeline, the loss of the most valuable components of oil entering the composition of ASP-B [2]

Problems of ASP-B are a rather complex structure. A lot of factors influence the formation of ASP-B and its formation, and the process of deposition is possible both in the bottomhole formation zone [3] and in the pipeline of prepared oil [4-5].

Currently, a fairly wide range of methods and means of disposal, preventing the formation of ASP-B is applied. A huge amount of reagents, solvents with excellent performance indicators was developed. But this is not the limit. The problem in this area is the lack of empirical dependencies between the physico-chemical characteristics of oil and the choice of the most effective method of preventing deposits. At the moment, the selection of reagents and the choice of the method of protection is determined in a practical way in the laboratory, which complicates and narrows the possible choice of means of influencing oil [5-7].

The purpose of this work is to determine the group composition of ASP-B, to study solutions of group components of ASP-B, and to make a comparative analysis of the data obtained. Which, in turn, can be the initial data for modeling the processes of formation and prevention of ASP-B.

## METHODS

Determination of particle size of oil dispersed systems was carried out by conductometric method using the Coulter Counter analyzer of the TA-II model of IDF Production (UK) [8]. The determination of dispersity by the conductometric method is based on measuring the electrical resistance at the moment when the particles pass through the calibrated micro-holes [8].

To determine the particle size of the disperse system, working apertures (tubes) of different diameters were used, the working volume of the sample was 0.5 ml.

The determination of the composition of ASP-B was carried out by liquid chromatography. The technique is based on the different solubility of the components of ASP-B in various solvents and their different sorption capacities for the silica gel.

## RESULTS

In the course of the work, 3 samples of ASP-B sediments were examined from the pipelines of NGDU "Zainskneft", NGDU "Nurlatneft". OGPU Pocachevneft PJSC Tatneft and 2 samples of sediments ASP-B of the Zyuzeyevskoye deposit of JSC Tatneftprom-Zyuzeyevneft. The results of the studies are presented in [Table 1].

### KEY WORDS

asphalt and resin paraffin substances, particle size, conductometric method, chromatography, group composition.

Received: 14 Oct 2018  
Accepted: 19 Dec 2018  
Published: 2 Jan 2019

### \*Corresponding Author

Email:  
valievdz@bk.ru  
Tel.: +79274367606

**Table 1:** Compositions of ASP-B deposits

Sample name	Composition, in %				
	Minerals	Asphaltenes	Resins	Hydrocarbons	Losses and water
Zainskneft	1,32	13,68	12,5	65,57	6,73
Pokachevneft	5,66	3,33	6,92	79,04	5,03
Nurlatneft	0,66	37,2	2,55	55,62	3,97
Zyuzejevskoye fld., well No. 2321	1,5	5,1	22,5	62,1	6,0
Zyuzejevskoye fld., well No. 961	8,6	5,5	18,0	62,0	5,8

Based on the data obtained, we classify the type of these deposits, for the convenience of selecting the most effective solvent ASP-B. The results are shown in [Table 2].

**Table 2:** Classification of ASP-B

Name	P / (C + A)	Content of the impurity mixture	ASP-B Type	Type
Zainskneft	2,47	1,32	Paraffinic	P <sub>3</sub>
Pokachevneft	7,71	5,66	Paraffinic	P <sub>3</sub>
Nurlatneft	1,4	0,66	Paraffinic	P <sub>3</sub>
Zyuzejevskoye fld., well No. 2321	0,15	0,15	Asphaltene	A <sub>1</sub>
Zyuzejevskoye fld., well No. 961	0,17	0,19	Asphaltene	A <sub>1</sub>

As can be seen from [Table 2], the samples of ASP-B deposits of PJSC Tatneft belong to the paraffin type, therefore the most effective solvent for them will be solvents on a paraffinic, naphthenic or unsaturated basis, since the main deposit mass is paraffin hydrocarbons, and the removal process These deposits will be more effective when dissolving the paraffinic part of the sediments.

Samples of deposits ASP-B of JSC Tatneftprom-Zyuzejevneft belong to the asphaltene type. For ASP-B asphaltene type, the most effective solvent is an aromatic solvent [9]. These solvents have a good dissolving power with respect to asphalt-resinous substances. The nature of the action of the solvent consists in dissolving the resins, which are the binding agent of paraffin agglomerates and the partial dissolution of asphaltenes, transferring deposits on pipelines into suspended particles that are easily carried away by the flow.

Also in the course of this paper, solutions of each component of deposits were analyzed on a particle size analyzer and particle size analyzer Coulter Counter, in order to determine the particle size and comparative evaluation of sizes, their ratios in sediments of various oils, the results of the studies are presented in [Table 3-7] and [Fig. 1 -3].

**Table 3:** Particle sizes of ASP-B of NGDU "Zainskneft" PJSC "Tatneft"

Channel range µm	% of the total number of particles		
	Paraffins	Resins	Asphaltenes
1	2	3	4
1,26-1,59	0	0	0
1,59-2	5,6	5,5	6,2
2-2,52	7,1	7,3	7,6
2,52-3,17	5,8	7	6,1
3,17-4,00	7,1	8,2	7,5
4,00-5,04	6,1	5,5	6,1
5,04-6,35	7	6,8	6,8
6,35-8,00	7,1	6,5	6,9
8,00-10,1	4,6	5	4,3
10,1-12,7	8,8	8,6	7,7
12,7-16,0	8,3	8,2	6,9
16,0-20,2	6,9	6,3	5,9
20,2-25,4	6,4	6,6	5,8
25,4-32	6,2	5,8	6,5
32-40,3	5,3	5,3	5,1
40,3-	7,3	7,4	7,9

**Table 4:** Particle sizes of ASP-B "Pocachevneff" PJSC "Tatneff"

Channel range µm	% of the total number of particles		
	Paraffins		Paraffins
1,26-1,59	0	0	0
1,59-2,00	6,3	6,1	6,5
2,00-2,52	7,6	7,5	7,6
2,52-3,17	6,1	6,1	6,1
3,17-4,00	7,5	7,5	7,6
4,00-5,04	6,3	6	6,2
5,04-6,35	6,8	6,8	6,9
6,35-8,00	6,8	6,8	6,7
8,00-10,1	4,3	4,3	9,3
10,1-12,7	7,7	7,8	7,7
12,7-16,0	6,8	6,8	6,7
16,0-20,2	5,8	5,8	5,8
20,2-25,4	5,8	5,9	3,5
25,4-32	6,4	6,4	6,6
32-40,3	5	5,2	5,1
40,3-	7,9	8	7,7

**Table 5:** Particle sizes of ASP-B of NGDU Nurlatneff PJSC Tatneff»

Channel range µm	% of the total number of particles		
	Paraffins		Paraffins
1,26-1,59	0	0	0
1,59-2,00	6,3	6,1	7,2
2,00-2,52	7,6	7,5	7,6
2,52-3,17	6,1	6,1	5,9
3,17-4,00	7,5	7,5	7,2
4,00-5,04	6,3	6	5,9
5,04-6,35	6,8	6,8	6,7
6,35-8,00	6,8	6,8	7,3
8,00-10,1	4,3	4,3	4,2
10,1-12,7	7,7	7,8	7,5
12,7-16,0	6,8	6,8	6,7
16,0-20,2	5,8	5,8	5,2
20,2-25,4	5,8	5,9	5,7
25,4-32	6,4	6,4	6,7
32-40,3	5	5,2	5,2
40,3-	7,9	8	8,7

**Table 6:** Particle sizes of ASP-B in the Zyuzeyevskoye oilfield well No. 2321. JSC Tatneftprom-Zyuzeyevneff

Channel range µm	% of the total number of particles		
	Paraffins		Paraffins
1	2	3	4
1,26-1,59	0	0	0
1,59-2,00	6,7	6,9	7,1
2,00-2,52	8,2	7,9	8,7
2,52-3,17	5,9	6,3	6,3
3,17-4,00	7,5	7,7	7,4
4,00-5,04	6,5	6,3	5,8
5,04-6,35	6,7	6,8	6,8
6,35-8,00	7,9	7,7	7,5
8,00-10,1	4,8	4,3	4,3
10,1-12,7	8,1	7,9	7,7
12,7-16,0	7,1	7	6,8
16,0-20,2	5	5,4	5,3
20,2-25,4	5,9	5,8	5,7
25,4-32	5,3	4,3	5,2
32-40,3	4,9	5	5
40,3-	8	7,9	7,8



**Table 7:** Particle sizes of ASP-B in the Zyuzeevsky deposit, borehole. No. 961 of JSC Tatneftprom-Zyuzeyevneft

Channel range $\mu\text{m}$	% of the total number of particles		
	Paraffins		Paraffins
1	2	3	4
1,26-1,59	0	0	0
1,59-2,00	6,1	6,8	7,6
2,00-2,52	7,5	7,7	8
2,52-3,17	6,1	6,1	6,2
3,17-4,00	7,5	7,5	7,6
4,00-5,04	6,1	6	6,2
5,04-6,35	6,8	6,7	6,8
6,35-8,00	6,9	7,5	7,6
8,00-10,1	4,3	4,2	4,3
10,1-12,7	7,8	7,6	7,7
12,7-16,0	6,9	6,8	6,8
16,0-20,2	5,9	5,3	5,4
20,2-25,4	5,8	5,6	5,8
25,4-32	6,6	5	4,6
32-40,3	5	5	5
40,3-	8,2	7,8	7,9

### DISCUSSION

The purpose of this work was a comparative analysis of five different deposits of ASP-B. All deposits were taken from different deposits, therefore, they represented sediments of various oils. As indicated above, these sediments differ in the group composition of the components. And the most interesting task was to reveal the similarity of the group components of some sediments with the group components of others. It was decided to investigate 1% solutions of each component for size and particle size ratio and give a comparative description of the data obtained. In parallel, work was carried out to study the structural and group composition, which, in turn, can confirm or disprove the results of this work.

The particle sizes are represented as the Poisson distribution in [Fig. 1–3].

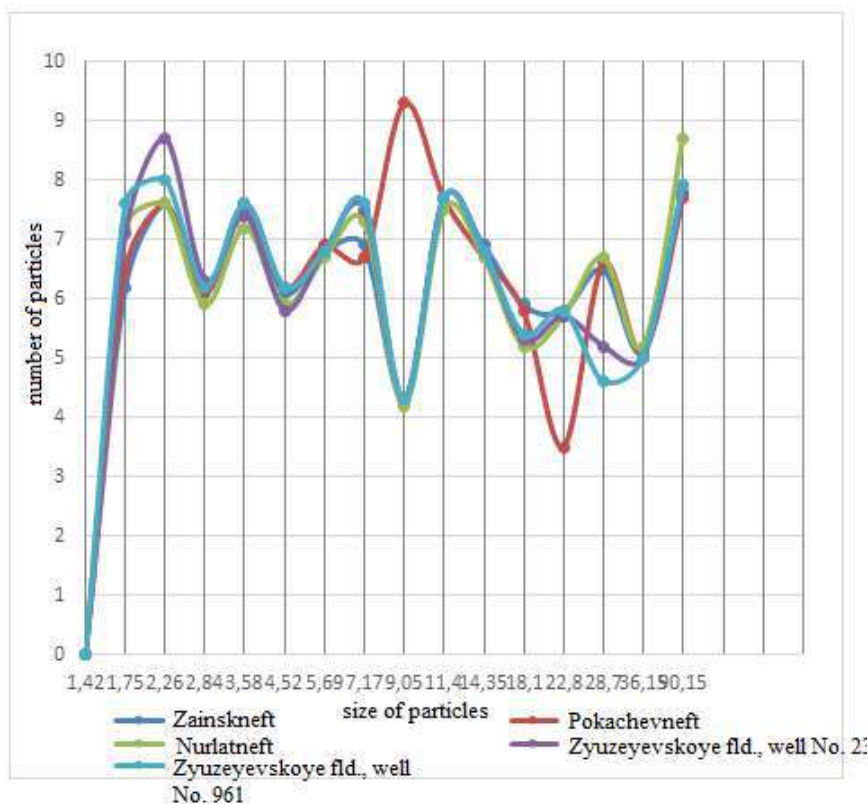


**Fig. 1:** Poisson distribution of asphaltene particles in a solution of benzene.

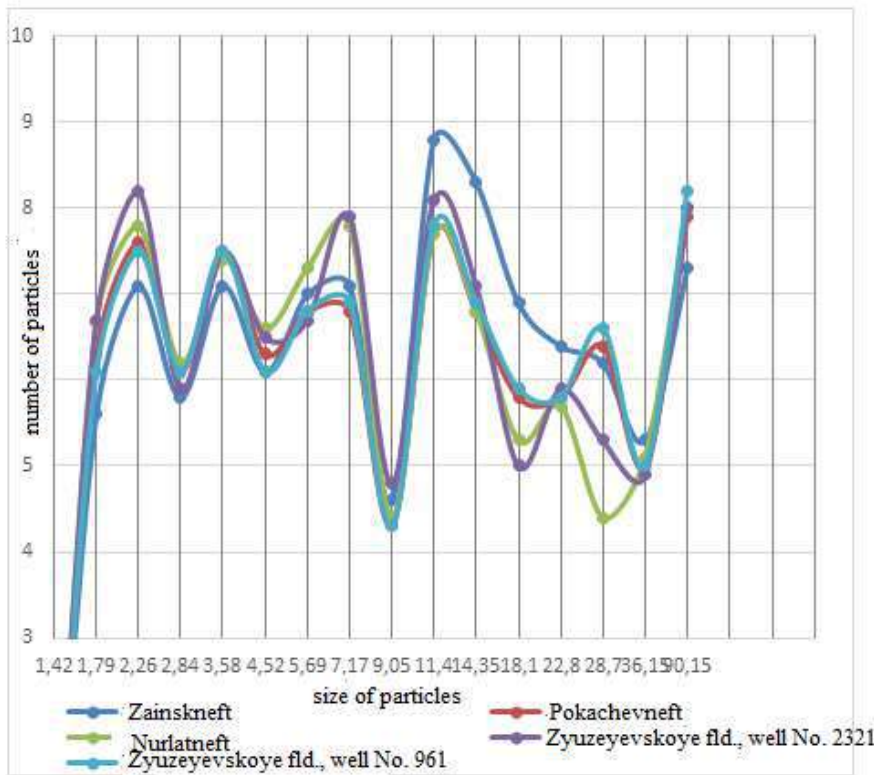


Fig. 2: Poisson distribution of paraffin particles in a solution of hexane.

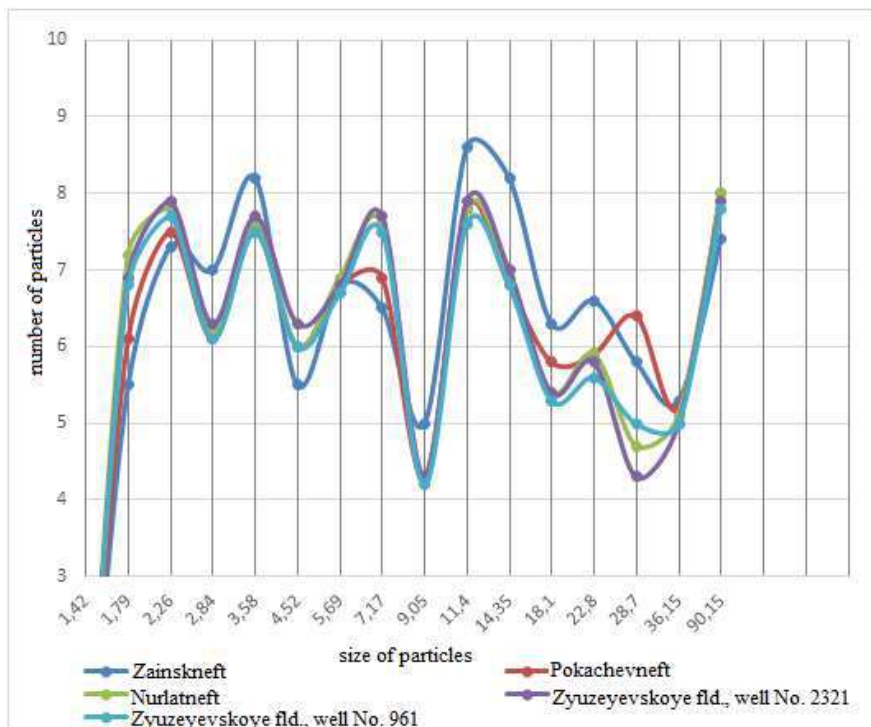


Fig. 3: Poisson distribution of resin particles in a solution of benzene.

As can be seen from the graphs, almost identical repetition of the curves obtained during the analysis of the group components of various ASP-B is observed. In our opinion, this gives the right to preliminarily conclude that in the investigated sediments, despite the different origin and differences in the group composition, the components of the ASP-B do not differ in their characteristics from each other in their characteristics. It is possible to assume that the group components have approximately the same molecular mass and structure [10].

## SUMMARY

In the course of this paper, various ASP-B deposits were analyzed, and the results suggested the similarity of the group components of different ASP-B.

It was revealed that 3 deposits of ASP-B (PJSC Tatneft) belong to the paraffin type, therefore the most effective solvent for these ASP-B will be solvents on a paraffinic, naphthenic or unsaturated basis, since the main deposit mass is paraffin hydrocarbons, and The process of removing these deposits will be more effective when dissolving the paraffinic part of the sediments.

2 deposits of ASP-B (JSC Tatnefteprom-Zyuzeyevneft) belong to the asphaltene type. For ASP-B asphaltene type, the most effective solvent is an aromatic solvent. These solvents have a good dissolving power with respect to asphalt-resinous substances. The nature of the action of the solvent consists in dissolving the resins, which are the binding agent of paraffin agglomerates and the partial dissolution of asphaltenes, transferring deposits on pipelines into suspended particles that are easily carried away by the flow.

In the work, solutions of each component of the sediment were measured at the Coulter-Counter particle distribution counter, in order to determine the particle size and the comparative estimation of the sizes, their ratios in the sediments of various oils. Based on the results of the studies, almost identical repeatability of the curves obtained in the analysis of the group components of various ASP-B is observed. It was revealed that in the investigated sediments, despite the different origin and differences in the group composition, the components of the ASP-B do not differ in their characteristics from each other in their characteristics, so it is possible to assume that the group components have approximately the same molecular mass and structure.

## CONCLUSION

The process of formation of ASP-B is determined by many factors, among which are the operating conditions of the process equipment for the extraction, transportation and storage of hydrocarbons, the properties of the hydrocarbons themselves. Particular importance in a number of factors that determine the propensity of hydrocarbons to form ASP-B, have high-molecular components of oil, namely, their composition, structure and percentage ratio. Knowing the properties and composition of hydrocarbons, their thermal and hydrodynamic conditions in the reservoir, and correctly selecting methods of combating ASP-B sediments, it will be possible to avoid deterioration of oilfield equipment and pipeline communications, which at one time is economically beneficial for the oil and gas industry, to reduce the number of repairs and reduce downtime of wells, will allow to extend the service life of equipment, to ensure rhythmic work of the fishery and to reduce the cost of oil production.

## CONFLICT OF INTEREST

The authors declare no conflict of interest relating to the material presented in this paper.

## ACKNOWLEDGEMENTS

The work is performed according to the Russian Government Program of Competitive Growth of Kazan Federal University. This work was funded by the subsidy allocated to Kazan Federal University for the state assignment in the sphere of scientific activities (10.7636.2017/7.8).

## FINANCIAL DISCLOSURE

None

## REFERENCES

- [1] Tatyana OS. [2008] Investigation of the conditions of formation of deposits in the oil transport system OS. Tatyana RZ, Sakhabutdinov FR. Gubaidullin Oilfield business. 8:43 - 46.
- [2] Sorokin SA, Khavkin SA. [2007] Features of physicochemical mechanism of formation of AFS in wells Drilling and oil. 10:30-31.
- [3] Sunyaev ZI. [1990] Oil dispersed systems ZI. Syunyaev RZ, Syunyaev RZ, Safiyev. Moscow: Chemistry. 226. 8.
- [4] Acevedo S. [2007] Relations between asphaltene structure and their physical and chemical properties: the rosary-type structure S. Acevedo A, Castro JG, Negrin A, Fernandez G, Escobar V. Piscitelli Energy & Fuels. 21:2165 - 2175.
- [5] Kyeongseok Oh. [2004] Asphaltene aggregation in organic solvents Oh Kyeongseok A, Ring Terry D. Deo Milind Journal of Colloid and Interface Science. 271:212 - 219.
- [6] Mastobayev BN. [2002] Chemical means and technologies in pipeline oil transport BN, Mastobayev AM, Shammazov EM, Movsumzadeh. Moscow: Chemistry. 296. 3
- [7] Kemalov F, Kemalov RA. Scientific and Practical Bases of the Physico-Chemical Mechanics and Statistical Analysis of Disperse Systems: Educational Textbook [in Russian], Izdate'stvo Kazanskogo Gosudarstvennogo Tekhnologiiicheskogo Universiteta, Kazan' [2008]. 6
- [8] Kemalov F. [2005] Dissertation for Doctor of Technical Sciences, Kazanskii Gosudarstvennyi Tekhnologicheskii, Universities, Kazan'. 4
- [9] Yagudin ShG. [2006] Composite reagents for extraction and preparation of heavy high-viscosity oils: the author's abstract of the dissertation of the candidate of technical sciences: 02.00.13 Yagudin Shamil Gabdulkhavich. Kazan. 19. 7
- [10] Kemalov AF, Kemalov RA, Valiev DZ. [2013] Study of the structure of complex structural units of heavy oil from Zyuzeevskaya field by NMR relaxometry and rheological studies. Oil Industry. 2: 63-65.

## ARTICLE

# PERFORMANCE AS THE MAIN FACTOR OF EXPANDED REPRODUCTION

Anas A Nurullin<sup>1</sup>, Asiya K Subaeva<sup>1\*</sup>, Natalya R Aleksandrova<sup>2</sup>

<sup>1</sup>Chistopol Branch of Kazan Federal University, Kazan, RUSSIA

<sup>2</sup>Ulyanovsk State Agrarian University, Boulevard Novy Venets, Ulyanovsk, RUSSIA

## ABSTRACT

Scientific and technological progress increasingly replaces aged equipment with more efficient and less expensive one. This makes it possible to significantly reduce labor costs for a unit of output and increase the total production volume. In the agrarian economy of Russia, the important issue remains the problem of labor productivity growth, the solution of which is largely achieved through factors that affect the reduction of labor costs per unit of output. To increase the efficiency of production, it is necessary to use all factors of labor productivity growth; only then the agricultural commodity producer can obtain tangible results of saving labor and financial resources [1]. Accelerating the growth of labor productivity is an important stage in the further development of production and the raising of human wellbeing. The purpose of the study is to analyze the productivity of labor in the Ulyanovsk region of the Russian Federation, to identify the main factors affecting the level of labor productivity and the reserves of growth of these indicators. When analyzing indicators reflecting the effectiveness of labor in agriculture in the Ulyanovsk region, econometric methods (time series analysis and forecasting, statistical grouping, multifactor correlation-regression modeling) were used. The main factors influencing the level of labor productivity in the region are determined. Point and interval predictions of analyzed labor productivity indicators are made. In the agrarian sector of the Ulyanovsk region, there are enough reserves for the growth of labor productivity in the form of raising the capital-labor ratio level in the agrarian sector, wages in agriculture, and the professional and qualification level of workers. The conducted research and the presented conclusions can be used as an example of the development of a separate agricultural enterprise when planning production and economic activities or when developing programs aimed at improving the efficiency of the agrarian branch of the region [1].

## INTRODUCTION

One of the important indicators reflecting the results of production activities, that characterize the efficiency and level of production intensification is labor productivity. This indicator most deeply reflects economic factors and characterizes the socio-economic level of labor productivity, and outlines the prospects for labor relations.

The growth of labor productivity is a complex system changing under the influence of many factors. At the same time, it is important that the influence of groups of factors on the increase of labor activity is achieved only when a new economic mechanism for managing is developed and new economic relations based on it is organized.

## MATERIALS AND METHODS

Labor productivity in agriculture is changing under the influence of many factors.

Preliminary assessment of factors allowed us to form a set of factorial indicators that determine the quantitative assessment:

- Capital/labor ratio of agricultural labor (X 1), thousand rubles / person;
- Specific weight of the active part of fixed assets in enterprises (X 2), %;
- Degree of replacement of fixed assets (X 3);
- Level of wages of agricultural workers (X 4), thousand rubles;
- Share of the wage fund in total production costs (X 5), %;
- Share of agricultural workers in the total number of employees (X 6), %.

A resultant indicator is the annual labor productivity calculated with the use of the gross product value.

Correlation-regression analysis of the influence of selected factors on the simulated indicator was carried out based on data of 137 agricultural organizations in the Ulyanovsk region and using the integrated program Statistica 10.0.

The estimation of the partial correlation coefficients made it possible to select the most significant indicators and exclude the weak influence and multi collinearity:

- Capital-labor ratio of agricultural labor (X 1), thousand rubles / person;
- Level of wages of agricultural workers (X 4), thousand rubles;
- Share of the labor compensation fund in total production costs (X 5), %.

### KEY WORDS

labor productivity, factors, prediction, efficiency, qualification, engineering and technical personnel.

Received: 10 Oct 2018  
Accepted: 11 Dec 2018  
Published: 2 Jan 2019

### \*Corresponding Author

Email: subaeva.ak@mail.ru  
Tel.: 9375224482



The first indicator is caused by the influence of scientific and technological progress on the productivity of agricultural labor, the other two are organizational indicators and they reflect the labor potential of an enterprise, the use of modern forms of labor organization and its payment, and the system of motivation and stimulation of labor in agriculture.

The degree of relationship strength between the selected indicators and the resultant indicator is reflected in [Table 1].

**Table 1:** Matrix of Pairwise Correlation Coefficients

Indicators	Convention	Labor productivity, Y, thousand rubles / person
Capital-labor ratio of agricultural labor, thousand rubles	X <sub>1</sub>	0.403
The level of remuneration of agricultural workers, thousand rubles	X <sub>4</sub>	0.565
The share of payroll in total production costs, %	X <sub>5</sub>	-0.400

As a result, the equation of the simulated indicator, labor productivity, has the following form:

$$Y = 1087.20 + 0.91X_1 + 14.80X_4 - 89.11X_5.$$

According to the equation obtained, the share of agricultural capital-labor ratio labor and the level of have a positive effect on the result. Thus, an increase in the capital-labor ratio on average by 1 000 rubles (with the invariability of the remaining facts of the model) promotes growth of labor productivity in agricultural organizations in an average by 910 rubles. The increase in the level of labor remuneration by 1,000 rubles leads to an increase in the effective indicator by an average of 14.8 thousand rubles.

The share of the wage fund in total production costs is characterized by a negative impact on the productivity of agricultural labor. The growth of the share of wages in the total costs of enterprises for production promoted the reduction of the labor productivity level by 89.11 thousand rubles.

The statistical significance of the corresponding regression coefficients can be judged from the t Student's t-test which value corresponds to  $t_{b1} = 6.11$ ;  $t_{b4} = 11.2$ ;  $t_{b5} = -6.97$ .

The multiple correlation coefficient equal to 0.791 indicates a close relationship between the selected factors and the effective indicator. The coefficient of determination equal to 0.626 indicates that the cumulative influence of the three factors determines 62.6% of changes in the annual labor productivity, and the remaining 37.4% are the factors unaccounted for in the model.

The multiple coefficient of determination corrected for loss of degrees of variation freedom  $R^2_{correct} = 0.617$ ;

The resulting equation is statistically significant, since Fisher's F-test is significantly higher than the critical value for a given probability level, F table- 2.7.

Correlation-regression analysis made it possible to determine that the capital-labor ratio is one of the main factors in the growth of production efficiency associated with scientific and technological progress. The value of the beta coefficient of capital-labor ratio indicates that if the capital-labor ratio increases by 1%, then labor productivity will increase by 0.33%.

**Table 2:** Grouping of agricultural enterprises by the level of annual labor productivity

Labor productivity, thousand rubles	The average level of labor productivity, thousand rub.	Number of enterprises	Capital-labor ratio, thousand rubles	Average monthly wage, thousand rub.	Fund's share of wages in total production costs, %
Less than 1094.0	601.0	46	658.1	105.9	29.5
1094.0 - 2278.4	1533.6	45	795.6	143.4	16.7
More than 2278,4	5629,0	46	1466.4	192.3	7.4
Total, average	2562,1	137	974.7	147.2	17.9

The grouping of 137 agricultural enterprises in the Ulyanovsk Region according to the level of their annual labor productivity showed that with the increase in the capital-labor ratio from 658.1 to 1466.4 thousand rubles and the average level of wages from 105.9 to 192.3 thousand rubles there is an increase in labor productivity from 601.0 to 5629.0 thousand rubles, that is in 9.4 times [Table 2]. The share of the wage fund is characterized with the opposite tendency: with an increase in labor productivity, the share of wages in total production costs is reduced from 29.5 to 7.4%, or in 4.0 times.

It should be noted that the agricultural enterprises of the region that are part of the first and second groups by the level of labor productivity are characterized by the values of the variables and the

performance factors lower than the average for the aggregate. Consequently, these organizations have a significant reserve to improve their level of labor productivity.

According to the tree of solutions built in the Deductor software, a high level of labor productivity in the region is achieved in the following cases:

- 1) The share of the wage fund in production costs does not exceed 8.7%;
- 2) The share of the wage fund in production costs is from 8.7 to 21.7%, the average wage level in agriculture is from 149 thousand rubles, and the capital-labor ratio has two values: less than 377.4 or more than 940.4 thousand rubles.

To construct a decision tree to achieve a high level of labor productivity in agriculture, the quantization method was used, what allowed us to break all the factors and the resultant indicator into three groups and to reveal the relationship within each group. As shown by the analysis, an average wage value in agriculture has the greatest impact on the formation of a high level of labor productivity. The level of the capital-labor ratio in agriculture labor plays an essential role in this.

## RESULTS AND DISCUSSION

The main direction in the growth of labor productivity is the development of scientific and technological progress. However, the introduction of world scientific achievements depends, first of all, on the agrarian enterprises themselves, and primarily on their financial capabilities. In this case, the main factor in the growth of the financial well-being of an organization is its technical re-equipment. Technical progress manifested in increasing the quantity and quality of agricultural machines is an important process of the gradual replacement of manual labor by machinery, that is, the most active part of fixed productive assets [2].

Intensive and effective use of fixed assets is essential in the increase of labor productivity, what makes it possible to reduce downtime of agricultural machinery and to increase the output per unit of equipment by 19-26% [3, 4]. Drawback of this fact on technical re-equipment is the seasonality in the use of much agricultural machinery. All this leads to an extension of the payback period and financial instability for farmers, because the main problem of crop production is a short period of use of planting and harvesting equipment. In this regard, the production of new high-tech agricultural machinery is most relevant.

Growing of the equipment status of agriculture due to equipping with machinery made it possible to strengthen its material and technical base, to increase energy supply and energy capacity of labor, to create the necessary conditions for increasing its productivity.

The machine and tractor fleet of agricultural organizations in Russia is losing ground every year. For the period since 1995, only 22.2% of the tractor fleet, 17.4% of tractor plows, 20.5% of various seeders, 11.0% of beet harvesters, 19.9% of mowing machines, 12.7% of sprinkling and irrigation machines, and 16.0% of milking plants remained [Table 3].

**Table 3:** Dynamics of technical equipment level of agriculture in the Russian Federation, thousand pieces

Type of technology	1995	2000	2005	2012	2013	2014	2015	2015 in % to 1995
Tractors	1052.1	746.7	480.3	276.2	259.7	247.3	233.6	22.2
Plows	368.3	238.0	148.8	76.3	71.4	67.8	64.1	17.4
Cultivators	403.5	260.1	175.5	108.7	102.2	97.8	93.2	23.1
Seeders	457.5	314.8	218.9	115.4	107.5	100.7	93.6	20.5
Combine harvesters	291.8	198.7	129.2	72.3	67.9	64.6	61.4	21.0
Forage harvesters	94.1	59.6	33.4	17.6	16.1	15.2	14.0	14.9
Potato harvester	20.6	10.0	4.5	2.7	2.6	2.4	2.3	11.2
Beet harvesting machines	20	12.5	7.2	2.8	2.5	2.4	2.2	11.0
Mowers	161.6	98.4	63.9	37.5	35.6	33.9	32.2	19.9
Irrigation systems and installation	46.3	19.2	8.6	5.2	5.2	5.7	5.9	12.7
Milking machines	157.3	88.7	50.3	28.6	27.3	26.3	25.1	16.0

Also there is a decrease in the number of combine harvesters of all types and purposes. In the year of 1995, Russia had 291.8 thousand combine harvesters, by 2015, this indicator decreased to 61.4 thousand, or by 21.0%. Of the 94.1 thousand units forage harvesters, there were 14.0 thousand units, or 14.9%, the reason was a sharp decrease in the number of livestock, which affected the number of equipment. The number of potato harvesters has changed quite dramatically and amounted to only 12.8% of this equipment in 2015 in relation to 1995.

Since 2010, production assets have increased annually, and the capital-labor ratio had increased, but this is due to a decrease in the number of agricultural workers. If the index of capital-labor ratio in agriculture as compared to 2005 by 2016 has doubled, then labor productivity has grown insignificantly.

Rational specialization and the strengthening of agricultural production to the optimum level facilitate more efficient use of machinery, mechanisms, material and labor resources. Expensive and high-performance machines and equipment can be used with their maximum loading in large specialized farms. This will significantly increase the yield of gross agricultural products and reduce the labor intensity of their production.

Reducing the labor intensity of products is also observed when introducing intensive and progressive technologies in agricultural production. If we apply intensive technologies in plant growing, we can provide a lower cost per unit of output by approximately 19 - 23%. This can be achieved using more intensive technologies, new kinds of crops or fertilizers in agricultural production [3,5]. In this regard, we consider the dynamics and prediction of the level of labor productivity in agricultural organizations in the Ulyanovsk region.

**Table: 4.** Dynamics of labor productivity in agricultural organizations in the Ulyanovsk Region

Years	The average annual labor productivity, thousand rubles / person	Average hourly productivity, rub / person-h
2008	527.7	301.2
2009	494.8	265.7
2010	546.5	432.3
2011	829.0	495.5
2012	915.5	615.6
2013	1077.6	814.6
2014	1223,0	929.8
2015	1662,1	1215.6
2016	2100.4	1276.3

The dynamics of 2009 - 2016 years shows that in the agricultural organizations of the Ulyanovsk region there was a tendency of an increase in the average annual labor productivity by 189.9 thousand rubles. At the same time, the average annual output in the period under study was 1041.8 thousand rubles per employee. The average hourly production [4, 5] during this period also tended to increase by 134.4 rubles annually, and its average level was 705.1 rubles [Table 4]

To compile a point prediction of labor productivity, an analytical equalization for a dynamical series of the indicators of the average and average hourly labor productivity using the straight line equation was applied:

$$Y_t = a + bt, \tag{1}$$

Where  $Y_t$  - equalized (fluctuation-free) level of labor productivity, thousand rubles;

$a$  - the average level of labor productivity in the period under study, thousand rubles (since 2009 to 2016);

$b$  - the value of the average change in labor productivity in the period under study, thousand rubles;

$t$  - time periods (years).

The results of the analysis are shown in [Table 5].

**Table 5:** Results of the labor productivity prediction in agricultural organizations in the Ulyanovsk region

Indicators	The average annual labor productivity, thousand rubles / person	Average hourly productivity, rub / person-h
Trend equation	$Y_t = 1041.84 + 189.91x$	$Y_t = 705.18 + 134.4x$
Coefficient of fluctuation, %	5.2	2.1
Stability factor, %	94.8	97.9
Point prediction for 2018	2373.2	1645.9
Interval prediction for 2019	$2373.23 \pm 187.37$	$1645.9 \pm 82.87$

According to the study, the average annual labor productivity in agricultural organizations of the Ulyanovsk region in 2018 will be 2373.2 thousand rubles per person, and the average hourly productivity will be 1645.9 rubles. The prediction of the labor productivity level for 2019 is determined taking into account the intervals of the indicator change (the mean statistical error). As a result, in 2019, the level of average

annual labor productivity upon introduction of intensive and progressive technologies in agricultural production will fall within the range from 2185.9 to 2560.6 thousand rubles per person, and the average hourly rate will make from 1563.0 to 1728.8 rubles per person per hour.

However, introduction of new technologies in production does not guarantee the growth of labor productivity in the case of low skill of workers. At the present stage, many suppliers of agricultural machinery, together with the supply of equipment, conduct training for a representative of the buyer enterprise. In the main, agrarian enterprises send their engineering personnel for training, with the subsequent training of workers of the enterprise. However, due to the increase in the age of a significant proportion of agricultural workers, there are no highly skilled workers at enterprises that can cope with digital technology and new computer programs. All this once again raises the question on interconnection between all aspects of the development of the agrarian sector and the necessity to involve young personnel into the agricultural production process.

## CONCLUSION

The use of new and intensive industrial technologies [6, 7] leads to a rationalization in the organization of labor and labor processes. The organization of labor must be directed towards the use of labor resources and the growth of labor productivity. To date, the lowest level of labor productivity is observed in livestock production, where, in comparison with crop production, there are differences not only in the degree of mechanization of labor-intensive processes in industries but in organizational matters. In livestock production there is a discrepancy between the forms of division and cooperation of the labor of workers in basic and auxiliary occupations and the progressive level of production mechanization and the requirements of progressive technologies, what has led to a difference in the degrees of loading level of milkmaids and cattlemen. Labor productivity in livestock is dependent on the sanitary and hygienic criteria of production and microclimate in livestock buildings [4]. Thus, enterprises using the achievements of scientific and technological progress in their work [8, 9] use a combination of organizational, managerial, socio-economic and moral-psychological principles of labor motivation and have highly qualified specialists, can compete effectively in the direction of increasing labor productivity and reproduction of fixed assets, and are able to provide the country with sufficient food and create food security.

### CONFLICT OF INTEREST

There is no conflict of interest.

### ACKNOWLEDGEMENTS

The work is carried out according to the Russian Government Program of Competitive Growth of Kazan Federal University.

### FINANCIAL DISCLOSURE

None

## REFERENCES

- [1] Buraeva EV. [2015] Labor productivity in agriculture of the agro-oriented region: problems and growth factors (by the example of the Orel region) EV. Buraeva Regional economy: theory and practice. 37:44-57.
- [2] Rofe AI. [2015] Labor Economics: textbook AI. Rofe-3rd edition, supplemented and revised. M.: Knorus. 374. 7.
- [3] Chaldaeve LA. [2015] Economics of an enterprise: A textbook and a practical work for the academic bachelor's degree LA. Chaldaeve. Moscow: Yurayt. 435. 3
- [4] Dubrovin IA. [2012] Labor Economics: A textbook IA. Dubrovin AS. Kamensky. Moscow: Dashkov and K. 232. 2
- [5] Potapenko MV, Sharopatova AV. [2017] Factors and ways to increase labor productivity in agriculture MV Potapenko AV. Sharopatova Innovative trends in the development of Russian science. Part I: materials of the X International Scientific and Practical Conference of Young Scientists dedicated to the Year of Ecology and the 65th Anniversary of the Krasnoyarsk State University of Automation (March 22-23, 2017) Krasnoyarsk State Agrarian University. Krasnoyarsk. 254-256.
- [6] Subaeva AK. [2016] Economic mechanism of technical support in agriculture: monograph AK Subaeva. Kazan: Publishing and Printing Company Brig. 216. 3
- [7] Subaeva AK. [2016] Classification of agro industrial complex technical provision effectiveness indexes AK. Subaeva AA. Zamaidinov Journal of economics and Economic education research. 4(17):8-14:1533-3590
- [8] Subaeva AK. [2015] Methods of agricultural machinery market regulation. AK Subaeva, AA Zamaidinov International Business Management. 9(7): 1780-1784. ISSN: 1993-5250.
- [9] Van Duijn JJ. [1981] Fluctuations in innovations over time. Futures. 13(4):264-273.



## ARTICLE

# ANALYSIS OF NATURAL FREQUENCIES OF OSCILLATIONS OF THE BALANCING MACHINE AND ROTOR GTD-16M

Sergey A Nazarychev<sup>1</sup>, Sergey O Gaponenko<sup>2\*</sup>, Aleksandr E Kondratiev<sup>2</sup>, Andrey V Busarov<sup>3</sup>

<sup>1</sup>The Alexander Butlerov Institute of Chemistry, Kazan Federal University, Kazan, RUSSIA

<sup>2</sup>Kazan State Power Engineering University, Kazan, RUSSIA

<sup>3</sup>Center of Expertise of Industrial Safety, Kazan, RUSSIA

## ABSTRACT

Descriptions of the general structure of the ANSYS program using the finite element method are given. The basic structures of the modal analysis and the position of the finite element method are studied. For reliable calculation, accuracy and suitability for elemental applications, equations in the form of matrix systems are described. A modal analysis is performed that characterizes the frequency and nature of the natural oscillations of a given structure. The calculation of natural frequencies of oscillations of the main elements of the balancing machine and the turbocharger rotor is performed. Presented is the imported GTD-16M rotor model, finite element mesh on the GTD-16M rotor model. The calculation of the natural frequencies of the bed and the support assembly of the balancing machine is performed. To calculate the natural frequencies and modes of natural oscillations of the machine bed, the bed model is loaded into the ANSYSWB environment. The first 24 modes of oscillations of the examined support assembly of the balancing machine are determined. The results are shown in the table. The calculation of natural frequencies and modes of natural oscillations of the support assembly of the balancing machine is carried out. The reference node model is loaded into the ANSYSWB environment. An informative frequency range has been obtained that allows balancing rotors in the pre-resonance mode of operation. The results of experimental studies are presented and presented graphically.

## INTRODUCTION

Such automated production and design systems such as AutoCAD, Pro / Engineer, Uni graphics, DUCT and Solids Works are widely used in computer prediction of unusual form standards, creation of control systems for CNC machines and production of techniques, however such group numerical prediction packages do not have developed methods analysis. Concepts of this kind, such as ABAQUS, ANSYS, COSMOS, I-DEAS, NASTRAN, which are mechanisms of automatic engineering analysis, allow performing high-quality forecasting of projects of different physical nature, and studying the response of such programs to external influences in the form of temperature, velocity, stress distribution, electromagnetic fields and other factors.

## MATERIALS AND METHODS

### Application of ANSYS

The ANSYS system is a convenient, reliable resource for design and research. The specificity of ANSYS is that all the incoming resources of this program are compatible and defined for all platforms used. This program operates in a group of operating systems often used by hardware. The multi functionality of this program allows the possibility of applying the same model for solving such intertwining problems as the influence of magnetic fields on the strength of a structure, the action of heat and mass transfer in an electromagnetic field, and stability under thermal loading. All this provides the subscribers of the program with reliable methods and options for solving a vast field of engineering issues [1-2].

Carrying out calculations by the ANSYS system, possibly thanks to basic engineering concepts and rules. With the help of proven numerical methods, these concepts can be expressed in the form of matrix equations that are maximally suitable for finite-element equations. In the mathematical model of the system, which consists of the integrity of the final branches (elements), interconnected at a finite number of points (nodes), it is necessary to evaluate its order and analyze the changes. The degrees of freedom of the nodes of the elemental finite model are key unknowns, namely, displacements, magnetic or electric field potentials, pressures, temperatures, velocities and rotations. The exact content of degrees of freedom is established with the type of element that is conjugated to this node. According to the degrees of freedom, for each component of the model, the mass, rigidity (or thermal conductivity) and resistance (or specific heat) matrices are determined.

### Basic concepts of the finite element method and modal analysis

To date, widely used numerical methods, preferably the finite element method (FEM), to evaluate the dynamic parts of structural elements [3].

The decisive dynamic tasks are: the dynamic effect on the load, due to the duration; calculation of free design vibrations; propagation of waves [5].

### KEY WORDS

ANSYS, finite element method, vibration modes, pre-resonance regime, balancing.

Received: 11 Oct 2018  
Accepted: 18 Dec 2018  
Published: 3 Jan 2019

### \*Corresponding Author

Email:  
sogaponenko@yandex.ru  
Tel.: 89874170041

In this work the ANSYS software complex was applied, which allows to perform the modal analysis (an important part of any dynamic analysis, since it allows estimating the dynamic behavior of the object) to determine the forms and frequencies of the object's own vibrations.

Own (free) oscillations are a necessary characteristic of linear systems. They manifest themselves in the absence of external forces, natural movements.

Modal analysis of the ANSYS system has solvers, it makes it possible to find the own values of the task. The Block Lanczos module is such a solver. It is used when a large sample contains elements of incorrect form 2- and 3-dimensional, for calculating a large number of modes. When a model consists of shell parts or their combinations and solidities, the Block Lanczos module works well. In comparison with the method of iteration in the subspace, the performance is faster, and the memory requirements are higher by 50% [6].

Applying the method of finite elements, the discrete equations of motion of the construction can be represented in the form of equations, presented in the educational material, Leontiev N.V. "Application of the ANSYS system to solving modal and harmonic analysis problems" [7].

The most important problem of finite element analysis is the justification of the uniqueness of the size of the computational grid. At the heart of the order, the ANSYS system is a means of estimating the calculation error used in performing linear strength and thermal analysis of elements due to the grid-based sampling, there is also a choice of rejecting it [7-8].

### Calculation of the natural vibration frequencies of the basic elements of the balancing machine and rotor design

Modal analysis consists of the following basic steps: creating a geometric model of the object of control; setting properties of materials; creation of contact conditions; determination of calculation methodology; the creation of a finite element grid (CE); course of calculation; view calculated results and create a report. The geometric characteristic of the object forms the basis for the analysis. There are two ways to create a model of the object under study in ANSYSWB-importing a model from an external CAD and creating geometry with internal tools. For this reason, Autodesk Inventor 2016 CAD software imports the geometry of the rotor into the ANSYSWB environment [Fig. 1].

The properties of the materials are specified:

- density: kg / m<sup>3</sup>;
- modulus of elasticity: N / m<sup>2</sup>;
- Poisson's ratio:  $\nu = 0,3$  .

The contact conditions are established: fixed fixation along the lateral faces of the model along the axis of rotation of the rotor and cylindrical fastening in the places of support of the rotor shaft. Due to the fact that the modal analysis is linear, the inclusion of contacts in this calculation can be neglected.

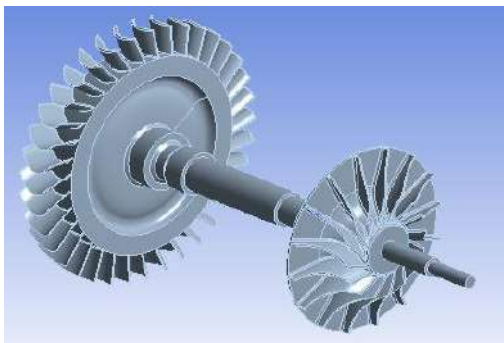


**Fig. 1:** Imported rotor model GTD-16M.

Execution of the finite element grid. When determining the calculation options, note, for modal analysis, the main assumptions and limitations: the absence of damping; the stiffness matrix [K] and masses [M] are constant; fluctuations are free; the behavior of the system is linear; the form of free oscillations is calculated in relative units and does not allow to determine absolute displacements [9].

To create the CE grid [Fig. 2], the following parameters are selected:

- grid on a solid body (grid type);
- standard grid (used splitting);

- high (quality of the grid);
- 44015 (number of nodes);
- 23219 (number of items).

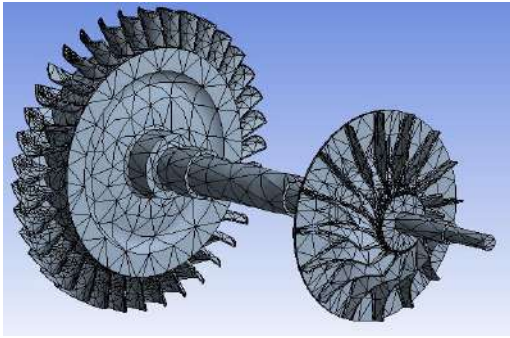


**Fig. 2:** The finite element mesh created on the GTD-16M rotor model.

As a result of the study, 24 first modes of oscillations of the calculated rotor are determined. When analyzing the results of the modal calculation, it is necessary to take into account that the form of free oscillations is calculated in relative units and does not allow determining absolute displacements.

The vibration shape of the first mode of the balancing rotor at a frequency of 269.67 Hz is shown in [Fig. 3].

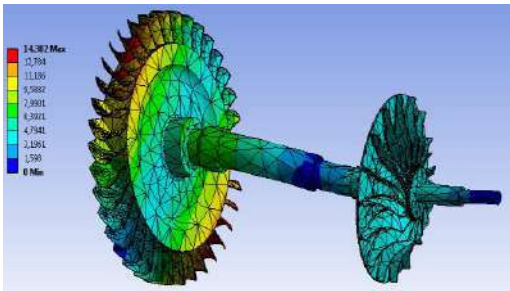


**Fig. 3:** Shape of vibration of the first mode of the rotor of the turbocharger.

The results are summarized in [Table 1].

**Table 1:** Modes of vibrations of the rotor in question

Mode of oscillation	Frequency, Hz	Mode of oscillation	Frequency, Hz	Mode of oscillation	Frequency, Hz
1	269,67	9	1594,7	17	3190,8
2	394,52	10	1597	18	3227,2
3	395,1	11	1947,4	19	3550,9
4	428,13	12	2463,5	20	3564,6
5	703,52	13	2475,4	21	4022,3
6	704,88	14	2931,6	22	4147,5
7	1309,6	15	2936	23	4263,2
8	1313,1	16	3086,5	24	4267,8

Using the obtained frequency range of the natural oscillations of the rotor, it is necessary to determine the natural frequencies of the balancing machine base in order to subtract these frequencies from the frequency modes of the rotor under investigation [10].

Calculation of the natural frequencies of the bed and support assembly of the balancing machine  
To calculate the natural frequencies and modes of natural oscillations of the machine bed, the bed model is loaded into the ANSYSWB environment [Fig. 4].

The frame is made of polymer granite and this material has the following properties:

- density: kg / m<sup>3</sup>;
- modulus of elasticity: N / m<sup>2</sup>;
- Poisson's ratio:  $\nu = 0,25$  .

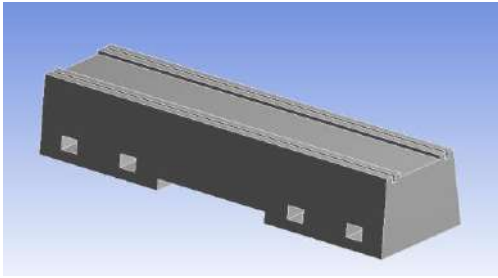


**Fig. 4:** Loaded geometry model of the frame in ANSYSWB.

When creating a finite element grid [Fig. 5], select:

- grid type: grid on a solid body;
- used partitioning: standard grid;
- grid quality: high;
- number of nodes: 9817;
- number of elements: 5471.

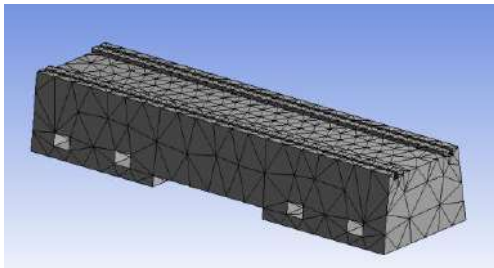


**Fig. 5:** The finite element grid on the bed model.

As a result of the modal examination of the frame, 24 first modes of oscillation are determined.

The results are summarized in [Table 2]

**Table 2:** Modes of oscillations of the examined bed of the balancing machine

Mode of oscillation	Frequency, Hz	Mode of oscillation	Frequency, Hz	Mode of oscillation	Frequency, Hz
1	1015,5	9	2288,1	17	3144,5
2	1083,4	10	2290	18	3229,8
3	1339,7	11	2404,2	19	3231,1
4	1419,6	12	2620,7	20	3311
5	1603,6	13	2678,3	21	3389,9
6	1769,2	14	3003,8	22	3432,5
7	1927,8	15	3030,6	23	3515,8
8	2019,5	16	3112	24	3567,8

The shape of the oscillation of the first mode of the machine bed at a frequency of 1015.5 Hz is shown in [Fig. 6].

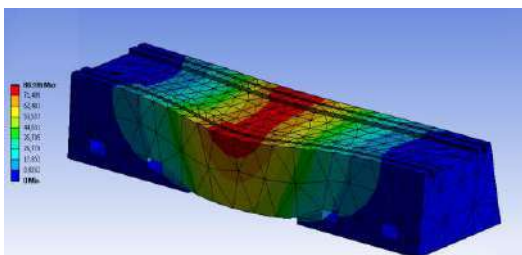


**Fig. 6:** The shape of the oscillation of the first mode of the machine bed of the balancing machine.



Similarly, the calculation of natural frequencies and modes of natural oscillations of the support assembly of the balancing machine is performed. The reference node model is loaded into the ANSYSWB environment [Fig. 7].

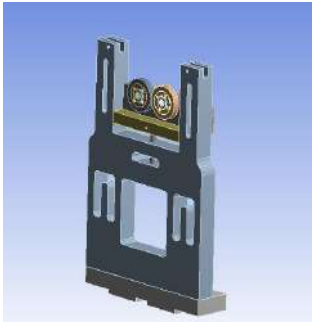


**Fig. 7:** Geometric model of the reference node in ANSYSWB.

The material properties are defined and a finite element grid is created [Fig. 8].

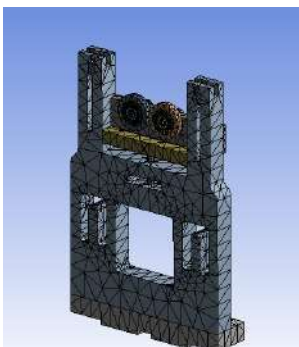


**Fig. 8:** The finite element grid on the model of the reference node.

As a result of the modal examination of the reference node, 24 first modes of oscillation are determined.

The shape of the oscillation of the first mode of the machine bed at a frequency of 1015.5 Hz is shown in [Fig. 9].

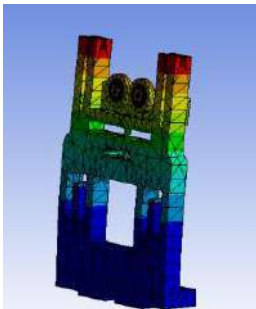


**Fig. 9:** Shape of oscillation of the first mode of the balancing machine support assembly.

The results are summarized in [Table 3].

**Table 3:** Modes of oscillations of the examined support unit of the balancing machine

Mode of oscillation	Frequency, Hz	Mode of oscillation	Frequency, Hz	Mode of oscillation	Frequency, Hz
1	2	3	4	5	6
2	714,75	9	1478,3	17	2369,5
3	920,95	10	1501,3	18	2380,7
4	1135,6	11	1697	19	2517,7
5	1170,1	12	1703,8	20	2691,4
6	1184,1	13	1760,2	21	2703,5
7	1247,9	14	1984,7	22	2728,1
8	1304,3	15	2159,2	23	2817,8
9	1440,7	16	2219,6	24	2839,1

## RESULTS AND DISCUSSION

As a result of this calculation, the range of the natural frequencies of the oscillations of the reference assembly of the balancing machine is determined.

When comparing [Tables 1- 3], it can be seen that the frequencies of the first 6 modes of the natural frequencies of the rotor oscillations lie below the natural oscillation frequencies of the frame and the supporting unit of the machine. Frequency range 0-705 Hz is the most informative frequency range on which it is necessary to carry out pre-resonance balancing of the rotor.

As a result of the modal analysis of the rotor, the bed and the support assembly of the balancing machine, an informative frequency range was obtained which allows balancing the rotors in the pre-resonance mode of operation. The balancing machine of the pre-resonance type is more efficient, because on this machine balancing is performed without calibration starts, high balancing accuracy is achieved and balancing of any rotor types corresponding to the overall dimensions of the machine is possible.

## CONCLUSION

In this work, a modal analysis (one of the methods for determining the forms and frequencies of natural oscillations) was performed using the ANSYS software and results were obtained. As a result of the studies, the goal and objectives were fully met. The general structure of the ANSYS program using the finite element method was considered, the natural vibration frequencies of the basic elements of the balancing machine and the turbocharger rotor were calculated.

### CONFLICT OF INTEREST

There is no conflict of interest.

### ACKNOWLEDGEMENTS

The work is performed according to the Russian Government Program of Competitive Growth of Kazan Federal University.

### FINANCIAL DISCLOSURE

None

## REFERENCES

- [1] Bryuka VA. Engineering Analysis in ANSYS Workbench: A Training Manual VA Bryuyaka, VG Fokin, EA Soldusova, NA Glazunov, IE Adeyanov. [2010] Samara: Samara State Technical University. 271.
- [2] Shirman A, Soloviev A. [1996] Practical vibration diagnostics and monitoring of mechanical equipment Moscow. 276.
- [3] Gaponenko SO, Kondratiev AE. [2017] Device for calibration of piezoelectric sensors, PROCEDIA ENGINEERING, Series International Conference on Industrial Engineering, ICIE 2017, Publishing: Elsevier Ltd. 146-150.
- [4] Gaponenko SO, Kondratiev AE, Zagretidinov AR. [2016] Low-frequency vibro-acoustic method of determination of the location of the hidden canals and pipelines, PROCEDIA ENGINEERING, Series International Conference on Industrial Engineering, ICIE 2016, Publishing: Elsevier Ltd. 150:2321-2326.
- [5] Nazarychev SA, Gaponenko SO, Kondratiev AE. [2018] Determination of informative frequency ranges for buried pipeline location control, Helix. 8(1):2481- 2487.
- [6] Sekita K, Fujisawa T, Sago K. [1982] Method of determining the location of the imbalances in rotary machines: Per. from English. Design and technology of mechanical engineering.M.: World. 104(21):26-31.
- [7] Leontiev NV. [2006] Application of the ANSYS system to solving modal and harmonic analysis problems Nizhny Novgorod. 368
- [8] Sidorov VA, Sotnikov AL, Sushko AE, Tsyba SA. [2009] A technique for assessing the economic efficiency of balancing rotors in production conditions. Vibration of machines: measurement, reduction, protection. 38-43.
- [9] Dyer D, Stuart R. [1978] Detection of rolling bearing damage by statistical vibration analysis: Per. with English. Design and technology of mechanical engineering. M.: Mir. 100(2):23-31.
- [10] Matthew D, Alfredson R. [1984] Vibration analysis Application to control the technical condition of rolling bearings: Per with English. Design and technology of mechanical engineering. M.: World. 106(3):100-108.
- [11] Rogov VA, Poznyak GG, Mukharyamov RG. [2005] Theoretical bases of balancing of rotors of turbochargers. Bulletin of the Kazan State Technical University. AN Tupolev. 8-11.
- [12] Aretakis N, et al. [2003] Turbocharger unstable operation diagnosis using vibroacoustic measurements ASME Turbo Expo 2003, collocated with the 2003 International Joint Power Generation Conference. American Society of Mechanical Engineers. 361-369.
- [13] Reshetov A, Arakelyan AK. [2010] Nondestructive testing and technical diagnostics of power facilities AK Arakelyan. Cheboksary: Publishing house. Chuvash University. 3:164.

## ARTICLE

# APPLICATION OF LOW-FREQUENCY ACOUSTIC VIBRATIONS FOR TECHNICAL WATER TREATMENT

Sergey A Nazarychev<sup>1</sup>, Sergey O Gaponenko<sup>2\*</sup>, Aleksandr E Kondratiev<sup>2</sup>, Eduard A Ahmetov<sup>2</sup>

<sup>1</sup>The Alexander Butlerov Institute of Chemistry, Kazan Federal University, Kazan, RUSSIA

<sup>2</sup>Kazan State Power Engineering University, Kazan, RUSSIA

## ABSTRACT

This paper describes the general structure of the LabVIEW program package. The program was developed using the National Instruments LabVIEW software package. The algorithm of operation of the automated system of the experimental setup is described. For experimental studies, an automated system for determining and maintaining the natural oscillations of an experimental plant for technical water treatment by acoustic oscillations was specially developed and manufactured. A schematic diagram of an automated system for determining and maintaining the natural oscillations of an experimental plant for technical water treatment by acoustic oscillations is presented. The results of experimental studies are presented and presented graphically. To compare the results of changes in the concentration of suspensions as a function of time, we plotted the effects of sedimentation for each sensor at different impact frequencies. The purpose of the experimental studies was to confirm the calculations of the optimum frequency of resonance formation in the pipe and the intensity of precipitation at frequencies other than of resonance formation, but adjacent thereto in the interval of  $\pm 15$  Hz and  $\pm 30$  Hz.

## KEY WORDS

LabVIEW, technical water, acoustic oscillations, sedimentation, resonance, ultrasonic vibrations (US), acoustic transducer (AT), acoustic speed, technical water, scale.

## INTRODUCTION

Increasing energy efficiency and introducing energy-saving technologies are priority areas for the development of heat and power engineering.

The concept of using ultrasonic technology to prevent the formation of scale on heat exchange equipment is based on the excitation of ultrasonic vibrations (ultrasonic waves) on the surface of a heat exchanger or in a heat carrier (water) [1, 2].

For shell-and-tube heat exchangers (water heaters), the welded connection of radiators with the tube board of the water heater is the most optimal method of transferring ultrasonic waves from the ultrasound emitter to the excited medium [Fig. 1.1]. Distributed along the tube board, ultrasonic vibrations are transmitted through welded or rolling joints into the tube bundle, preventing deposition of scale or deposits of other origin, for example, organic matter on the heat exchanger surface. In the case of a steam or hot water boiler, the radiators are welded to the drums and collectors of the side and rear screens [Fig. 1.2], which provides protection against the scale in high-temperature boiler sections. For plate heat exchangers, the formation of ultrasonic oscillations in the water column is preferable [Fig. 1.3], which is achieved due to a certain change in the design of the radiators. The frequency of forced ultrasonic vibrations is 15-25 kHz and is selected from the results of numerous studies, as optimal to prevent the formation of deposits and friendly to welded and rolled joints [3, 4].

Ultrasound technology (UST) is designed to prevent the formation of scale, which ensures high-quality indicative results of operation in a relatively short time. Its maximum efficiency is achieved by the parallel equipping of heat exchange equipment with instrumentation and automation, subject to consideration of energy-saving technologies and recording of heat consumption and supply as a single direction in a series of technical measures for the development of heat power engineering. [5, 6, 7]

## MATERIALS AND METHODS

The algorithm of operation of the automated system of the experimental setup.

For experimental studies, an automated system for determining and maintaining the natural oscillations of an experimental plant for technical water treatment by acoustic oscillations has been developed and constructed.

Fig. 2.1 shows a schematic diagram of an automated system for determining and maintaining the natural oscillations of an experimental plant for technical water treatment by acoustic oscillations. The principle of the plant is described in the utility model patent No. 104319 dated 03.12.2010 "A device for laboratory studies of the intensity of industrial water treatment from suspended solids" by Kondratiev A.Ie., Iliasov N.Kh., Gaponenko S.O. [8,9,10, 11].

\*Corresponding Author

Email:  
sogaponenko@yandex.ru  
Tel.: 89874170041

Received: 6 Oct 2018  
Accepted: 15 Dec 2018  
Published: 3 Jan 2019



**Fig. 1.1:** Installation of Acoustics-T on a shell-and-tube water heater.



**Fig. 1.2:** Installation of an Acoustics-T device on a DKVr-10 boiler.



**Fig. 1.3:** Installation of an Acoustics-T device on a plate heat exchanger.

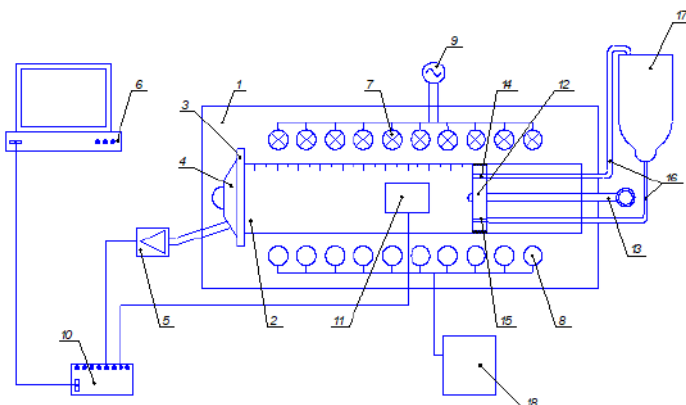


**Fig. 2.1:** An automated system for determining and maintaining the natural oscillations of an experimental plant for technical water treatment by acoustic oscillations: 1 - base; 2 - pipe, length 620 mm and diameter  $\square 45 \times 2$ ; 3 - membrane; 4 - acoustic radiator; 5 - signal amplifier; 10 - ADC-DAC; 6 - the computer with LabVIEW installed; 7 - light-emitting diodes; 8 - photocells; 9 - power adapter; 18 - milli voltmeter; 12 - movable piston; 13 - stem; 14 - output valve; 15 - input valve; 16 - flexible hoses; 17 - expansion tank.

[Fig. 2.2] presents a photo of an experimental plant for technical water treatment by acoustic vibrations.

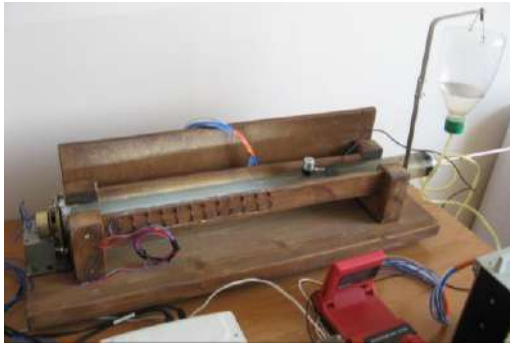


**Fig. 2.2:** A photo of an experimental plant for technical water treatment by acoustic vibrations.

## RESULTS AND DISCUSSION

Experimental studies were carried out in several stages: with natural precipitation, with an acoustic effect on the water under investigation at 605 Hz, which, as the calculations show, is the optimum frequency of resonance in the tube.

The purpose of the experimental studies was to confirm the calculations of the optimum frequency of resonance formation in the pipe and the intensity of precipitation at frequencies other than of resonance formation, but adjacent thereto in the interval of  $\pm 15$  Hz and  $\pm 30$  Hz.

### Experiment no.1.

The purpose of the first experiment is to determine the dependence of the change in the concentration of suspensions on time under natural precipitation. For this, the turbid water filled in a transparent pipe is illuminated by light-emitting diodes and by means of photocells we take readings of the change in concentration every 15 seconds from the measuring device for the concentration of inorganic contaminants. The data is entered in [Table 3.1]. After processing the results, the data looks as follows [Table 3.2].

**Table 3.1:** Time-based change in the concentration of suspensions with natural precipitation

Sec No.	1	2	3	4	5	6	7	8	9	10
15	0.226	0.235	0.234	0.193	0.194	0.205	0.206	0.215	0.211	0.226
30	0.208	0.217	0.215	0.169	0.171	0.183	0.186	0.191	0.189	0.211
45	0.189	0.191	0.198	0.155	0.156	0.17	0.176	0.18	0.178	0.197
60	0.179	0.181	0.19	0.148	0.149	0.162	0.171	0.174	0.17	0.186
75	0.173	0.174	0.186	0.142	0.141	0.159	0.167	0.17	0.165	0.178
90	0.168	0.169	0.182	0.138	0.135	0.154	0.164	0.166	0.162	0.174
105	0.167	0.167	0.179	0.135	0.133	0.152	0.162	0.164	0.16	0.172
120	0.165	0.164	0.178	0.132	0.13	0.15	0.161	0.162	0.157	0.168
135	0.164	0.162	0.175	0.129	0.126	0.148	0.159	0.161	0.155	0.164
150	0.16	0.159	0.172	0.125	0.121	0.145	0.157	0.16	0.153	0.16

**Table 3.2:** Time-based change in the concentration of suspensions with natural precipitation after processing the results

Sec %	1	2	3	4	5	6	7	8	9	10
15	1	1	1	1	1	1	1	1	1	1
30	0.92	0.923	0.918	0.875	0.881	0.892	0.902	0.888	0.895	0.933
45	0.836	0.812	0.846	0.803	0.804	0.829	0.854	0.837	0.843	0.871
60	0.792	0.77	0.812	0.766	0.768	0.79	0.83	0.809	0.805	0.823
75	0.765	0.74	0.794	0.735	0.726	0.775	0.81	0.79	0.782	0.787
90	0.743	0.719	0.777	0.715	0.695	0.751	0.796	0.772	0.767	0.769
105	0.738	0.71	0.765	0.699	0.685	0.741	0.786	0.762	0.758	0.761
120	0.73	0.697	0.76	0.683	0.67	0.731	0.781	0.753	0.744	0.743
135	0.725	0.689	0.747	0.668	0.649	0.722	0.771	0.748	0.734	0.725
150	0.708	0.676	0.735	0.647	0.623	0.707	0.762	0.744	0.725	0.708



Experiment no.2

The purpose of the second experiment is to determine the dependence of the change in the concentration of suspensions on time under acoustic impact at 605 Hz. For this, the turbid water filled in a transparent pipe is illuminated by light-emitting diodes and by means of photocells we take readings of the change in concentration every 15 seconds from the measuring device for the concentration of inorganic contaminants. Acoustic impact occurs through the combined operation of an acoustic generator, an acoustic radiator and a membrane. The turbidity level should correspond to the initial value of the turbidity index in experiment 1. The applied frequency is set at a value of 605 Hz, which, according to the calculations, is the optimum frequency for resonance in the pipe. The data is entered in [Table 3.3]. After processing the results, the data looks as follows [Table 3.4].

**Table 3.3:** Time-based change in the concentration of suspensions under acoustic impact at 605 Hz

Sec No.	1	2	3	4	5	6	7	8	9	10
15	0.239	0.237	0.253	0.193	0.192	0.196	0.2	0.204	0.203	0.217
30	0.186	0.186	0.204	0.151	0.155	0.157	0.169	0.173	0.171	0.181
45	0.166	0.167	0.189	0.138	0.135	0.147	0.159	0.165	0.162	0.171
60	0.16	0.16	0.185	0.133	0.13	0.144	0.156	0.161	0.155	0.167
75	0.158	0.157	0.181	0.129	0.125	0.141	0.154	0.158	0.152	0.163
90	0.156	0.155	0.179	0.126	0.122	0.139	0.152	0.154	0.15	0.161
105	0.155	0.153	0.178	0.124	0.119	0.137	0.151	0.152	0.148	0.157
120	0.152	0.151	0.176	0.122	0.117	0.136	0.15	0.151	0.147	0.156
135	0.151	0.15	0.175	0.121	0.116	0.135	0.149	0.15	0.146	0.153
150	0.15	0.15	0.175	0.12	0.114	0.134	0.148	0.149	0.145	0.151

**Table 3.4:** Time-based change in the concentration of suspensions under acoustic impact at 605 Hz after processing the results

Sec No.	1	2	3	4	5	6	7	8	9	10
15	1	1	1	1	1	1	1	1	1	1
30	0.778	0.784	0.806	0.782	0.807	0.801	0.845	0.848	0.842	0.834
45	0.694	0.704	0.747	0.715	0.703	0.75	0.795	0.808	0.798	0.788
60	0.669	0.675	0.731	0.689	0.677	0.734	0.78	0.789	0.763	0.769
75	0.661	0.662	0.715	0.668	0.651	0.719	0.77	0.774	0.748	0.751
90	0.652	0.654	0.707	0.652	0.635	0.709	0.76	0.754	0.738	0.741
105	0.648	0.645	0.703	0.642	0.619	0.699	0.755	0.745	0.729	0.723
120	0.636	0.637	0.695	0.632	0.609	0.693	0.75	0.74	0.724	0.718
135	0.631	0.632	0.691	0.626	0.604	0.688	0.745	0.735	0.719	0.705
150	0.627	0.632	0.691	0.621	0.593	0.683	0.74	0.73	0.714	0.695

To compare the results of changes in the concentration of suspensions as a function of time, we plotted the effects of sedimentation for each sensor at different impact frequencies.

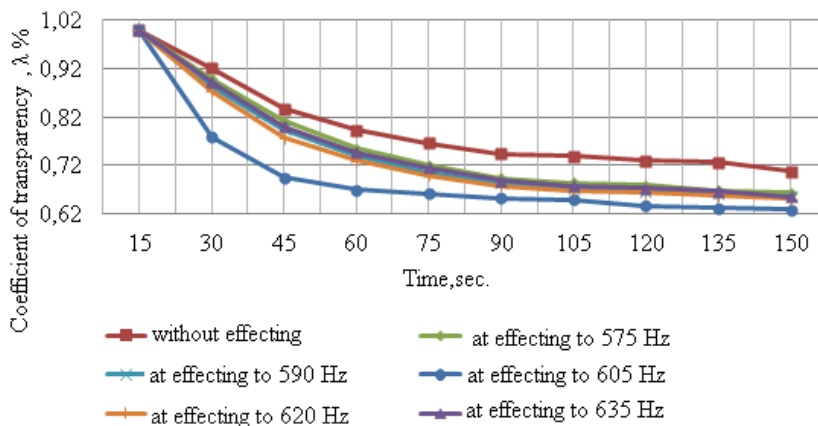


**Fig. 3.1:** Diagram of the change in the transparency index as a function of time for the 1st sensor.

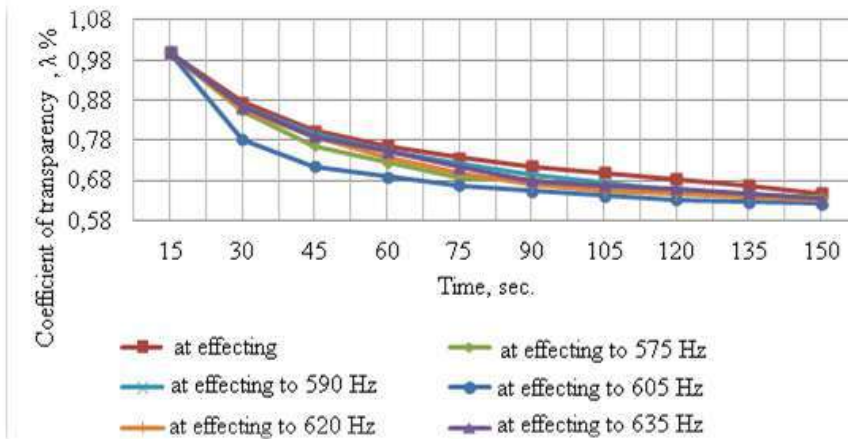


Fig. 3.2: Diagram of the change in the transparency index as a function of time for the 2nd sensor.

## CONCLUSION

As we can see, the percent change in the concentration of suspensions flows much faster at a frequency of 605 Hz, which, according to calculations, was the optimal frequency of resonance formation than with natural precipitation.

For experimental studies, an automated system for technical water treatment by acoustic oscillations was developed and constructed. The program was developed in the LabVIEW software environment to determine and maintain natural oscillations. The automated system for determining and maintaining the natural oscillations of an experimental plant for technical water treatment by acoustic oscillations was developed and constructed. Analysis of the obtained experimental data shows that the percent change in the concentration of suspensions is much faster when water is exposed to the frequency at which a standing wave forms than in the case of natural precipitation.

## CONFLICT OF INTEREST

There is no conflict of interest.

## ACKNOWLEDGEMENTS

The work is performed according to the Russian Government Program of Competitive Growth of Kazan Federal University.

## FINANCIAL DISCLOSURE

None

## REFERENCES

- [1] Khokhriakova EA, Reznik IaE. [2007] Authors compilers. Water treatment: Reference book / Ed. Doctor of Technical Sciences, full member of the Academy of Industrial Ecology SE Belikov. M.: Aqua-Therm. 240 www.aqua-therm.ru/
- [2] Voronov Viu. [2006] Water drainage and sewage treatment: a textbook. - revised edition No.4. M.: Publishing House of the Association of Construction Universities. 702.
- [3] Budykina TA, Emelianov SG. [2010] Processes and apparatus for protecting the hydrosphere: a textbook for student of high vocational institutions. M.: Publishing Center Akademia. 288.
- [4] Riabchikov BE. [2004] Modern methods of water treatment for industrial and domestic use. M.: DeLi print. 328.
- [5] Fedotkin IM, et al., Use of ultrasound to prevent the formation of scale in evaporators, Sugar industry. 4:64-66.
- [6] LLC Ultrasonic technique-in the laboratory /http://en.utinlab.ru
- [7] Shadley JR, Shirazi SA, Dayalan E, Rybicki EF. [1998] Prediction of erosion-corrosion penetration rate in carbon dioxide environment with sand, Corrosion/98. 59, NACE.
- [8] Norton MP. [2003] School of Mechanical Engineering, University of Western Australia and DG Karczub, SVT Engineering Consultants, Perth, Western Australia/ Fundamentals of Noise and Vibration Analysis for Engineers, Second edition/ CAMBRIDGE UNIVERSITY PRESS, 621.
- [9] Buckin V. Department of Chemistry, University College Dublin, Belfield, Dublin 4, Ireland, Breda O'Driscoll and Cormac Smyth, Ultrasonic Scientific, Block 1, Richview Office Park, Clonskeagh, Dublin 4, Ireland in collaboration with Arno C. Alting and Ronald W. Visschers, Wageningen Centre for Food Sciences (WCFS), Wageningen, The Netherlands Ultrasonic spectroscopy for material analysis. Recent advances. 20-25.
- [10] Doosti MR, Kargar R, Sayadi MH. Environment and Civil Eng Dept, University of Birjand, Birjand, Iran Water treatment using ultrasonic assistance: A review. 110.
- [11] Gaponenko SO, Kondratiev AE. [2017] Device for calibration of piezoelectric sensors, PROCEDIA ENGINEERING, Cep International Conference on Industrial Engineering, ICIE, Publishing: Elsevier Ltd. 146-150.
- [12] Gaponenko SO, Kondratiev AE, Zagretidov AR. [2016] Low-frequency vibro-acoustic method of determination of the location of the hidden canals and pipelines, PROCEDIA ENGINEERING, Cep International Conference on Industrial Engineering, ICIE, Publishing: Elsevier Ltd. 150:2321-2326.
- [13] Nazarychev SA, Gaponenko SO, Kondratiev AE. [2018] Determination of informative frequency ranges for buried pipeline location control, Helix. 8(1): 2481- 2487.
- [14] Panfil PA, Andreev AG. Anti-scaling ultrasonic technology, http://www.rosteplo.ru
- [15] Kondratiev Ale, Iliasov NKh, Gaponenko SO. RF patent No. 104319 dated 03.12.2010 A device for laboratory studies of the intensity of industrial water treatment from suspended solids.

## ARTICLE

# ON INFLUENCE OF TURNING THE KOCH FRACTAL DIPOLE ARMS ON ITS BASE FREQUENCY AND BANDWIDTH

Dmitrii Tumakov\*, Alexey Ovcharov, Dmitry Chickrin, Petr Kokunin

*Institute of Computational Mathematics and Information Technologies, Kazan Federal University, Kazan, RUSSIA*

## ABSTRACT

A dipole wire antenna of the Koch is considered. The antenna represents a wire dipole symmetrical with respect to the point of feeding. Arms of the dipole have the geometry of Koch prefractal. A family of antennas is singled out, in which the antennas differ from each other by an angle of arms turning. Antennas having the geometry of the first two iterations of a Koch curve are chosen for the analysis. Dipoles based on the Koch pre-fractals of the first two iterations having different wire thicknesses obtained by rotating one of the arms around a given coordinate axis is considered. Graphs depicting dependence of the base frequency and bandwidth for the frequency on angles of rotation around the axes are presented. Rotations of the dipole arms by small angles do not exert influence on the frequency and bandwidth. However, in the case of large angles of the arms rotation, the values of base frequency increase and bandwidth reduce significantly.

## INTRODUCTION

A classical symmetric electric dipole containing two identical arms fed in the middle represents one of the most well explored objects in the theory of antennas [1]. There exist various methods of improvement of electrodynamic characteristics of such dipoles [2]. For example, the improvements can come from varying an angle between the arms and obtaining the so-called V-shaped antennas [3] as well as from mutual influence of radiation originating from the arms on each other. Another method of improvement of the symmetric dipole's characteristics is related to placing the arms in an antisymmetric manner. The method was applied in [4] for improving several resonance characteristics of the classical Koch and quadratic Koch fractal dipole antenna; the study also compared the obtained antennas with each other. A dual-band dipole antenna with asymmetric arms was presented in [5] for WLAN applications.

For improving the electrodynamic characteristics of dipoles, modification of the ratio of sizes (areas) of the dipole's arms is also utilized. For example, study [6] considered a dipole antenna consisting of two printed strips of unequal lengths and presented graphs for reflection coefficients and radiation patterns of the proposed antenna. The wide operating band is obtained at the fundamental and second resonances of the rod dipole by using manipulations related to changing the feed [7]. A balanced-to-unbalanced transformer or balun is also often used [8]. The study [9] considered a printed dipole antenna with a microstrip balun and demonstrated an influence of sizes of the balun on return loss. In the study [10], inductive load was added for reducing the base frequency.

Multiple folded arms are can also used. The studies [11, 12] considered antennas consisting of an axially symmetric array of four and six conductor arms forming a spherically shaped structure and demonstrated influence of increase in the number of arms on quality factor and bandwidth.

For reducing the sizes of the dipoles, one can alter topology of the arms, so that the electric length of the antenna increases, while radius of the sphere covering the dipole remains unchanged. For that purpose, one can roll the arms into a helix [13, 14] or perform various fractal transformations [15]. In this regard, the following antennas can be specified: an antenna which is based on the Koch curve [16, 17], Minkowski curve [18, 19], Sierpinski carpet [20, 21], a rounded fractal antenna [22, 23] and complex fractal combinations [24-26].

Characteristics of the dipole can be further improved by rotating its arms in space with respect to each other. For example, properties of the Koch dipole during rotating the arms in one plane (in the antenna's plane) were studied in [27]. In the present study, we analyze the effect of rotation of the Koch dipole's arms around its axes on base frequency and bandwidth. We investigate changes in such basic properties of the antenna as base frequency and bandwidth on angles of rotation around the axes. As a result, we present graphs and draw the relevant conclusions.

## STATEMENT OF THE PROBLEM

The first fractal antenna, whose electromagnetic and directional properties were studied most completely and extensively, was the antenna based on the pre-fractal Koch curve. When constructing a Koch line, the initial interval of length  $L_0$ , referred to as an initiator of the fractal, is split into three equal parts. The central part is replaced with an equilateral triangle having sides of length  $L_0/3$ . As a result, there appears a broken line consisting of four links; each of the links has length  $L_0/3$  [Fig. 1]. The process is carried out for each segment of the broken line.

### KEY WORDS

Koch antenna, base frequency, bandwidth, arms rotation, influence of turning.

Received: 12 Oct 2018  
Accepted: 20 Dec 2018  
Published: 3 Jan 2019

\*Corresponding Author  
Email:  
dtumakov@kpfu.ru  
Tel.: +7(965)5867997

We consider symmetric dipoles based on the Koch pre-fractal (DBKP) of the first two orders. The zeroth order DBKP coinciding with the ordinary dipole is shown in [Fig. 1(a)], the first order DBKP is shown in [Fig. 1(b)] and the second order DBKP is shown in [Fig. 1(c)]. The feed point for all the dipoles is located exactly in the middle.

We assume that initially the antenna lies in the plane ( $z=0$ ). We rotate the right arm in space relative to the starting position [Fig. 2]. Moreover, we consider three sub-problems, each of which represents rotation around a particular axis [Fig. 2(a)-(c)].

We seek base frequency and bandwidth ( $S_{11} < -10$  dB) of the obtained new dipoles by rotating an arm. It should be noted that rotation around the  $x$ -axis does not influence electromagnetic characteristics in vicinity of the base frequency. A difference shows up only at higher frequencies in vicinity of the second resonance. The same conclusion regarding comparison of the symmetric and antisymmetric dipoles was drawn in [4]. Therefore, we will hereafter explore only rotations around the  $y$ -axis and  $z$ -axis.

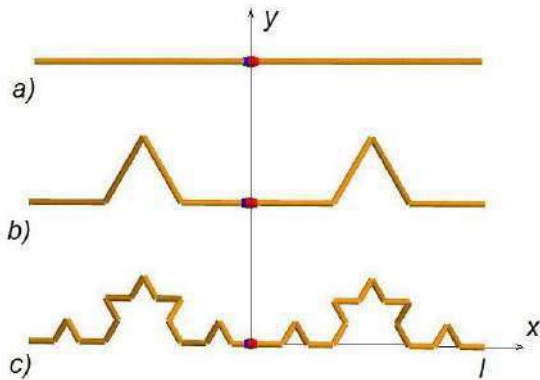


**Fig. 1:** Symmetric Koch fractal dipole. Arm length  $l=7.5$  cm, wire radius  $r=1$  mm. a) zeroth-order dipole (ordinary dipole); b) first-order dipole; c) second-order dipole.

Calculations in the present work were carried out using the FEKO software. In all cases, length of the segment partitions was selected to be five times greater than radius. It was assumed that the wire was made of copper of a circular cross-section. Main calculations were conducted for wires having radiuses equal to  $r=1.0$  mm,  $r=1.5$  mm and  $r=2.0$  mm.

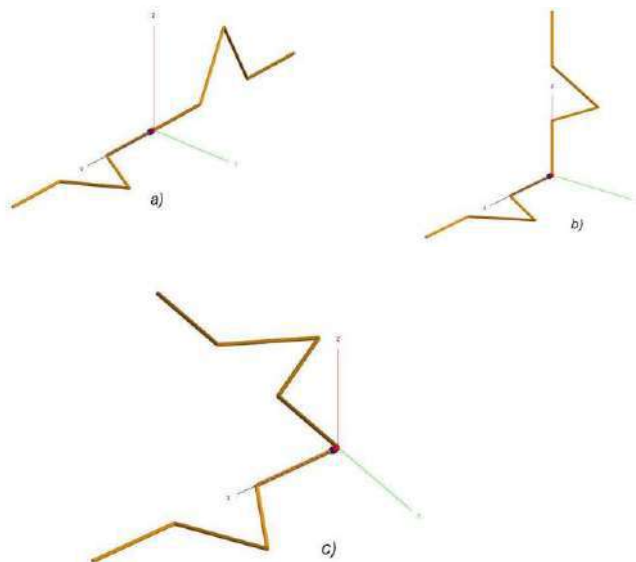


**Fig. 2:** Options for rotation of an arm around the axes: a) rotation around the  $x$ -axis (twisting); b) rotation around the  $y$ -axis; c) rotation around the  $z$ -axis.

For numerical implementation, we perform cycles with angle steps equal to 1-2 degrees. For determining the resonance angles with high accuracy, we decrease the angle step size to 0.01 degrees and frequency step size to 10 kHz.

### BASE FREQUENCY OF THE DIPOLE

One of the main advantages of the fractal antenna is the increase of its electrical length, while its linear dimensions remain unchanged. For example, length of the Koch curve  $L_m$  increases for every new  $m$ -th iteration in line with formula [28]

$$L_m = \left(\frac{4}{3}\right)^m L_0, \quad (1)$$

where  $L_0$  is length of the initial curve. This reduces base frequency  $f_m$  while maintaining the linear dimension  $l$  unchanged.

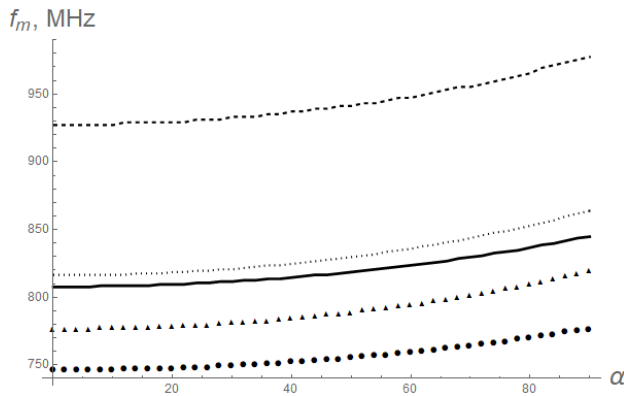


**Fig. 3:** Dependence of  $f_m$  on  $\alpha$ . The solid line corresponds to  $r=1.0$  mm and the DBKP of the 1st order; the dotted line –  $r=2.0$  mm and the DBKP of the 1st order; circles –  $r=1.0$  mm and the DBKP of the 2nd order; triangles –  $r=2.0$  mm the DBKP of the 2nd order. The dashed line – the ordinary dipole with  $r=1.0$  mm.  $l = 7.5$  cm.

Graphs presented in [Fig. 3 and 4] serve as a proof for this particular statement. Here, the dashed lines in the figures correspond to the ordinary dipole (DBKP of the zeroth order); the continuous lines corresponds to the DBKP of the 1st order, and the circles correspond to the DBKP of the second order. These three graphs are drawn for the wire of radius  $r=1$  mm. It can be seen that base frequency of the dipoles decreases with increase in electrical length of the arms. For example, for symmetric position of the arms,  $f_0$  decreases from 927 MHz corresponding to the ordinary dipole to 746 MHz corresponding to the 2nd order DBKP.

Rotation of an arm of the ordinary dipole having radius  $r=1$  mm around the  $y$ -axis in the interval of  $\alpha \in (0^\circ, 90^\circ)$  leads to a monotonic increase in base frequency  $f_0$  from 927 MHz to 977 MHz. For the 1st order DBKP, variation of base frequency occurs in the range from 808 MHz to 845 MHz, while for the 2nd order DBKP, variation occurs in the range from 746 MHz to 776 MHz. Thus, increase in the angle  $\alpha$  leads to a continuous increase in base frequencies for all types of the considered dipoles [Fig. 3]. At increasing the dipole geometry's complexity, difference between the values of  $f_m$  at  $\alpha=0^\circ$  and  $\alpha=90^\circ$  becomes smaller. For the classical dipole, the frequency  $f_m$  decreases by 50 MHz; for the 1st order DBKP, the difference decreases and makes 37 MHz; for the 2nd order DBKP, the difference drops even further and makes 30 MHz.

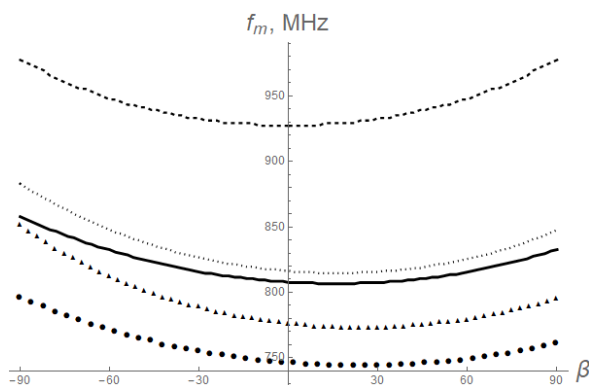


**Fig. 4:** Dependence of  $f_m$  on  $\beta$ . The solid line corresponds to  $r=1.0$  mm and the DBKP of the 1st order; the dotted line –  $r=2.0$  mm and the DBKP of the 1st order; circles –  $r=1.0$  mm and the DBKP of the 2nd order; triangles –  $r=2.0$  mm the DBKP of the 2nd order. The dashed line – the ordinary dipole with  $r=1.0$  mm.  $l = 7.5$  cm.



Radius  $r$  of the wire also affects resonance frequency. Values of  $f_m$  increase with increase of  $r$ . For the 1st order DBKP having an arm of length  $l=7.5$  cm, for a change in radius from 0.5 mm to 2.0 mm, one can obtain the following relation expressed using dimensionless variables:

$$f_1(d) \approx f_1(0.5) + 12(d - 0.5)^{0.7} = 800.5 + 12(d - 0.5)^{0.7}, \quad (2)$$

where  $r$  is expressed in mm while the resulting value of  $f_1$  is expressed in MHz. For the 2nd order DBKP, the dependence takes the form

$$f_2(d) \approx f_2(0.5) + 42(d - 0.5)^{0.8} = 721.1 + 42(d - 0.5)^{0.8}. \quad (3)$$

Comparison of the formulas (2) and (3) with each other shows that increase of  $r$  leads to a significant increase of  $f_m$  for pre-fractals of higher orders. This be confirmed by analyzing the distances between the solid line and the dotted line (for  $r=1$  mm) and the distances between circle signs and triangle signs (for  $r=2$  mm) in [Fig. 3] and [Fig. 4].

In rotating the arm around the  $z$ -axis, a change in  $f_m$  follows a slightly more different pattern. For the 1st order DBKP, rotation by a negative angle ( $\beta < 0$ ) significantly increases base frequency from 808 MHz to 858 MHz. At the same time, rotation by a positive angle, at first, slightly reduces  $f_m$  down to the minimum value  $f_m \approx 807$  MHz at  $10^\circ < \beta < 22^\circ$ . A further increase in the angle  $\beta$  leads to increase in base frequency up to the value  $f_m \approx 833$  MHz at  $\beta = 90^\circ$ .

A quite similar pattern is also observed for the 2nd order DBKP. In this case, the minimum value of base frequency is achieved at the angle values in the range  $12^\circ < \beta < 36^\circ$ ; at  $\beta = 0^\circ$ , the values decrease from 746 MHz to 744 MHz.

As a result of analysis of the base frequency values  $f_m$ , it can be concluded that rotations of the dipole arms by small angles do not exert influence on the frequency. However, in the case of large angles of the arms rotation, the values of base frequency  $f_m$  increase significantly. For a more complete understanding of the dependence of frequency on angles of rotation, you can use regression analysis on a number of other parameters [29, 30].

### DIPOLE BANDWIDTH

We assume that the frequency range near the base frequency  $f_m$ , in which  $S_{11} < -10$  dB, is, indeed, the bandwidth BW. In rotation around the  $y$ -axis by small angles ( $\alpha < 40^\circ$ ), width of the frequency range for the ordinary dipole behaves differently than for the DBKP. For the ordinary dipole, bandwidth increases with increase in the rotation angle from 86 MHz to 93.3 MHz at  $\alpha \approx 64^\circ$ , then decreases again and reaches its initial value at  $\alpha = 90^\circ$ . For the DBKP, values of BW always decrease with increase in  $\alpha$  [Fig. 5] and  $\beta$  [Fig. 6].

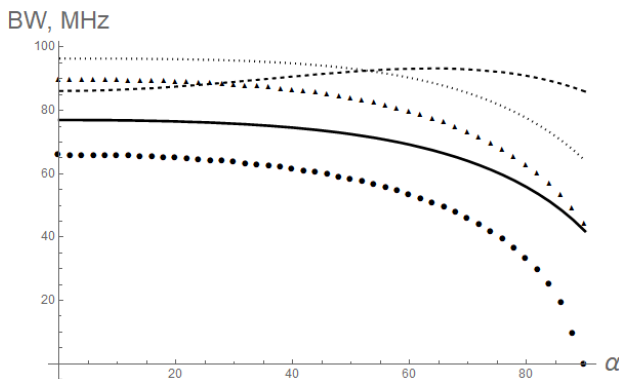


**Fig. 5:** Dependence of BW on the rotation angle  $\alpha$  of the arm around the  $y$ -axis relative to the normal dipole. The solid line corresponds to  $r=1.0$  mm and the DBKP of the 1st order; the dotted line –  $r=2.0$  mm and the DBKP of the 1st order; circles –  $r=1.0$  mm and the DBKP of the 2nd order; triangles –  $r=2.0$  mm and the DBKP of the 2nd order. The dashed line – the ordinary dipole with  $r=1.0$  mm.  $l = 7.5$  cm.

Narrowing of the frequency range is insignificant for small angles of rotation ( $\alpha < 40^\circ$ ) around the  $y$ -axis. For example, for the 1st order DBKP, the value decreases from 77 MHz to 74.5 MHz for  $r=1.0$  mm, and from 96.5 MHz to 95 MHz for  $r=2.0$  mm. For the 2nd order DBKP, dispersion of the intervals becomes slightly more discernible at  $r=1.0$  mm with the values decreasing from 66 MHz to 61.5 MHz; at  $r=2.0$  mm, the values decrease from 90 MHz to 86.5 MHz.

After passing the value  $\alpha = 40^\circ$ , the BW values decrease more significantly. For example, for the 1st order DBKP, the interval width decreases (at  $\alpha \rightarrow 90^\circ$ ) down to 42 MHz and 64 MHz for  $r=1.0$  mm and  $r=2.0$  mm, respectively. For the 2nd-order DBKP, the interval width decreases down to 0 MHz and 44 MHz for the same values of  $r$ , respectively.

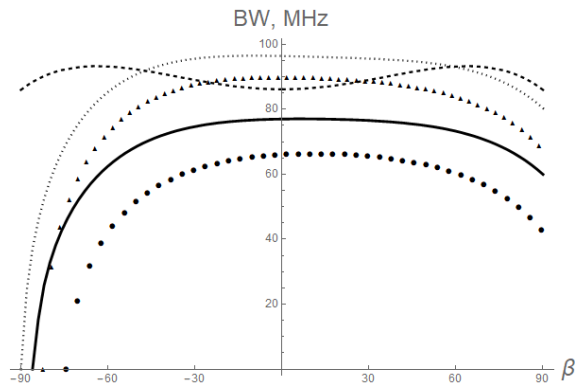


**Fig. 6:** Dependence of BW on the rotation angle  $\beta$  of the arm around the z-axis relative to the normal dipole. The solid line corresponds to  $r=1.0$  mm and the DBKP of the 1st order; the dotted line –  $r=2.0$  mm and the DBKP of the 1st order; circles –  $r=1.0$  mm and the DBKP of the 2nd order; triangles –  $r=2.0$  mm and the DBKP of the 2nd order. The dashed line – the ordinary dipole with  $r=1.0$  mm,  $l = 7.5$  cm.

In rotation around the z-axis, the bandwidth behavior remains identical to that observed in rotation around the y-axis. The BW values slightly decrease in rotation by a small angle. Decrease in BW becomes significant with a further increase in the angle  $\beta$ .

Let us consider a change for the 1st order DBKP. A dipole having radius 1 mm does not have a bandwidth at the angles  $\beta < -86^\circ$ . If  $\beta \in (-28^\circ, 50^\circ)$ , slight variations are observed in the bandwidth:  $BW \in (75 \text{ MHz}, 77 \text{ MHz})$ . For a dipole having  $r=2$  mm, the bandwidth disappears only at  $\beta = -90^\circ$ . An approximate 2 MHz-spread of the maximum bandwidth  $BW \in (94.3 \text{ MHz}, 96.4 \text{ MHz})$  occurs at nearly the same values of the angle  $\beta \in (-32^\circ, 50^\circ)$ .

For the 2nd order DBKP, the pattern is very similar. The critical angle  $\beta$ , below which "the antenna does not work", is approximately  $-74^\circ$  for a wire of radius  $r=1$  mm and  $-82^\circ$  for a wire of radius  $r=2$  mm. Small variations in bandwidth occur within the interval  $BW \in (62 \text{ MHz}, 64 \text{ MHz})$  at  $\beta \in (-18^\circ, 43^\circ)$  and within the interval  $BW \in (88 \text{ MHz}, 90 \text{ MHz})$  at  $\beta \in (-27^\circ, 45^\circ)$ .

Thus, small rotations around the y-axis within the angle range  $\alpha < 40^\circ$  slightly reduce the bandwidth. Rotations around the z-axis in the range  $-20^\circ < \beta < 40^\circ$  reduce BW by no more than 2 MHz. In large angle rotations, the bandwidth reduces significantly.

## CONCLUSION

Rotations of the arms around their own axis (the x-axis) do not exert any influence on electromagnetic characteristics in vicinity of the base. The main effects occur in rotation around the axis of the feed line (y-axis) as well as in the antenna's plane (z-axis). Rotations of the dipole arms by small angles around the y-axis and the z-axis do not affect the resonance frequency. In the case of large angle rotations of the arms, the resonance frequency values increase significantly. Small rotations around the y-axis by the angle within the range  $\alpha < 40^\circ$  reduce slightly the bandwidth. Rotations around the z-axis by the angle in the range  $-20^\circ < \beta < 40^\circ$  reduce the bandwidth by no more than 2 MHz. At larger angles of rotation, the bandwidth becomes significantly narrower. It should be noted that rotation around the z-axis can be considered as more advantageous because it is carried out in the plane of the antenna, and rotations around the z-axis can be generalized to the case of the micro strip antennas.

In most cases, the turns of the antennae leads to a slight increase in the values of the base frequency and a decrease in the bandwidth. However, turning the arms at small angles does not significantly change the frequency and bandwidth. This fact can be useful if other electrodynamic characteristics when turning will improve.

### CONFLICT OF INTEREST

There is no conflict of interest.

### ACKNOWLEDGEMENTS

The work is performed according to the Russian Government Program of Competitive Growth of Kazan Federal University.

### FINANCIAL DISCLOSURE

None

## REFERENCES

- [1] Balanis CA. [1997] Antenna theory: analysis and design, John Wiley & Sons, New Delhi.
- [2] Volakis JL. [2007] Antenna engineering handbook, McGraw-Hill.
- [3] Milligan TA. [2005] Modern Antenna Design, John Wiley & Sons.
- [4] Das AK, Gupta RK, Pal M, Ghatak R. [2015] Resonance characteristics of asymmetric fractal shaped dipole antennas, IJECT. 6(1):91-94.
- [5] Chiu CH, Lin CC, Huang CY, Lin TK. [2014] Compact dual-band dipole antenna with asymmetric arms for WLAN applications, International Journal of Antennas and Propagation. 195749(4).
- [6] Jin XH, Huang XD, Cheng CH, Zhu L. [2011] Super-wideband printed asymmetrical dipole antenna, Progress in Electromagnetics Research Letters. 27:117-123.
- [7] Su SW, Chang FS. [2009] Wideband rod-dipole antenna with a modified feed for DTV signal reception, Progress in Electromagnetics Research Letters. 12:127-132.
- [8] Lewallen RW. [1985] Baluns: What they do and how they do it, in ARRL Antenna Compendium. 1:157-164.
- [9] Votis C, Christofilakis V, Kostarakis P. [2010] Measurements of Balun and Gap Effects in a Dipole Antenna, Int J Communications, Network and System Sciences. 3:434-440.
- [10] B. Gong RLi, Zhao S, Shi L, Zhang H. [2014] A novel planar dipole antenna with distributed inductive load for size reduction, Advanced Materials Research. 846-847:452-456.
- [11] Stuart HR, Tran C. [2007] Small spherical antennas using arrays of electromagnetically coupled planar elements, IEEE Ant Wireless Prop Lett. 6:7-10.
- [12] Stuart HR, Best SR, Yaghjian AD. [2007] Limitations in relating quality factor to bandwidth in a double resonance small antenna, IEEE Ant Wireless Prop Lett. 6:460-463.
- [13] Best SR. [2005] Low electrically small linear and elliptical polarized spherical dipole antennas, IEEE Trans. Antennas Propag. 53(3):1047-1053.
- [14] Thal HL. [2006] New radiation limits for spherical wire antennas, IEEE Trans. Antennas Propag. 54(10):2757-2763.
- [15] Krzysztofik WJ. [2013] Fractal geometry in electromagnetics applications - from antenna to metamaterials, Microwave Review. 19(2):3-14.
- [16] Baliarda CP, Romeu J, Cardama A. [2000] The Koch monopole: A small fractal antenna, IEEE Transactions on Antennas and Propagation. 48(11):1773-1781.
- [17] Li D, Mao JF. [2012] A Koch-like sided bow-tie fractal dipole antenna, IEEE Transactions on Antennas and Propagation. 60(5):40-49.
- [18] Comisso M. [2009] Theoretical and numerical analysis of the resonant behaviour of the Minkowski fractal dipole antenna, Microwaves, Antennas and Propagation. 3(3):456-464.
- [19] Mahatthanajatuphat C, Saleekaw S, Akkaraekthalin P, Krairiksh M. [2009] A rhombic patch monopole antenna with modified Minkowski fractal geometry for UMTS, WLAN, and mobile WiMAX application, Progress In Electromagnetics Research. 89:57-74.
- [20] Puente-Baliarda C, Romeu J, Pous R, Cardama A. [1998] On the behavior of the Sierpinski multiband antenna, IEEE Transactions on Antennas and Propagation. 46(4):517-524.
- [21] Ghatak R, Karmakar A, Poddar DR. [2013] Hexagonal boundary Sierpinski carpet fractal shaped compact ultrawideband antenna with band rejection functionality, Int J Electron Commun. 67:250-255.
- [22] Ghatak R, Karmakar A, Poddar DR. [2011] A circularshaped Sierpinski carpet fractal UWB monopole antenna with band rejection capability, Progress In Electromagnetics Research C. 24:221-234.
- [23] Li D, Mao JF. [2013] Scircularly arced koch fractal multiband multimode monopole antenna, Progress in Electromagnetics Research. 140:653-680.
- [24] Li D, Mao JF. [2012] Sierpinskized Koch-like sided multifractal dipole antenna, Progress in Electromagnetics Research. 130:204-227.
- [25] Nasr MHA. [2013] Z-Shaped Dipole Antenna and Its fractal Iterations, International Journal of Network Security and Its Applications. 5(5):139-151.
- [26] Tumakov DN, Abgaryan GV, Chickrin DE, Kokunin PA. [2017] Modeling of the Koch-type wire dipole, Applied Mathematical Modelling. 51:341-360.
- [27] Ghatak R, Poddar DR, Mishra RK. [2009] A moment-method characterization of V-Koch fractal dipole antennas, Int J Electron Commun. 63:279-286.
- [28] Kim Y, Jaggard DL. [1986] The fractal random array in Proc of the IEEE. 74(9):1278-1280.
- [29] Abgaryan GV, Tumakov DN. [2017] Relation between base frequency of the Koch wire dipole, fractal dimensionality and lacunarity, Journal of Fundamental and Applied Sciences. 9(1S):1885-1898.
- [30] Abgaryan GV, Markina AG, Tumakov DN. [2017] Application of correlation and regression analysis to designing antennas, Revista Publicando. 4:13(2):1-13.

## ARTICLE

# KOCH FRACTAL DIPOLE MATCHING BY TURNING OF THE ARMS

Dmitrii Tumakov\*, Alexey Ovcharov, Dmitry Chickrin, Petr Kokunin

*Institute of Computational Mathematics and Information Technologies, Kazan Federal University, Kazan, RUSSIA*

## ABSTRACT

A dipole wire antenna of the Koch is considered. The antenna represents a wire dipole symmetrical with respect to the point of feeding. Arms of the dipole have the geometry of Koch prefractal. A family of antennas is singled out, in which the antennas differ from each other by an angle of arms turning. Antennas having the geometry of the first two iterations of a Koch curve are chosen for the analysis. Dipoles based on the Koch pre-fractals of the first two iterations having different wire thicknesses obtained by rotating one of the arms around a given coordinate axis is considered. Graphs depicting dependence of the reflection coefficient at the base frequency on angles of rotation around the axes are presented. Resonance angles of rotation of a "perfectly my" matched antenna's arms are obtained. A conclusion is drawn on possibility of significant improvement of antenna matching by turning the dipole arms with respect to each other.

## INTRODUCTION

A classical symmetric electric dipole containing two identical arms fed in the middle represents one of the most well explored objects in the theory of antennas [1]. There exist various methods of improvement of electrodynamic characteristics of such dipoles [2]. For example, the improvements can come from varying an angle between the arms and obtaining the so-called V-shaped antennas [3] as well as from mutual influence of radiation originating from the arms on each other. Another method of improvement of the symmetric dipole's characteristics is related to placing the arms in an antisymmetric manner. The method was applied in [4] for improving several resonance characteristics of the classical Koch and quadratic Koch fractal dipole antenna; the study also compared the obtained antennas with each other. A dual-band dipole antenna with asymmetric arms was presented in [5] for WLAN applications.

For improving the electrodynamic characteristics of dipoles, modification of the ratio of sizes (areas) of the dipole's arms is also utilized. For example, study [6] considered a dipole antenna consisting of two printed strips of unequal lengths and presented graphs for reflection coefficients and radiation patterns of the proposed antenna. A balanced-to-unbalanced transformer or balun is also often used [7]. The study [8] considered a printed dipole antenna with a micro strip balun and demonstrated an influence of sizes of the balun on return loss.

On can also make use of multiple folded arms. For example, the folded dipole of two and more elements was used as an impedance transformer to match the antenna to a line of higher characteristic impedance in [9]. In addition, multi armed related structures are also used. The studies [10, 11] considered antennas consisting of an axially symmetric array of four and six conductor arms forming a spherically shaped structure and demonstrated influence of increase in the number of arms on quality factor and bandwidth.

For reducing the sizes of the dipoles, one can alter topology of the arms, so that the electric length of the antenna increases, while radius of the sphere covering the dipole remains unchanged. For that purpose, one can roll the arms into a helix [12, 13] or perform various fractal transformations [14]. In this regard, the following antennas can be specified: an antenna which is based on the Koch curve [15, 16], Minkowski curve [17, 18], Sierpinski carpet [19, 20], a rounded fractal antenna [21, 22] and complex fractal combinations [23-26].

Characteristics of the dipole can be further improved by rotating its arms in space with respect to each other. For example, properties of the Koch dipole during rotating the arms in one plane (in the antenna's plane) were studied in [27]. In the present study, we analyze the effect of rotation of the Koch dipole's arms around its axes on the reflection coefficient at the base frequency on angles of rotation around the axes. As a result, we present graphs and draw the relevant conclusions. We draw a conclusion that that by turning the arms by a certain angle one can essentially improve the antenna matching.

## STATEMENT OF THE PROBLEM

The first fractal antenna, whose electromagnetic and directional properties were studied most completely and extensively, was the antenna based on the pre-fractal Koch curve. When constructing a Koch line, the initial interval of length  $L_0$ , referred to as an initiator of the fractal, is split into three equal parts. The central part is replaced with an equilateral triangle having sides of length  $L_0/3$ . As a result, there

### KEY WORDS

Koch antenna, matching, reflection coefficient, arms rotation, influence of turning.

Received: 17 Oct 2018  
Accepted: 14 Dec 2018  
Published: 3 Jan 2019

### \*Corresponding Author

Email:  
dtumakov@kpfu.ru  
Tel.: +7(965)5867997

appears a broken line consisting of four links; each of the links has length  $L_0/3$  [Fig. 1]. The process is carried out for each segment of the broken line.

We consider symmetric dipoles based on the Koch pre-fractal (DBKP) of the first two orders. The zeroth order DBKP coinciding with the ordinary dipole is shown in [Fig. 1(a)], the first order DBKP is shown in [Fig. 1(b)] and the second order DBKP is shown in [Fig. 1(c)]. The feed point for all the dipoles is located exactly in the middle.

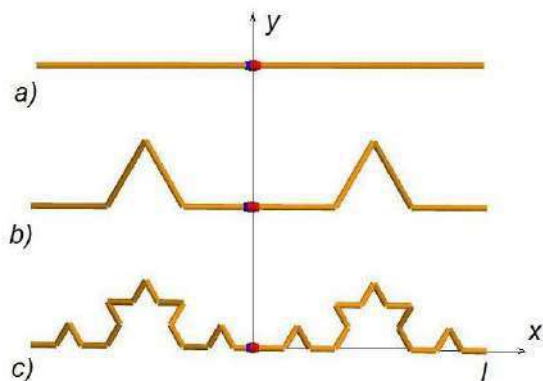


**Fig. 1:** Symmetric Koch fractal dipole. Arm length  $l=7.5$  cm, wire radius  $r=1$  mm. a) zeroth-order dipole (ordinary dipole); b) first-order dipole; c) second-order dipole.

We assume that initially the antenna lies in the plane  $\{z=0\}$ . We rotate the right arm in space relative to the starting position [Fig. 2]. Moreover, we consider three sub-problems, each of which represents rotation around a particular axis [Fig. 2(a)-(c)].

We seek the reflection coefficient of the obtained new dipoles by rotating an arm. It should be noted that rotation around the x-axis does not influence electromagnetic characteristics in vicinity of the main resonance. A difference shows up only at higher frequencies in vicinity of the second resonance. The same conclusion regarding comparison of the symmetric and antisymmetric dipoles was drawn in [4]. Therefore, we will hereafter explore only rotations around the y-axis and z-axis.

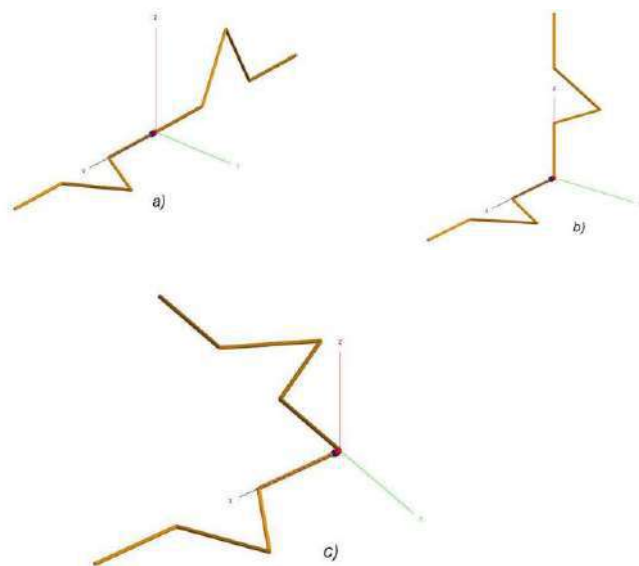


**Fig. 2:** Options for rotation of an arm around the axes: a) rotation around the x-axis (twisting); b) rotation around the y-axis; c) rotation around the z-axis.

Calculations in the present work were carried out using the FEKO software. In all cases, length of the segment partitions was selected to be five times greater than radius. It was assumed that the wire was made of copper of a circular cross-section. Main calculations were conducted for wires having radiuses  $r$  equal to  $r=1.0$  mm,  $r=1.5$  mm and  $r=2.0$  mm.



For numerical implementation, we perform cycles with angle steps equal to 1-2 degrees. For determining the resonance angles with high accuracy, we decrease the angle step size to 0.01 degrees and frequency step size to 10 kHz. It should be noted that such a high accuracy theoretically allows determining the optimum rotation angle guaranteeing a perfect match. However, for all practical purposes, large steps are of more interest due to the fact that it is not so easy technically to perform rotations with accuracy of one hundredths of a degree.

### REFLECTION COEFFICIENT

Let us consider a dependence of values of the first (main) minimum of the reflection coefficient  $S_{11}$  on location of the arms. When changing the radius  $r$  from 1.0 mm to 1.5 mm for the ordinary dipole, the minimum is reached at the value of angle  $\alpha$  equal to approximately  $78^\circ$ . The angle  $\alpha$ , corresponding to the minimum of the reflection coefficient  $S_{11}$ , slightly increases with increase in  $r$  and reaches the value  $\alpha \approx 80^\circ$  at  $r=2.0$  mm. The value of  $S_{11}$  itself remains at the value close to -45 dB.

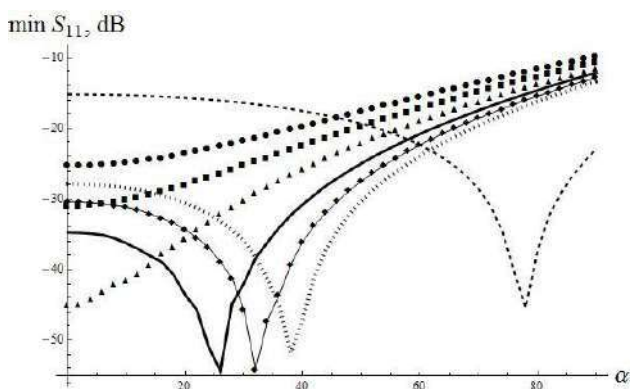


**Fig. 3:** Dependence of minimum of  $S_{11}$  on  $\alpha$ . The arm's length  $l$  is 7.5 cm. The solid line corresponds to radius of the wire  $r=1.0$  mm and the DBKP of the first order; diamond signs correspond to  $r=1.5$  mm and the DBKP of the first order; dotted line corresponds to  $r=2.0$  mm and the DBKP of the first order; circle signs correspond to  $r=1.0$  mm and the DBKP of the second order; square signs correspond to  $r=1.5$  mm and the DBKP of the second order; triangle signs correspond to  $r=2.0$  mm and the DBKP of the second order. The dashed line corresponds to the ordinary dipole having radius  $r=1.0$  mm,  $l=7.5$  cm.

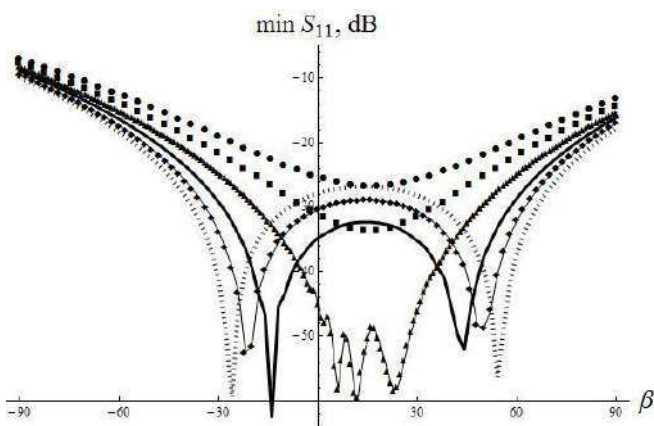


**Fig. 4:** Dependence of minimum of  $S_{11}$  on  $\beta$ . The solid line corresponds to radius of the wire  $r=1.0$  mm and the DBKP of the first order; diamond signs correspond to  $r=1.5$  mm and the DBKP of the first order; dotted line corresponds to  $r=2.0$  mm and the DBKP of the first order; circle signs correspond to  $r=1.0$  mm and the DBKP of the second order; square signs correspond to  $r=1.5$  mm and the DBKP of the second order; triangle signs correspond to  $r=2.0$  mm and the DBKP of the second order. The dashed line corresponds to the ordinary dipole having radius  $r=1.0$  mm,  $l=7.5$  cm.

A similar pattern is also observed for the first order DBKP when rotating around the y-axis. For smaller values of  $r$ , extreme values of  $S_{11}$  are achieved at smaller values of the angle  $\alpha$ . The values of  $\alpha$

continuously increase from 26° to 38° when changing r from 1.0 mm to 2.0 mm. The minimum values remain at the level S<sub>11</sub>~55 dB.

**Table 1:** Extreme values of S<sub>11</sub> when rotating around the y-axis

Radius $r$ , mm	Angle $\alpha$	Minimum $S_{11}$ , dB
1.0	25.07°	-100
1.5	32.73°	-96.5
2.0	38.14°	-95.5

At larger values of the angle  $\alpha$ , the difference between antennas, having different radiuses, practically disappears. The reflection coefficient of the first-order DBKP for  $\alpha \rightarrow 90^\circ$  fluctuates around the value -13 dB.

For the second order DBKP [Fig. 3, 4], the reflection coefficients take on larger values at smaller radiuses. This means that the dipoles of the second order are better matched for large values of r. As the angle  $\alpha$  increases [Fig. 3], the minimum value of S<sub>11</sub> monotonically increases for the second order DBKP. The exact values obtained for a finer grid (angle step size is 0.01° and frequency step size is 20 kHz) are presented in [Table 1]. Note that for an ordinary dipole, the exact value of the minimum of the reflection coefficient S<sub>11</sub>~90 dB having radius of the wire 1 mm is achieved at the rotation angle of 77.68°.

**Table 2:** Extreme values of S<sub>11</sub> when rotating around the z-axis

Radius $r$ , mm	Angle $\beta$	Minimum $S_{11}$ , dB
1.0	-14.34°	-120
1.0	+43.31°	-99
1.5	-21.30°	-99
1.5	+49.72°	-97.5
2.0	-26.46°	-98
2.0	+54.38°	-97

Regarding the rotation around the z-axis, we can state only the following. First, we can draw the coordinate axis min S<sub>11</sub> not for the value  $\beta=0^\circ$ , but, instead, for the value  $\beta=20^\circ$ . Note that in this case, speculations concerning the rotations by angles greater than 20° and by angles less than 20° remain the same as speculations for the case of rotation around the y-axis.

Note that for the second order DBKP having the wire radius of 2 mm, the minimum of S<sub>11</sub> in the range  $0^\circ < \beta < 30^\circ$  follows a complicated oscillatory pattern (triangles in [Fig. 4]). However, on the outside of the range, the curve of min S<sub>11</sub> for a given antenna demonstrates behavior, which is similar to rotation around the y-axis.

Extreme values of S<sub>11</sub> during rotation around the z-axis, determined with high accuracy, are presented in [Table 2].

### BEST ANTENNAS

Let us consider radiation characteristics of the optimal dipoles. We present graphs depicting the reflection coefficients values for optimal antennas having the wire of radius r=1 mm. In line with [Tables 1 and 2], they correspond to antennas obtained at the rotation angles  $\beta=-14.34^\circ$ ,  $\beta=43.31^\circ$  and  $\alpha=25.07^\circ$ . It can be seen that behavior of the reflection coefficient at the first resonance frequency (around 810 MHz)

is practically identical for the three proposed antennas. Differences in graphs of S<sub>11</sub> show up at the second frequency around 2.4 GHz.

Analysis of electrodynamic characteristics, conducted at turning the antenna around various axes, allows stating the following. Turning the antenna around the x-axis does not alter electromagnetic characteristics of the first resonance frequency; influence of the turns becomes discernible only at higher frequencies (see, for example, [4]). Optimum angles of turning the antenna in the antenna's plane (around the z-axis) and optimum angles of turning the antenna around the y-axis produce almost identical very well matched antennas. Based on this observation, we can recommend turning the arms in the antenna's plane (around the z-axis) for the purpose of improving characteristics of the antenna. In this case, sizes of the antenna do not change, and matching of the dipole can be significantly improved.

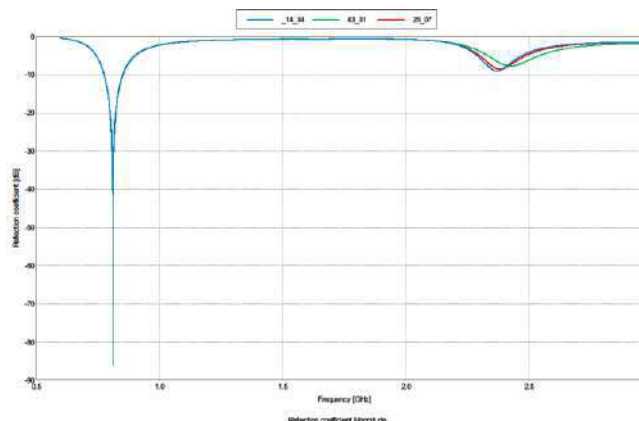


**Fig. 5:** Graphs of S<sub>11</sub> for optimal antennas (l=7.5 cm; r=1.0 mm). The case of the DBKP of the first order. The solid line corresponds to  $\beta = -14.34^\circ$ , the dashed line corresponds to  $\beta = 43.31^\circ$  and the dotted line corresponds to  $\alpha = 25.07^\circ$ .

In addition, it should be noted that for some applications, it is required that the antenna must be stretched. From this viewpoint, a change in its geometry by means of turning in the plane of the antenna is undesirable. However, from the classical point of view, the surface area, occupied by the antenna, is expressed in terms of radius of a circle covering the antenna itself. In this case, turning the arms in the antenna's plane does not affect the area of the dipole.

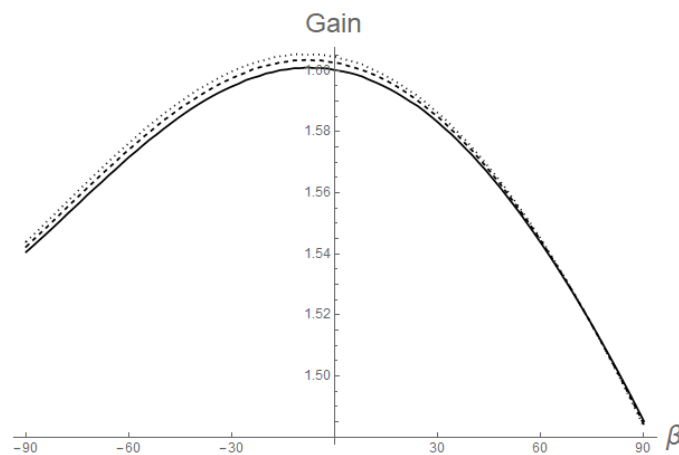


**Fig. 6:** Dependence of the gain on the rotation angle  $\beta$  for the DBKP of the first order. The solid line corresponds to  $r = 1.0$  mm; the dashed line corresponds to  $r = 1.5$  mm; the dotted line corresponds to  $r = 2.0$  mm.  $l = 7.5$  cm.

Dependence of the gain on the rotation angle  $\beta$  for the DBKP of the first order. The solid line corresponds to  $r = 1.0$  mm; the dashed line corresponds to  $r = 1.5$  mm; the dotted line corresponds to  $r = 2.0$  mm.  $l = 7.5$  cm. From the physical point of view, the effect of improving the antenna matching is explained by mutual influence on each other of separate component segments of the antenna (more precisely, influence on each other of electromagnetic fields emitted by the segments). At certain angles, the influence turns out

to be optimal. A more widespread variant consists in changing geometry of the arms. In both cases, the physical effect turns out to be the same.

Let us present dependence of the gain on the main resonance frequencies for dipoles with the arms representing the Koch pre-fractal of the first order [Fig. 6], and for dipoles with the arms representing the Koch pre-fractal of the second order [Fig. 7]. The values of the gain change in the range from 1.48 to 1.6, reaching the maximum values for the dipole having arms, which remain in the initial position.

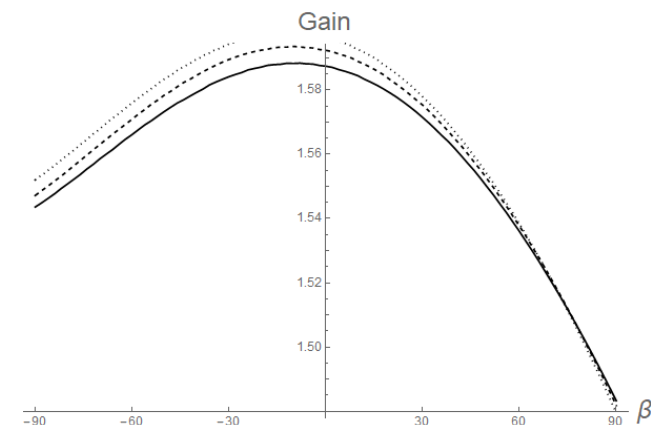


**Fig. 7:** Dependence of the gain on the rotation angle  $\beta$  for the DBKP of the second order. The solid line corresponds to  $r=1.0$  mm; the dashed line corresponds to  $r=1.5$  mm; the dotted line corresponds to  $r=2.0$  mm.  $l=7.5$  cm.

Note that dipoles of large diameters possess large values of the gains. The difference for the Koch pre-fractal of the second order is found to be stronger than that for the Koch pre-fractal of the second order.

One can expect that for dipoles having a more complex geometry, despite a more complicated behavior of influence of the dipole's elements on each other, there also exist "optimum" turnings of the arms. At the same time, the graphs depicting dependence of reflection coefficients on angles of rotations must become much more complicated in case of complications of geometry of the arms.

## SUMMARY

Rotations of the arms around their own axis (the x-axis) do not exert any influence on electromagnetic characteristics in vicinity of the main resonance. The main effects occur in rotation around the axis of the feed line (y-axis) as well as in the antenna's plane (z-axis). In the case of the optimal rotation around the y-axis and the z-axis, "perfect" antenna matching can be achieved.

## CONCLUSION

The antenna matching can be significantly improved by small angle rotations of the dipole arms. It should be noted that rotation around the z-axis can be considered as more advantageous because it is carried out in the plane of the antenna, and rotations around the z-axis can be generalized to the case of the micro strip antennas.

### CONFLICT OF INTEREST

There is no conflict of interest.

### ACKNOWLEDGEMENTS

The work is performed according to the Russian Government Program of Competitive Growth of Kazan Federal University.

### FINANCIAL DISCLOSURE

None

## REFERENCES

- [1] Balanis CA. [1997] Antenna theory: analysis and design, John Wiley & Sons, New Delhi.
- [2] Volakis JL. [2007] Antenna engineering handbook, McGraw-Hill.
- [3] Milligan TA. [2005] Modern Antenna Design, John Wiley & Sons.

- [4] Das AK, Gupta RK, Pal M, Ghatak R. [2015] Resonance characteristics of asymmetric fractal shaped dipole antennas", *IJEET*. 6(1):91-94.
- [5] Chiu CH, Lin CC, Huang CY, Lin TK. [2014] Compact dual-band dipole antenna with asymmetric arms for WLAN applications, *International Journal of Antennas and Propagation*, Article ID 195749(4).
- [6] Jin XH, Huang XD, Cheng CH, Zhu L. [2011] Super-wideband printed asymmetrical dipole antenna, *Progress in Electromagnetics Research Letters*. 27:117-123.
- [7] Lewallen RW. [1985] Baluns: What they do and how they do it, in *ARRL Antenna Compendium*. 1:157-164.
- [8] Votis C, Christofilakis V, Kostarakis P. [2010] Measurements of Balun and Gap Effects in a Dipole Antenna, *Int J Communications, Network and System Sciences*.3:434-440.
- [9] Guertler R. [1950] Impedance transformation in folded dipoles, *Proc IRE*. 38(9):1042-1047.
- [10] Stuart HR, Tran C. [2007] Small spherical antennas using arrays of electromagnetically coupled planar elements, *IEEE Ant Wireless Prop Lett*. 6:7-10.
- [11] Stuart HR, Best SR, Yaghjian AD. [2007] Limitations in relating quality factor to bandwidth in a double resonance small antenna, *IEEE Ant Wireless Prop Lett*. 6:460-463.
- [12] Best SR. [2005] Low electrically small linear and elliptical polarized spherical dipole antennas, *IEEE Trans. Antennas Propag*. 53(3):1047-1053.
- [13] Thal HL. [2006] New radiation limits for spherical wire antennas, *IEEE Trans. Antennas Propag*. 54(10):2757-2763.
- [14] Krzysztofik WJ. [2013] Fractal geometry in electromagnetics applications from antenna to metamaterials, *Microwave Review*. 19(2):3-14.
- [15] Baliarda CP, Romeu J, Cardama A. [2000] The Koch monopole: A small fractal antenna, *IEEE Transactions on Antennas and Propagation*. 48(11):1773-1781.
- [16] Li D, Mao JF. [2012] A Koch-like sided bow-tie fractal dipole antenna, *IEEE Transactions on Antennas and Propagation*. 60(5):40-49.
- [17] Comisso M. [2009] Theoretical and numerical analysis of the resonant behaviour of the Minkowski fractal dipole antenna, *Microwaves, Antennas and Propagation*. 3(3):456-464.
- [18] Mahatthanajatuphat C, Saleekaw S, Akkaraekthalin P, Krairiksh M. [2009] A rhombic patch monopole antenna with modified Minkowski fractal geometry for UMTS, WLAN, and mobile WiMAX application, *Progress In Electromagnetics Research*. 89:57-74.
- [19] Puente-Baliarda C, Romeu J, Pous R, Cardama A. [1998] On the behavior of the Sierpinski multiband antenna, *IEEE Transactions on Antennas and Propagation*. 46(4):517-524.
- [20] Ghatak R, Karmakar A, Poddar DR. [2013] Hexagonal boundary Sierpinski carpet fractal shaped compact ultrawideband antenna with band rejection functionality, *Int J Electron Commun*. 67:250-255.
- [21] Ghatak R, Karmakar A, Poddar DR. [2011] A circular shaped Sierpinski carpet fractal UWB monopole antenna with band rejection capability, *Progress In Electromagnetics Research C*. 24:221-234.
- [22] Li D, Mao JF. [2013] Scircularly arced koch fractal multiband multimode monopole antenna, *Progress in Electromagnetics Research*. 140:653-680.
- [23] Li D, Mao JF. [2012] Sierpinskized Koch-like sided multifractal dipole antenna, *Progress in Electromagnetics Research*. 130:204-227.
- [24] Nasr MHA. [2013] Z-Shaped Dipole Antenna and Its fractal Iterations, *International Journal of Network Security and Its Applications*. 5(5):139-151.
- [25] Abgaryan GV, Markina AG, Tumakov DN. [2017] Application of correlation and regression analysis to designing antennas, *Revista Publicando*. 4(13) (2): Pr1-Pr13.
- [26] Tumakov DN, Abgaryan GV, Chickrin DE, Kokunin PA. [2017] Modeling of the Koch-type wire dipole, *Applied Mathematical Modelling*. 51:341-360.
- [27] Ghatak R, Poddar DR, Mishra RK. [2009] A moment-method characterization of V-Koch fractal dipole antennas, *Int J Electron Commun*. 63:279-286.



## ARTICLE

# PRODUCTION OF MOTOR OILS ON A MINERAL AND SEMI-SYNTHETIC BASIS

Aliyorbek Alisher O'g'li Umaraliev\*

*Institute of Geology and Petroleum Technologies, Kazan Federal University, Kazan, RUSSIA*

## ABSTRACT

*In this work, the production of oils on a mineral and semi-synthetic basis is considered and studied in detail. Objective of the work is to study and analyze the production of motor oils. In the process of our work, we conducted research of the production of motor oils. We performed an analytical review of the data, where we have considered the basic and technical requirements for petroleum oils, the classification of products and symbols of commercial oils. In the course of studies, we have also reviewed and carried out technological calculations of a dewaxing plant. We considered the process of cleaning crude oils, the classification of petroleum oils and the main indicators of their quality, cleaning methods, and continuous-flow types of motor oils production. Oil additives, their purpose, classification and mechanism of action were also studied. We studied the working conditions of motor oils and the process of preparing commercial oils.*

## INTRODUCTION

**KEY WORDS**  
motor oils, synthetic oils,  
semisynthetic oils,  
mineral oils, analysis, raw  
materials, depareft,  
supplements.

Motor oil is a substance that is used to service parts of various kinds of mechanisms. Motor oil is one of the important elements of engine design. It is divided into synthetic, semi-synthetic, mineral and hydrocracking oils. Many people believe that synthetic products work better than mineral products, but not everyone has an idea of what synthetic and mineral motor oils are and what they are intended for.

Mineral motor oils are simply refined oil, but synthetic oil was created in laboratory conditions. Mineral oils are productive in use and have the least destructiveness to details. In many cases, they are not applied in pure form and therefore about 10% of various additives are added to them. And due to additives, mineral motor oil becomes anti-corrosion, more corrosion preventive and have higher detergent properties. The main disadvantage is the accelerated wearing and also due to additives mineral oil cannot maintain a stable mixture homogeneity for a long time. Mineral oils are divided into several types, such as: aromatic, paraffinic and naphthenic. The increased viscosity of such oils minimizes the formation of oil leaks in parts with increased wear.

Synthetic oils are designed to provide our engine with a higher level of protection against wear and temperature rise. In addition, when we use synthetics, the resistance level is lower and because of this, our engine shows higher power and fuel economy. The main disadvantage of synthetic oil is its high cost. Synthetic oil differs from mineral oil, first of all, at the molecular level. It is not necessary to add a large amount of additives to a synthetic oil, as to a mineral one; the necessary substances are already synthesized in its composition when it is created.

Semi-synthetic oils are a mixture of petroleum products with synthetic ones. The composition of semi-synthetics allowed for to combine the best characteristics of mineral and synthetic oils, as a result, we get a product with excellent performance characteristics and low cost. The most important characteristics of semi-synthetics are: low evaporation, high viscosity index, etc.

## METHODS

Petroleum oils are a complex hydrocarbon mixture (the number of carbon atoms is 20-60; molecular weight is 300-750, boiling point is 300-650°C). Raw materials for the production of motor oils are fuel oil, and the main process of processing is vacuum distillation, as a result of which narrow (close cut) oil fractions (from 1 to 4) and tar are obtained [1].

Resinous asphaltene, polycyclic aromatic and high molecular weight paraffinic hydrocarbons are undesirable components that impair the physicochemical and operational properties of commercial oils, therefore the production technology of the base oils is based on selective removal of undesirable hydrocarbons from the oil fractions while preserving the components that provide the required physical-chemical and operational properties of resulting commercial oils. Some components are usually considered harmful and can be very valuable in some areas:

- Resins, fatty and naphthenic acids increase the stickiness and durability of the adsorption film of the oil (improve lubricity);
- Some sulfur and nitrogen compounds exhibit antioxidant properties; therefore, during deep cleaning of the oil, some of its lubricating, antioxidant and anticorrosion properties may deteriorate [1].

Received: 22 Oct 2018  
Accepted: 19 Dec 2018  
Published: 3 Jan 2019

\*Corresponding Author  
Email:  
Aliyorbek.Umaraliev@gmail.com  
Tel.: +79274353171

Cleaning removes:

- sulfur compounds and organic acids;
- resinous and asphaltene compounds;
- unsaturated hydrocarbons;
- solid hydrocarbon compounds dissolved in oil;
- polycyclic compounds.

Viscosity index characterizes the change in viscosity of lubricating oils depending on temperature. A relatively small change in viscosity occurs with temperature for oils with a high viscosity index; oils with low viscosity index feature a significant change in viscosity.

A simple treatment with sulfuric acid, lime and bleaching clay turns distillates into products with acceptable quality and a low viscosity index. For the production of products with high and medium viscosity index, it is necessary to use certain types of extraction with solvents separating colored, unstable and having low viscosity index components. At the final stage, the oil is dewaxed (that is, paraffins are removed from it) to obtain a product with a pour point of from minus 10° C to minus 20° C. This process is carried out by dissolving the oil in methyl ethyl ketone (MEK) followed by cooling and filtration [1].

At most plants, three or four fractions are obtained by mixing of which the whole range of marketable oils is produced.

### Synthetic base products

Synthesis processes make it possible to create molecules of relatively simple compounds with the desired properties. The main classes of synthetic materials used as components of oils [1] are listed in [Table 1].

With the exception of poly glycolic fluids, all synthetic base oils have a viscosity within the limits typical of the lightest high-index distillate mineral oils. However, their viscosity index and flash point are higher, and their pour point is significantly lower [1].

**Table 1:** Main classes of synthetic materials

Type	Main application
Alkylated aromatics	Automobile and industrial oils
Oligomers of drying agents	Automobile and industrial oils
Dibasic acid esters	Aviation and automobile oils
Polyol esters	Aviation and automobile oils
Polyalkylene glycol	Industrial oils
Phosphoric acid esters	Industrial oils

The main disadvantage of synthetic oils is that by their very nature they are more expensive than mineral ones. This limits their use in the field of special oils and lubricants. Ester-type fluids have another one drawback: they cause more swelling degree for sealing materials than hydrocarbons, so they should be used with care in applications where they can come into contact with elastomers designed for working with mineral oils.

### Methods for cleaning oil fractions are the following

1. Chemical methods with the use of reagents (acid, alkali, hydrogen) that chemically interact with the components to be removed (alkalization, sulphate or hydrogenation process)
2. Physical methods with separation of the oil fraction into 2 parts without changing the chemical structure of hydrocarbons:
  - a) Extraction processes - deasphalting, selective cleaning;
  - b) The process of extractive crystallization (a kind of extraction process) - dewaxing;
  - c) Adsorption cleaning with the use of adsorbents [2].

### Types of additives applied to motor oils

Antioxidant additives which protect oil hydrocarbons from oxidation [3].

Antifricition, antiwear and extreme pressure additives - contribute to reducing friction, wear and tearing of the rubbing surfaces of metals [4].

Corrosion inhibitors and anti-corrosion additives protect metal parts of machines and mechanisms (during their storage and operation) from environmental exposure (oxygen, moisture, chemically active products) [4].

Detergents (or detergent and dispersant additives) prevent deposits, varnishes and sediments from forming on engine parts [5, 6].  
 Depressor additives lower the pour point of the oils [4].  
 Viscous additives improve viscosity and temperature properties.  
 Antiseptics increase the resistance of oils to fungi and bacteria [4].  
 Anti-foam additives prevent the formation of oil foams.  
 Adhesive additives increase adhesion and prevent the spreading of oils [4].  
 Multifunctional and multicomponent additives simultaneously improve several performance properties of oils [4].

## RESULTS AND DISCUSSION

Let's consider the process of extractive crystallization

There are two dewaxing processes:

1. Conventional dewaxing with obtaining oils having a freezing point of -10 to -15 o C,
  2. Deep dewaxing is obtaining oils with a freezing point of -30 o C and below.
- Dewaxing is a low temperature process.

Cooling agents are propane or ammonia. The first stage of crystallization is the isolation from a supersaturated solution of nuclei of crystals which are the smallest particles of a crystallizing substance [6].

The optimum composition of the solvent is determined in a practical way; solvent composition, % (mass.) - MEK (60-75), toluene (25-40). The higher the viscosity of the raw material and the content of paraffin in it, the greater the dilution ratio; the ratio of solvent to solvent: raw materials for distillate raw materials – 2.8: 1 to 4: 1; for residual raw materials - from 4: 1 to 4.5: 1).

The final cooling temperature must be below the set pour point of deparaffinate by the value of TED (5-10 o C) [temperature effect of dewaxing] [6].

In this paper, calculations were made of the installation of oil dewaxing.

Regeneration department: Calculation of a regenerative crystallizer.

Baseline data for the calculation:

- Fresh feed rate:  $G_c = 250$  thousand tons / year = 684.93 t / day = 28538.75 kg / h;
- Since the scheme has four parallel streams identical with each other, the performance of one stream is  $G_1 = 7,233.75$  kg / h.
- The ratio of solvent to the raw material is 5: 1;
- The solvent is fed in portions; each portion is served in a 1: 1 ratio
- Temperature of raw materials supply to regenerative crystallizers  $T = 303$  K.

The solvent is a mixture of methyl ethyl ketone and toluene in a ratio of 60:40 wt.

We determine the physical and chemical indicators of raw materials and filtrate of the first stage in charts 1, 2, 3.

In this section, technological calculations of the heat exchange surface of the regenerative crystallizer were carried out.

We calculated the speed of raw materials and filtrate movement in the mold. We determined the parameters of the 1st stage filter where the data on the composition and heat capacity of the filtrate, and the absolute density of the raw materials were entered, and from these values the average heat capacity and density of the raw materials supplied from the raw material reservoirs were found.

The heat capacity of the oil fraction is determined by the formula:

$$C = \frac{1}{\sqrt{\rho_{15}^{15}}} \times (0.762 + 0.0034 \times T) \quad , \text{ kJ / kg K} \quad (1)$$

Where  $\rho_{15}^{15}$  is the density of the oil fraction at a temperature of 15 ° C; T - K process operating temperature;

The oil fraction density at a temperature of 15 ° C is determined by the formula:

$$\rho_{15}^{15} = \rho_{4}^{20} + 5a \quad (2)$$

where,  $\rho_{4}^{20}$  is the density of the oil fraction at a temperature of 20 ° C;

a - the coefficient which is determined by the table.

The speed of movement is found by the formula:

$$W = \frac{Gc}{3600 \cdot \rho c \cdot S_{\text{c}} \cdot \Delta T} \quad (3)$$

where, Gc- raw material consumption kg / m<sup>3</sup>; ρc is the density, kg / m<sup>3</sup> ; S<sub>c</sub> - cross-sectional area, m<sup>2</sup> ; Next, based on the criteria of Reynolds, Prandtl and Nusselt, we calculated the speed of movement of raw materials and filtrate in the mold.

Reynolds criterion:

$$Re = \frac{D \cdot W}{\nu} \quad (4)$$

where D is the internal diameter of the pipe, m; W- flow velocity, m / s; ν - kinematic viscosity m<sup>2</sup> / s

Prandtl criterion:

$$Pr = \frac{C_c \cdot \mu}{\lambda} \quad (5)$$

where C<sub>c</sub> is the heat capacity, kJ / kg K; μ - dynamic viscosity, Pa • s; λ - coefficient of thermal conductivity, W / m K

Nusselt criterion:

$$Nu = 0.21 \cdot Re^{0.8} \cdot Pr^{0.43} \cdot \left( \frac{Pr_{ct}}{Pr} \right)^{0.25} \quad (6)$$

where Re is the Reynolds criterion; Pr - Prandtl criterion; Pr<sub>ct</sub> - determined at the temperature of the pipe wall.

Similarly, the heat transfer coefficient from the wall to the filtrate solution was calculated in the same way. According to the data obtained, we selected a standard mold with a heat exchange surface of 70 m<sup>2</sup>, while the surface margin was 44%.

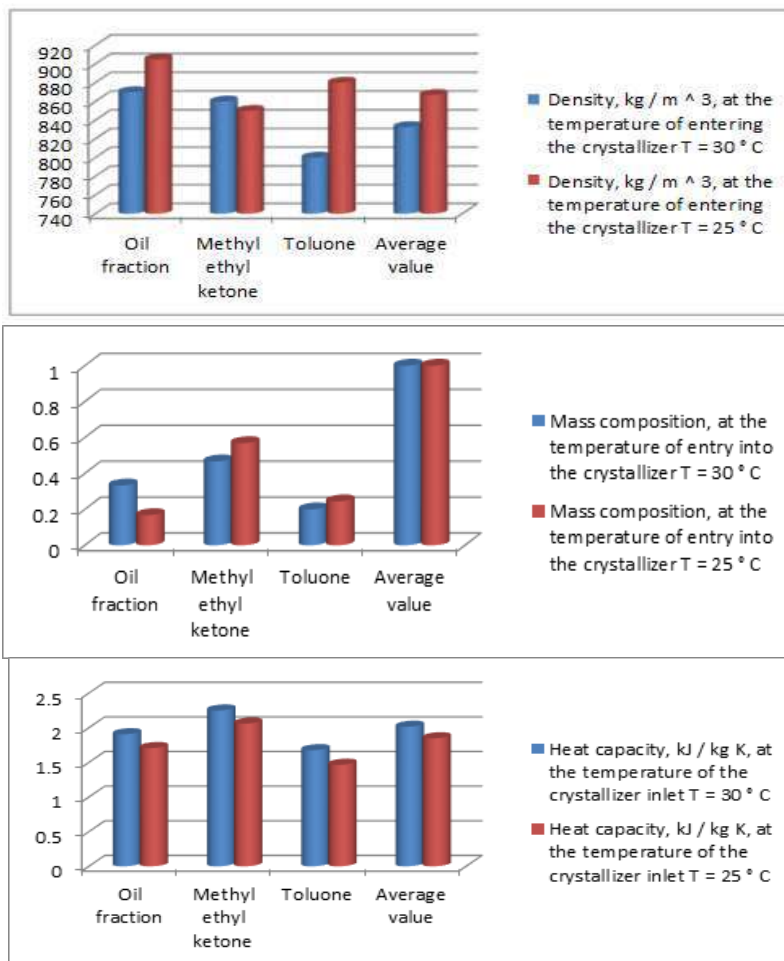


Fig. 1, 2, 3: Physical and chemical parameters of the first stage.

### Calculation of the ammonia crystallizer

Before entering the cooled suspension into the ammonia crystallizer, the third portion of the cooled solvent (second stage filtrate) is added to the raw material and then cooled. The heat capacity and density of the oil fraction were determined. We found the amount of ammonia required for cooling the suspension from the heat balance equation.

We calculated the coefficient for heat transfer from the wall to the filter solution according to the cross-sectional area, the amount of ammonia vapors formed, and the linear velocity of ammonia vapors according to Reynolds, Prandtl and Nusselt criteria. Then we determined the heat transfer coefficient.

Next, we calculated the heat exchange surface and selected a standard mold with a heat exchange surface of 70 m<sup>2</sup>, while the surface margin was 41%. [7,8]

### CONCLUSION

Varieties of dewaxing processes that can be introduced into production:

1. Dewaxing with propane (propane is used as a solvent, a cooling agent and an inert gas), the ratio to the raw material is 0.8: 1 up to 2: 1 (because of its high dissolving capacity), and its disadvantage is deep cooling [7].
2. The Edeleanu process (solvent: a mixture of dichloroethane 40-70% [precipitates solid HC] and methylene chloride 60-30% [dissolves non-crystallizing components]); high filtration rate (200kg / h); solvents are non-combustible, therefore they do not require an inert gas in the system, low temperature TED (0-1 o C); the disadvantage is the low thermal stability of solvents (they decompose at 130-140 o C with the formation of corrosive products).
3. The Dilchil process. Solvent: mixture of MEK with methyl isobutyl ketone or toluene using Dilchil crystallizers of the original design (direct injection of cooled solvent and flow of dewaxed raw material heated in a steam heater) [7].
4. Hydrocatalytic dewaxing: a decrease in the freezing temperature of diesel fuels and lubricating oils through selective hydrocracking and hydroisomerization of n-paraffins on selective catalysts.
5. Urea dewaxing: the process intended for obtaining low-hardening fuels, low-viscosity oils and liquid paraffins is carried out at positive temperatures. It is based on the ability of urea to produce crystalline complexes with n-structure paraffins (the number of atoms is less than 6). Pure carbamide has a tetragonal structure; in the process of complex formation, the crystal structure is rearranged to a hexagonal structure consisting of six carbamide molecules arranged in a spiral. Inside the spiral, a channel is formed with a diameter of 5.25 Å. The cross section of the molecules of n- alkanes is about 4.2 Å, which allows them to fit into the channel and to be held by the van der Waals forces.
6. The process of microbiological dewaxing: it is based on the ability of certain types of microbes to selectively oxidize n-structure paraffins as a source of energy for their vital activity. Deparaffinate is used as a component of winter diesel fuel, and biomass is used to produce feed protein. [9]

In this paper, we conducted a study of methods for the production of motor oils. We studied the requirements, classifications and system designations of motor oils. We performed an analytical review of the data, where we have reviewed the basic and technical requirements for petroleum oils, the classification of products and symbols of commercial oils. [9]

The following issues were considered: the process of refining oil feedstock, the classification of petroleum oils and the main indicators of their quality, methods of refining, and flow-through schemes for the production of oils. Also we studied additives to oils, their purpose, classification and mechanism of action, the operating conditions of motor oils and the process of preparing commercial oils.

#### CONFLICT OF INTEREST

There is no conflict of interest.

#### ACKNOWLEDGEMENTS

The work is performed according to the Russian Government Program of Competitive Growth of Kazan Federal University.

#### FINANCIAL DISCLOSURE

None

### REFERENCES

- |  |  |
|--|--|
| [1] Reznikov VD. [1985] A brief guide to the properties of lubricants and fuels, VD Reznikov. 168. | [3] Shkolnikov VM. [1989] Fuels, lubricants, and technical liquids, VM Shkolnikov. M.: Chemistry.                  |
| [2] Dyachkova SG. [2011] Technology of production of petroleum oils, SG Dyachkova. - Irkutsk: 63.  | [4] Almagambetova MZh. [2017] Technology of production of lubricants, Mzh Almagambetova. Uralsk: Study Guide. 117. |



- [5] Glavati OL. [1989] Physical chemistry of dispersing additives to oils. OL Glavati. Kiev: Naukova Dumka. 184.
- [6] Sytz WE, Laurent JW. [1975] In: Reports of the JSLE-ASLE International Lubrication Conference, 9-11 June, Tokyo, 277.
- [7] Wilson JV, Samy SF. SAE Paper N 770636.
- [8] Smalheer CV, Mastin TW. [1956] J Inst Petrol. 42:337-347.
- [9] Dawson C, Ratner A, Roberts L. [1959] Production of the high-basic detergent additives for engine oils, Amer Chem Soc. 4(3):45-50.
- [10] Patent 2088509. France. Detergent additives for lubricating oils. - Published on 11.02.72.

## ARTICLE

# THE CONCEPT OF MAINTAINING THE EFFICIENCY OF AUTOMOBILE ENGINES METHODS TRIBODIAGNOSTICS

Ilnar F Suleimanov<sup>1\*</sup>, Aleksandr T Kulakov<sup>1</sup>, Elena P Barylnikova<sup>1</sup>, Ruslan F Kalimullin<sup>2</sup>, Nikolay N Yakunin<sup>2</sup>

<sup>1</sup>Naberezhnye Chelny Institute, Kazan Federal University, Naberezhnye Chelny, RUSSIA

<sup>2</sup>Orenburg State University, Orenburg, RUSSIA

## ABSTRACT

The article presents an analysis of the process of changing of technical state of the automobile engine mobile interfaces from the beginning of operation until depletion of established service life in the form of life ageing structure that includes a complex of repair and maintenance cycles. During the operational phase, periodic multiple repetition of cycles of deterioration and stepwise recovery of the technical state occurs. Within a single cycle, deterioration of technical state forms a monotonic and relatively slow wear of the parts and their aperiodic sudden failures. If within a single maintenance cycle there is a complex of working cycles that include engine operation at startup, idle and under load, and maintenance itself, the regularity of the technical state change will be determined by wear rate at each of these modes. Consideration of this "micro level" in the structure of wear is a feature and novelty of the described here repair and maintenance cycle of engine. According to this structure, taking into account the assumptions and limitations made, the dependence between the mobile interface lifetime and the lifetime of the lubricating layer under the influence of a complex of operational factors: torque, crankshaft speed, modes and duration of run-in phase, duration of operation at start-up, idling, under load is received. The objective function of an automobile engine durability improvement is proposed. The results of calculations show that the mobile interfaces lifetime is significantly increased if the maximum lifetime of the lubricating layer is provided during run-in, start-up, idle and under load conditions. Thus, based on the idea of regularity of the technical state change of mobile interfaces in operation, the scientific concept of maintaining the automobile engine efficiency in operation is proved. The concept is presented in the form of a structure containing the goal, criteria, limitations, scope, stages, technical and organizational solutions. The novelty of the concept is that conditions for limiting the crankshaft bearings wear during the operating cycles are created in the structure of repair and maintenance cycle of an automobile engine, due to the development of the lubrication control system.

## INTRODUCTION

An essential factor for increasing the competitiveness of automobile transportation is minimizing costs of ensuring working capacity of vehicles and their components. Engine is one of the major automobile component, which determine both its operation efficiency and the amount of maintenance costs. The efficiency of the automobile engines operation is determined by a variety of factors - constructive, road, natural-climatic, operational, etc. [1-3]. At the same time, a wide range of opportunities for increasing the efficiency of its operation provides management of operational factors.

At the stages of production and technical operation of automobile engines, there is a change in parameters of the technical state of its units, mechanisms and systems, initial indicators values of which are formed during production [2]. During running-in of new or overhauled engine, change in parameters is directed towards improvement, however, during subsequent operation time, a multiple repetition of cycles of technical state deterioration and its stepwise recovery through repair is carried out with a regularity of maintenance. Within a single maintenance cycle, the regularity of change in the technical state forms a monotonic and relatively slow wear of mobile interfaces and aperiodic sudden failures.

Strict adherence to periodicity and volume of maintenance work, timeliness of repair performance slows the monotonous deterioration of the technical state parameters. At the same time, the authors concluded that there is a significant reserve in maintaining the automobile engines performance if additional measures are taken to reduce the rate of technical state deterioration within a single cycle.

Based on Cause and Effect Analysis of the factors of changes in the technical state of mobile interfaces in operation, it is concluded that the control of the technical condition is associated with the control of the lubrication process [4, 5]. Preconditions of such control were studied based on the study of scientific publications and practical developments in the field of maintaining of automobile engines efficiency in operation [6 -12].

It is established that the common problem holding back quality improvement of run-in, technical state definition and prediction, minimization of starting and operational wear of mobile interfaces, is insufficiently developed operational, reliable, low-cost and available methods and tools for evaluating the lubrication process.

Analysis of the present situation showed that the problem of increasing the automobile engine durability could be solved by controlling the lubrication process in mobile interfaces. However, the effective practical implementation of such operational method of maintaining the automobile engine efficiency is currently hindered due to insufficient development of theoretical and methodological provisions of the lubrication management system. Therefore, development of methods for effective maintenance of automobile engines performance based on the lubrication process management helps to reduce costs of resources and losses during operation.

## KEY WORDS

engine, efficiency,  
crankshaft,  
tribodiagnosics,  
lubrication process.

Received: 18 Oct 2018  
Accepted: 21 Dec 2018  
Published: 3 Jan 2019

## \*Corresponding Author

Email:  
ecolog\_777@mail.ru  
Tel.: 89179045977

In this regard, research aimed at developing methods and instruments to maintain the automobile engine performance are relevant.

**METHODS**

The main scientific propositions and results presented in the article are based on the developed theoretical background and results of experimental studies of the operational reliability of automobile engines, the use of tribo diagnostics and study of regularities of change in the automobiles and aggregates technical state [13].

Change process of mobile interfaces technical state from beginning of operation until depletion of established service life is complex, and it can be more simply represented as the structure of operational wear process. It includes a set of repair and maintenance cycles, formed by stages of repair and operation [14].

If within a single maintenance cycle there is a complex of working cycles that include engine operation at startup, idle and under load, and maintenance itself, the intensity of the technical state change will be determined by regularities of wear at each of these modes. Consideration of working cycles in the structure of wear is a feature and novelty of the repair and maintenance cycle of engine.

According to the accepted structure, the current diametral clearance  $\Delta$  in the mobile interface is formed by the clearance value after mounting (assembly)  $\Delta_M$  and the total current operational wear  $I^{\Sigma}$  generated by wear during the running-in  $I^{OB}$  and current operational wear  $I^{\rho}$ , which, in turn, consists of wear at start-up  $I^I$ , when the engine is idling  $I^X$  and under load IH:

$$\Delta = \Delta_M + I^{\Sigma} = \Delta_M + I^{OB} + I^{\rho} = \Delta_M + I^{OB} + I^I + I^X + I^H. \tag{1}$$

Based on this, the objective function of operational wear can be represented as following:

$$I^{\Sigma} = I^{OB} + I^I + I^X + I^H \rightarrow \min.$$

Linear wear  $I$  of the rubbing surfaces is equal to:

$$I = i_h \cdot \tau, \tag{2}$$

where  $i_h$  - wear rate,  $\mu\text{m} / \text{h}$ ;  $\tau$  - duration of friction, h.

It is assumed that the wear rate  $i_h$  is proportional to frictional work and, accordingly, to duration of the contact interaction (in case of lubricating layer absence) of friction surfaces, torque  $M$  and crankshaft speed  $n$ :

$$i_h = A(1 - E_g) M n K_{\delta}, \tag{3}$$

where  $A$  - coefficient of proportionality, depending on the physical-mechanical and geometric properties of friction surfaces;  $E_g$  - parameter of the lubricating layer lifetime in the mobile interface;  $K_{\delta}$  - coefficient of the mode dynamism taking into account an increase in wear intensity during an unsteady mode of the engine operation in comparison with the steady one.

The operational wear is summarized from the wear values at each mode: start-up  $I_l^I$ , idling  $I_l^{\delta}$  and under load  $I_l^I$  in all operating cycles:

$$I^{\rho} = \sum_{l=1}^{L_j} (I_l^I + I_l^{\delta} + I_l^I) = A^i \sum_{l=1}^{L_j} \sum_{j=1}^{j=I_j} (1 - E_{gij}^I) \dot{I}_{ij}^I n_{ij}^I \tau_{ij}^I \hat{E}_{\alpha ij}^I + A^{\delta} \sum_{l=1}^{m-I_j} (1 - E_{gim}^{\delta}) \dot{I}_{lm}^{\delta} n_{lm}^{\delta} \tau_{lm}^{\delta} \hat{E}_{\alpha lm}^{\delta} + A^I \sum_{l=1}^{L_j} \sum_{k=1}^{k=I_j} (1 - E_{gik}^I) \dot{I}_{lk}^I n_{lk}^I \tau_{lk}^I \hat{E}_{\alpha lk}^I. \tag{4}$$

where  $T_{II}, T_X, T_H - \tau_{ij}^{II}$  - the number of start-up, idling and load modes in one operating cycle respectively;  $\tau_{ij}^{II}$  - duration of the engine operation in  $l$ -th cycle on the  $j$ -th operating mode at start-up, h;  $\tau_{lm}^X$  - duration of the engine operation in the  $l$ -th operating cycle on the  $m$ -th operating mode at idle, h;  $\tau_{lk}^{II}$  - duration of the engine operation in the  $l$ -th operating cycle on the  $k$ -th operating mode under load, h;

$LE$  - number of working cycles in operation;  $(\dot{I}_{lj}^I, n_{lj}^I), (\dot{I}_{lm}^{\delta}, n_{lm}^{\delta}), (\dot{I}_{lk}^I, n_{lk}^I)$ , - parameters of loading modes in each working cycle;  $E_{glj}^I, E_{glm}^{\delta}, E_{gik}^I$ , - parameter of the relative lifetime of the lubricating layer in each working cycle for each stage;  $\hat{E}_{\alpha ij}^I, \hat{E}_{\alpha lm}^{\delta}, \hat{E}_{\alpha lk}^I$ , is the dynamic factor in each working cycle for each stage.

Duration  $\tau_{lk}^H$  of the engine operation under load is determined by an automobile mileage  $L_{lk}$  (km) with an average speed  $V_{lk}$  (km/h) according to the formula:

$$\tau_{lk}^i = \frac{L_{lk}}{V_{lk}} \quad (5)$$

The maximum permissible operational wear will be:

$$I^{\Delta PPP} = \Delta_{PPP} - \Delta_M - I^{OB}, \quad (6)$$

where  $\Delta_{PPP}$  - maximum permissible value of diametal clearance in mobile interface.

On the assumption that parameters in the groups  $(\tau_{lj}^{\Pi}, \tau_{lm}^{\dot{O}}, \tau_{lm}^{\dot{I}})$ ,  $[(\dot{I}_{lj}^{\dot{I}}, n_{lj}^{\dot{I}}), (\dot{I}_{lm}^{\dot{O}}, n_{lm}^{\dot{O}}), (\dot{I}_{lk}^{\dot{I}}, n_{lk}^{\dot{I}})]$ ,  $(E_{glj}^{\dot{I}}, E_{glm}^{\dot{O}}, E_{glk}^{\dot{I}})$ ,  $(\hat{E}_{\dot{a}lj}^{\dot{I}}, \hat{E}_{\dot{a}lm}^{\dot{O}}, \hat{E}_{\dot{a}lk}^{\dot{I}})$  have the same values, wear at running-in will be:

$$I^{OA} = \dot{A}^{\dot{I}A} (1 - E_g^{OA}) \dot{I}^{OA} n^{OA} \dot{O}^{OA} \hat{E}_{\dot{a}}^{\dot{I}A}, \quad (7)$$

maximum permissible operational wear will be:

$$I^{\dot{Y}ID} = \dot{A}^{\dot{I}} (1 - E_g^{\dot{I}}) \dot{I}^{\dot{I}} n^{\dot{I}} L_{\dot{Y}} T^{\dot{I}} \hat{E}_{\dot{a}}^{\dot{I}} + \dot{A}^{\dot{O}} (1 - E_g^{\dot{O}}) \dot{I}^{\dot{O}} n^{\dot{O}} L_{\dot{Y}} T^{\dot{O}} \hat{E}_{\dot{a}}^{\dot{O}} + \dot{A}^{\dot{I}} (1 - E_g^{\dot{I}}) \dot{I}^{\dot{I}} n^{\dot{I}} \frac{L_l}{V_l} \hat{E}_{\dot{a}}^{\dot{I}} \quad (8)$$

where  $T^{OB}, T^{\Pi}, T^X, T^H$  - total operation time at run-in, start-up, idling, under loading modes respectively, h;  $M^{OB}, M^{\Pi}, M^X, M^H$  - average values of torque at run-in, start-up, idling and under load operation respectively, Nm;  $n^{OB}, n^{\Pi}, n^X, n^H$  - average values of rotational frequency at run-in, start-up, idling and under load respectively, min-1;  $V_l$  - average speed of the vehicle, km / h;  $L_l$  - vehicle mileage for one working cycle, km.

Let us assume that lifetime of the mobile interface is equal to:

$$L_D = L_{\dot{Y}} L_l, \quad (9)$$

and the number of working cycles in operation will be:

$$L_{\dot{Y}} = \frac{\Delta_{\dot{Y}ID} - \Delta_{\dot{I}} - \dot{A}^{\dot{I}A} (1 - E_g^{OA}) \dot{I}^{OA} n^{OA} \dot{O}^{OA}}{\dot{A}^{\dot{I}} (1 - E_g^{\dot{I}}) \dot{I}^{\dot{I}} n^{\dot{I}} T^{\dot{I}} + \dot{A}^{\dot{O}} (1 - E_g^{\dot{O}}) \dot{I}^{\dot{O}} n^{\dot{O}} T^{\dot{O}} + \dot{A}^{\dot{I}} (1 - E_g^{\dot{I}}) \dot{I}^{\dot{I}} n^{\dot{I}} \frac{L_l}{V_l}} \quad (10)$$

Then the mathematical model of lifetime expenditure of mobile interface can be represented in the form:

$$L_p = L_l \frac{\Delta_{\dot{Y}ID} - \Delta_M - A^{OB} (1 - E_g^{OB}) M^{OB} n^{OB} T^{OB} K_{\dot{O}}^{OB}}{A^{\Pi} (1 - E_g^{\Pi}) M^{\Pi} n^{\Pi} T^{\Pi} K_{\dot{O}}^{\Pi} + A^X (1 - E_g^X) M^X n^X T^X K_{\dot{O}}^X + A^H (1 - E_g^H) M^H n^H \frac{L_l}{V_l} K_{\dot{O}}^H} \quad (11)$$

The target function of increasing the automobile engines durability is:

$$L_{\dot{O}} \rightarrow L_p(max) \quad (12)$$

Under limitations:

$$E_{g.\dot{a}i\dot{I}} < E_g \leq 1; n_{\dot{O}\dot{O}} \leq n \leq n_{\dot{I}\dot{I}}; \hat{E}_{\dot{a}} \geq 1; L_{lmin} \leq L_l \leq L_{lmax} \\ V_{lmin} \leq V_l \leq V_{lmax}; T_{min} \leq T \leq T_{max}; A_{min} \leq A \leq A_{max}.$$

Results of the theoretical study show that value change of parameter  $E_g$  has the greatest impact on the value  $L_p$  when working under load. Thus, when value of  $E_g$  parameter is reduced by 0,02 relatively to the average value of 0,97, the lifetime is reduced by 1,5 times. However, with an increase in parameter by 0,02 relatively to the average value, the lifetime rises already 2,1 times. In general, to increase the lifetime, it is necessary to ensure a high level of values of the parameter  $E_g$  both at run-in and at the stages of operating modes. So, while simultaneously taking into account the maximum values of  $E_g$  at run-in (0.8), starting (0.9), idling (0.7) and under load (0.99), the increase in lifetime reaches 2.6 times.

## RESULTS AND DISCUSSION

Based on a common understanding of regularities of change in technical state of mobile interfaces in operation, the scientific concept of maintaining the automobile engines efficiency is proved, which differs in terms of limiting the wear intensity of mobile interfaces in repair and maintenance cycle based on the development of tribo diagnostics methods.

Conceptual provisions are formulated as follows:

- aim is to reduce cost of transportation process support by increasing the durability of automobile engines through maintaining their efficiency by means of tribo diagnostics methods;
- criterion is maintenance of automotive engine efficiency based on management of technical state change of limiting the lifetime mobile interfaces due to minimization of wear intensity and lubrication process control;
- limitation is the assumption that deterioration of the technical state occurs due to wear, the intensity of which depends on the parameters of the lubrication process;
- scope are stages of repair and operational cycle of engine: run-in, operation modes for the intended purpose, maintenance and repair;
- stages include development of theoretical and methodological provisions of the lubrication process control in mobile interfaces; development of the lubrication process control system in mobile interfaces: information, technical, intellectual component;
- technical solutions are software and hardware complex of tribo diagnostics [14]; application programs packages; methods and technology of management [15-18]
- organizational solutions are methods of maintaining efficiency at the stages of the repair and maintenance cycle of the engine [10], guidelines, personnel training.

## CONCLUSION

The concept of maintenance of automobile engines working capacity in operation due to restriction of wear intensity of mobile interfaces on the basis of development of mathematical, information, technical and organizational support of the lubricating process control system by application of tribo diagnostics methods is formulated. The presented results of scientific research can be used for development of new technical and organizational solutions to effectively maintain the automobile engine performance based on the development of lubrication management system using modern and prospective methods of tribo diagnostics.

### CONFLICT OF INTEREST

There is no conflict of interest.

### ACKNOWLEDGEMENTS

The work is performed according to the Russian Government Program of Competitive Growth of Kazan Federal University.

### FINANCIAL DISCLOSURE

None

## REFERENCES

- [1] Denisov AS. [1999] Fundamentals of the formation of the maintenance and repair cycle of vehicles, Saratov: SSTU. 352.
- [2] Denisov AS, Kulakov AT. [2007] Ensuring the reliability of automotive engines, Saratov: SSTU. 422.
- [3] Barylnikova EP, Talipova IP, Kulakov AT. [2018] Influence of the technical state of the power unit components on the automobile efficiency, Scientific and Technical Bulletin of the Volga Region. 1:43-45.
- [4] Yakunin NN, Kalimullin RF. [2014] Transitional lubricating process in plain bearings in machines, Life Science Journal. 11(12):427 – 423.
- [5] Barylnikova EP, Makushin AA. [2013] Influence of operational factors on the lubrication conditions of crankshaft bearings of automotive engines” Tractors and farm machinery. 5:33-36.
- [6] Holmberg K, Andersson P, Nylund NO, Mäkelä K, Erdemir A. [2014] Global energy consumption due to friction in trucks and buses, Tribology International. 78:94-114.
- [7] Priest M, Taylor CM. [2000] Automobile engine tribology - approaching the surface, Wear. 241(2):193-203.
- [8] Stachowiak, Gwidon W, Andrew W. [2006] Batchelor, Hydrodynamic Lubrication, Engineering Tribology: Third Edition. 103-204.
- [9] Tung SC, McMillan ML. [2004] Automotive tribology overview of current advances and challenges for the future, Tribology International. 37(7):517-536.
- [10] Kalimullin RF. [2016] Scientific basis for maintaining the automobile engines efficiency by methods of tribodiagnostics, Orenburg: OOO IPK "University". 272.
- [11] Kalimullin RF. [2015] the Concept of increasing the automobile engines durability in operation, Bulletin of the Orenburg state University. (9):144 – 152.
- [12] Kalimullin RF, Kovalenko SYU. [2013] The concept of resource-saving operation of automobile engines, Bulletin of Saratov State Technical University. 2(71) 2:30 - 35.
- [13] Podmasteryev KV. [2012] Status and tool maintenance of electrical methods of friction units monitoring, Izvestiya Tula State University (Izvestiya TulGU). Technical Sciences. 7:221-234.
- [14] Kazakov AV, Kalimullin RF, Yakunin NN. [2016] Information and measuring system of the evaluation of lubrication in bearings of internal combustion engines, International Scientific and Research Journal. 11(53):60-63, 2016.
- [15] Barylnikova EP, Kulakov OA, Kulakov AT. [2016] Adaptive system of supplying lubricant to the internal combustion engine, Innovative engineering technologies, equipment and materials. 27-31.
- [16] Kulakov A, Gattarov I, Frolov A. [2015] Provision of gas engine bus performance with air-fuel mixture Journal of Environmental Management and Tourism. 6(1):91-100.
- [17] Barylnikova EP, Kulakov AT, Kulakov OA. [2017] Adaptive system of supplying lubricant to the internal combustion engine//IOP Conference Series: Materials Science and Engineering. 240(1):012-010.
- [18] Kulakov AT. [2014] Providing normal conditions of lubricating of diesel engine during its operation. Kulakov AT, Gafiyatullin AA, Barylnikova EP. IOP Conference Series: Materials Science and Engineering. 69(1):012-027.



## ARTICLE

# NEURAL NETWORK MODEL AND SOFTWARE COMPLEX TO DETERMINE PERSON'S FUNCTIONAL STATE

Ilyas I Ismagilov<sup>1\*</sup>, Svetlana F Khasanova<sup>2</sup>, Alexey S Katasev<sup>3</sup>, Amir M Akhmetvaleev<sup>3</sup>, Dina V Kataseva<sup>3</sup>, Dmitriy G Petrosyants<sup>3</sup>

<sup>1,2</sup> *Institute of Management, Economics and Finance, Kazan Federal University, Kazan, RUSSIA*

<sup>3</sup> *Kazan National Research Technical University named after A.N. Tupolev, Kazan, RUSSIA*

## ABSTRACT

This article deals with the definition of an intoxicated person functional state. They performed the analysis of pupillary response peculiarities to illumination changes. It is proposed to use the method of pupillometry for the analysis of pupillary reactions. They concluded that it is necessary to evaluate the values of the papillo gram parameters on the basis of the neuro net approach. The task was to develop a mathematical model and software to determine the functional state of a person's intoxication. The solution of this problem is carried out on the basis of neural network collective, formed according to the bootstrapping method. They proposed the methods to collect and prepare the initial data for analysis, to develop a neural network model, as well as the method and the algorithm to optimize the composition of the input and the number of hidden neurons of its neural networks. ROC analysis is used to find an optimal clipping point for solution classes generated at the output of neural network models. They provided the description of the neural network model, the developed software package, as well as the results of the research conducted on its basis. For the purpose of approbation, the problem of a person's intoxication is solved during a pre-trip medical examination. The conclusion is made about material, technical and time cost reduction during the survey conduct using the proposed approach, as well as the possibility and the effectiveness of its practical use in other areas.

## INTRODUCTION

**KEY WORDS**  
functional state, neural network, pupillometry, diagnostics, ROC analysis, bootstrapping, reduction, genetic algorithm, pre-trip medical examination.

At present, the task of a person functional state (FS) determination acquires an urgency in various subject areas. A number of works are devoted to this problem solution. The change of mammal pupil size under the influence of light flashes was recognized as a reliable marker of brain activity, including human brain [1,2]. In addition to brightness change adaptation, the changes of a pupil diameter correlate with a person's excitation, attention, and perception changes [3-5]. Such diagnostic methods based on the evaluation of the pupillary response of a person refer to the methods of pupillometry. In [6] they proposed to use this method to determine the FS of athletes.

There are different classes of human FS [7]: normal, borderline, pathological ones. Among the latter they determine the FS, characteristic of alcohol or drug intoxication. In most cases, intoxication leads to a human visual system disorder. This feature allows you to identify human FS in medical diagnostic systems. Many scientists have been involved in this area research [8-11]. However, diagnostic systems, including those based on the methods of pupillometry, require the participation of qualified experts, the creation of special conditions and significant material, technical and time costs. These features of pupillometry method application in medical diagnostics reduce the possibility of its use in other areas.

The pupillometry allows to obtain the data, according to the analysis of which it is possible to classify the human FS. This problem should be solved on the basis of the neural network approach [12,13], which proved its effectiveness in diagnostic systems [14,15] and decision making support [16,17]. Many scientists contributed to the development of neuro cybernetics and the development of decision making support systems [18, 19]. However, they did not study completely the issues of neural network (NS) use in the determination of human FS based on pupillometry. This actualizes the need to develop new neural network models, the methods and the algorithms that can solve the task effectively. Thus, in order to determine the human FS according to the analysis of its pupillary response to light impulse, it is necessary to develop mathematical model and software based on the neural network approach.

## METHODS

One of the criteria that affect the quality of a person's life is his FS, in particular the state of intoxication (alcoholic or narcotic). In this state, the intensity of pupillary reaction decreases, and the pupils are narrowed or widened as much as possible.

Pupillometry is an effective method of intoxication state diagnostics. In this method, the dynamics of a pupil size change is represented in the form of a time series - the pupillogram [Fig. 1].

The following parameters are indicated on the figure: ID - initial diameter, FD - final diameter, HCD - half constriction diameter, MD - minimum diameter, LRT - latent reaction time, HCT - half constriction time, HET - half expansion time, CT - constriction time, AC - the amplitude of constriction, and ET - the expansion time. Pupillometry also uses such parameters as the rate of narrowing (CC) and the rate of expansion (CP), calculated according to the initial data. Thus, each set of parameter values can be associated with the

Received: 13 Oct 2018  
Accepted: 9 Dec 2018  
Published: 4 Jan 2019

\*Corresponding Author  
Email:  
iismag@mail.ru

state of "norm" or "deviation". The totality of such values is the data to develop a model for a person intoxication state determination.

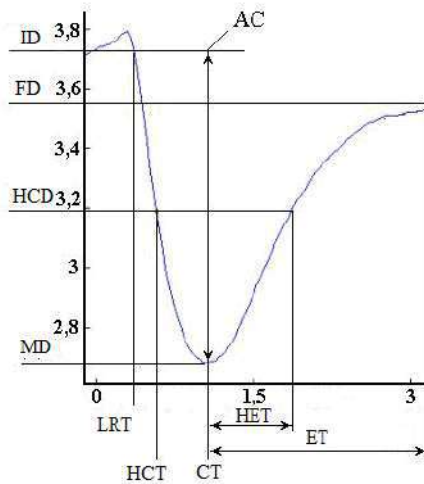


Fig. 1: Example of a pupillogram and its parameters.

The solution of time series problem analysis from pupillometry results is based on various methods. Discrete transformations are widely used in pupillometry. It is proposed to use a transient Fourier transformation in [20] to estimate the mental load. The parabolic and elliptic Haf transformations are used to recognize and measure a pupil size obtained from web camera data [21]. Wavelet transformations are used to analyze the results of pupillometry in [22]. Discrete Walsh transformations and their generalizations can be used effectively during the solution of time series analysis problems in the methods of pupillometry [23, 24].

At present, statistical methods are used to solve the problem under consideration: parametric, linear-discriminant, clustering, etc. The effectiveness of their use depends on data quality. At low detail of an image, the accuracy of the diagnosis is reduced. Therefore, in order to analyze the values of the pupillogram parameters under the specified conditions and to develop the binary classification model, it is important to use the methods of data analysis, in particular the NN, whose effectiveness is conditioned by their universal approximating ability, which allows them to solve practical problems with a high degree of accuracy.

Thus, in order to determine the state of a person intoxication on the basis of a neural network approach, the following developments are required:

- 1) the methods for the collection and preparation of baseline data for analysis;
- 2) the neural network model and the methods of its development;
- 3) the numerical method and neural network model algorithm reduction to increase the efficiency of its practical use;
- 4) software complex implementing the proposed methodologies, model, method and algorithm.

The methodology has been developed in order to collect and prepare data for analysis, consisting of the following steps:

- 1) the collection of initial data in changing illumination conditions;
- 2) the evaluation of source data quality;
- 3) source data cleaning;
- 4) the calculation of pupillogram parameter values;
- 5) the development of the initial data table with the calculated values;
- 6) quality assessment, data table cleaning and obtaining for analysis.

To implement the first stage, they developed the laboratory stand that includes a video camera and software to record and analyze the images of human eyes. All images were recorded for 3 seconds with a light pulse provision. The obtained data include noise, anomalous and missing values [25]. Therefore, during the second and the third stage of the methodology, the data quality is assessed and its cleaning takes place [26].

During the fourth stage, they calculate the values of the pupillogram parameters. Let us have the pupillogram  $P = \{(t_0, D_0), \dots, (t_i, D_i), \dots, (t_k, D_k)\}$ , where  $t_0$  is the initial time moment (0 seconds),  $t_k$  is the

final time moment (3 seconds),  $D_0$  is the initial diameter of a pupil,  $D_k$  is the final diameter of the pupil. Then the values of the parameters will be calculated by the following formulas:

- $D_{min} = \min(D_i), i = \overline{0, k}$  - MD;
- $t_s = t_i | D_i = D_{min}$  - CT;
- $D_{ps} = \frac{D_0 + D_{min}}{2}$  - HCD;
- $t_{ps} = t_i < t_s | D_i = D_{ps}$  - HCT;
- $t_{pr} = t_i - t_s | D_i = D_{ps}, t_i > t_s$  - HET;
- $t_r = t_k - t_s$  - ET;
- $A_s = D_0 - D_{min}$  - AC;
- $V_s = \frac{A_s}{t_s}$  - CC;
- $V_r = \frac{D_k - D_{min}}{t_r}$  - CP;
- $t_l = \min(t_i) | D_i < D_0$  - LRT.

During the fifth stage, the obtained values are reduced to the table showing the class of the human FS. During the sixth stage, quality assessment, purification and the obtaining of a ready-made data table for analysis are performed see [Table 1].

**Table 1:** Data fragment to develop a neural network model

No	$D_0$	$D_{min}$	$D_{ps}$	$D_k$	$A_s$	$V_s$	$V_r$	$t_l$	$t_s$	$t_r$	$t_{ps}$	$t_{pr}$	Class
1	5,4	4	4,7	5,2	1,4	2,6	0,5	0,2	0,5	2,4	0,2	1,1	0
2	5,5	4,1	4,8	5,4	1,5	2,8	0,6	0,2	0,5	2,3	0,2	1	0
3	5,4	4,1	4,7	5,2	1,2	2,2	0,5	0,2	0,6	2,2	0,2	1	0
4	5,5	4	4,7	5,1	1,5	2,8	0,3	0,2	0,5	2,2	0,2	1,1	0
5	2,6	2,6	2,6	2,6	0,1	0,1	0,1	0,3	0,3	2,4	0,1	1,1	1
6	2,6	2,6	2,6	2,6	0,1	0,2	0,1	0,2	0,4	2,4	0,1	1,1	1
7	7,1	6,7	6,9	6,9	0,3	0,6	0,1	0,2	0,5	2,2	0,2	1	1
8	7,3	6,7	7,1	7,1	0,6	1,1	0,2	0,3	0,5	2,2	0,2	1	1

In order to develop a neural network model based on the analysis of the obtained data, the following procedure was developed:

- 1) To form the structure of the NN on the basis of Arnold-Kolmogorov-Hecht-Nielsen theorem for the whole set of input parameters [18];
- 2) To develop an initial neural network model of the given structure, to find an optimal cut-off point for class solution by the ROC-analysis method and to estimate the model error by bootstrapping method [26];
- 3) in order to increase the accuracy and to reduce the dimension of an original model structure, to reduce it by clarifying the composition of the input and the number of hidden neurons based on the genetic algorithm.

In order to solve this problem, the perceptron model NS was developed. The number of its hidden neurons is determined by the corollary of the Arnold-Kolmogorov-Hecht-Nielsen theorem on the basis of the following expression [18]:

$$N_h \leq 2 \times N_{in} + 1, \tag{1}$$

where  $N_h$  is the number of hidden neurons, and  $N_{in}$  is the number of input neurons.

Thus, taking into account (1), the initial model consists of 12 input neurons, 25 hidden neurons and one output neuron.

In order to select an optimal clipping point to cut off solution classes in the neural network model, the ROC analysis method was used. The criterion for an optimal cut-off point  $Cutt\_off_0$  selection is the reduction of errors of the first kind according to the rule:

$$Cutt\_off_o = Cutt\_off_k \left| Se = \max_{k=1,K}(Se_k) \right. \& k = \max[1, K]$$

[Fig. 2] shows the example of cut-off point selection rule.

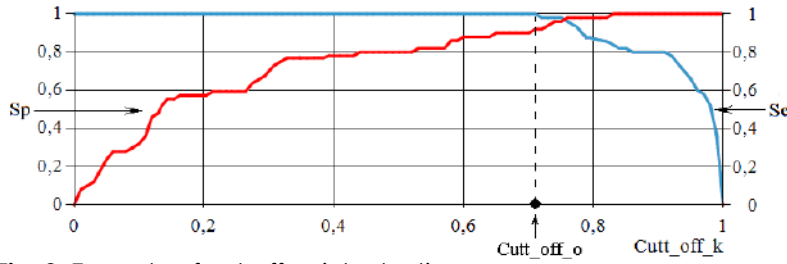


Fig. 2: Example of cut-off point selection.

Therefore, among the set of all cut-off points K, the optimal point should be on the right side of the maximum sensitivity range (Se) boundary, at which the specificity (Sp) is maximum.

In order to estimate the model error, the bootstrap method is used to form N random sets of training and test samples with the calculation:

-  $\epsilon_{train} = \frac{n_{train}}{N_{train}}$  - model error in learning, where  $n_{train}$  is the number of correctly classified learning examples,  $N_{train}$  is the volume of the training sample;

-  $\epsilon_{test} = \frac{n_{test}}{N_{test}}$  - model error in testing, where  $n_{test}$  is the number of correctly classified test cases,  $N_{test}$  is the volume of the test sample.

After the i-th ( $i = 1..N$ ) iteration, the error is calculated:  $\epsilon_i = 0,632 * \epsilon_{test_i} + 0,368 * \epsilon_{train_i}$ .

$$\text{Final model error: } \epsilon = \frac{\sum_{i=1}^N \epsilon_i}{N} \times 100\%.$$

Thus, during bootstrapping, the team of N NS of the same architecture is developed. The result of the classification is the aggregation of all NN decisions on the basis of voting see [Fig. 3].

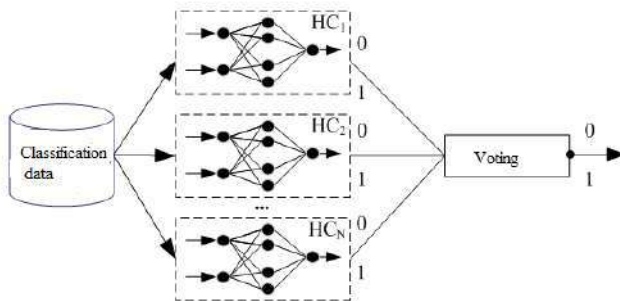


Fig. 3: NN collective model application scheme.

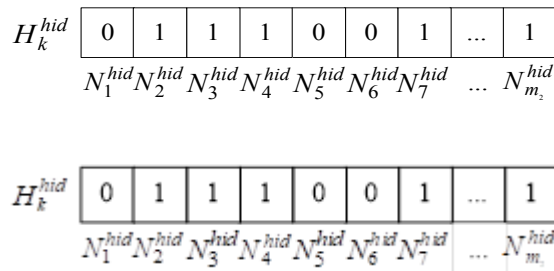
Typical results of bootstrapping at N = 7 are presented in [Table 2].

Table 2: Typical bootstrapping results

Item №	$\epsilon_{train}$	$\epsilon_{test}$	$\epsilon_i$	$\epsilon, \%$	Model accuracy
1	0,04	0,09	0,07	6,8	91%
2	0,06	0,05	0,05		
3	0,03	0,02	0,02		
4	0,04	0,11	0,08		
5	0,08	0,09	0,09		
6	0,03	0,12	0,08		
7	0,04	0,09	0,07		

According to the presented results, the adequacy of the initial model is not high. The accuracy of the model can be improved by the elimination of its constituent redundancy. To solve this problem, the method and the algorithm for genetic optimization has been developed to reduce the number of input and hidden neurons. Let the set  $N^{in} = \{N_1^{in}, N_2^{in}, \dots, N_{m_1}^{in}\}$  contains the neurons of the input layer  $N_j^{in}, j = \overline{1, m_1}$  (m1 - the number of input neurons), and the set  $N^{hid} = \{N_1^{hid}, N_2^{hid}, \dots, N_{m_2}^{hid}\}$  are the neurons of the hidden layer  $N_l^{hid}, l = \overline{1, m_2}$  (m2 - the number of hidden neurons). Let's encode the input layer of the network in the form of the chromosome  $H_i^{in} = \{h_{ij}^{in}\}$ , where the single gene  $h_{ij}^{in}$  means the presence of the input layer neuron, and the zero gene is its absence. The hidden layer of the network is encoded as the chromosome  $H_k^{hid} = \{h_{kl}^{hid}\}$  with a similar representation of the gene  $h_{kl}^{hid}$ .

The examples of chromosome encoding of the input and hidden layers:



The creation of the initial population of chromosomes of the input layer (volume m1) is performed by the inclusion of the parent chromosome in the population from single genes and a set of descendants obtained as the result of random mutation of its genes with the probability of 0.5. The reduction of NN structure is reduced to the search for chromosomes of the input and hidden layers, under which the final model error and the number of elements of its structure are minimal.

The fitness function is determined as follows:

$$F(H_{ik}) = \frac{\sum_{b=1}^N 0,632 * \epsilon_{test_b}^{ik} + 0,368 * \epsilon_{train_b}^{ik}}{N} \rightarrow \min_{\forall H_{ik}}, \quad (2)$$

where  $H_{ik} = H_i^{in} + H_k^{hid}$  - the chromosome for NN structure coding.

Let's consider the implementation of genetic operators. At the first stage, according to the formula (1), the NN generation is performed corresponding to the initial chromosomes of the input layer. The following is performed for each network:

- 1.1) the creation of the initial chromosome population of the hidden layer (volume m2) in the following composition: the parent chromosome from single genes and the set of descendants obtained as the result of random mutation of its genes with the probability of 0.5;
- 1.2) the estimation of all chromosome fitness according to the formula (2);
- 1.3) the selection of 2 parent chromosomes based on the roulette wheel method;
- 1.4) the crossing of the parent chromosomes to obtain 2 descendants;
- 1.5) the mutation of offspring by the inversion of their genes with the probability of 0.02;
- 1.6) the evaluation of descendant fitness according to the formula (2);



1.7) the reduction of the 2 worst chromosomes to form a new population.

The steps 1.3-1.7 are performed until chromosomes with better fitness appear. After that, the chromosome  $H_i \Leftrightarrow \min F(H_k^{hid})$  is selected. Adaptability of input layer chromosomes:

$$F(H_i^{in}) = F(H_i) = \min F(H_k^{hid}).$$

The second stage is the search of a set corresponding to the NN with a minimum classification error. To do this, the steps similar to the first step are performed. This stage is repeated until chromosomes with better fitness appear. The best one determining the structure of the desired NN is chosen from the final set of chromosomes.

[Fig. 4] shows the desired NN collective model, obtained after the reduction of its constituents.

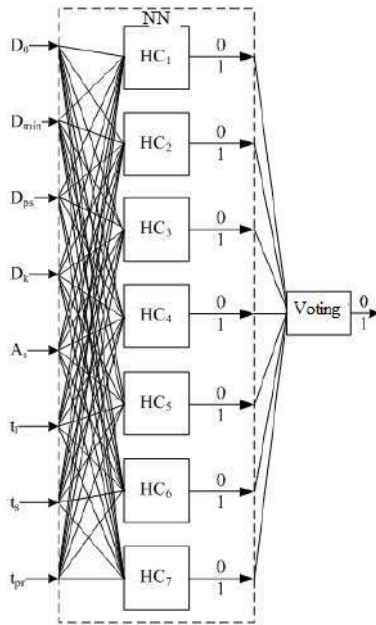


Fig. 4: NN collective model.

The desired model consists of 7 reduced NN with 10 hidden neurons and 8 input neurons, whose composition is determined by the following parameters: D0, Dmin, Dk, Dps, As, tl, ts, and tpr. After the reduction, the accuracy of the model made 96.7%, which corresponds to the error of 3.3%. Since the error makes no more than 5%, the obtained model is adequate.

## RESULTS AND DISCUSSION

Based on the proposed methodologies, method and algorithm, the software package was implemented in Microsoft Visual Studio environment via C# language. This complex consists of three programs see [Fig. 5].

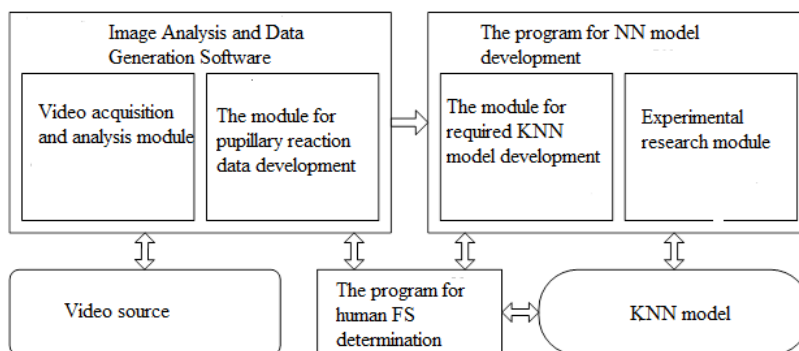


Fig. 5: Software complex structure.

The first program consists of two modules responsible for video image obtaining and analysis and pupil response data generation. The second program consists of the modules for neural network model development, the evaluation of their adequacy, the reduction and the conduct of studies to assess the impact of various parameters on the NN collective model adequacy. The third program is used to determine the human FS.

Let us consider the results of the studies on the evaluation of method effectiveness and NN reduction algorithm see [Table 3].

Table 3: NN reduction results

№	Input parameters of the model	Amount		Model accuracy, %	Stage number $\Gamma A_1 / \Gamma A_2$	Reduction time, in min.
		In. neuron	Hidden neuron			
1	$D_0, D_{min}, D_{ps}, V_s, t_i, t_s, t_{ps}, t_{pr}$	8	11	96,2	20/492	40
2	$D_{min}, D_{ps}, A_s, t_i, t_s, t_r, t_{pr}$	7	4	94	20/490	36
3	$D_0, D_{min}, D_{ps}, V_r, t_i, t_s, t_{ps}, t_{pr}$	8	8	96,2	28/716	71
4	$D_0, D_{min}, D_{ps}, D_k, t_i, t_s, t_{pr}$	7	7	94,2	20/480	30
5	$D_0, D_{min}, D_{ps}, D_k, A_s, t_i, t_s, t_{pr}$	8	10	96,7	24/758	59
6	$D_0, D_{ps}, D_k, A_s, t_i, t_s, t_r, t_{pr}$	8	7	94,7	21/505	49
7	$D_{ps}, D_k, V_s, t_i, t_s, t_r, t_{pr}$	7	5	95,6	20/438	38
8	$D_0, D_{min}, t_i, t_s, t_r, t_{pr}$	6	3	96,4	24/660	59
9	$D_{min}, D_{ps}, D_k, A_s, t_i, t_s, t_r, t_{pr}$	8	5	95,3	24/726	67
10	$D_0, D_{ps}, D_k, A_s, t_s, t_{ps}, t_{pr}$	7	5	96,1	24/682	69

During the fifth experiment, the set of model parameters was obtained, which achieves the accuracy of 96.7%. At that, each NN in the model structure consists of 8 neurons of the input layer and 10 neurons of the hidden layer.

Let us consider the results of the proposed approach approbation to intoxicated man FS definition using the example of pre-trip medical examination procedure passing by a driver see [Fig. 6].

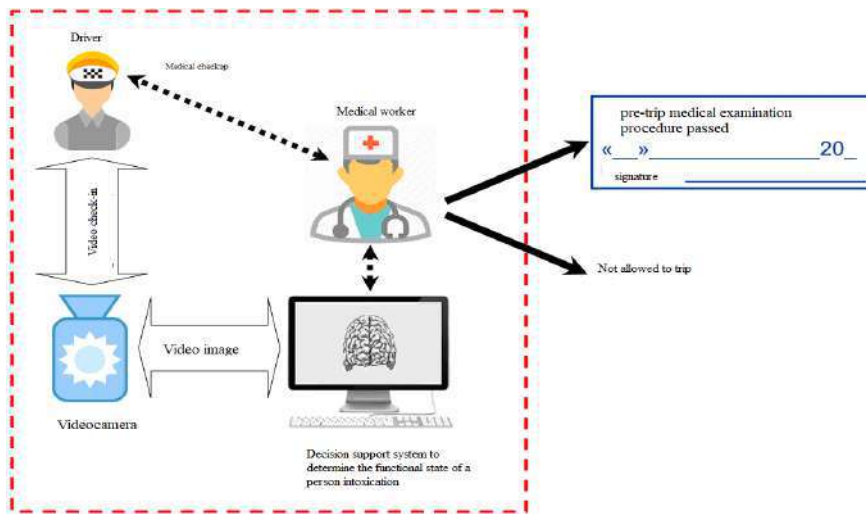


Fig. 6: Pre-trip medical examination passing scheme.

In this scheme the software complex is used in the form of a decision support system to determine whether drivers have medical restrictions for vehicle driving. A medical worker makes the conclusion on the admission of drivers to drive a car based on the results of the medical examination and taking into account the driver's FS assessment by neural network (sober / drunk).

The developed system was put into trial operation in the trucking industry of the city of Kazan. They performed the estimation of its efficiency from the point of view of material, technical and time expenses reduction see [Table 4].

By approbation results it is possible to draw the conclusion about the effectiveness of the developed software. Its use to determine the state of a person intoxication in the procedure of pre-trip medical examination allows to reduce material and technical (no less than 90%) and time (no less than 10 times) costs.

**Table 4:** Evaluation effectiveness results from the system use

Item No	Cost indicators (per driver)	Costs	
		Prior to introduction	After introduction
1	Material-technical	consumables for alcohol level testing (~ 20 rubles per test) and the presence of psychoactive substances (~ 195 rubles per test)	Consumables for alcohol level testing
2	Time	no less than 10-15 minutes	no more than 1 minute

## CONCLUSION

Thus, the developed neural network model is an effective tool to determine human FS. In particular, its use is effective when the drivers of motor vehicles undergo pre-trip medical examinations. The great advantage of the neural network model use in the framework of the described technology, as compared with the classical papillometric survey, is the absence of stringent requirements for laboratory and special technical support. Besides, there is no need to put an expert diagnostician in each area of medical examination, since the role of the expert is performed by NN.

The conducted researches have shown a high efficiency of neural network model and the possibility of its use in various spheres of human activity. First of all, the definition of intoxication FS is relevant in the sphere of public safety to identify potentially dangerous people whose abnormal condition is a threat to society, economy and the state. In order to develop a scientific trend concerning the definition of human FS, it is advisable to improve the mathematical model and software, as well as to develop, implement and use new applied intelligent decision support systems in various subject areas.

### CONFLICT OF INTEREST

There is no conflict of interest.

### ACKNOWLEDGEMENTS

The work is performed according to the Russian Government Program of Competitive Growth of Kazan Federal University. This work was supported by the Russian Federation Ministry of Education and Science, project № 8.6141.2017/8.9.

### FINANCIAL DISCLOSURE

None

## REFERENCES

- [1] Tolias AS. [2014] Pupil fluctuations track fast switching of cortical states during quiet wakefulness. *Neuron*. 84:355–362. doi:10.1016/j.neuron.2014.09.033
- [2] Schwalm M, Jubal ER. [2017] Back to pupillometry: How cortical network state fluctuations tracked by pupil dynamics could explain neural signal variability in human cognitive neuroscience. *Neuro*. 4(6):0293-16. DOI: 10.1523/ENEURO.0293-16.
- [3] Einhäuser W, Stout J, Koch C, Carter O. [2008] Pupil dilation reflects perceptual selection and predicts subsequent stability in perceptual rivalry. *Proc Natl Acad Sci USA* 105:1704–1709.
- [4] Murphy PR, Vandekerckhove J, Nieuwenhuis S. [2014] Pupil-linked arousal determines variability in perceptual decision making. *PLoS Comput Biol* 10:e1003854. doi:10.1371/journal.pcbi.1003854.
- [5] Breeden AL, Siegle GJ, Norr ME, Gordon EM, Vaidya CJ. [2017] Coupling between spontaneous pupillary fluctuations and brain activity relates to inattentiveness. *European Journal of Neuroscience*. 45(2):260-266. DOI: 10.1111/ejn.13424.
- [6] Matveev IA, Varchenko NN, Gankin KA. [2015] Using binocular pupillometry method for evaluating the functional state of persons. *Sports Technology*. 8(1-2):67-75. DOI: 10.1080/19346182.2015.1117478.
- [7] Leonova AB. [1984] Psychodiagnosis of human functional states. - Moscow: Mosk. University publishing house. 200.
- [8] Kalinitskaya VE, Pogrebnoy AI, Yakobashvili VA. [2003] Pupillogram features among drug addicts during the period of acute abstinence, *Actual problems of physical training and sports*. 6:221-230.
- [9] Steffen S. [2012] Diss by the Cand. of phys.-math. sciences, University of Eberhard Carls, Tübingen (Germany). 131.
- [10] McLaren JW, Erie JC, Brubaker RF. [1992] Computerized analysis of pupillo-grams in studies of alertness. *Invest Ophthalmol Vis Sci*. 33(3):671-676.
- [11] [1980] Risto Fried Pupillometry: the psychology of the pupillary response, *Journal of Personality Assessment*. 44(4):441-444.
- [12] Akmetvaleev A. [2017] Katasev. Neural network model and software complex to determine a person's functional state, *Automation of control processes*. 3 (49):88-95.
- [13] Akhmetvaleev A, Katasev A. [2015] The scheme of contactless identification of persons in intoxicated state, *Information and security*. 18(3):360-365.
- [14] Katasev AS, Kataseva DV. [2016] Neural network diagnosis of anomalous network activity in telecommunication systems. *Dynamics of Systems, Mechanisms and Machines, Dynamics*. 7819020.
- [15] Katasev AS, Kataseva DV. [2016] Expert diagnostic system of water pipes gusts in reservoir pressure maintenance processes. *2nd International Conference on Industrial Engineering, Applications and Manufacturing, ICIEAM 2016 - Proceedings* 7911651.
- [16] Wen L, Li X, Gao L, Zhang Y. [2018] A new convolutional neural network-based data-driven fault diagnosis method. *IEEE Transactions on Industrial Electronics*. 65(7):5990-5998.
- [17] Mrzygłód B, Hawryluk M, Gronostajski Z, Ziemia J, Zwierzchowski M. [2018] Durability analysis of forging tools after different variants of surface treatment using a decision-support system based on artificial neural networks. *Archives of Civil and Mechanical Engineering*. 18(4):1079-1091.
- [18] Hecht-Nielsen R. [1987] Kolmogorov's mapping neural network existence theorem, *IEEE First Annual International Conference on Neural Networks*. San Diego. 3:11-13.

- [19] Kohonen T. [1997] Self-Organizing Maps (2-nd edition), Springer.
- [20] Lew R, Dyre BP, Werner S, Wotring B, Tran T. [2008] Exploring the potential of short-time Fourier transforms for analyzing skin conductance and pupillometry in real-time applications Proceedings of the Human Factors and Ergonomics Society. 3:1536-1540.  
<https://www.scopus.com/inward/record.uri?eid=2-s2.0-70350591760&partnerID=40&md5=c15e98e3415ec2cbfaed66a26ec991a1>
- [21] Nasim A, Maqsood A, Saeed T. [2017] Multicore and GPU based pupillometry using parabolic and elliptic hough transform International Journal of Mechanical Engineering and Robotics Research. 6(5):425-433. DOI: 10.18178/ijmerr.6(5):425-433
- [22] Nowak W, Szul-Pietrzak E, Hachol A. [2014] Wavelet Energy and Wavelet Entropy as a New Analysis Approach in Spontaneous Fluctuations of Pupil Size Study - Preliminary Research IFMBE Proceedings. 41:807-810. DOI: 10.1007/978-3-319-00846-2\_200
- [23] Ismagilov II. [2001] Discrete transforms in basis of piecewise-exponential functions and their properties Izvestiya Vysshikh Uchebnykh Zavedenij. Radioelektronika. 44(3):54-60.
- [24] Ismagilov II. [1996] Slant Rademacher functions: properties and application to the problems of digital signal processing Izvestiya VUZ: Radioelektronika. 39(12):11-16.
- [25] Akhmetvaleev AM, Kataev AS, Shlyemovich MP. [2016] Improving the efficiency of a person's face and eyes detection on a video image during the tasks of contactless detection of potentially dangerous persons Information and Security. 19:4 (4):519-522.
- [26] Paklin NB, Oreshkov VI. [2009] Business analytics: from data to knowledge. St Petersburg: Peter. 624.

## ARTICLE

# THE COMPARATIVE ANALYSIS OF METHODS FOR DETECTING PEDESTRIANS FOR UNMANNED VEHICLES

Rustem R. Ziyatdinov\*, Ravil A. Biktimirov, Ksenia V. Klochkova

*Naberezhnye Chelny Institute of Kazan Federal University, Naberezhnye Chelny, RUSSIA*

## ABSTRACT

Advanced driver assistance systems and unmanned vehicles require an environmental recognition function to make management decisions. To solve such problems, for example recognition of pedestrians, one of the methods of detecting dynamic objects should be used. To date, there are quite a lot of similar methods that differ in the quality and speed of recognition. The use of classical neural network architectures in such problems is of low efficiency. Therefore, to solve the pedestrian recognition problem, the convolutional neural networks were chosen as the main algorithm, since they provide invariance to small changes in input images, such as changing the survey angle, scale, rotation, displacement and other distortions. This paper presents a comparative analysis of methods for detecting objects in pedestrian recognition: SSD, YOLO, HOG + SVM methods. Comparison of these algorithms for the speed of work when recognizing pedestrians in the video stream was made in two modes of operation: using a central processor (CPU) and a graphics processor (GPU). The results of the work showed that the most promising method of detection in pedestrian recognition problems is the Tiny YOLO convolutional neural network method. Good results on the speed of work were also demonstrated by HOG + SVM. The use of GPU allowed to significantly increase the speed of object recognition.

## INTRODUCTION

Recognition of objects is quite a difficult task due to the diversity of both the recognized objects, and the methods used. The need for such systems exists in different areas - from recognition of malfunctions in automated diagnostic systems to the management of unmanned vehicles. Especially, this task is relevant in the development of automated systems for the recognition of the environment for use in advanced driver assistance systems (ADAS) and unmanned vehicles. In this case, the detection methods used must provide high recognition accuracy and real-time operation [1-4].

The object of the study are methods for detecting objects in pedestrian recognition, based on artificial neural networks and providing the ability to perform calculations by the graphics (GPU) or central (CPU) processors. The main advantage of using neural networks for detecting pedestrians is their learning ability based on previously obtained samples of images.

## METHODS

The problems of image recognition most often use classical neural networks (a network of radial-basis functions, a multilayer perceptron, etc.). However, the analysis of experimental data obtained using such networks shows that the use of classical neural network architectures in such problems is of little effectiveness for the following reasons:

- recognizable images often have large dimensions, which leads to an increase in the structure of the neural network;
- a large variety of parameters increases the size of the system, which leads to an increase in the need for a larger training sample and, consequently, an increase in the complexity of computations and the time required for training the system;
- provision of high efficiency of the recognition system requires the use of several neural networks trained with a different order of providing the initial images and the initial values of the synaptic coefficients. This leads to an increase in the complexity of the solution to the problem and the time of its performance;
- high sensitivity to various changes in the geometry of input images, such as changing the shooting angle, image scale and other distortions [5].

Subject to the above facts, to solve this problem of recognition of pedestrians, the convolutional neural networks were used as the main algorithm. This is due to the fact that they have some resistance to small scale changes, angle changes, shifts, turns, and other distortions.

The structure of classical convolutional neural networks contains many layers. These layers, as a rule, are of two types: convolutional and sub-sampling, alternating with each other [Fig. 1].

Neurons located within the layer are organized in the form of a plane. Each of the layers has a set of a corresponding number of planes. In this case, neurons in the same plane have the same synaptic coefficients, connecting them with all the local sections of the previous layer. Each neuron of the layer is connected to the area of the previous layer so that the input image of the previous layer is scanned

**KEY WORDS**  
pattern recognition,  
convolutional neural  
networks, pedestrian  
detection, ADAS  
systems, unmanned  
vehicles.

Received: 21 Oct 2018  
Accepted: 18 Dec 2018  
Published: 6 Jan 2019

\*Corresponding Author  
Email:  
rust.kfu@gmail.com  
Tel.: 9534874499



through a small window. Then it is passed through the system of synaptic coefficients and fixed by the corresponding neuron of the current layer. The plane sets are feature maps, and each plane finds the corresponding parts of the image on the previous layer. The size of the scanning window is determined at the stage of development of the neural network.

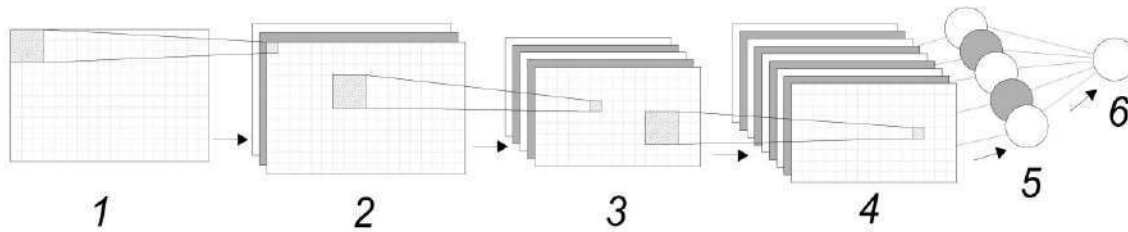


**Fig. 1:** The architecture of convolutional neural networks.  
1 - input; 2,4 - convolutional layers; 3 - sub-sample layer; 5 - fully connected layer; 6 - neural network output.

The sub-sample layer reduces the dimensionality of the generated feature maps by locally averaging the values of the neuron outputs. As a result of this operation, the network becomes more invariant to the size of the input image. The map on each subsequent layer decreases in size, but the number of feature cards increases. This leads to the ability to recognize complex feature hierarchies [5].

Gradually, the neural network learns to distinguish the key characteristics of the necessary patterns in the incoming images. The responses of the neural network form maxima in the locations of these images [Fig. 2] [5, 6].

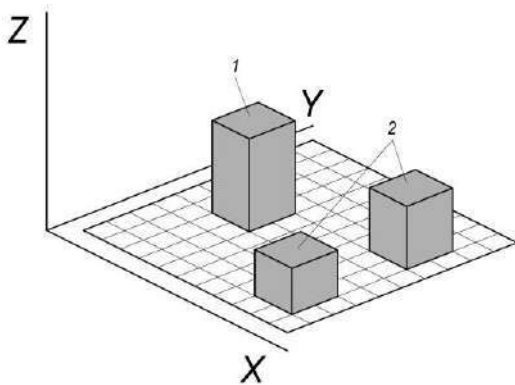


**Fig. 2:** Feedback from a convolutional neural network.  
1 - the most probable position of the source pattern on the image; 2 - the least likely pattern finding on the image (noise).

The most significant limitation in the development of neural network algorithms is the extremely high computational cost of implementing these methods. The main and traditional ways to address this problem include the organization of distributed and parallel computing using specialized hardware, such as systolic neural processors, neural chips, distributed cluster systems, programmable logic integrated circuits (PLD), and GRID technologies.

A Compute Unified Device Architecture (CUDA) was designed to use graphics processors (GPU) to accelerate scientific and engineering calculations and perform various computations comparable in performance to cluster systems [7, 8]. The main difference between these architectures is the following: the execution of commands on the cluster takes place according to the MIMD architecture (each processor independently executes a different set of instructions, processing different data sets), and in the CUDA environment it is characterized by the SIMD architecture (a number of processors execute the same set of commands over different data, for example, array elements).

For convolutional neural networks, NVIDIA developed the CUDA Deep Neural Network (cuDNN) library. Unlike NVIDIA CUDA, which provides the ability to perform various calculations on the GPU, the cuDNN library is designed specifically for training deep neural networks. This library contains the optimized for the graphics processors implementation of convolutional and recurrent networks, various activation functions (sigmoidal, semilinear, hyperbolic tangent), back propagation algorithm, etc. cuDNN allows training neural networks on graphics processors several times faster than just CUDA.

## RESULTS AND DISCUSSION

As the main models of convolutional neural networks for pattern recognition in the image, the following were used:

1. SSD: Single Shot Multi Box Detector. An object detection system with a single network based on Caffe – the framework for deep learning. This approach is based on dividing the output space of the bounding rectangles into a set of standard fields with different proportions and scales for each feature card. In forecasting, this method calculates the probability of having each category of objects in each such field and makes its corrections to better match the shape of the object [9].
2. YOLO: You Only Look Once. An advanced online object detection system, which uses a multiscale method of learning convolutional neural networks. YOLO can work with images of different sizes, offering a compromise between speed and accuracy [10].
3. HOG + SVM. To compare the speed of convolutional neural networks with classical classification algorithms, a pedestrian recognition system consisting of the HOG (Histogram of Oriented Gradients) algorithm, necessary for preliminary search for a pattern in an image and SVM (Support Vector Machine) classifier, is used to recognize the found assumptions [11].

For training, the COCO Image Dataset (for the Tiny YOLO convolutional neural network) and INRIA Person Dataset (for the SVM classifier) were used.

The results of using the pedestrian detection method are shown in [Fig. 3].



**Fig. 3:** shows the results of using pedestrian detection methods (from top to bottom): SSD, YOLO, HOG+SVM.

Comparison of these algorithms for the speed of work when recognizing pedestrians in the video stream was made in two modes of operation: using a central processor (CPU) and a graphics processor (GPU). To test the algorithms, various pre-trained models of convolutional neural networks and the SVM classifier were used. Compilation of the source code of programs was carried out in Visual Studio 2013 using Microsoft Visual C++ 2013.

The testing of the received programs was carried out on a computer with a 2GB video card NVIDIA GeForce GTX 950M, with an Intel Core i5-7200U processor and 8GB RAM. The original resolution of the test video: 640x360 pixels. This comparison does not take into account the accuracy of recognition, and the key emphasis is on the speed of the algorithms and the maximum number of frames per second. For each method, the detected image is considered positive at the threshold of 0.5.

The results of testing the methods are given in [Table 1].

**Table 1:** Results of comparison of the pedestrian detection methods

Method	The model used	Operating mode	Method operating time, msec	Number of frames per second
HOG+SVM	OpenCV	CPU	105	9.5
		GPU	33	29.4
YOLO	Tiny YOLO	CPU	525	1.9
		GPU	22	43
	YOLOv2 416x416	CPU	2250	0.43
		GPU	63	15.8
	YOLOv3-320	CPU	2605	0.38
		GPU	95	10.2
	YOLOv3-416	CPU	4942	0.20
		GPU	137	7.2
SSD	PASCAL VOC COCO	CPU	2269	0.43
		GPU	83	10.6
	PASCAL VOC 07+12	CPU	2215	0.45
		GPU	82	10.7
	PASCAL VOC 07++12	CPU	2317	0.42
		GPU	103	9.2
	ILSVRC2016	CPU	2833	0.35
		GPU	115	8
	COCO	CPU	2453	0.40
		GPU	98	9

The columns in [Table 1] show:

- Method: methods used;
- The model used: the used pre-trained model;
- Operating mode: the mode of operation of the compiled program (on a graphics processor (GPU) or using CPU resources);
- Method operating time: operation time of the method in milliseconds (not subject to the time of additional actions for preliminary and post-processing of images);
- Number of frames per second: the maximum number of frames per second for the video stream.

## CONCLUSION

The results of testing these methods for detecting pedestrians in a video stream shows that the use of the GPU improves the speed of operation by an average of more than 25 times.

The best model without considering the accuracy of speed recognition is the Tiny YOLO convolutional neural network algorithm with 43 frames per second. The classic SVM classification algorithm also showed a high result with 29 frames per second. The low speed of the other models of convolutional networks is due to a large pre-trained model and a large number of layers embedded in their architecture. Using a more powerful graphics card in conjunction with the processor will allow these algorithms to be used in real-time operation.

The Tiny YOLO and HOG + SVM methods of the convolutional neural network can be used to detect various objects (cars, pedestrians, etc.) in the implementation of automated systems for the recognition of the environment for unmanned vehicles and advanced driver assistance systems. This will improve the safety of driving and reduce the number of road accidents.

## CONFLICT OF INTEREST

There is no conflict of interest.

## ACKNOWLEDGEMENTS

The work is performed according to the Russian Government Program of Competitive Growth of Kazan Federal University.

## FINANCIAL DISCLOSURE

None

## REFERENCES

- [1] Ziyatdinov RR, Biktimirov RA, Klochkova KV. [2017] The comparative analysis of classification of algorithms in the problems of pattern recognition. *Journal of Fundamental and Applied Sciences*, [S.l.]. 9(1S):1790-97,1112-9867.
- [2] Ziyatdinov RR, Mukhametzyanov VR, Nabiullina GI. [2015] Application of neural networks for the diagnosis of depth sucker rod pumps *International Journal of Applied Engineering Research*. 10-24(1):45022-26.
- [3] Sharafieva LN, Ziyatdinov RR. [2016] Application of artificial neural network in the problems of diagnosis of borehole pumps *Information Technology. Automation. Actualization and solving the problems of training highly qualified personnel: Proceedings*

- of the international conference Naberezhnye Chelny. 83-87. (in Russian)
- [4] Ziyatdinov R, Shigabiev R, Talipov D. [2017] Automated road marking recognition system. IOP Conf. Series: Materials Science and Engineering. 240. 012070 doi:10.1088/1757-899X/240/1/012070.
  - [5] Yu N, Notkin BS, Sedov VA. [2009] Neuro iterative algorithm of tomographic reconstruction of the distributed physical fields in the fibre optic measuring systems Computer optics. 33(4):446-455.
  - [6] Wilson DR, Martinez TR. [2004] The general inefficiency of batch training for gradient descent learning, Neural Networks. 16(4):1429-1451.
  - [7] Fatica M. [2009] CUDA for High Performance Computing: materials of HPC-NA Workshop 3.
  - [8] FASTR: Belgian researchers develop desktop supercomputer. Available at: <http://fastra.ua.ac.be/en/index.html> (accessed 15 April 2018).
  - [9] SSD: Single Shot Multi Box Detector. Available at: <https://github.com/weiliu89/caffe/tree/ssd> (accessed 17 April 2018).
  - [10] YOLO: Real-Time Object Detection. Available at: <https://pjreddie.com/darknet/yolo/> (accessed 24 April 2018).
  - [11] Open CV: Open Source Computer Vision Library. Available at: <https://opencv.org/> (accessed 01 April 2018).

## ARTICLE

# METHODS AND ENVIRONMENTAL ASPECTS OF UTILIZATION OF ASPHALTENE SEDIMENTS AS A HARD WASTE OF THE OIL PRODUCING INDUSTRY

Alim F Kemalov, Dinar Z Valiev\*, Ruslan A Kemalov

*Institute of Geology and Petroleum Technologies, Kazan Federal University, Kazan, RUSSIA*

## ABSTRACT

*In this paper, possible methods for the prevention and disposal of waste asphaltene sediments (AS) are systematized. The practical importance of the rational use of existing methods for prevention of AS sediments occurrence, as well as the recycling methods are represented. The practical value is considered by the example of the Unvinskoye oilfield, enterprises of the Russian Federation and the USA. The formation of wastes from asphaltene sediments is possible during the drilling of wells, as well as in the course of operation during the overhaul of wells and cleaning of drainage tanks. This type of waste is mostly paraffinic, so a mechanical method of prevention (scrapers) is adopted. This paper summarizes the existing technologies for utilization and processing of sludge using them as alternative energy sources. The problem of their utilization is now solved by processing in the existing scheme for the preparation of commercial oil. Full utilization of liquid petroleum wastes, even at a single enterprise, ensures a reduction in the total amount of petroleum wastes by more than 70% and the return of marketable oil to resource turnover. The paper presents the results of calculations of waste generation during construction and operation. We also considered classification of hazardous waste to the environmentally dangerous. Promising areas of processing asphaltene sediments are presented.*

## INTRODUCTION

The most important environmental problem at present is the management of waste contaminated with oil and oil products [1].

The output of oil sludge in refineries is about 7 kg / ton of refined oil. These heavy oil residues contain on average 10-56% of petroleum products, 30-85% of water, and 1.3 - 4.6% of solid impurities. Based on the list of wastes it follows that the problem of handling such wastes as oil sludge is relevant for enterprises of many industries. The problem is compounded by the fact that industrial wastes containing petroleum products are toxic and flammable, and there are practically no efficient technologies for their processing or disposal. Due to their high danger they are not accepted for burial at city dumps. Therefore, sludge is accumulated in the territories of enterprises, is stored in sludge caps, earth storages, etc. being a permanent, chronic source of environmental pollution (EP). Processing and disposal of oil sludge is an important environmental and economic challenge [2]. Considering the problem of oil sludge utilization, it should be noted that oil sludge is also a valuable secondary material resource [3], a potential source of additional raw materials that can be processed to extract useful products or used as fuel. Using it as a raw material is one of the rational ways of its disposal, since it achieves a certain environmental and economic effect [4]. According to the state of aggregation, oil waste can be divided into liquid and solid ones [Fig. 1].

Of the greatest commercial interest is liquid oil waste which represents water-oil emulsions with an oil content of up to 90% wt. The problem of their utilization is now solved by their reprocessing in the existing scheme for commercial oil treatment. Full utilization of liquid oil waste, even at a single enterprise, ensures a reduction in the total amount of oil waste by more than 70% and the return of marketable oil to resource turnover [5].

All solid oil waste generated at the stages of production, treatment and transportation of oil and gas can be divided into three types: repair waste, asphaltene sediments (AS); ground oil waste. The composition of oil waste directly depends on the result of what operation they are formed [Table 1].

In practice, most often all types of waste, regardless of their state of aggregation and composition, are jointly collected in accommodation facilities (excluding some liquid oil waste disposed of at special facilities) [2]. Therefore, traditionally, the processing of oil waste is carried out by technologies "at the end of the pipe", which do not contribute to the differentiation of waste streams at the stage of formation and increase the proportion of the oil that can be used as secondary resources.

## METHODS

The methods used to control deposits in oil field equipment are determined by the specific conditions of the field and suggest two directions: prevention of formation and removal of already formed sediments [6]. The classification scheme for methods for controlling asphaltene sediments is presented in [Fig. 2].

## KEY WORDS

asphaltene sediments,  
ecology, waste, sludge,  
disposal, methods.

Received: 19 Oct 2018  
Accepted: 18 Dec 2018  
Published: 6 Jan 2019

\*Corresponding Author  
Email: valievdz@bk.ru  
Tel.: + 79274367606



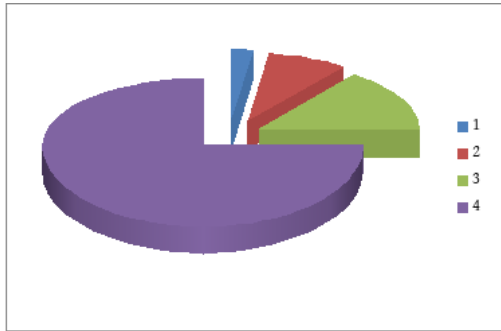


**Fig. 1:** The structure of oil waste oil and gas companies: 1 - maintenance waste; 2 - asphaltene sediments; 3 - ground oil waste; 4 - liquid oil waste.

**Table 1:** Classification of oil waste of an oil and gas production enterprise

Waste name	Technological process which generates waste	Composition of oil waste	% by weight
Solid Oil Waste			
Maintenance waste (asphaltene sediments + ground oil waste)	Well repair. Stripping of oil storage tanks	Organic substances Mechanical impurities Water	25-35 20-45 30-45
Asphaltene sediments	Repair of a well with steam cleaning of production tubing	Organic substances Mechanical impurities Water	50-93 5-49 1-5
Ground oil waste	Cleaning the area after a pipeline rupture in a warm season. Oil spill	Organic substances Mechanical impurities Water	15-20 45-65 20-35
Liquid oil waste			
Intermediate layer	Storage of oil in tanks	Organic substance Mechanical impurities Water	80-90 0-10 1
Oil polluted snow	Pipeline ruptures	Organic substance Mechanical impurities Water	2-10 40-60 38-50

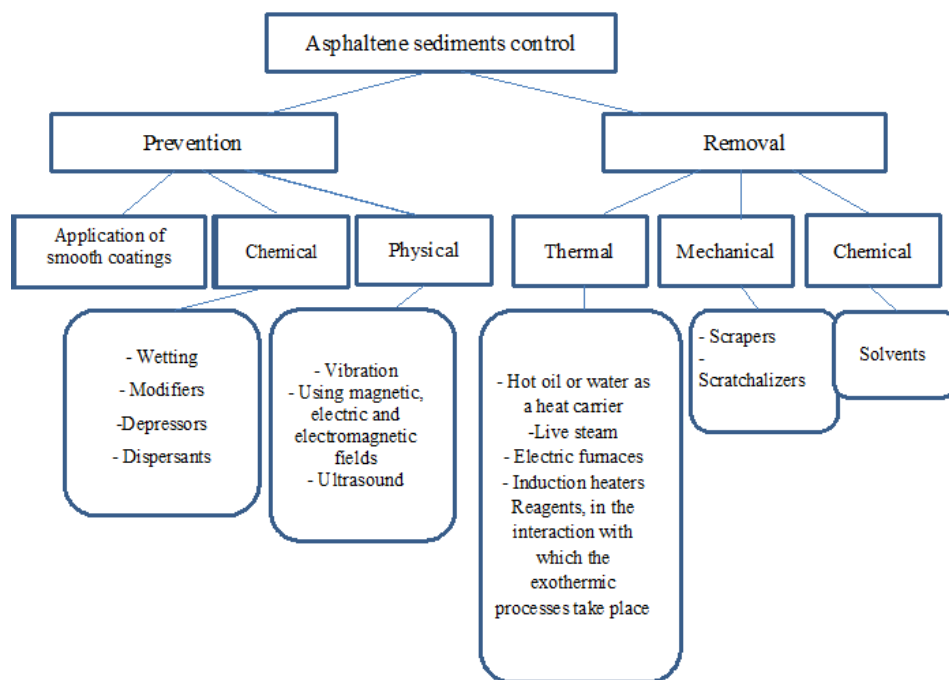


**Fig. 2:** Scheme for classification of asphaltene sediments control methods.

## Ways to prevent formation of deposits

Under conditions of intensive formation of paraffin deposits, the inter-cleaning operation period of a well is significantly reduced (less than 30 days), the number of washes with heated agents or hydrocarbon solvents increases, what leads to an increase in oil production costs and a negative impact on the bottom-hole formation zone [7]. In such operating conditions, the best method to control asphaltene sediments is to prevent them by application of protective coatings, physical methods or special chemicals [8], [9], [10].

## Methods of asphaltene sediment removal

The removal of asphaltene sediments can be carried out by a variety of methods, among which there are:

- thermal methods: flushing the downhole equipment with hot oil, creating a local heat flux using submerged electric heaters, heating cable lines or high-frequency electric field;
- chemical methods: removal with solvents and technical detergents;
- physical methods: destruction by ultrasonic action;
- biological methods: elimination using aerobic and anaerobic bacteria.

This classification of methods for controlling paraffin deposits is based on practical methods for removing or preventing the formation of deposits.

## RESULTS

To consider the formation of oil waste and their disposal in practice, the calculation of the formation of asphaltene sediments during the well construction and infrastructure development at the multiple-well platform of the Unvinskoye oilfield (at the stage of developing project documentation) [11], [12] was made.

To prevent the formation of asphaltene sediments in the wellbores, semi-automatic dewaxing mechanisms of the SDU-80 type are provided. When drilling wells of the multiple-well platform, the formation of asphaltene sediments may occur during the process of cleaning the drainage tank. In the course of operation, asphaltene sediments may be formed as a result of workover of wells. The calculation of waste generation is presented in [Table 2].

**Table 2:** Calculation of waste generation during construction and operation

Item. No	Waste name	Oil slime quantity, t / year
For the period of drilling		
1	Sludge from cleaning pipelines and tanks (barrels, containers, cisterns, road aids) from oil	13,500
For the period of construction and operation		
2	Waste from the extraction of oil and gas (asphaltene sediments, fuel oil contaminated soil)	1,062
3	Sludge from pipelines and tanks (barrels, containers, cisterns, road aids) from oil	0.162

In order to reduce the environmental impact of a waste, this waste has to be disposed of. According to the contract of a contracting organization, they are transferred to an enterprise that is capable of utilizing this type of waste. According to the norms and rules of transportation, waste is transferred to the organization with a passport for the type of asphaltene sediment waste in a certain amount specified in the contract.

To prevent the formation of asphaltene sediments, at the Unvinskoye field in the Perm region of the Russian Federation (RF) [11], semi-automatic mechanisms for dewaxing of wells were provided (mechanical method). The waste generated during the repair of wells and the cleaning of drainage tanks were transferred to the technological site, where the work technology provided for their saturation with commercial oil and their further use. This solution made it possible to avoid the release of hazardous waste into the soil and water bodies, and emissions from the source of pollution were minimized, too.

An example of the enterprise that can utilize, recycle and neutralize this type of waste is "Priroda-Perm" LLC. One of those technologies is the saturation of asphaltene sediments with commercial oil (microbiological remediation technology). The technology has already been introduced at the Yarino-Kamenolozhskoye oil field in the Perm Territory.

[Fig. 3] presents a diagram of the main possible ways on processing and using wastes of asphaltene sediments.

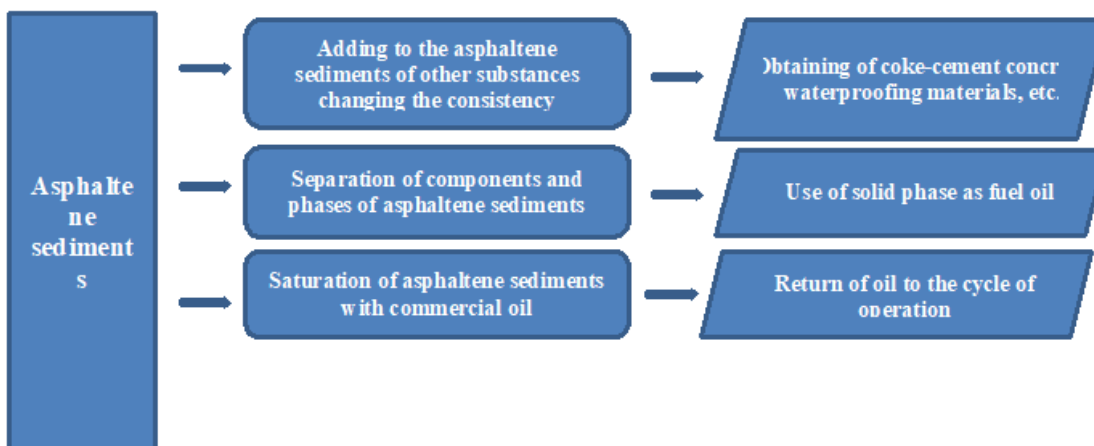


Fig. 3: Possible ways of reprocessing of asphaltene sediments.

At present, it is known, for example, that in the Republic of Tatarstan in the Russian Federation the JV Tatoiilgaz has built for the processing of oil waste an installation using the technology in which the waste was divided into water and solid sludge. The latter contains up to 5% of oil, the rest is dry black powder, which is used as a road surface.

Experimental studies have shown that the use of ground oil waste with asphaltene sediments and lime in certain proportions allows obtaining a waterproofing material for covering solid waste landfills with high physico mechanical properties [11], [13]. New schemes and technologies are being developed for processing this waste and methods of its secondary use, reducing its negative impact on the environment.

## DISCUSSION

The currently existing numerous methods of dealing with paraffin deposition can significantly increase the inter-cleaning period for a well, but it is not possible to completely avoid the formation of deposits. Therefore, when carrying out routine and capital repairs of wells and pipelines or other technological operations, a mechanical sweeping (or steaming) of oilfield equipment is a necessary condition. As a result, a significant amount of solid oily waste is generated. As a rule, asphaltene sediments make up about 80% of the total amount of solid oil-contaminated waste generated [14].

From an environmental point of view, the chemical aggressiveness of deposits against environment is determined by the resins and asphaltenes contained in it. Carcinogenic polycyclic aromatic hydrocarbons containing sulfur, oxygen, nitrogen and trace elements are concentrated in asphaltene sediments. The latter can be divided into 2 groups: non-toxic (silicon, iron, calcium, magnesium, phosphorus, etc.) and toxic (vanadium, nickel, cobalt, lead, copper, molybdenum, etc.), affecting living organisms as poisons. Accordingly, the use of a single integral indicator relative to asphaltene sediments may affect the results of the obtained calculations of the hazard class, distorting them to lower values. Therefore, the determination of the hazard class of asphaltene sediments, taking into account the expanded list of indicators, is an urgent task both in terms of the correctness of hazard class calculations and for choosing a rational and safe temporary storage, disposal or recycling of this type of waste.

The organic component of asphaltene sediments can be considered as an alternative source of raw materials for petrochemical products. So, in the USA, the technology of cleaning asphaltene sediments was implemented according to the scheme: deasphalting and tertiary treatment at a refinery with obtaining high-quality white paraffins and high-melting ceresins or paraffin-ceresin compositions. However, the processes of isolating individual components or a mixture of substances are complex, time consuming, lengthy and costly. In this case, of the greatest interest is the possibility of using the purified heavy oil deposits without separation as a component of various industrial products or, realizing the principle of asphaltene sediments recovery, the return of some materials for reuse in the same process [6], [15].

Of particular interest in this context is the possibility to return of previously cleaned asphaltene sediments to commercial oil, which, on the one hand, increases the likelihood of re-precipitating heavy components of oil during its transportation through main pipelines. On the other hand, depending on the mass of the asphaltene sediments introduced into the oil, its quantitative yield increases and, accordingly, the financial benefit for a production enterprise increases. But the most important thing is the circulation of these substances is thus carried out, without the formation of asphaltene sediments as oil waste.

Existing to date developments on the involvement of the organic part of the deposits as raw materials for the production of a number of products are presented in [Table 4].

**Table 4:** Perspective directions of reprocessing the asphaltene sediments

Directions of reprocessing	Composition of the product	Application area
Preservative lubricant manufacturing	Petrolatum 10-20% in asphaltene sediments 80-90%, Anticorrosive additive MNI-7 0.9-1.1%	Protection of metal structures against corrosion
Rope grease	Plasticizer PN-6k-15-25%; ceroxone amide -3-7; asphaltene sediments - 20-40%; petroleum oil - up to 100%.	Lubrication of steel cables to reduce friction and wear between the individual strands of steel cables with friction mechanisms, as well as to prevent corrosion.
As a component in the production of insulation and construction bitumen	Additive 20-30% of asphaltene sediments to bitumen	Road, industrial and civil construction, the production of soft roofing and waterproofing materials, and other industries.
Waterproof roofing material	Water up to 15% wt.; Oil sludge (asphaltene sediments) - 50- 60% wt. and ceramsite cinder - 40-50% wt.;	As a material for soft roofs, as well as waterproofing basements and foundations
Waterproofing screen for landfills	Clay 45-50%, sand 15-20%, lime 10-15%, asphaltene sediments 20-25%.	Watertight material with hydrophobic properties that reduce the emission of seepage water
Waterproofing coating	Asphaltene sediments 40-50% LDPE waste 60-50%	Watertight material with hydrophobic properties
Solid carbon-containing fuel (composition for briquetting fuel)	Peat 1-10% coal, asphaltene sediments 1-40% coal 72-78%, asphaltene sediments 22-28%	For use in the fuel industry and for domestic needs

The presented directions for using asphaltene sediments are determined, first of all, by their specific properties due to their composition. Accordingly, asphaltene sediments have anti-corrosion properties and can be used as protective coatings, with good adhesion to the surface due to the presence of surfactants [6].

Therefore, a possible direction of disposal of asphaltene sediments that can be considered is using them as a basis for the preparation of special conservation coatings, for example, as alternatives to film-forming inhibited oil compositions.

## CONCLUSION

In order for such type of waste as asphaltene sediments could not form, works are provided for to prevent the formation of deposits and their removal. Despite the numerous methods for controlling asphaltene sediments, there is no universal and effective one, since the deposits differ significantly by their properties and composition, what makes it necessary to constantly search for the best methods to prevent and remove asphaltene sediments. Considering the methods of waste disposal, we can say that most enterprises transfer waste to specialized organizations, and do not use it as a secondary raw material. The activities of enterprises engaged in the processing of asphaltene sediments are mainly aimed at turning this type of waste into commercial oil and its reusing.

In connection with the foregoing and with unfavorable trends associated with a decrease in oil reserves and the difficulties of its production, as well as a decrease in the raw material base of components for preservation materials, asphaltene sediments can be considered as valuable, affordable and cheap raw material due to their high organic content and useful properties.

The search for directions on reprocessing asphaltene sediments is particularly relevant in the context of expanding the resource base in the Russian Federation of heavy highly viscous and high-paraffinic oils, with a high content of resins, asphaltenes and paraffins prone to sedimentation, the production of which will be accompanied by the formation of substantial amount of asphaltene sediments.

The development and implementation of resource-saving technologies for the disposal of asphaltene sediments with the production of popular products is an important national economic task. Its solution will, on the one hand, reduce the technogenic load on natural geosystems by reducing the number or elimination of oily waste sites, and on the other hand, will ensure a more rational use of non-renewable natural resources by replacing primary raw materials with secondary ones.

### CONFLICT OF INTEREST

The authors declare no conflict of interest relating to the material presented in this paper.

### ACKNOWLEDGEMENTS

The work is performed according to the Russian Government Program of Competitive Growth of Kazan Federal University. This work was funded by the subsidy allocated to Kazan Federal University for the state assignment in the sphere of scientific activities (10.7636.2017/7.8).

### FINANCIAL DISCLOSURE

None

## REFERENCES

- [1] Yagafarova GG et al. [2010] Modern methods of sludge processing, Chemistry, 190.
- [2] Zharov OA, Lavrov VL. [2004] Modern methods of oil sludge processing, Ecology of production. 5:43-51.
- [3] Yagafarova GG, Nasyrova LA, Shakhova FA, et al. [2007] Engineering ecology in the oil and gas complex. Ufa: UGNTU Publishing House. 334.
- [4] Mastobaev BN, Yagafarova GG. [2008] Impact of the oil industry on the state of environment. Actual problems of technical, natural and human sciences: materials of the International Scientific and Technical Conference. Ufa: Publishing house UGNTU. 279.
- [5] Valinejad R, Nazar AR. [2013] An experimental design approach for investigating the effects of operating factors on the wax deposition in pipelines. Solaimany Fuel. 106:843 – 850.
- [6] Miller VK. [2016] An integrated approach to solving the problem of asphaltene sediments from highly-watered oils (for example, oil fields in Udmurtia): thesis of the candidate of technical sciences: 02.00.13 / Veronika Konstantinovna Miller. Moscow. 196.
- [7] Mosheva AM. [2014] Overview of the main methods of dealing with asphaltene sediments and methods for estimating reliability parameters for discharge lines to oil fields. Problems of development of hydrocarbon and ore mineral deposits. 1:253-255.
- [8] Kelechukwu EM. [2010] Influencing factors governing paraffin wax deposition during crude production, International Journal of Physical Sciences. 5(15):2351-2362.
- [9] Gavriyuk YuA et al. [2014] Experience of using fiberglass tubing in the fields of Udmurtneft OJSC. Scientific and Technical Bulletin of Rosneft. 1:44-48.
- [10] Kemalov AF, Kemalov RA, Valiev DZ. [2013] Study of the structure of complex structural units of heavy oil from Zyuzeevskaya field by NMR relaxometry and rheological studies. Oil Industry. 2: 63-65.
- [11] Karataeva SV. [2014] Possible methods and ways of utilization of waste oil industry (for example, asphaltene sediments), SV Karataeva, Bulletin of PNRPU. Geology. Oil - gas and mining industry. 10:114-120.
- [12] Lu X, Redelius P. [2006] Compositional and structural characterization of waxes isolated from bitumens. Energy & Fuels. 20:653-660.
- [13] Akbarzadeh K et al. [2005] Association Behavior of Pyrene Compounds as Models for Asphaltenes. Energy & Fuels. 19:1268-1271.
- [14] Acevedo S, et al. [2007] Relations between asphaltene structure and their physical and chemical properties: the rosary-type structure. Energy & Fuels. 21:2165 – 2175.
- [15] Kyeongseok Oh. [2004] Asphaltene aggregation in organic solvents. Oh Kyeongseok, A Ring Terry, D Deo Milind. Journal of Colloid and Interface Science. 271:212 – 219.



## ARTICLE

# IMPROVED METHODS OF MONITORING AND MANAGING THE MOVEMENT OF URBAN PASSENGER TRANSPORT

Ilnar F. Suleimanov<sup>1\*</sup>, Elena V. Moskova<sup>1</sup>, Igor I. Lyubimov<sup>2</sup>, Aleksey N. Melnikov<sup>2</sup>, Vladimir I. Rassokha<sup>2</sup>

<sup>1</sup>Naberezhnye Chelny Institute of Kazan Federal University, Kazan, RUSSIA

<sup>2</sup>Orenburg State University, Orenburg, RUSSIA

## ABSTRACT

Research is focused on improving quality of urban passenger transport (UPT) service by assessing and eliminating the negative consequences arisen in the process of vehicles operation on routes. The improvement of the proposed methodology is based on the existing theories of road transport operation, passenger transportation, decision-making theory and the provisions of the system analysis. The selection criterion for backup vehicle based on its search and dispatching to the origin of emergency situation (ES) has been developed. At the same time, the search should be carried out both among the backup vehicles of the park, the central dispatch service (CDS), and among the vehicles operating on routes. Expert assessments of the time spent by control system in processing information and making a decision have been formed. Time estimates of movement of the backup vehicle directed from the route to the place of ES are received. Methodology for estimating the efficiency of control system implementation based on assessment of the main indicators of the reliability of the urban passenger transportation system is proposed, which makes it possible to evaluate its basic reliability indicators. The reliability of the research is based on the analysis of sufficient number of sources directly related to the research topic.

## INTRODUCTION

Selection criterion for backup vehicle is the minimum expected time of arrival of backup vehicle at place of emergency with restriction: passenger capacity of the backup vehicle should not be less than required. We consider all options for searching backup vehicle - on the line, in the reserve of the park, in the reserve of central dispatch service [1].

In case of emergency situation, search and supply time of vehicle of the operational reserve  $T_s$ , it is necessary to evaluate the following components:  $T_{sit}$  - time spent on obtaining information about the situation that has arisen;  $T_{ass}$  - time spent on assessing the situation by criteria;  $T_r$  - time spent on searching and selection of alternative capabilities of the backup vehicle;  $T_d$  - delay time, which passes from the moment when dispatcher takes a decision till the selected backup vehicle starts to move to the place of ES occurrence;  $T_{mov}$  - time of the backup vehicle movement to the target [2].

## METHODS

On the basis of the existing control system of urban passenger transport in the city of Orenburg, as well as taking into account review of the analysis of modern foreign and domestic control systems, assessments of possible values of variables  $T_{sit}$ ,  $T_{ass}$ ,  $T_r$ ,  $T_d$  on a three-point scale of qualitative assessments a) "perfectly" b) "satisfactorily" c) "unsatisfactorily" were formed (adopted at the level of expert) to characterize operation of the control system during ES.

The rating "perfectly" corresponds to the best achievable indicators when using modern technologies and techniques.

If the control system in ES spends no more than one minute to report the occurrence of the ES, and for one minute to assess the situation, analyze alternative options, make a decision and report the decision to the executor, then such actions of the control system deserve the rating "perfectly".

Based on the analysis of graphs of values estimating waiting time of the backup vehicle, it is assumed that if this value does not exceed 3 minutes, then the operation of the vehicle reservation system can also be evaluated as "perfect". In the accepted designations, waiting time for the departure of the backup vehicle (delay time) is  $T_d \leq 3$  [3, 4].

The satisfactory rating should correspond to the situation in which mobile communication systems are used to ensure the transmission of message to the control center while the vehicle is in the zone of final destination (FD), as well as the stationary communication facilities of linear central dispatch service, using automated control technologies. The following values of the variables are adopted for the assessment "satisfactory":

Time for communication with the center  $T_{sit} \leq 5$ ; Time to assess the situation  $T_{ass}$ , search for alternatives  $T_{ass} \leq 3$ . Time for decision making and information transfer to the performer  $T_r \leq 3$ . Delay time. Then

## KEY WORDS

control system,  
passenger  
transportation, road  
transport, reliability,  
dispatching.

Received: 20 Oct 2018  
Accepted: 18 Dec 2018  
Published: 6 Jan 2019

## \*Corresponding Author

Email:  
ecolog\_777@mail.ru  
Tel.: 89179045977

sum of the values of the variables  $[T_c + T_{ass} + T_r] \leq 5 + 3 + 3 \leq 11$ . Waiting time of the backup vehicle  $T_d \leq 7$ .

The Unsatisfactory rating corresponds to the situation in which traditional automated control technologies are used, as well as stationary communication facilities of linear central dispatch service, without using mobile communication and navigation.

The following values are adopted for «unsatisfactory» variables:

Time for communication with the center  $T_{sit} \leq 15$ ; Time to assess the situation, search for alternatives  $T_{ass} \leq 5$ . Time for decision making and information transfer to the performer  $T_r \leq 5$ .  
 $[T_{sit} + T_{ass} + T_r] \leq 15 + 5 + 5 \leq 25$ .

The delay time for the backup vehicle departure  $T_d \leq 15$  (a small number of vehicles on the routes, lack of reserves in the park at the time of the emergence). The resulting values of assessments are presented in [Table 1] [5, 6].

Let us proceed to estimation of variable  $V_A = V_A(t, d)$  - average speed of vehicle depending on the time of day  $t$  and day of week  $d$ . This dependence of the vehicle speed in a modern city is determined by the characteristics of the transportation flow, which are dependent on the time of day  $t$  and day of the week  $d$ .

**Table 1:** Adopted estimates of the characteristics of the control system and the reservation system

The adopted rating	Characteristic of the control system "time Consumption in the control system": the sum of the values of variables $[T_{sit} + T_{ass} + T_r]$ , evaluating the quality of the communication system and the control system, min.	Characteristics of the reservation system " time Spent waiting for a free backup vehicle» The value of the variable $T_d$ , evaluating the redundancy system vehicle, min.
«perfectly»	$1+1+1 \leq 3$	$\leq 3$
«satisfactorily»	$5+3+3 \leq 11$	$\leq 7$
«unsatisfactorily»	$15 + 3 + 3 \leq 21$	$\leq 15$

In accordance with [7], the transportation flow is divided into six groups according to vehicle speed characteristic: 1) free; 2) stable; 3) almost stable 4) close to unstable; 5) unstable; 6) constrained.

Performance characteristics of urban streets, depending on the characteristics of the traffic flow [Table 2].

Thus, having determined characteristics of the transportation flow for each route of backup vehicle, depending on the time of day  $t$  and weekday  $d$ , on the basis of the relation (1), the required estimate of the traveled distance was obtained by substituting instead of  $V_A$  its value from [Table 2].

$$S_s = \frac{1}{2D_1 D_2} \quad (1),$$

где  $S_s$  - the area of search,  $D_n$  - the diagonal of a square search.

**Table 2:** The operational performance of urban streets

Characteristics of traffic flow	The speed of movement of the vehicle on a city street, km/h
A Free	$\geq 48$
B Stable	$\geq 40$
C Almost stable	$\geq 32$
D Close to the unstable	$\geq 24$
E Unstable	$\approx 24$
F Constrained	$< 24$

Combining the results of the control system and traffic situation analysis, we will obtain generalized characteristics of the control system at liquidation of ES consequences under various conditions [Table 3].

When considering the vehicle location, the following assumptions are made: 1) all vehicles are equipped with either satellite or local navigation; 2) The location of the vehicle must be determined by the navigational data received by the system. In this case, method of determining the vehicle location depends on what type of navigation equipment is installed on the vehicle's board.

**Table 3:** Generalized description of the capabilities of the control system and the backup system of the vehicle at liquidation of consequences of ES

Evaluation of the characteristics of the control system and the reservation system of the vehicle	Characteristics of the control system "time Spent in the control system", min.	Characteristics of the reservation system "time Spent waiting for a free standby vehicle", min.	Characteristics of traffic flow	The speed of movement of the vehicle on a city street, km/h
«perfectly»	≤ 3	≤ 3	Free	≥48
			Stable	≥40
			Almost stable	≥32
			Close to the unstable	≥24
			Unstable	≈24
			Constrained	<24
«satisfactorily»	≤ 11	≤ 7	Free	≥48
			Stable	≥40
			Almost stable	≥32
			Close to the unstable	≥24
			Unstable	≈24
			Constrained	<24
«unsatisfactorily»	≤ 21	≤ 15	Free	≥48
			Stable	≥40
			Almost stable	≥32
			Close to the unstable	≥24
			Unstable	≈24
			Constrained	<24

Calculation should be carried out stepwise in the following sequence.

- 1) Calculation of probability of vehicle arrival at each FD for each route in the standby vehicle search area at time l (one minute), depending on the period of the day.
- 2) Calculation of waiting time of vehicle at each FD in the standby vehicle search area with a probability of at least 0.95.

The ratio (2) is taken as the basis for calculating the delay time for the arrival of reserve vehicles at the place of ES occurrence.

$$P(T_{d=t}) = \sum_{i=1}^m P A_i(t) - \sum_{i=1}^m \sum_{j=1}^m (P A_i(t) P A_j(t)) + \sum_{i=1}^m \sum_{j=1}^m \sum_{k=1}^m (P A_i(t) P A_j(t) P A_k(t)) + \dots \quad (2)$$

$$\dots + (-1)^{m+1} (P A_1(t) P A_2(t) \dots P A_m(t))$$

where  $P(T_{d=t})$  - probability of arrival of the vehicle at least on one of m routes to the FD in Td minutes; - probability of arrival of vehicle at the i-th FD in t minutes.

Necessary calculations of the probabilistic characteristics of the routes were carried out by the example of the municipal state-owned enterprise "Orenburg Passenger Transportation" of the city of Orenburg. The calculation of the probabilities for all routes is based on the ratios (3, 4).

$$t_{int_i} = \frac{t_{ret_i}}{n_i(t)} \quad (3)$$

where  $t_{int_i}$  - estimated time of the movement interval, min.;  $t_{ret_i}$  - turnaround time, min..

$$P(A_1(t) \cup A_2(t) \cup \dots \cup A_m(t)) = P(A_1(t)) + P(A_2(t)) + \dots + P(A_m(t)) - P(A_1(t)A_2(t)) - \dots \quad (4)$$

$$\dots - P(A_{n-1}(t)A_n(t)) + P(A_1(t)A_2(t)A_3(t)) + \dots + (-1)^{m+1} P(A_1(t)A_2(t) \dots A_m(t))$$

Event with probability of 0.95 and higher will be considered practically reliable. Thus, the estimated time of arrival of at least one vehicle at FD is equal to the estimated arrival time with a probability of 0.95 or more. On the basis of ratio (2), the following parameters are accepted as the initial calculation parameters.

- average traffic interval of vehicle on routes (in minutes). To simplify calculations and obtain a universal analytic dependence, we will assume that traffic interval is the same on all the considered routes. We will accept in our calculations range of traffic interval variation from 5 to 40 minutes.

m - number of FDs, at which the arrival of vehicle is expected. We will accept in our calculations change of this parameter from 1 to 20, which most closely corresponds to a possible variety of practical situations.

t - current waiting time of arrival of at least one vehicle (in minutes), for which the probability of arrival is estimated. It is a cycle variable and can take values from 1 minute to the accepted in calculations traffic interval in minutes.

We will consider arrival of the vehicle at FD as a reliable event for the period of time that equals traffic interval. Traffic interval is the highest variable.

The calculation is performed alternately for each specified traffic interval from 5 to 40 minutes in increments of 1 minute. That is, the limit value of the variable is 40 minutes.

Thus, the "amount of FD" is a variable of the first nested cycle. Based on practical experience, we assume in calculations the limiting value of this variable - 20.

The initial number of FD is one. The probability of arrival for 1 minute, for two minutes, etc. is calculated. Estimated waiting time for the arrival of vehicle is a variable of the second nested cycle. The maximum waiting time is 40 minutes. Calculation of the second nested cycle ends when the number of waiting minutes is determined, for which the probability of arrival of at least one vehicle equals or exceeds 0.95.

Then the number of FDs in calculation increases by 1. If the limit quantity of 20 is not exceeded, then the calculation for the second nested cycle is repeated.

## RESULTS AND DISCUSSION

Assessment of the main reliability indicators of UPT system shall be carried out according to the scheme applicable to production technological systems according to GOST 27.503-81 "Dependability/Reliability in technics. Key indicators" [8], GOST 27.204-83 "Industrial product dependability. Technical requirements for methods of reliability evaluation on productivity parameters" [9] and in accordance with GOST 27.301-95 "Dependability in technics. Dependability prediction. Basic principles" [10].

When assessing vehicle reliability on productivity parameters, in accordance with GOST 27.204-83, four levels of consideration of the vehicle are distinguished: technological operation vehicle; technological process vehicle; production department vehicle (workshop, site, etc.); enterprise vehicle.

We will choose and interpret levels as follows: level of technological operation vehicle - level of transportation system in a single trip; level of technological process vehicle - level of the passenger transportation system on a single route; level of the enterprise vehicle - level of the transportation system by one enterprise.

When choosing reliability indicators, one of the most important concepts of reliability theory is a failure. In accordance with GOST 27.002-83 [11] failure is interpreted as inability of the system to perform one of its main functions.

GOST 27.204-83 [Table 2] [9] regulates four main indicators of reliability of technological systems: 1) probability of failure-free operation; 2) mean time between failures; 3) gamma-percentile operating time to failure; 4) preset operating time before corrective adjustment; 5) Mean restoration time.

On the basis of this, we shall choose the following indicators of reliability: 1) probability of execution of volume of transportation; 2) probability of trouble-free operation on routes with the announced schedule. Assessment of reliability of the existing UPT system is also important in assessing the various options of the management system implementation.

Taking into account specifics of the UPT transportation, we shall calculate «probability of volumes execution» of transportation only for city routes and according to transport modes (bus, trolleybus) for routes with interval traffic.

In accordance with GOST 27.204-83 (clause 1.13), calculation of reliability indicators for the current state of transportation system can be carried out by calculation methods according to experimental-statistical data in accordance with GOST 27.503-81 [12].

For the accounting calendar period, we shall select main operational/strategic planning period for UPT - 24 hours.

In this case, the assessment of the indicator "probability of traffic volumes execution per day":

$$P_{day} = \frac{Q_{fday}}{Q_{pday}} \quad (5)$$

где  $P_{day}$  - "probability of execution without failure" of a single flight of UPT per day;  $Q_{fday}$  - actually performed the traffic volumes for the day;  $Q_{pday}$  - planned volume of traffic per day.

For routes with the announced schedule, including suburban routes, we shall use the second indicator: "probability of trouble-free operation on routes".

From the point of view of the passenger, non-execution of flight on route with the declared schedule for any reason is a failure of transportation. Therefore, for route with a declared schedule, "probability of carrying out without traffic on the route" is equal to probability of carrying out without failure of all scheduled flights.

Let  $n_i$  be the planned number of flights on the route  $i$ . Then, taking into account the expression (5), we obtain the following estimate of the probability of execution without traffic failure on the route  $i$  with the announced schedule per day:

$$P_{day}^i = \frac{R_{fday}^i}{R_{pday}^i} \quad (6)$$

где  $P_{day}^i$  - "the probability of execution without failure" of traffic on  $i$ -th route for the day;  $R_{fday}^i$  - the actual number of flight movements at the  $i$ -th route for the day;  $R_{pday}^i$  - the actual number of flight movements at the  $i$ -th route for the day.

These estimates (5, 6) are applicable to the existing transport system, since they use statistical information.

Reliability assessment for future possible states of the system when implementing one or another version of control system, in accordance with GOST 27.301-95 [4], can be based on forecasting methods using, in particular: a typical model of transportation system functioning under control of modernized transportation management system; structure and distribution of functions between dispatchers and means of automatic monitoring (control) of state and object management; types and characteristics of human-machine interfaces that determine parameters of working capacity and reliability of the operators; level of personnel qualification; quality of software tools used in the facility; planned technology and organization of transportation for each version of the management system implementation.

Adequacy of the chosen calculation method and constructed calculation models to the goals and objectives of the object reliability forecast should be characterized by: completeness of use in the forecast of all available information about passenger transportation system and capabilities of control system in the event of traffic failure liquidation; validity of admissions and assumptions made while constructing transportation process models and models of control system functioning; degree of correspondence of the complexity level and accuracy of the calculation models of the object reliability to the available accuracy of the initial data for calculation.

## CONCLUSIONS

- 1 Main characteristics of Orenburg UPT as well as the topological features of city bus routes are considered.
- 2 A methodology for collecting and analyzing experimental data on ES and violations in UPT operation in the city of Orenburg has been developed.
- 3 It was established that there is a need to process the available statistical data in two areas: ES and situations that arise in case of the transportation process violation, associated with the emergence of undesirable social consequences, but not connected with threat to life and health of passengers.
- 4 Technique of estimation of arrival time of reserve vehicles to the place of ES occurrence of is developed.
- 5 The minimum expected time of arrival of backup vehicle at place of emergency can act as a selection criterion for backup vehicle.
- 6 The main reliability indicators of UPT system were evaluated at various levels before and after system implementation.

Adequacy of the chosen calculation method should be characterized by completeness of use in the forecast of all available information about passenger transportation system and capabilities of control system in case of traffic failure liquidation; validity of admissions and assumptions made while constructing transportation process models and models of control system functioning; degree of correspondence of the complexity level and accuracy of the calculation models of the object reliability to the available accuracy of the initial data for calculation.

### CONFLICT OF INTEREST

There is no conflict of interest.

### ACKNOWLEDGEMENTS

The work is performed according to the Russian Government Program of Competitive Growth of Kazan Federal University.



## FINANCIAL DISCLOSURE

None

## REFERENCES

- [1] Lyubimov II, Melnikov AN, Trubin NA [2016]. The Control System Improvement of the City Motor Transportation. *Procedia Engineering*, 150:1192–1199.
- [2] Melnikov AN, Lyubimov II, Manayev KI. [2016] Improvement of the Vehicles Fleet Structure of a Specialized Motor Transport Enterprise.: *Procedia Engineering*. 150:1200–1208.
- [3] Suleimanov IF, Mavrin GV, Kalimulina MR, et al. [2017] Increasing the availability of urban passenger transport on objective control data basis. *J Fundam Appl Sci*. 9(2S):1067-1076.
- [4] Webster FV. [1958] *Traffic Signal Settings*, Department of Transport, Road Research Technical Paper No. 39, HMSO, London.
- [5] Yang H, Yagar S. [1995] Traffic assignment and signal control in saturated road networks. *Transportation Research Part A*. 29 (2):125 - 139.
- [6] Bie J, Lo HK. [2010] Stability and attraction domains of traffic equilibria in a day-to-day dynamical system formulation. *Transportation Research Part B*. 44(1):90-107.
- [7] Arkhipov SG. [1999] Increasing the efficiency of city buses maintenance due to their rational adaptation to the conditions of traffic routes: Candidate of Technical Sciences, 170.
- [8] Standartov MI. [1983] Industrial product dependability. Technological systems. Technical requirements for methods of reliability evaluation on productivity parameters. GOST, 27.204-83
- [9] Standartov MI. [1989] Industrial product dependability. General principles. Terms and definitions. GOST, 27.204-83
- [10] Standartov MI. [1990] Industrial product dependability. Dependability requirements: contents and general rules. GOST, 27.003-90.
- [11] Golenitsky YuV. [1999] Modeling of priority traffic of buses: Diss ... Candidate of Technical Sciences, Volgograd, RGSU. 168.
- [12] Standartov MI. [1981] Industrial product dependability. Main Indicators. GOST, 27.503-81.

## ARTICLE

# SORPTION OF WATER FROM PETROLEUM PRODUCTS BY POLYACRYLAMIDE-BASED SUPERABSORBENT

Dinar D Fazullin, Nikita M Novikov\*, Gennady V Mavrin, Ilnar A Nasyrov

Department of Chemistry and Ecology, Naberezhnye Chelny Institute, Kazan Federal University, RUSSIA

## ABSTRACT

Maintaining of high quality of petroleum products is an urgent task, since the use of low-quality fuel containing dissolved or emulsified water can increase the likelihood of rapid deterioration or breakdown of an internal combustion engine which uses the fuel. Water is present in petroleum products and in oil in various states: in a dissolved state, in a free state, and in the form of an emulsion. The transition of water from one state to another is determined by the following factors: pressure, temperature, pH, viscosity and chemical composition of the fluid. If free water is removed by conventional methods such as settling, coalescence, and centrifugation, then removal of bound water (emulsified and dissolved water) is a difficult task. The method of chemical absorption of water was investigated for the purification of gasoline from dissolved water, and polyacrylamide-based superabsorbent and cellulose fiber were considered as absorbents. The filtration rate of gasoline with a content of 10.6% emulsified water through a layer of sorbent 10 cm and a diameter of 0.9 cm was 4.3 cm<sup>3</sup> / min. The degree of removal of water by the absorbent containing 30% polyacrylamide was 99.8%. The absorbent can be used to clean fuels from emulsified and dissolved water.

## INTRODUCTION

At oil-producing and oil-refining enterprises there is an acute problem of utilization of water-in-oil emulsions formed during the production of a number of petroleum products. Water in petroleum products is in a dissolved, emulsified and free state. To separate these types of emulsions, various processes and devices are used, which work is based both on centrifugal and gravitational forces, separation using reagents and various adsorbents, and on specific processes such as ultrasound, magnetic field, and radio emission [1-3].

The recently spread on the market coalescent filters which well separate water (for example, filter elements manufactured by Pall Company), do not work efficiently enough when there is a large amount of mechanical impurities in the initial diesel fuel.

In [4], the authors used calcium oxide to remove moisture from petroleum products. Oil containing water was passed through a tube filled with an adsorbent under dynamic conditions at a speed of 0.5 m / h and a temperature of 20-25° C. The consumption of calcium oxide was more than 0.21% by the volume of refined petroleum products. To remove the formed calcium hydroxide flakes, the authors used filtration methods.

Also in the literature there are many works on the drying of various petroleum fractions and petroleum products: fuels, oils, olefins, alcohols, etc. with the use of NaA molecular sieves. Compared with the existing methods of drying oil and petroleum products based on heating them to the water evaporation temperature, drying with the use of molecular sieves has significant advantages. Its disadvantages are: clogging of pores and the formation of gels on the surface, what leads to a decrease in the filtration rate, which requires frequent replacement and regeneration of zeolites.

The patent for the method of processing diesel fuel provides for that fuel is heated; the volumetric content of water in the fuel is adjusted to 1-4 % and the fuel is homogenized. Then, by means of a filtering porous partition made of a hydrophobic material with a cleaning fineness of 1-10 microns, joint processes of dehydration and fine filtration are carried out [5].

In the study [6], superhydrophobic and super-ophilous silane-modified cotton fibers were obtained. The obtained fibers showed selective sorption capacity for oils from water, a high sorption capacity, and high sorption rate. Fibers also have outstanding superhydrophobic stability against various aggressive solutions and hot water, which allows them to be used to separate oils from harsh waters. The efficiency of separation water from oil is more than 91%.

In the study [7], nanoparticles of Fe<sub>3</sub>O<sub>4</sub> and a subsequent hydrophobic modification were applied on the surfaces of cotton fibers. The results show that the prepared fibers exhibit excellent superhydrophobicity and magnetic sensitivity. Compared to the original cotton fibers, the sorption capacity of the modified fibers as to hexane, toluene, chloroform, gasoline, and diesel fuel increases by 70.8%, 58.5%, 23%, 37.3% and 30.5%, respectively.

In the work [8], a hollow fiber membrane was used to remove water from motor fuel. The removal of water is as follows: oil containing emulsified water flows along one side of the hollow-fiber membrane; air flowing

### KEY WORDS

Oil products, gasoline, water sorption,

Received: 21 Oct 2018  
Accepted: 24 Dec 2018  
Published: 6 Jan 2019

### \*Corresponding Author

Email:  
novikovchem@yandex.ru  
Tel.+8 (8552) 42-62-40

on the other hand removes water from the oil through a hydrogel membrane available within the wall of the hollow fiber membrane. The water content in the emulsion was 1-4%. The degree of removal of emulsified water was more than 90%. The disadvantage of this method of removing emulsified water is clogging of the pores of the membranes, what leads to an increase in working pressure.

In the studies [9-13], separation of emulsified water from petroleum products performed with the use of absorbents from various composite resins, carbon nanotubes modified by teflon fibrils, super hydrophilic oleophobic sponges, aerogels, zeolites, calcium chloride, nanoparticles and other sorption materials.

Also, to remove water from gasoline, ethanol is added to the fuel in a volume of from 1 to 15% [14].

## METHODS

The scientific significance of solving the problem lies in the development of methods for the cleaning of petroleum products from emulsified and dissolved water based on chemical adsorption methods.

For the cleaning of petroleum products from dissolved water, a method of chemical water absorption was investigated, and superabsorbent based on polyacrylamide and cellulose fiber were considered as absorbents (desiccants).

The absorbent was obtained from polyacrylamide and recycled cellulose fiber. The recycled cellulose fibers have different lengths, from 100 microns to 2000 microns. The thickness of the cellulose fibers is from 10 to 100 nm. Cellulose fibers are insoluble in water, acids and alkalis, and in organics; they hold and absorb liquid well. Cellulose fibers are the main component of the sorbent on the surface of which polyacrylamide powder with a size of 100-300 microns is applied.

Super absorbents (SA) are hydrophilic polymer networks that, when swelled, absorb and retain huge amounts of water and aqueous solutions, going into gels. The water-holding capacity of super absorbents ranges from 50-100 g / g to 2200 g / g. For example, for the commercially available water-holding polymer "Aquasorb" this value is more than 500 grams of water per gram of absorbent. Hydrogels are obtained by the method of radical polymerization of acrylic acid or its salts (acrylates) at temperatures above 56 oC in an atmosphere of nitrogen or carbon dioxide. A crosslinking agent is introduced into the reaction mass to create a three-dimensional structure at the stage of polymerization. In this case, crosslinking occurs simultaneously with the growth of the polymer. The mass content of cellulose fiber in the sorbent is 70%, and 30% of polyacrylamide.

Dissolved and emulsified water was removed from the model emulsion prepared as follows. 30 ml of water and 10 g of sodium dodecyl sulfate were added to 300 ml of gasoline AI-92. To obtain an emulsion, the mixture was stirred at 3000 rpm for 15 minutes.

The model emulsion was filtered under dynamic conditions through a column filled with a sorbent weighing 2 g, the height of the sorbent was 10 cm.

The filtration rate was determined by passing 100 ml of gasoline and emulsion through a column with absorbent for a certain time.

The scheme of the laboratory installation for absorption of the inverse emulsion of the "water in oil" type in dynamic conditions is shown in [Fig. 1]. Original emulsion is fed into the column with filter loading, the emulsion is filtered through a polymer load under the action of gravity, and the filtrate is collected in a flask.

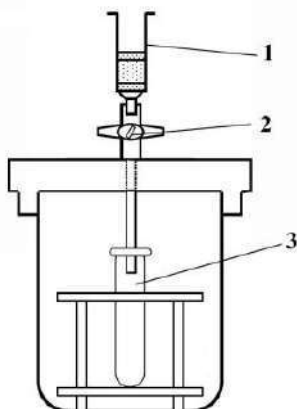


**Fig. 1:** Scheme of laboratory: 1 - column with superabsorbent; 2 - the crane; 3 - a flask for collecting oil.

.....  
 The water content in petroleum products is determined before and after treatment in accordance with GOST 2477-2014 (Oil and petroleum products; method for determination of water content). The essence

of the method is as follows: the product being tested is heated inside a flask with a refrigerator in the presence of a solvent not miscible with water, which is distilled along with the water in the sample. Condensed solvent and water are constantly separated in the trap, with the water remaining in the graduated compartment of the trap, and the solvent is returned to the distillation vessel.

### RESULTS AND DISCUSSION

[Fig. 2] and [Table 1] present the results of measurements of particle sizes and  $\zeta$ -potential of the dispersed phase of the inverse emulsion of water in gasoline.

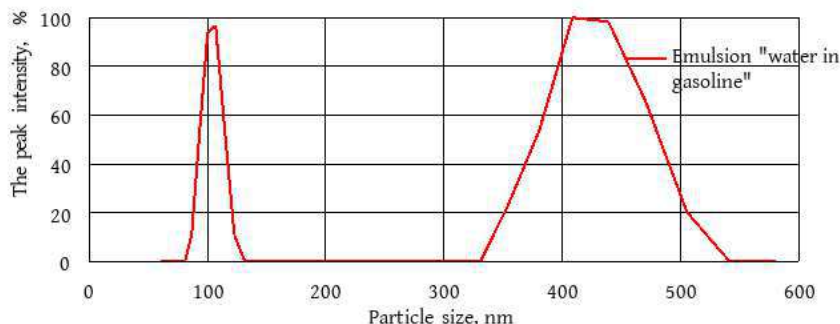


**Fig. 2:** Graphs of particle size distribution of the dispersed phase of the reverse emulsion of water in gasoline.

**Table 1:** The values of the particle size and the  $\zeta$ -potential of the dispersed phase of the reverse emulsion "water in gasoline"

Emulsion	Particle size, nm	$\zeta$ -potential, mV
Emulsion "water in gasoline"	86-124; 355-542	-19 $\pm$ 2

According to the data presented in [Fig. 2], the inverse emulsion "water in gasoline" is a poly disperse system with particle sizes from 86 to 542 nm. From the data of [Table 1], it follows that the emulsion has the absolute value of the  $\zeta$ -potential equal to -19 mV and is a stable system. The higher the absolute value of the  $\zeta$  - potential of the emulsion, the stronger the particles repel each other, what does not allow the emulsion to separate.

The filtration rate for gasoline and the inverse emulsion "water in gasoline" through a column with absorbent are presented in [Table 2].

**Table 2:** The rate of filtration of gasoline and emulsion water in gasoline through a column with absorbent (30% polyacrylamide, 70% cellulose fiber)

Name of liquid	Water content in gasoline, %	Filtration rate through absorbent, cm <sup>3</sup> / min
Gasoline	<0.01	9.7
Emulsion water in gasoline	10.6	4.3

The filtration rate of gasoline through the sorbent layer of 10 cm and a diameter of 0.9 cm is 9.7 cm<sup>3</sup> / min, and when filtering gasoline with a content of 10.6% emulsified water, the filtration rate falls to 4.3 cm<sup>3</sup> / min.



**Fig. 3:** Left to right: source gasoline; emulsion with 10.6% water in gasoline; gasoline, purified from water absorbent.

[Fig. 3] shows that the emulsion “water in gasoline” is turbid and has sediments at the bottom of the flask; after filtering the emulsion, the water is trapped in cellulose fiber and is set by polyacrylamide. The cleaned gasoline in [Fig. 3] (right) is transparent. The water content in gasoline was determined by the method of GOST 2477-2014, the results are presented in [Table 3].

**Table 3:** Degree of removal of water from gasoline by an absorbent

Absorbent	Water content in gasoline, %		Degree of water removal, %
	before	after	
10% polyacrylamide, 90% cellulose fiber	10.6	0.5	95.3
30% polyacrylamide, 70% cellulose fiber		<0.01	99.8

From the results of [Table 3], the water removal degree with an absorbent containing 10% polyacrylamide is 95.3%, and when the mass content of polyacrylamide is 30%, the cleaning rate is 99.8%.

Inverse emulsion water in gasoline is a poly disperse system with particle sizes from 86 to 542 nm. Having an absolute value of the  $\zeta$ - potential equal to -19 mV, the emulsion is a stable system. The higher the absolute value of the  $\zeta$  - potential of the emulsion, the stronger the particles repel each other, what does not allow the emulsion to separate.

The filtration rate of gasoline through the sorbent layer of 10 cm and a diameter of 0.9 cm is 9.7 cm<sup>3</sup> / min, and when filtering gasoline with a content of 10.6% emulsified water, the filtration rate falls to 4.3 cm<sup>3</sup> / min. The emulsion “water in gasoline” is turbid; it has sediments, and after filtration through a layer of sorbent it becomes transparent.

The water removal degree with an absorbent containing 10% polyacrylamide is 95.3%, and when the mass content of polyacrylamide is 30%, the cleaning rate is 99.9%. For comparison, the degree of removal of emulsified water from petroleum products using cotton fiber modified with silane is 91%, and the application of Fe3O4 nanoparticles onto cotton fiber increases the degree of water removal from gasoline by 37% compared to the original fiber [6, 7]. The degree of removal of emulsified water from the engine oil using a hollow-fiber membrane, on which the hydrogel is applied, is more than 90% [8].

Thus, the proposed absorbent from cellulose fiber and polyacrylamide has a high degree of removal of emulsified and dissolved water from gasoline.

## CONCLUSION

According to the research results, it was determined that a superabsorbent consisting of polyacrylamide and cellulose fiber effectively cleans gasoline from emulsified and dissolved water under dynamic conditions. When the content of polyacrylamide is no less than 30% (by weight) in the composition of the absorbent, the water removal degree reaches 99.8%. The fuel filtration rate is from 4 to 5 cm<sup>3</sup> / min. This absorbent can be used to clean fuels and waste solvents from emulsified and dissolved water.

### CONFLICT OF INTEREST

There is no conflict of interest.

### ACKNOWLEDGEMENTS

The work is performed according to the Russian Government Program of Competitive Growth of Kazan Federal University.

### FINANCIAL DISCLOSURE

None

## REFERENCES

- [1] Osipov OP, Sannikov SG. [2001] Oil refining and petro chemistry. M.: TsNIITeneftkhim. 6:12-14.
- [2] Proskuryakov VD, Smirnov OV. [1992] Cleaning of petroleum products and oily water by electrical treatment. St. Petersburg: Chemistry. 17-18.
- [3] Shepelev II, Tverdokhlebov VP, Fomova NA. [2001] Oil refining and petro chemistry. TsNIIT Eneftkhim. 8:14-17.
- [4] Yablokova MA, Ponomarenko EA. [2013] Promising methods for cleaning diesel fuel from water and mechanical impurities. Current problems of science and education. 3. URL: <http://www.science-education.ru/ru/article/view?id=9246> (appeal date: 05/14/2018).
- [5] Zege ON. [1996] The method of processing diesel (mostly watered) fuel, installation for its implementation and a vortex apparatus: RF Patent No. 2054572. 5
- [6] Jintao W et al. [2017] Hydrothermal fabrication of robustly super hydrophobic cotton fibers for efficient separation of oil/water mixtures and oil-in-water emulsions. Journal of industrial and engineering chemistry. 54:174-183.
- [7] Jintao W et al. [2016] Magnetically superhydrophobic kapok fiber for selective sorption and continuous separation of oil from water. Chemical Engineering Research and Design. 115:122-130.



- [8] Li Y et al. Bio-inspired onboard membrane separation of water from engine oil. *Journal of membrane science*. 378:1-2.
- [9] Jingjie H. [2018] Removal of Oil from Water Surface by Novel Composite NSM-g-P(MMA-co-BA) Super Oil-Absorption Resin. *Polymer composites*. 39(4):1051-1063.
- [10] Padmajan SS et al. [2018] Multiwall carbon nanotube reinforced teflon fibrils for oil spill cleanup and its effective recycling as textile dye sorbent. *Journal of environmental management*. 211:198-205.
- [11] Chunping S et al. [2017] A magnetic superhydrophilic oleophobic sponge for continuous oil-water separation. *Chemical engineering journal*. 309:366-373.
- [12] Filho MC et al. [2017] Efficient simultaneous removal of petroleum hydrocarbon pollutants by a hydrophobic silica aerogel-like material. *Colloids and Surfaces A: Physicochemical and Engineering Aspects*. 520:550-560.
- [13] Ghanbari S, Vaferi S. [2015] Experimental and theoretical investigation of water removal from DMAZ liquid fuel by an adsorption process. *Acta Astronautica*. 112:125.
- [14] El-Faroug Musaab O et al. [2016] Spark Ignition Engine Combustion, Performance and Emission Products from Hydrous Ethanol and Its Blends with Gasoline. *ENERGIES*. 9(12):984.

## ARTICLE

# HEAVY METAL EMISSION FROM PYROLYSIS PRODUCTS OF CARBON-CONTAINING WASTES AFTER ASHING

Ilnar A Nasyrov\*, Gennady V Mavrin, Dinar D Fazullin, Aliya R Ahmetshina, Rudel N Safarov

Department of Chemistry and Ecology, Naberezhnye Chelny Institute, Kazan Federal University, RUSSIA

## ABSTRACT

In this paper, they studied the emission of heavy metals from a potential sorption material obtained by pyrolysis from silt sediments and treated with "dry" ashing. The use of a solid pyrolysis product after ashing involves the purification of waste water from contaminants. The content of heavy metal ions in aqueous extraction and in the extraction with an acetate-ammonium buffer of a solid pyrolysis product from carbon-containing waste was determined by atomic emission spectrometry. By mass concentration in the order of its value decrease, heavy metal ions in the aqueous extract of the pyrolysis product from mud sediments are arranged in the following series: Si, Sr, V, Mn, Zn, Mo, Ba, Sb, Cu. In the acetate-ammonium extract, heavy metals are in order of value decrease and arranged in the following series: Si, Mn, Zn, Al, Sr, Cr, B, V, Fe, Ba, Ni, Mo, Se, Pb, Sb. They compared the content of harmful ingredients in the aqueous extract of solid pyrolysis products from carbon-containing waste relative to the normative indices of the aquatic environment. They calculated the concentration coefficients compared with the standards for drinking water, fishery water and sewage for the discharge to the centralized system. The obtained results show that the aqueous extracts of the solid pyrolysis products from carbon-containing waste after treatment with "dry" ashing do not exceed the normative indices for sewage by heavy metal content. They determined that the pyrolysis product does not pollute the wastewater after the treatment with ashing, which justifies the possibility of its use from environmental positions with the restriction of wash water discharge from the solid pyrolysis product directly to the fishery water reservoirs.

## INTRODUCTION

The protection of the environment from the pollutants entering into it is an important task at the present stage of scientific and technical progress development. With household economic and industrial activity of a person, liquid wastes are formed in the form of sewage, which are discharged into the sewage system. The purification of domestic and industrial wastewater is an urgent problem for urban areas [1].

Various methods are used, including sorption, for the purification of sewage from heavy metal ions (HMI). Activated carbons, zeolites, natural materials, etc. are used as sorbents. Often these materials have a high cost and require the use of natural resources [2]. The technical solutions in the field of cleaning are very useful and relevant, which make it a low-waste. The use of carbon-containing waste (CCW) as a valuable secondary material resource will significantly reduce the environmental burden and will allow to obtain a new type of industrial products. There is no need to develop mining or grow new raw materials, which inevitably leads to new pollution of the environment [3].

CCW contain organic components and often mineral substances that are converted to gaseous pyrolysis fuel, liquid pyrolysis fuel and solid pyrolysis product (SPP) during pyrolysis. SPP, formed at high temperature, is a potential sorbent, the sorption properties of which can be improved by a special procedure - "dry" ashing. [4]

In order to create highly effective sorption materials, a qualitative and a quantitative analysis is necessary to determine the content of mobile and water-soluble forms of the ingredients in their composition.

## METHODS

The study of the aqueous extract and the extract by the acetate-ammonium buffer of the pyrolysis products after the treatment with ashing to determine HMI emission volumes was carried out by atomic-emission spectrometry with inductively coupled plasma using Agilent 720-OES spectrometer [5,6].

The water extract for analysis was prepared by the dissolution of 30 g of the sample in 150 ml of distilled water. After that, the suspension was treated for 30 minutes in a laboratory shaker, and then it was settled and filtered. Similarly, the extract with acetate-ammonium buffer was prepared, by the means of which more ions of heavy metals can be transferred to the liquid phase in comparison with a usual aqueous extract [7,8].

The pH values of the solutions were measured with ANION 4100 ionomer. The conductivity meter ANION-7020 was used to measure mineralization and specific electrical conductivity [9].

## RESULTS AND DISCUSSION

As a research object, they took the product sample of CCW pyrolysis treatment, obtained by low-temperature pyrolysis under production conditions. The following CCW were subjected to pyrolysis: the sediment of sewage biological treatment. Subsequently, the obtained pyrolysis product of CCW was

subjected to ashing in a muffle furnace at  $t = 800\text{ }^{\circ}\text{C}$ . We studied the emission of HMI from the obtained samples.

SPP treated with "dry" ashing is a dark brown powder [Fig. 1].



**Fig. 1:** Solid pyrolysis product after ashing.

pH, mineralization and UEP were determined in the aqueous extract of SPP. The results of measurements and normative indices for water bodies are given in [Table 1].

**Table 1:** Indices of aqueous extract of solid pyrolysis product after ashing

sample	pH, units pH	SEC, $\mu\text{S}$ / cm	mineralization by NaCl, mg / $\text{dm}^3$
sludge	7.05	307	146.5
TLVdrinking water	6.0-9.0	-	1000
TLVopen reservoirs	6.5-8.5	-	1000
LVwaste water	6.0-9.0	-	3000

pH value 7.05 indicates almost a neutral aqueous extract medium and does not exceed the pH standard for the waters of household and cultural value, fishery and sewage waters, which is in the range of 6-9 pH units [Table 1]

The results of HMI content determination in an aqueous extract and in the extraction of acetate-ammonium buffer are given in [Table 2].

[Table 3] indicates, for comparison, the maximum permissible concentration of the ingredient in the water of domestic and cultural facilities (TLVdrinkingwater), the maximum permissible concentration of the ingredient in the water of fishery facilities (TLVopenreservoirs), the permissible concentration of pollutants in wastewater admitted to discharge into a centralized water disposal system (LVwastewater) [10].

**Table 2:** The content of heavy metal ions in the aqueous extract, the content of heavy metal ions in the extract by ammonium-acetate buffer, standards

element	concentration in aqueous extract, mg / $\text{dm}^3$	concentration in extract by acetate-ammonium buffer, mg / $\text{dm}^3$
Al	<0.1	2.77
Ba	0.079	0.381
Be	<0.01	<0.01
Cd	<0.05	<0.05
Co	<0.2	<0.2
Cr	<0.15	<0.15
Cu	0.001	0.869
Fe	<0.05	0.385
Mn	0.234	9.94
Mo	0.110	0.126
Ni	<0.001	0.150
Pb	<0.001	0.081
Sb	0.007	0.008
Se	<0.005	0.086

Si	0.996	23.7
Sr	0.515	2.32
Ti	<0.1	<0.1
V	0.267	0.846
Zn	0.175	3.08
B	<0.1	0.861
Ag	<0.3	<0.3
As	<1	<1

**Table 3:** Standards for heavy metals

Element	TLVdrinking water	TLVopen reservoirs	LVwaste water
Al	0.2	0.04	3
Ba	0.7	0.74	-
Be	0.0002	0.0003	-
Cd	0.001	0.005	0.015
Co	0.1	0.01	-
Cr	0.05	0.02	0.5
Cu	1	0.001	0.5
Fe	0.3	0.05	3
Mn	0.1	0.01	1
Mo	0.25	0.001	-
Ni	0.1	0.01	0.25
Pb	0.01	0.006	0.25
Sb	0.05	0.005	-
Se	0.01	0.002	-
Si	10	-	-
Sr	7	0.4	2
Ti	0.1	0.06	-
V	0.1	0.001	-
Zn	1	0.01	1
B	0.5	0.5	-
Ag	0.05	-	-
As	0.01	0.05	0.01

According to the analysis results, the sample of SPP CCW after the treatment with "dry" ashing contains the following metals in the mobile form in the order of concentration decrease [Table 4]

**Table 4:** Ranks of priority of heavy metals in aqueous extract

sludge	Si, Sr, V, Mn, Zn, Mo, Ba, Sb, Cu
--------	-----------------------------------

The acetate-ammonium extract TM has the following series in the order of value decrease [Table 5]

**Table 5:** Ranks of priority of heavy metals in extract by acetate-ammonium buffer

sludge	Si, Mn, Zn, Al, Sr, Cr, B, V, Fe, Ba, Ni, Mo, Se, Pb, Sb
--------	--

In order to evaluate the impact of SPP CCW on water objects of the environment after the treatment by heavy metal ion leaching with water and acetate-ammonium buffer they calculated the concentration coefficients relative to TLVdrinkingwater, TLVopenreservoirs, LVwastewater. according to the following formulae:

a) the concentration coefficient of HMI in SPP extract after the treatment with respect to TLVHMI in the water of domestic and cultural objects.

$$K_{\text{drinking water}} = \frac{C}{\text{TLV}_{\text{drinking water}}} \quad (1)$$

b) the concentration coefficient of HMI in SPP extract after treatment with respect to TLV in the water of fishery reservoirs.

$$K_{\text{open reservoirs}} = \frac{C}{\text{TLV}_{\text{open reservoirs}}} \quad (2)$$

b) the concentration coefficient of HMI in SPP extract after treatment with respect to the permissible concentration of pollutants in the wastewater admitted for discharge to the centralized water disposal system.

$$K_{\text{waste water}} = \frac{C}{\text{LV}_{\text{waste water}}} \quad (3)$$

The calculation results are given in [Table 6 and 7].

**Table 6:** Coefficient of concentration of heavy metals in aqueous extract relative TLV

element	$K_{dw}$	$K_{or}$	$K_{ww}$
Al	-	-	-
Ba	0,113	0,107	-
Be	-	-	-
Cd	-	-	-
Co	-	-	-
Cr	-	-	-
Cu	0,001	1	0,002
Fe	-	-	-
Mn	2,34	23,4	0,234
Mo	0,440	110	-
Ni	-	-	-
Pb	-	-	-
Sb	0,140	1,40	-
Se	-	-	-
Si	0,100	-	-
Sr	0,074	1,29	0,258
Ti	-	-	-
V	2,67	267	-
Zn	0,175	17,5	0,175
B	-	-	-
Ag	-	-	-
As	-	-	-

**Table 7:** Coefficient of concentration of heavy metals in extract by acetate-ammonium buffer relative TLV

element	$K_{dw}$	$K_{or}$	$K_{ww}$
Al	13,9	69,3	0,923
Ba	0,544	0,515	-
Be	-	-	-
Cd	-	-	-
Co	-	-	-
Cr	-	-	-
Cu	0,869	869	1,74
Fe	1,28	7,70	0,128
Mn	99,4	994	9,94
Mo	0,504	126	-
Ni	1,50	15	0,600
Pb	8,10	13,5	0,324
Sb	0,160	1,60	-
Se	8,60	43	-



Si	2,37	-	-
Sr	0,331	5,80	1,16
Ti	-	-	-
V	8,46	846	-
Zn	3,08	308	3,08
B	1,72	1,72	-
Ag	-	-	-
As	-	-	-

The use of SPP after ashing involves the purification of waste water from pollutants. The obtained results show that the water extract of SPP after its treatment with "dry" ashing does not exceed the normative indices for sewage by HMI content.

The comparison by K<sub>ww</sub> series according to all indicators [Table 6] is illustrated by the diagram of [Fig. 2], provided for convenience by the value K<sub>ww</sub> in logarithmic scale according to the base 10.

[Fig. 2]: the elements whose content in the extract exceeds LVwaste water are located above the horizontal line, and the HMI with the content less than the norm is below the horizontal line.

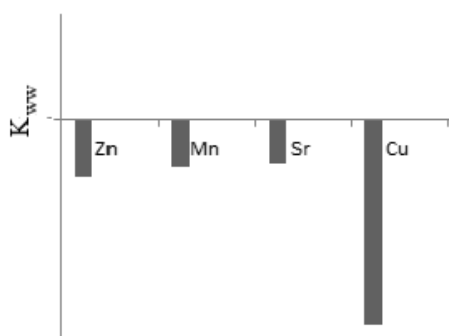


**Fig. 2:** Coefficient of concentration of ingredients of aqueous extract of solid pyrolysis product after ashing relative to TLVforwaste water in base 10 logarithmic scale.

Thus, in order of K<sub>ww</sub> decrease HMI in the water extract are located in the following row [Table 8]:

**Table 8:** Ranks of priority of heavy metals in aqueous extract as reduction of danger to waste water

sludge	Sr, Mn, Zn, Cu
--------	----------------

The absence of HMI normative index exceeding in water bodies indicates a low toxicity of the obtained sample. The use of it as a sorption material is also limited by the possible toxicity. Therefore, there is a need to determine SPP toxicity after ashing experimentally by the mortality of the test object *Daphnia magna* Straus. The results of the study are shown in [Table 6].

**Table 6:** Toxicity of solid pyrolysis product after ashing

sample	hazard class	
sludge	1	5

Thus, the studied pyrolysis product of biological wastewater treatment sediment is relatively safe for use as a sorption material.

### CONCLUSION

They studied the solid product of carbonaceous waste (sludge) pyrolysis after the treatment with "dry" ashing as the sources of migration into the aqueous phase of harmful ingredients in the form of HMI.

They obtained the values of the observed specific electric conductivity, NaCl mineralization and HMI mass concentration in aqueous extract and in the extraction of the acetate-ammonium buffer of SPP CCW.

HMI subjected to emissions into the water phase are arranged in the order of value decrease according to the following series: Si, Sr, V, Mn, Zn, Mo, Ba, Sb, Cu.

They are arranged in the following series in the acetate-ammonium extract of TM, in the order of value decrease: Si, Mn, Zn, Al, Sr, Cr, B, V, Fe, Ba, Ni, Mo, Se, Pb, Sb.

They compared the content of harmful ingredients in the water extract of SPP CCW relative to the normative indices of the aquatic medium. The concentration coefficients were calculated relative to the standards for drinking water, fishery water, the sewage for discharge to the centralized system.

The obtained results show that in the overwhelming majority the water extract of SPP after the treatment with "dry" ashing does not exceed the normative indices for sewage according to HMI content.

They determined SPP toxicity of the studied CCW after ashing experimentally by the mortality of *Daphnia magna* Straus test object. According to the criteria for hazardous waste classification as a hazard class for the environment [11], the CCW of rubber waste under study belongs to the fifth hazard class.

It has been established that SPP CCW after the treatment with ashing does not have a negative effect on sewage, which justifies the possibility of SPP use from environmental positions with the restriction of SPP wash water discharge into the fishery water reservoirs.

#### CONFLICT OF INTEREST

There is no conflict of interest.

#### ACKNOWLEDGEMENTS

The work is performed according to the Russian Government Program of Competitive Growth of Kazan Federal University.

#### FINANCIAL DISCLOSURE

None

## REFERENCES

- [1] Svergzuzova SV, Sevastyanov VS, Sapronov JA, Spirin MN, Shaikhiev IG. [2013] Using sediment from wastewater treatment and reclamation of sludge cards - an urgent task environmental management. Bulletin of Kazan State Technological University. 16 (4):199-202.
- [2] Gulyaev IS, Dyakov MS, Savinova YN, Glushankova IS. [2012] Analysis and study of methods of neutralization and disposal of sewage sludge biological treatment plant. The bulletin of PNIPU. Protection of the environment, transport, safety of life. 2:18-32.
- [3] Lynda H, Wartelle K, Thomas Klasson, Chanel A, Fortier, Isabel M, Lima. [2011] J Agric Food Chem. Influence of Pyrolysis Temperature on Biochar Property and Function as a Heavy Metal Sorbent in Soil. *Minor Uchimiyu*. 59(6):2501-2510.
- [4] Ilnar A, Nasyrov, Vilnus M, Ahmetov, Munir N, Miftahov, Gennady V, Mavrin, Mikhail P. [2016] The problem of disposal sludge treatment plants. Sokolov, International Journal of Pharmacy & Technology. 8(2):14359-14365.
- [5] Deliyanni EA, Peleka EN, Matis KA. [2009] Modeling the sorption of metal ions from aqueous solution by iron-based adsorbents. *Journal of Hazardous Materials* 172:550-558.
- [6] Zaini MAA, Okayama R, Machida M. [2009] Adsorption of aqueous metal ions on cattle-manure-compost based activated carbons. *Journal of Hazardous Materials* 170:1119-1124.
- [7] Ilnar A Nasyrov, Stanislav V Dvoryak, Ildar G Shaikhiev. [2016] Sorption properties of carbon waste pyrolysis product for biological wastewater treatment. *Acta Technica*. 61 (4B):307-314.
- [8] Ilnar A Nasyrov, Aigul I Ahmadiyeva, Dinar D Fazullin, Gennady V Mavrin, Mikhail P Sokolov. [2017] Petroleum containing wastewater products purification by carbon-containing wastes pyrolysis products. *The Turkish Online Journal of Design, Art and Communication TOJDAC*. 7:1713-1728.
- [9] Ilnar A Nasyrov, Gennady V Mavrin, Aliya R Ahmetshina, Aigul I Ahmadiyeva. [2017] Sorption properties of pyrolysis products of sludge, wood waste and rubber waste for heavy metal ions. *Journal of Fundamental and Applied Sciences*. 9(1S):1615-1625.
- [10] Bespamyatnov GP. Threshold limit values of harmful substances in air and water. The handbook for the choice and hygienic assessment of methods of neutralization of industrial wastes. 2nd prod the lane and additional L.: Chemistry.
- [11] Order No. 536 of the Ministry of Natural Resources and Environmental Protection of the Russian Federation from 12/4/2014. About the approval of criteria of reference of waste to the I-V classes of danger on degree of negative impact on the environment of waste.

## ARTICLE

# FEATURES OF THE APPLICATION SOFTWARE COMPLEX AUTODESK INVENTOR TO BUILD 3D MODELS ROTOR GTE-16M

Sergey A Nazarychev<sup>1</sup>, Sergey O Gaponenko<sup>2</sup>, Aleksandr E Kondratiev<sup>2</sup>, Aleksei O Malahov<sup>1</sup>

<sup>1</sup>The Alexander Butlerov Institute of Chemistry, Kazan Federal University, RUSSIA

<sup>2</sup>Kazan State Power Engineering University, RUSSIA

## ABSTRACT

This article discusses the features of using Autodesk Inventor software for modelling equipment, the advantages and effectiveness of this program. Graphics in the form of 3D (three-dimensional) looks much more realistic than the traditional two-dimensional graphics, in addition, it allows you to represent the object in the form in which it can be in reality, to consider it from all sides. Characteristics Autodesk Inventor allows you to create digital models of technological products, includes convenient mechanisms for finding components, forms design documentation. The primary means of intensification of production consist in the accuracy of automated design, the installation of technological management, to improve the quality of products and the efficiency of its production. The main thing in the development of modern equipment is the introduction and improvement of technical products, improving the quality of the system. The complexity of the technological processes that must ensure the lowest costs at the highest productivity, the need to select the optimal process, the multivariate available capabilities and the responsibility of the decisions made presupposes the rational application of CAD methods and tools (computer-aided design). Currently, CAD should provide the solution of the following tasks: to perform 3-dimensional modelling, geometric constructions, applying standard product dimensions; To work with the library of standard objects, as well as text technical documentation. Without the automation of design, the system cannot work in full efficiency, the modelling of the elements allows us to evaluate the prospect of introducing any equipment and improve the quality of the system as a whole.

## INTRODUCTION

To solve the task, the computer-aided design (CAD) system was chosen, namely Autodesk Inventor.

## KEY WORDS

CAD, Autodesk Inventor, graphic editor,

The Autodesk Inventor component library includes a large number of standard components for fastening and finished product models, partitions for design features, which is very convenient for the user. Including the GOST standard and all common world standards (ANSI, ISO, DIM, JIS, etc.). Currently, the number of standard parts in the library is approaching one million.

In addition to the library of finished parts, Autodesk Inventor also has a library of their individual elements that performs various forms of die cuts, holes, punches, selections, etc. [2]

Autodesk presents various versions of the Inventor product. Student's license Inventor is presented to students and teachers as a free version in an educational form, such version has a special mark on the created or edited files.

## METHODS

Among modern balancing machines, two main groups can be distinguished: pre-resonance machines with rigid supports and resonant ones, with elastically suspended supports of rotation. The most widespread are the resonant machines due to less stringent requirements to the foundations for which they are installed. However, the balancing performed in the pre-resonance frequency range makes it possible to obtain the greatest accuracy.

Features of the pre-resonance type of balancing machine:

- high accuracy of balancing in the pre-resonance mode;
- possibility of balancing without calibration starts;
- balancing of any types of rotors;
- cardan drive for rotors with large aerodynamic resistance and rotors of complex configuration;
- special saddle-shaped inserts for balancing aviation turbines and compressors in their own bearings;
- Manual drive belt;
- Constant (for long term) calibration factors.

## \*Corresponding Author

Email:  
sogaponenko@yandex.ru  
Tel.: 89874170041

Analyzing the characteristics of existing balancing machines presented in the Russian market, a large-scale horizontal pre-resonance balancing machine was developed from such large manufacturers as: DIAMEX, CIMAT, SCHENCK, and Techno balance.

Received: 22 Oct 2018  
Accepted: 29 Dec 2018  
Published: 7 Jan 2019

[Fig. 2.1] shows the assembly 3D model of the developed balancing machine.

The pre-resonance balancing machine consists of a bed 1 and two support units 2, which are adjustable in height. The support units can be displaced along a rail mounted on the frame relative to each other and equipped with a piezoelectric force sensor.

The cast base [Fig. 2.2] is made of a vibration-resistant polymer (20% more absorbs vibration than a cast-iron bed), mounted on special vibration-armor, covered with a vibration-absorbing layer, does not require a foundation. The total length of the bed is 1500 mm.

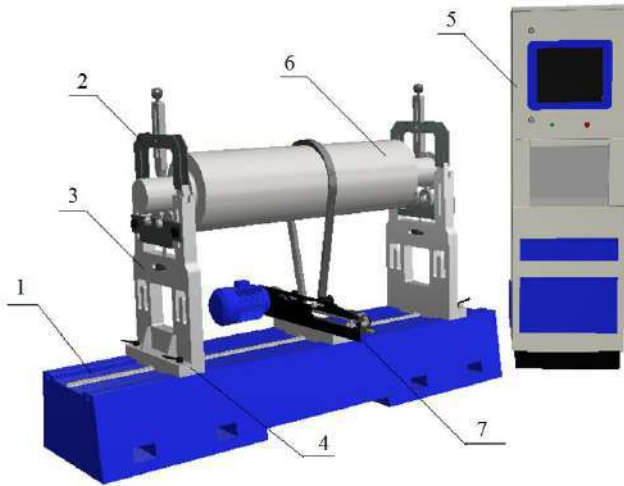


**Fig. 2.1:** 3D model of the balancing machine. 1 - bed; 2 - reference node; 3 - support base; 4 - support plate; 5 - control unit; 6 - the investigated rotor; 7 - middle support with electric motor.



**Fig. 2.2:** Stand of the pre-resonance machine together with the installed rail.

The support assembly [Fig. 2.3] includes the support base and the support plate. Piezoelectric force sensor, built into the support base. On each support cylindrical reinforced rollers are installed on which a balancing rotor is installed. The height of the support rollers is adjustable in height, thus this design feature allows covering a wide range of balancing rotors along the diameter of the support necks.

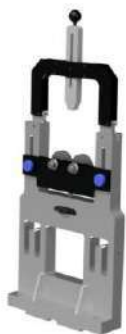


**Fig. 2.3:** Supporting assembly.

The operation of the machine in question is controlled by the control unit 5 (operator's rack), to which the force sensors mounted on each support and the driving motor are connected. Preconfigured frequency-controlled asynchronous electric drive allows controlling the rotor speed, acceleration and deceleration with the help of a belt drive and a number of guide rollers.

As a phase angle sensor for the belt drive, a laser tachometer is used [Fig. 2.4].



**Fig. 2.4:** Digital laser tachometer DT2234C +.

The operator's rack [Fig. 2.5] is equipped with a laser printer to output the balancing results on paper.

## RESULTS AND DISCUSSION

### Rotor GTD-16M

As the object of balancing, the rotor of the turbocharger of the gas turbine engine GTD-16M is considered. [Fig. 3.1] shows the turbo-generator unit TG-16M is an autonomous unit used to create the conditions for launching gas turbine engines of aircraft. GTE-16 serves for driving through the reducer of the generator and for all components of the maintenance of the TG-16 [14].



**Fig. 3.1:** General view of the turbo-generator unit TG-16M.

The rotor of the turbocharger [Fig. 3.2] is a shaft at one end of which is a turbine disk, on the other is a compressor impeller [Fig. 3.3] [14].

The rotor rotates on the rolling bearings installed in the compressor casing.



**Fig. 3.2:** Rotor shaft of the turbocharger with a disk: 1 - shaft; 2 - blade with blades.





**Fig. 3.3:** The impeller of the compressor.

The turbine is a single-stage, axial, designed to convert the thermal energy of hot gases into mechanical work and includes three main units: a nozzle apparatus, a turbine disk with blades and a turbine case. The disk of the turbine [Fig. 3.4] is made of steel EI437BU, along the edge of the disk 36 Christmas tree grooves are made, into which turbine blades are inserted. The disc hub is tightened to the shaft with interference and is fixed with 6 radial pins made of 18X2H4BA steel. The rotor shaft is solid, made of steel 38XMUA. The blades of the turbine are made of the alloy ZhS6-K. On the disc, the turbines are fixed with a plate lock, the protrusions of which are bent to the disc of the turbine. [3,9,10]



**Fig. 3.4:** Turbine disc GTE-16M.

For further calculations, a 3D model of the turbocharger rotor in the Autodesk Inventor CAD was simulated [Fig. 3.5]. According to the operating and maintenance manual for the turbo-generator unit TG-16M, the 3D model is designed in a scale of 1: 1 and takes into account all the geometric features of these parts of the unit.



**Fig. 3.5:** Modelled turbocharger rotor 3D model.

## CONCLUSION

The software package Autodesk Inventor allows you to automate, simplify the design of the installation, significantly reduces costs. In this article, the turbo-generator unit TG-16M, the gas turbine engine, and its components are considered: a reducer, a GS-24A-3C direct current generator and systems. For normal operation of the installation in accordance with the specifications, the gas turbine engine GTD-16, turbocharger rotor, turbine, turbine disk are their main characteristics and components of the material. All parts of the system, with the correct modelled view, ensure a balanced and efficient operation of the installation.

Modelled model allows you to analyze it in the process of assembly, if necessary, make changes without losing the quality of the model.

In this paper, using the Autodesk Inventor program, calculations were made, the materials of the parts and their physical and chemical properties were assigned and an assembly unit was created that includes 3 components: a shaft, a disk with blades and a compressor impeller.

Model of turbo-generator unit TG-16M 3D-model is designed in scale 1: 1 and takes into account all the geometric features of these parts of the unit.

#### CONFLICT OF INTEREST

There is no conflict of interest.

#### ACKNOWLEDGEMENTS

The work is performed according to the Russian Government Program of Competitive Growth of Kazan Federal University.

#### FINANCIAL DISCLOSURE

None

## REFERENCES

- [1] Database for automated design of universal assemblies by means of Autodesk Inventor /[https://otherreferats.allbest.ru/programming/00189074\\_0.html](https://otherreferats.allbest.ru/programming/00189074_0.html)
- [2] Autodesk Inventor: A new look at engineering design / <http://www.cad.dp.ua/obzors/inventor.php>
- [3] Kuklin NG, Kuklin GS. [1987] Machine parts: Proc. For machine building specialists for technical schools, 4-th ed., Rev. and add. Moscow: Higher School. 383.
- [4] Radchik VM, Tarakanov VA, Popov KK, Yakutin KI. Sutormin Balancing machine, patent search, <http://www.findpatent.ru/patent/256/2561249.html>
- [5] Kontsevich VG. [2007] Solid modelling of engineering products in Autodesk Inventor, Kiev, Moscow: DiSoftTM, DMK Press. 672.
- [6] Research methods for developing graphical editors in the example of CAD-systems pipelines /[http://masters.donntu.org/m2016/fknt/zimonin/diss/index\\_e.htm](http://masters.donntu.org/m2016/fknt/zimonin/diss/index_e.htm)
- [7] Aretakis N, Mathioudakis K, Kefalakis M, Papailiou KD. [2004] Turbocharger Unstable Operation Diagnosis Using Vibroacoustic Measurements, ASME Journal of Engineering for Gas Turbines and Power. 126(3):840-847
- [8] Autodesk Inventor 2018 Basics Tutorial. Kishore, [2017] 190. ISBN 9781547048403. (Tutorial Books).
- [9] John S. Mitchell. [1981] An Introduction to Machinery Analysis And Monitoring. 202-204, PennWell Publishing.
- [10] Chen HH, Jablonka GE, Mitsche JV, Lewis JB. [1980] Turbine-Generator Loss of Life Analysis Following a Faulty Synchronization Incident, Proceedings of the American Power Conference. 42.
- [11] Gaponenko SO, Kondratiev AE. [2017] Device for calibration of piezoelectric sensors, PROCEDIA ENGINEERING, Series. International Conference on Industrial Engineering, ICIE 2017, Publishing: Elsevier Ltd. 146-150.
- [12] Gaponenko SO, Kondratiev AE, Zagretdinov AR. [2016] Low-frequency vibro-acoustic method of determination of the location of the hidden canals and pipelines, PROCEDIA ENGINEERING, Series. International Conference on Industrial Engineering, ICIE, Publishing: Elsevier Ltd. 150:2321-2326.
- [13] Nazarychev SA, Gaponenko SO, Kondratiev AE. [2018] Determination of informative frequency ranges for buried pipeline location control, Helix. 8(1):2481- 2487.
- [14] Gareev AA. [2012] Disassembly and assembly of gas turbine engine GTD-16, [Electronic resource]: electron, method, instructions, Ministry of Education and Science of Russia, Samara State Aerospace University na SP. Korolev (National Research University), Samara. 25.

## ARTICLE

# PIT DESIGN TAKING INTO ACCOUNT WATER LEVEL REDUCTION USING THE SOFTWARE PACKAGE MIDAS GTS NX

A.N. Sekisov<sup>1</sup>, A.V. Varvarkina<sup>1</sup>, D.A. Gura<sup>2\*</sup>, A.A. Savenko<sup>3</sup>, A.A. Shikhovtsov<sup>3</sup>

<sup>1</sup> Department of Construction, Kuban State Agrarian University named after I.T. Trubilin, Krasnodar, RUSSIA

<sup>2</sup> Department of Cadastre and Geo-engineering, Kuban State Technological University, Krasnodar, RUSSIA

<sup>3</sup> Department of Technology, Organization, Economics of Construction and Real Estate Management, Kuban State Technological University, Krasnodar, RUSSIA

## ABSTRACT

Using Midas GTS NX software package, the groundwater drainage is possible on the basis of needle filters and wells. This software package allows you to analyze the parameters of soil in the process of excavation. Midas GTS NX is based on the finite element method. Since this package is geotechnical one, it has a significant number of mathematical models describing the behavior of soil, depending on its physical and mechanical characteristics. One of them is the Mohr-Coulomb model. Due to this, you can get a complete picture of soil stress-strain state, to analyze and take appropriate measures.

## INTRODUCTION

During the development of the pit, the groundwater level is often above the pit bottom. Thus a number of measures is required to implement artificial water drainage [1,2,3,4]. One of such methods is the device of needle-filtering units and wells.

During the implementation of the related activities, it becomes necessary to take into account the changes of developed soil physico mechanical properties [3,4,5].

The complex of calculations for the pit development is implemented in Midas GTS NX software package, taking into account dewatering. The presented complex provides the opportunity to analyze in detail the soil parameters during the excavation process. Midas GTS NX program allows you to apply the finite element method effectively. Since this complex is geotechnical, it includes a sufficient number of mathematical models that describe the behavior of soil depending on its physico mechanical characteristics [6–12]. One of them is the Mohr-Coulomb model.

## METHODS AND MATERIALS

The mathematical model of Mohr-Coulomb describes the dependence of tangential stresses on the magnitude of the normal stresses applied to the material. This is due to friction inside a solid body.

The dependence of the tangential stress of the material on the magnitude of the applied normal stresses is a bilinear dependence, which is the criterion of Mohr-Coulomb strength and is described by the following formula:

$$\tau = \sigma \tan(\varphi) + c$$

where  $\sigma$  – the value of normal stresses,

$\tau$  – the magnitude of the tangential stresses,

$c$  – the intersection of the strength criterion curve with  $\tau$  axis,

$\tan(\varphi)$  – slope angle tangent of the strength criterion curve.

If  $\varphi=0$ , the Mohr-Coulomb strength criterion turns into the Tresca criterion. If  $\varphi=90^\circ$ , then the Mohr-Coulomb strength criterion corresponds to the Rankine viscous medium model.

For the circles of Mohr it is true that:

$$\sigma = \sigma_m - \tau_m \sin \varphi; \tau = \tau_m \cos \varphi,$$

where  $\tau_m = \frac{\sigma_1 - \sigma_2}{2}$ ,  $\sigma_m = \frac{\sigma_1 + \sigma_2}{2}$

where  $\sigma_1$  – the maximum principal stress,

$\sigma_2$  – the minimum principal stress.

Therefore, the Mohr-Coulomb strength criterion can be represented as follows:

### KEY WORDS

well, stress-strain state, pit, groundwater level, dewatering, finite element method.

Received: 25 Oct 2018  
Accepted: 21 Dec 2018  
Published: 10 Jan 2019

\*Corresponding Author

Email:  
gda-kuban@mail.ru

$$\tau_m = \sigma_m \sin \varphi + c \cos \varphi$$

This type of Mohr-Coulomb strength criterion corresponds to the fracture on a plane parallel to the direction of the main stress  $\sigma_2$ .

The Mohr-Coulomb strength criterion is used to analyze the bearing capacity of soil massifs.

During loading soils work mainly on surface shear with the lowest bearing capacity. Therefore, shear strength is the defining strength characteristic for soils.

The destruction occurs at the moment when the magnitude of the shear (tangential) stress reaches the ultimate soil strength at shear. Therefore, the relationship between normal shear stresses is the criterion of strength for soils.

Let's consider the solution to this problem by example.

There is the evidence of the construction site engineering-geological profile [Fig. 1].

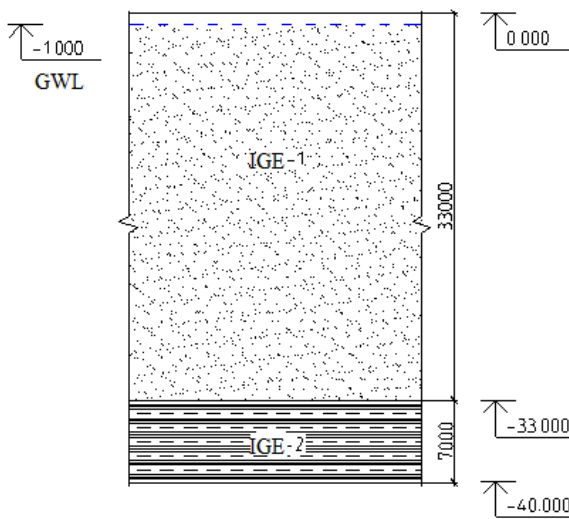


Fig. 1: Engineering-geological section.

The geotechnical data of the construction site is presented below [Table 1].

Table 1: Geotechnical data

Soil name	Specific soil adhesion with, kPa	The angle of internal friction, $\varphi$ , deg.	The modulus of the total strain E, MPa	The specific weight of soil particles $\gamma_w$	The specific weight of soil $\gamma_w$ , kN/m <sup>3</sup>	Poisson's ratio $\mu$	Layer thickness, m
IGE 1	1	35	$30 \times 10^6$	21	17	0.3	33
IGE 2	49	24	$42 \times 10^6$	21	19,5	0,32	7

During the excavation development, HYUNDAI R330LC-9A crawler excavator was used. The loading was carried out via MAN TGA 33.350 6X4 BB-WW dump truck with a bucket capacity of 15 m<sup>3</sup> [Fig. 2].

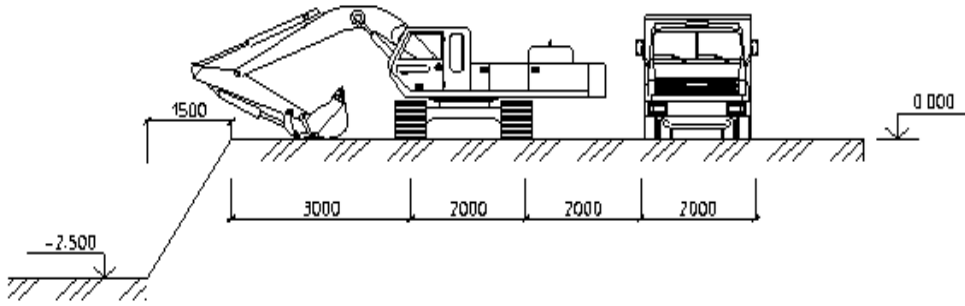


Fig. 2: Pit development scheme using construction machines and mechanisms.

The actual loads and impacts during the pit development at the construction site are presented below [Table 2].

Table 2: Loads and Impacts

Load name	Meas. Un.	Rated value	Safety factor	Design value
Constant				
Net weight of the 1st layer of soil (sand)	t/m <sup>3</sup>	1.7	1,1	1,87
Net weight of the 2nd layer of soil (clay)	t/m <sup>3</sup>	1.95	1,1	2,15
Temporal load				
Excavator	kN	75	-	75
Dump truck	kN	75	-	75

The design scheme of the excavation at the construction site is presented below [Fig. 3].

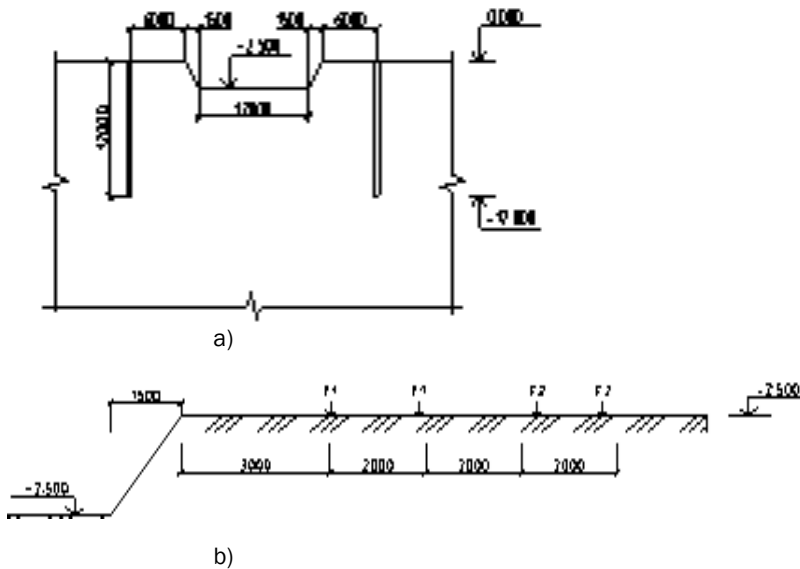


Fig. 3: The design scheme of the excavation design: a) the design of wells, b) the load from the construction machines and mechanisms.

The generated finite element model in Midas GTS NX software [Fig. 4].

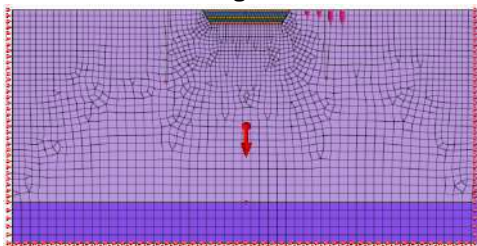


Fig. 4: Finite-element model.



[Fig. 5-13] demonstrate iso-fields at different stages of calculation (type of loading), which we consider in this problem.

The first stage is filtering, which we determine for the given soil conditions.

At the second stage, the stress-strain state (SSS) of soil strata is considered.

The third stage is characterized by the appearance of an excavator at a construction site for the development of soil (the load from an excavator).

The next calculation step is the accounting for the separation of the first excavation and its loading into a dump truck (a dump truck arrived at the construction site for excavated soil loading into it).

Then the separation of the second excavation and the loading of the excavated soil into the dump truck takes place. The truck has already been emptied from the first part of soil (took it to another part of the construction site where filling is required).

Then the calculation stage takes place with the separation of the third excavation and the loading of soil from the third excavation into the dump truck.

A similar situation is observed during the step 7 of the computational model, where the separation of the excavation 4 and the loading of the fourth soil into the dump truck takes place.

Step 8, the final one, the separation of the excavation 5 and the loading of the remaining soil in the dump truck.

During the current model calculation, the following values were obtained:

a) initial filtration [Fig. 5].

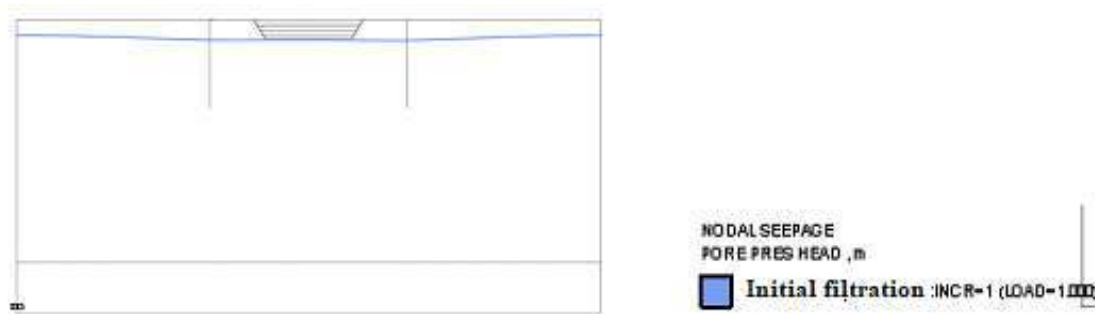


**Fig. 5:** Initial filtration.

The line shows the level of filtration in a given soil massif after water-lowering using a well device.

b) pore pressure, after the excavator arrival at the construction site [Fig. 6].



**Fig. 6:** Pore pressure.

The pore pressure isoline represents the calculation results in the software after the excavator arrival at the construction site to develop the excavation.

c) deformations (maximum and minimum) arising from the own weight of the excavator [Fig. 7].

The maximum and the minimum values of deformations along Y axis that occur during the excavation of the upper soil layer by the excavator [Fig. 7].

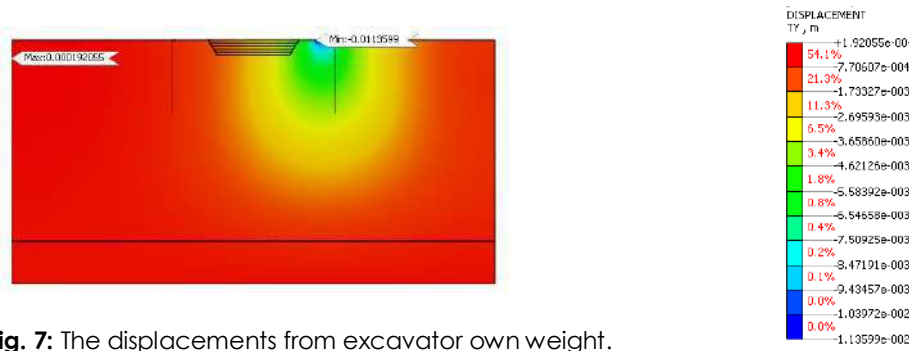


Fig. 7: The displacements from excavator own weight.

d) the deformations during the development of the first soil layer [Fig. 8].

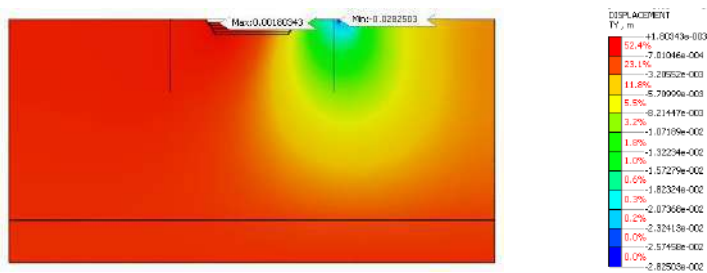


Fig. 8: Displacements from the excavator weight during the first soil layer development.

e) deformations during the development of the second layer of soil [Fig. 9].

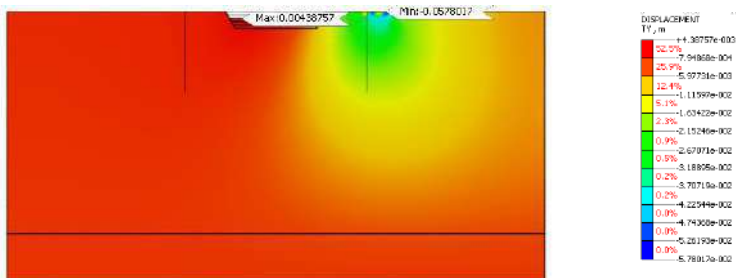


Fig. 9: The displacements from excavator and dump truck weight during the second soil layer development.

f) the deformations during the development of the third soil layer [Fig. 10].

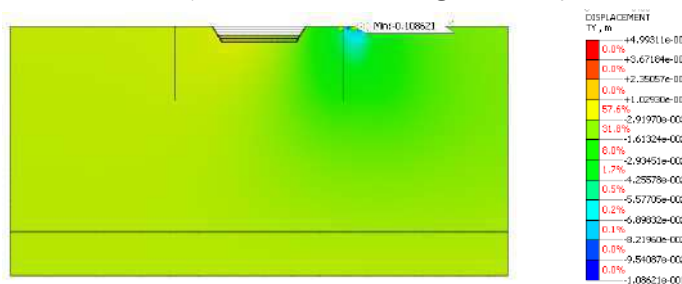


Fig. 10: The deformations from excavator and dump truck weight during the third layer of soil development.

g) The deformations during the fourth layer of soil development [Fig. 11].

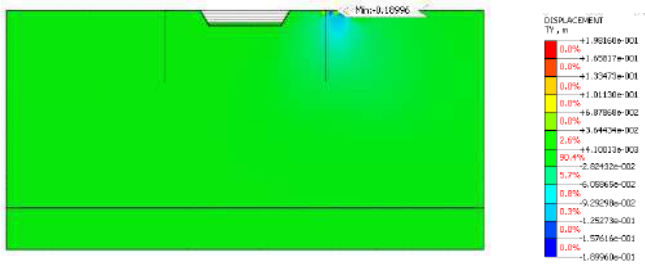


Fig. 11: Deformations from excavator and dump truck weight during the development of the fourth layer of soil.

h) deformations during the development of the fifth soil layer [Fig. 12].

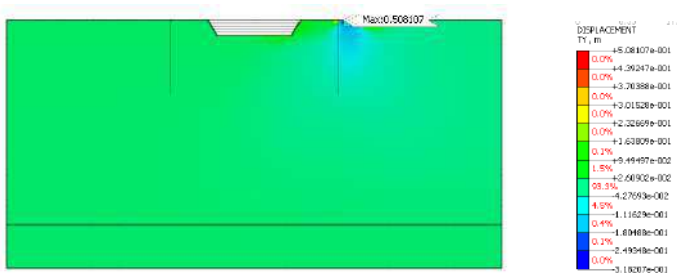


Fig. 12: Deformations from excavator and dump truck weight during the development of the fifth layer of soil.

i) The stresses in XY plane [Fig. 13].

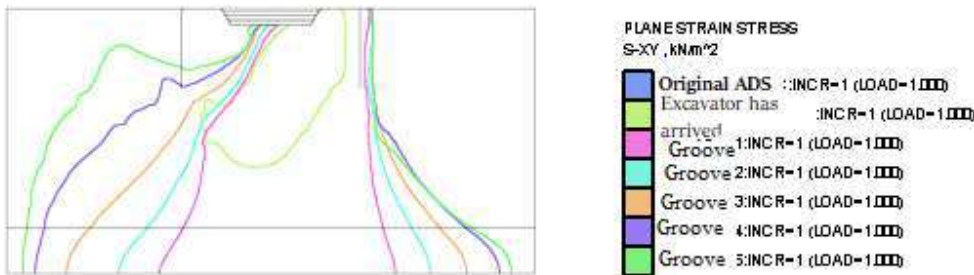


Fig. 13: The stresses in XY plane XY.

Iso fields display the stress distribution from the corresponding loads [Table 3].

Table 3: Calculation results

Load type	Pore pressure/ (stress), kPa/ (kN/m <sup>2</sup> )		Movement, m		Stress, kN/m <sup>2</sup>			
	Max	Min	Max	Min	Max		Min	
					XY	Y	XY	Y
1	382,5	-27,4	-	-	-	-	-	-
2	1,0	-382,5	-	-	1,3	-3,5	-1,2	-440,1
3	1,0	-382,5	1,9×10 <sup>-4</sup>	-1,1×10 <sup>-2</sup>	10,0	-0,5	-11,0	-442,6
4	1,0	-382,5	1,8×10 <sup>-3</sup>	-2,8×10 <sup>-2</sup>	23,3	4,9	-16,0	-447,7
5	1,0	-382,5	4,4×10 <sup>-3</sup>	-5,8×10 <sup>-2</sup>	37,4	55,3	-33,3	-452,4
6	1,0	-382,5	5,2×10 <sup>-2</sup>	-1,1×10 <sup>-1</sup>	59,7	147,3	-56,8	-796,5
7	1,0	-382,5	0,2	-0,2	107,4	324,0	-84,4	-1269
8	1,0	-382,5	0,5	-0,3	148,0	436,6	-137,1	-1850

Loading type: 1 - filtration; 2 - stress-strain state (SSS); 3 - the load from excavator; 4 - the separation of excavation 1 and the loading of the first soil into the dump truck; 5 - the separation of excavation 2 and

the loading of the second soil into the dump truck; 6 - the separation of the excavation 3 and the loading of the third soil into the dump truck; 7 - the separation of excavation 4 and the loading of the fourth soil into the dump truck; 8 - the separation of the excavation 5 and the loading the remaining soil into the dump truck.

Having analyzed the results of the calculations presented in [Table 3], let's develop the dependency graphs, thanks to which it will be possible to understand how the stress-strain state of soil depends on soil saturation with water. Analyzing [Fig. 14-16] it is possible to trace the physico mechanical changes in soil by stages.

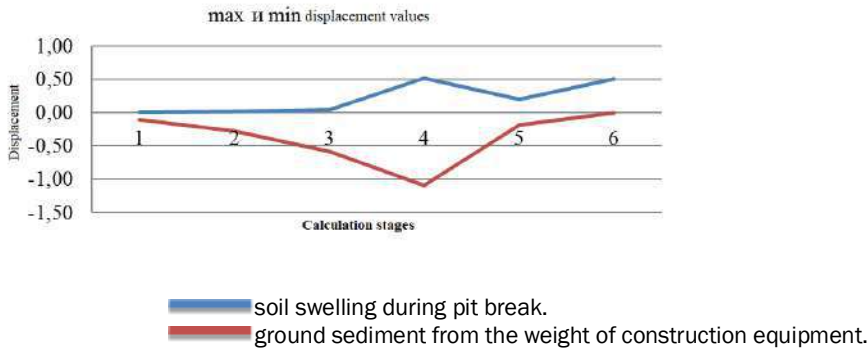


Fig. 14: The graph of maximum and minimum displacements.

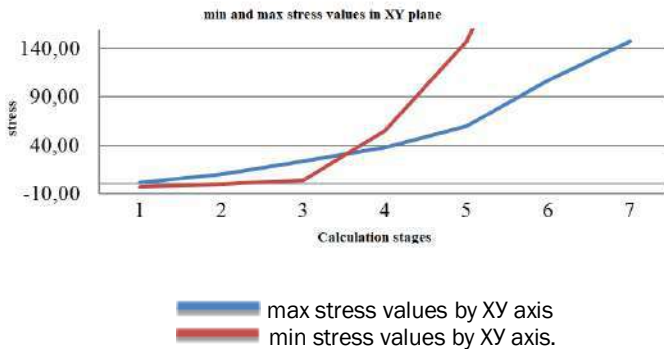


Fig. 15: The graph of maximal and minimal stresses.

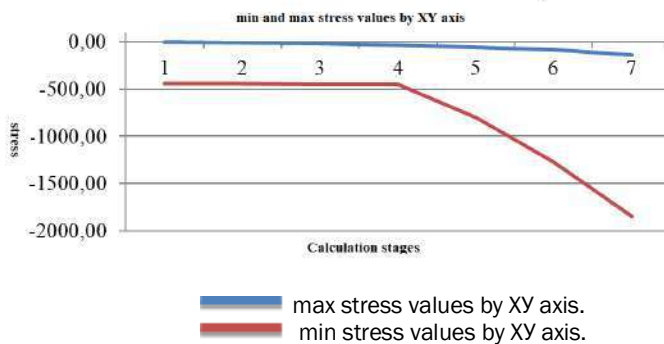


Fig. 16: The graph of maximum and minimum stresses along Y axis.

## RESULTS

Thus, under the action of a load applied to the base by construction machines, the stress state arises in soil, which causes the development of deformations leading to the displacement (the settlement) of the soil surface.

The analysis of soil problem solution results showed that SSS significantly depends on the degree of soil saturation with water. At the end of the primary (filtration) consolidation, the pore pressure at all stages makes 1, hence the sediment is caused solely by the shear deformations of the soil skeleton. Soil is compacted with water lowering.

This task, which was calculated in Midas GTS NX software package, can be used during drainage calculation, the determination of underground water supply source debit, the calculation of structure sediments over time, an artificial lowering of groundwater level and the digging out of pits.

## CONCLUSION

The scientific novelty of the study is in a new multifactorial approach for this problem solution, namely: the determination of the mathematical model for the soil conditions of the construction site, the selection of machines and mechanisms for pit excavation, the arrangement of water-reducing plants and the determination of their characteristics and step-by-step calculation in Midas GTS NX.

Only when the multifactorial nature of the problem and the availability of reliable data on the foundation soils are taken into account one can carry out the measures for water lowering successfully.

### CONFLICT OF INTEREST

There is no conflict of interest.

### ACKNOWLEDGEMENTS

None

### FINANCIAL DISCLOSURE

None

## REFERENCES

- [1] Degtyareva OG. [2016] Using CAE-systems for solving engineering problems, Scientific support of the agro-industrial complex. Collection of articles based on the materials of the 71st Scientific and Practical Conference of Teachers on the basis of research in 2015. Krasnodar: KubSAU, 2016: 462-463.
- [2] Degtyareva OG. [2014] Features of the analysis of the state of a building under construction in complex hydrogeological conditions of the city of Sochi", Polythematic network electronic scientific journal of the Kuban State Agrarian University, Krasnodar: Kuban State Agrarian University, 7: 1-25.
- [3] Degtyarev VG, et al. [2018] Modeling of the Building by Numerical Methods at Assessment of the Technical Condition of Structures. International conference on Construction and Architecture: theory and practice of industry development (CATPID-2018). Trans Tech Publications, Switzerland, 931: 141-147.
- [4] Degtyareva OG, et al. [2018] The Calculation of a Drain Seasonal Regulation Reservoir Volume Probability. International conference on Construction and Architecture: theory and practice of industry development (CATPID-2018). Trans Tech Publications, Switzerland, 931: 991-995.
- [5] Degtyarev VG, et al. [2018] The Foundation Pit Deep Site Ground State Design Modelling Process. International conference on Construction and Architecture: theory and practice of industry development (CATPID-2018). Trans Tech Publications, Switzerland, 931: 396-404.
- [6] Nehaj R, et al. [2017] Algorithm of composing the schedule of construction and installation works. IOP Conference Series: Earth and Environmental Science, 90 (1):1-8.
- [7] Sekisov AN, et al. [2018] Development of the Methods Improving the Production Costs Formation Process, International conference on Construction and Architecture: theory and practice of industry development (CATPID-2018). Trans Tech Publications, Switzerland, 931:1210-1213.
- [8] Litvinov SV, et al. [2018] Buckling of Glass Reinforced Plastic Rods of Variable Rigidity. International conference on Construction and Architecture: theory and practice of industry development (CATPID-2018). Trans Tech Publications, Switzerland, 931: 133-140.
- [9] Degtyarev GV, et al. [2018] Numerical modeling of condition of the bridge structure based on the results of national surveys. International Journal of Engineering & Technology, 7(2.13),226-230.
- [10] Yazyev BM, et al. [2018] The Definition of a Critical Deflection of Compressed Rods with the Creep by the Method of Bubnov-Galerkin. International conference on Construction and Architecture: theory and practice of industry development (CATPID-2018). Trans Tech Publications, Switzerland, 931: 127-132.
- [11] Gura DA, et al. [2017] Application of inertial measuring unit in air navigation for ALS and DAP // Journal of Fundamental and Applied Sciences, 9(1S): 732-741.
- [12] Kuzyakina MV, et al. [2018] Experimental analysis of srtm model by image processing and geostatistical methods, International Journal of Engineering and Technology(UAE). 7(4.7): 250-253.



## ARTICLE

# PROFILE RESEARCHES OF NATURAL AND AGROGENE CHERNOZEMIC SOILS BIOLOGICAL ACTIVITY IN THE BELT OF STEPPE MEADOWS OF CENTRAL CAUCASUS (KABARDINO-BALKAR REPUBLIC)

Olga N. Gorobtsova, Tatyana S. Uligova, Fatima V. Gedgafova\*, Rustam H. Tembotov, Elena M. Khakunova, Victoria A. Chadayeva, Nellie L. Tsepkova, Zalim M. Khanov, Albert Zh. Zhashuev

*Tembotov Institute of Ecology of Mountain Territories, Russian Academy of Sciences, RUSSIA*

## ABSTRACT

The profile research and the morphogenetic description of various subtypes of the natural and agrogene mountain chernozemic soils widespread in a belt of steppe meadows of the Elbrus option of zonation of Kabardino-Balkaria is conducted. Parameters of biological activity are set: content and a reserves of humus, rate of basal and substrate - induced respiration, content and reserves of carbon of microbial biomass, enzyme activity oxidoreductases (catalase, dehydrogenase) and hydrolase (invertase, urease, phosphatase) in profiles of virgin and arable mountain chernozemic soils ordinary, typical and leached. It is shown that the changes of parameters of biological activity which resulted from arable use have difficult and ambiguous character. Steady distinctions at the level of subtype, both in virgin, and in arable mountain chernozemic soils are not revealed. The main changes of indicators of biological activity are observed in the arable horizons. To establish the general level of biological activity and to estimate the extent of its change, the uniform estimated criterion - the integre index of an ecological and biological state of the soil (IIEBSS) is applied. High level of profile biological activity of natural and arable mountain chernozemic soils is established, and differences in IIEBSS values between profiles of agrogene and natural soils are practically absent. The IIEBSS values defined for the top horizons (0-20 cm) indicate noticeable easing of biological activity (for 16-43%) in the arable horizons of all subtypes of mountain chernozemic soils.

## INTRODUCTION

Mountain chernozemic soils - the unique, high-fertile soils occupying the space about 845 km<sup>2</sup> (500-1200 m above sea level) in Kabardino-Balkar Republic and actively used under an arable land, long-term plantings, haymakings and pastures. At agricultural influence there is a continuous and intensive influence on the main modes and properties of soils. At the same time a necessary condition of their further arable use is maintaining fertility and creation of optimum conditions of growth of cultural plants (corn, sunflower, etc.). Though the main changes of soil properties happen in the arable and subarable horizons [1], it is necessary to track the direction of dynamics of biological activity in all a profile of the processed soils that was highlighted with leading experts in the field of biology of soils [2]. Biological properties of mountain chernozemic soils of Central Caucasus were not investigated earlier, but in a number of works [3-5] the efficiency of studying of various biological characteristics of soils when determining extent of negative anthropogenic impact is shown.

Thus, a research objective is definition of extent of change of the general level of profile biological activity of various subtypes of arable mountain chernozemic soils in comparison with their virgin analogs in a belt of steppe meadows.

## METHODS

The explored area is located at the height of 560-850 m above sea level (a.s.l.) in the territory of the Elbrus option of zonation which differs in rather arid and continental climate which is formed under the influence of free circulation of winds of Prikaspiya [6]. Climatic conditions at which mountain chernozemic soils around researches function are characterized with the average annual air temperature of +7,80 C. The, rainfall has on average 560-700 mm/year, evaporability of 707 mm/year, duration of the no-frost period from March to November, the sum of average daily temperatures (more than +1000C) during active vegetation (174-177 days) makes about 30000 [7]. The hydrothermal mode of mountain chernozemic soils which is formed under such circumstances is favorable for activity of a soil biota and also cultivation of crops and long-term fruit plantings. Conditions of the Elbrus option contributed also to the development of dense natural grassy meadow and steppe vegetation on mountain chernozemic soils which quite often forms a dense organic mat at a protective covering of herbage about 100%.

Mountain chernozemic soils lie on plateau-like heights where possess the full-developed profile. The leveled sites almost completely are opened, as well as mild slopes. Soilforming breeds are products of aeration of carbonate dense sedimentary breeds - eluvia-slide-rocks of limestones, sandstones, limestones and marlstone, carbonate clays and loams [8, 9]. Rubble and stony inclusions of carbonate maternal breeds quite often meet from a surface and on all profile of mountain chernozemic soils.

## KEY WORDS

mountain chernozemic soils, biological activity

Received: 29 Oct 2018  
Accepted: 22 Dec 2018  
Published: 10 Jan 2019

\*Corresponding Author  
Email:  
ecology\_lab@mail.ru

Collecting and the analysis of soil samples for determination of physical and chemical and biological properties of natural and arable mountain chernozemic soils (ordinary, typical, leached) carried out by the standard methods in ecology and soil science [10]. Lying of cuts and sampling on the genetic horizons were made in the first decade of July, 2016 the soils not subject to slope erosive processes having characteristic morphogenetic properties and the full-developed profile were considered. Soil cuts were put in characteristic natural meadow biogeocenoses and in agrocenoses under crops of corn in a stage of formation of an ear [Table 1].

**Table 1:** The locations of cuts of mountain chernozemic soils in natural and agricultural biogeocenoses of the explored territories

Arable mountain chernozemic soils		Natural mountain chernozemic soils	
Name of the soil	Coordinates of the place of laying of a section	Name of the soil	Coordinates of the place of laying of a section
The chernozemic soil ordinary carbonate average thickness low-humus heavy loam on yellow-brown carbonate clays	Zolsky district, surrounding settlements of Kamennomostskoye, h-850 m a.s.l., 43°45'01 "N 43°1'34 "E	The chernozem is ordinary carbonate low-power average humus average loamy on yellow-brown carbonate loams	Zolsky district, surrounding settlements of Kamlyukovo, h-752 m a.s.l., 43°46'3 "N 43°12'41 "E
The chernozem typical average thickness low-humus heavy loam on yellow-brown carbonate clay breeds with pebble impurity	Baksan district, surrounding settlements Top Kurkuzhin, h-694 m a.s.l., 43°43'38 "N 43°21'16 "E	The chernozem is typical average thickness average humus average loamy on yellow-brown carbonate clay breeds with pebble impurity	Baksan district, surrounding settlements Top Kurkuzhin, h-856 m a.s.l., 43°41'39 "N 43°14'60 "E
The chernozem leached average thickness low-humus average loamy on brown carbonate loams with impurity of crushed stone and pebble	Baksan district, surrounding settlements Top Kurkuzhin, h-578 m a.s.l., 43°45'58 "N 43°22'46 "E	Leached chernozem average thickness low-humus average loamy on yellow-brown carbonate deposits of coarse-grained rough sand and crushed stone	Baksan district, surrounding settlements of Islamey, h-561 m a.s.l., 43°40'44 "N 43°26'42 "E

Besides, the method of "envelope" selected samples of various subtypes of the virgin and processed mountain chernozemic soils in a layer of 0-20 cm which reflect properties of the arable and humic and accumulative horizons of the explored soils, selection volume for each subtype was 16-18 samples. When determining places of sampling used the soil card and personal navigator GPS MAP 60 CEX [11]. Classification diagnostics of the studied subtypes of chernozemic soils was performed according to genetic classification of soils [12].

Lying of soil cuts and sampling of virgin mountain chernozemic soils were made within undisturbed natural meadow biogeocenoses. Geobotanical descriptions carried out on each site. Determined a protective covering and average height of herbage, specific structure and total number of species of plants, the index of sinantropization (a share of sinantropny types from total number) by A.M. Abramova's method [13].

Laboratory and analytical researches carried out in 3-9 multiple frequencies. The content of humus was determined by Tyurin's method in Nikitin [4] modification, pH of suspension (1:2,5) by electrometric. The activity of enzymes (invertase, urease, phosphatase, dehydrogenase) was determined by colorimetric and catalase by gasometric method by Galstyan's techniques in Haziyev's modification [14]. The received indicators were estimated by the scale by Gaponyuk and Malakhov [15]. The relative total profile enzymatic activity was calculated according to Zvyagintsev's method [16].

The physiological activity of soil microbial biomass was established using the basal and substrate - induced respiration (a BR and SIR) [17]. Definition was carried out according to methodical developments of N.D. Ananyeva [18, 19]. The preincubation of samples was carried out at optimum humidity of soils (60% of MMC) within 7 days at a temperature of 220C in plastic bags with air exchange. Quantitatively release of carbon dioxide was defined according to A.Sh. Galstyan's technique [20]. The SIR rate was estimated on the rate of respiration of microorganisms after enrichment of the soil glucose (0,2 ml/g of the dry soil; a caption of 0,05 g of glucose) and incubations during 4 hours at a temperature of 220C. For calculations of content of carbon of microbial biomass (C mic) the SIR rate expressed in ml CO<sub>2</sub>/g of soil / in hour. Cmic (mkg C/g soil) = SIR (mkl CO<sub>2</sub>/g soil/hour) × 40,04 + 0,37 [21]. The reserve of microbial biomass carbon in the 20 cm layer was calculated taking into account density of the explored soils: Cmic reserved (g/m<sup>2</sup>) = Cmic (mkg C/g soil) × d (g/cm<sup>3</sup>) × V, where the V - volume of the soil in a layer of 20 cm and the area of 1 m<sup>2</sup> = 10000 cm<sup>2</sup>. Density of soils (d (g/cm<sup>3</sup>)) defined according to state standard specification 5180-2015.

For definition and comparison of the general level of biological activity of various subtypes of chernozemic soils used a method of calculation of the integral index of an ecological and biological state of soils (IIEBSS) [22, 23]. For finding of IIEBSS the maximum value of each of indicators in selection was taken for 100%, and in relation to it expressed values of this indicator in relative percent in other samples: Bi = Bx/Bmax × 100 of %, where Bi - relative point of indicator; Bx - the actual value of an indicator; B max - the maximum value of indicator. Then summarized relative data of several indicators which absolute values

cannot be summarized since have different units of measure:  $Bav. = (B_1 + B_2 + \dots + B_p) / N$ , where  $Bav.$  - average estimated point of an indicator;  $N$  - number of indicators. IIEBSS was calculated by a formula:  $IIEBSS = (Bav. / Bav. max.) \times 100\%$ , where  $Bav.$  - average estimated point of all indicators;  $Bav. max.$  - the maximum estimated point of all indicators. At calculations used these activities of five studied enzymes, the rate of BR, reserves of humus and microbial biomass defined taking into account density of addition of the top horizons and therefore more precisely the reflecting properties of the explored soils.

Statistical processing of the obtained data was carried out in the Statistica-10.0 program. Reliability of distinction of the studied soil characteristics estimated at significance value  $\alpha \leq 0,05$ .

## RESULTS AND DISCUSSION

Lying of soil cuts, sampling and the description of vegetable communities within natural biogeocenoses were carried out on sites, free from intensive anthropogenic influence. Respectively this factor had no significant effect on the studied parameters of virgin mountain chernozemic soils that causes legitimacy of carrying out the comparative analysis of natural and agrogenic soils. Justification of the studied natural meadow wholeness bio geocenoses are the lack of a trail structure, traces of journey of agricultural machinery and a pasture of the cattle and also the results of geobotanical researches which revealed high values of the general projective covering and average height of herbage, considerable specific richness of flora and also low level of sinantropization of sites [Table 2]. As a part of forb-cereal steppe meadows of all three sites types of *Festuca pratensis* Huds and *Elytrigia repens*, characteristic of the area of researches dominate (L.) Desv. ex Nevski. From forb high abundance have *Galium verum* L., *Salvia verticillata* L., *Medicago falcata* L., *Achillea millefolium* L. *Cirsium ciliatum* (Murray) Moench, *Carduus crispus* L occur among sinantropny plants single copies., *Urtica dioica* L.

**Table 2:** The geobotanical description of the studied natural biogeocenoses of Central Caucasus Mountains (in borders of Kabardino-Balkaria)

Geobotanical characteristics of sites	Sites of natural biogeocenoses		
	Zolsky district, surrounding village of Kamlyukovo	Baksan district, surrounding page V. Kurkuzhin	Baksan district, surrounding village of Islamey
General projective covering, %	90	100	90
Height of herbage, cm	30	35	40
Number of species of plants	34	30	36
Index of a sinantropization, %	2,94	3,33	5,55
Level of anthropogenic pressure	Low	Low	Low

Acid-base conditions considerably define biological activity of the soil as exert impact on chemical properties of humus and the specific structure of microbial community and also enzyme activity showing high activity in the certain range of values pH (the invertase is most active in acidic conditions, urease - in neutral, phosphatase, dehydrogenase and catalase - in alkaline) [3, 4, 16]. Comparison of the data characterizing physical and chemical properties of the compared natural and arable mountain chernozemic soils [Table 3] shows that values pH (H<sub>2</sub>O) are in limits of genetically caused values corresponding to neutral and alkaline reaction of soil solution.

Density of addition of natural soils is lower, than processed. In profiles of chernozemic soils ordinary and typical even in the horizon of B1 the values of this indicator <1 g/cm<sup>3</sup> that is probably connected with action of powerful root system of grassy plants and also activity of earthworms and activity of other representatives of mesofauna. Values of density in the arable horizons can be considered close to optimum.

Down a profile of the processed soils density naturally increases, but even upon transition to maternal breed does not exceed 1,32 g/cm<sup>3</sup> that speaks about lack of reconsolidation of the described soils as a result of processing.

Dehumification of arable soils - well studied and conventional phenomenon. The data about decrease of content and reserves of humus are provided in the plain chernozemic soils of Kabardino-Balkaria by us earlier [24-27]. The cespitose layer of natural mountain chernozemic soils is characterized by high (> 6%) humus content, however, in our opinion, it is not quite correct to compare the content of humus in the arable horizon and cespitose. Comparison of parameters of the arable horizon and the humus-accumulative horizon A is more justified.

The noticeable difference in the humus content between the arable horizon and horizon A is established only for the typical chernozem (decrease in the arable horizon makes 24%). For chernozemic soils ordinary and leached quite comparable indicators are found. Calculations of stocks of humus in layer of 0-20 cm of natural and agrogenic chernozemic soils also speak about close values which can be characterized as averages: for chernozemic soils ordinary - 108 t/hectare and 110 t/hectare, chernozemic soils typical - 136 t/ha and 142 t/ha, leached - 117 t/ha and 112 t/ha respectively.

**Table 3:** Profile physical and chemical indicators of mountain chernozemic soils of Central Caucasus (in borders of Kabardino-Balkaria)

Arable mountain chernozemic soils					Natural mountain chernozemic soils				
Depth of sampling of the soil, cm	Content of humus, %	Reserves of humus, t/ha	Density, g/cm <sup>3</sup>	pH H <sub>2</sub> O	Depth of sampling of the soil, cm	Content of humus, %	Reserves of humus, t/ha	Density, g/cm <sup>3</sup>	pH H <sub>2</sub> O
Ordinary chernozemic soils									
Aar. 0-20	5,3	106	1,0	7,98	A0 0-5	7,0	32	0,9	6,63
A 20-37	4,6	86	1,1	7,95	A 5-18	5,8	68	0,9	6,83
AB 37-57	4,3	102	1,2	7,97	AB 18-33	5,0	69	0,9	7,42
B1 57-76	4,0	99	1,3	8,05	B1 33-47	3,4	48	1,0	7,62
Bca 76-104	2,6	95	1,3	8,05	Bca 47-84	3,0	122	1,1	7,64
BC 104-140	2,2	94	1,3	8,03	BC 84-110	2,4	75	1,2	7,63
Typical chernozemic soils									
Aar. 0-20	5,9	142	1,2	6,95	A0 0-6	9,3	45	0,8	6,42
A 20-46	5,1	146	1,1	7,52	A 6-26	7,8	125	0,8	6,86
AB 46-67	3,7	86	1,1	7,98	AB 26-50	3,7	80	0,9	7,05
B1 67-90	2,5	69	1,2	8,21	B1 50-73	2,4	50	0,9	7,80
Bca 90-140	2,0	130	1,3	8,25	B2 73-110	2,1	93	1,2	8,28
BC 140-180	2,0	104	1,3	8,56	BC 110-140	2,0	72	1,2	8,06
Leached chernozemic soils									
Aar. 0-20	5,1	112	1,1	7,80	A0 0-5	6,5	33	1,0	7,12
A 20-38	2,2	48	1,2	8,07	A 5-30	5,1	140	1,1	7,86
AB 38-64	2,1	66	1,2	8,26	AB 30-50	3,0	66	1,1	7,97
B 64-88	1,2	37	1,3	8,33	B 50-84	1,6	60	1,1	8,33
BC 88-120	1,1	46	1,3	8,52	BC 84-130	1,0	51	1,1	8,35

Decrease in humus content down a profile for all described soils (except for the agrochernozem leached) has similar character. Upon transition from A0 horizon to the horizon A (in natural soils) and also Aar. to the horizon A (in processed) the change of indicators comes for 13-22%. Sharper decrease (rather overlying horizon) is noted in a middle part of a profile (below AB horizon) where it makes 32-47%. It should be noted that in a profile of natural and arable chernozemic soils ordinary below the horizon of B1 the differences in sizes of the described indicator are less, than in the top horizons. In chernozemic soils typical similar values take place already in the horizon of AB and further down a profile. In ordinary and typical chernozemic soils - both virgin, and arable, rather high content of humus is observed even upon transition to maternal breed. It indicates existence of an organic substratum and activity of microbiological and biochemical processes and also zoogene transfer of organic substance down a profile. The set of biological processes and also mechanical transfer of organic substance forms the stretched humic profile of mountain chernozemic soils.

In a profile of the mountain agrochernozem leached there is sharp decrease in humus content (more than twice) in the subarable horizon owing to what the data characterizing humus condition of the horizons of A and AB practically coincide. In a profile of the virgin leached chernozem so noticeable difference in the humus content between the top horizons is not observed. Below the horizon of AB the differences in values of this indicator in virgin and arable soils are leveled and in the horizon of BC make about 1%. Therefore, it is possible to make the assumption that sharp reduction of contents (and a stock) humus in the subarable horizon of this subtype of the chernozem is connected with its processing. Clarification of the reason of so sharp falling demands a separate detailed research as it is not quite clear - whether noted feature is typical for arable mountain leached chernozemic soils and also - whether it is connected with high content of mobile humic fractions in these soils.

Calculation of profile reserves of humus showed that in the compared couples of agrogene and virgin mountain chernozemic soils ordinary (respectively 583 t/ha and 413 t/ha) and typical (677 t/ha and 465 t/ha) this indicator is higher than in the processed soils. The great values of density of addition established for all horizons of agrochernozemic soils and also more powerful profile of arable chernozemic soils ordinary and typical are the reason. Humus stocks in mountain chernozemic soils leached make for a profile of the arable soil - 309 t/ha, and virgin - 350 t/ha that, at comparable values of density and power of leached chernozemic soils, is a consequence of lower humus content in all profile of the agrochernozem.

Along with the profile researches selections of soil samples in a layer of 0-20 cm of natural and arable chernozemic soils were made. According to the obtained data, the average content of humus (the volume of selection of 16-18 samples for each subtype) in the processed chernozemic soils ordinary is  $5,28 \pm 0,52\%$ , in virgin -  $8,05 \pm 0,49\%$ ; in chernozemic soils typical -  $7,27 \pm 0,54\%$  and  $9,76 \pm 0,96\%$ ; in leached -  $6,41 \pm 0,69\%$  and  $8,50 \pm 0,93\%$  respectively. The given average values of the considered indicator allow judging the direction of process of change of humic state of the arable horizons of mountain chernozemic soils, in comparison with natural analogs. The decrease in humus content by 25-34% statistically significant ( $t > 2,3$  is established;  $p < 0,04$ ) for all subtypes, therefore, around a research humic degradation of the arable horizons of mountain chernozemic soils takes place.

Catalytic activity of soil enzymes is a traditional indicator of biological activity of the soil. The analysis of the obtained data confirms low activity of the studied enzymes in the processed mountain chernozemic soils. [Table 4] of the explored territories. In the arable horizons absolute values correspond to average and weak levels [15]. The exception is made by the urease showing high activity up to mountains of B1 in a profile of the agrochernozem ordinary that can be a consequence of recent introduction of nitrogen fertilizers. With a depth the activity of all enzymes gradually decreases, but, as a rule, remains (though very weak) even upon transition to maternal breed.

Comparison of absolute values of activity of enzymes in the natural and processed soils shows that activity of the oxidoreductases (catalase and dehydrogenase) participating in oxidation-reduction processes of synthesis of humic components changes as a result of agricultural influence to a lesser extent, than behavior of hydrolytic enzymes. Data are in limits of one category of activity, or decrease (in comparison with horizon A of virgin soils) from average - to weak or from weak - to very weak. Presumably, the aeration of the arable horizon of the soil happening when processing to some extent influences functioning of oxidoreductases therefore falling of their activity is not so essential compared to the representatives of hydrolase. Other authors investigating change of activity of soil enzymes under the influence of a complex of agrogenic factors [1, 14, 28] also came to similar conclusions.

**Table 4:** Profile enzymatic activity of arable and virgin mountain chernozemic soils of Central Caucasus (in borders of Kabardino-Balkaria)

Depth of sampling of the soil, cm	Dehydrogenase, mg TFF /10g/24h	Catalase, ml O <sub>2</sub> /1g/1min	Invertase, mg glucose 1g/24h	Urease mg NH <sub>3</sub> /10 g/ 24 h	Phosphatase, mg P <sub>2</sub> O <sub>5</sub> /100g / 1h
Arable chernozem ordinary					
Aar. 0-20	10,7	3,1	5,5	37,0	10,0
A 20-37	11,6	2,1	3,6	33,1	8,6
AB 37-57	8,8	2,6	2,0	30,3	8,5
B1 57-76	8,4	1,8	1,4	30,1	6,0
Bca 76-104	6,2	1,3	1,6	18,0	5,6
BC 104-140	1,4	0,2	0,4	4,9	3,4
Virgin chernozem ordinary					
A0 0-5	15,6	8,8	36,0	51,9	17,4
A 5-18	9,3	8,8	13,1	31,2	14,4
AB 18-33	6,4	5,6	5,9	9,3	15,3
B1 33-47	3,9	5,7	2,6	7,0	13,8
Bca 47-84	2,4	2,7	1,5	5,4	7,8
BC 84-110	0,5	0,4	0,5	3,7	3,5
Arable chernozem typical					
Aar. 0-20	2,0	5,1	9,4	14,6	13,3
A 20-46	1,6	2,1	3,8	4,4	7,5
AB 46-67	1,4	2,0	2,8	1,1	5,8
B1 67-90	1,1	0,2	1,7	0,6	4,9
Bca 90-140	0,9	0,2	1,6	0,5	4,8
BC 140-180	0,2	0,2	0,8	0	1,3
Virgin chernozem typical					
A0 0-6	2,7	5,7	28,7	15,4	18,0
A 6-26	2,5	5,0	15,8	11,5	11,4
AB 26-50	2,2	4,3	7,2	10,5	8,7
B1 50-73	2,3	3,5	4,4	5,1	5,0
B2 73-110	2,0	3,3	3,7	1,1	5,1
BC 110-140	1,1	2,8	3,5	0	4,4
Arable chernozem leached					
Aar. 0-20	3,6	5,2	11,1	29,6	12,4
A 20-38	1,7	1,4	2,5	15,2	6,3
AB 38-64	1,3	1,0	2,1	14,3	5,6
B 64-88	0,4	0,2	2,0	1,2	5,3



BC	88-120	0,3	0,1	2,0	0,6	5,4
Virgin chernozem leached						
A0	0-5	4,1	6,7	18,7	23,6	18,4
A	5-30	3,4	6,3	10,9	15,5	10,5
AB	30-50	3,2	4,9	5,5	14,7	7,9
B	50-84	0,7	2,6	4,4	2,1	5,4
BC	84-130	0,5	1,5	4,3	1,5	4,4

Differences of activity of hydrolytic enzymes in soils agro-and biogeocenoses are shown more and are 23-84% in the top horizons. Invertase catalyzes reactions of decomposition of sucrose to glucose and fructose - the substances which are a power source and carbon for plants and microorganisms. She shows average activity in the cespitose horizons of natural soils which decreases down a profile - to weak and very weak. In the arable horizons the invertase activity is weak, and down the profile of agrogene soils is very weak.

Phosphatase plays an important role in reactions of phosphoric exchange as mobilization of the phosphorus fixed in organic substances before the connections available to plants, is carried out by rather narrow group of the microorganisms producing specific enzymes - phosphatases [16, 4, 14, 29]. Profile dynamics of this enzyme both in natural, and in the processed chernozemic soils is similar to invertase.

However not all obtained data keep within the scheme of the unambiguous decrease in enzymatic activity which resulted from agricultural use. For example, in chernozemic soils leached the activity of urease in the arable horizon is slightly higher, than in the cespitose horizon of the natural soil, and down a profile of the compared soils absolute datas of urease activity practically coincide. Dynamics of activity of urease and in a profile of the agrochernozem ordinary where its high rates in the arable soil remain to horizon BCa is non-standard and also is even surpassed by similar characteristics of the natural soil. This enzyme participates in processes of regulation of nitric exchange, catalyzing decomposition of urea on ammonia and carbon dioxide that makes urea nitrogen available for plants and microorganisms [30]. In the presence of a substratum (mineral fertilizers) the catalytic role of urease increases that, perhaps is the reason of its activation in arable chernozemic soils ordinary and leached.

To track more general regularities in change of biochemical activity of mountain chernozemic soils when agrouing, the values of relative total profile enzymatic activity were calculated. When comparing genetic analogs of virgin and arable soils it is established that indicators of total profile activity of enzymes in the natural chernozem typical are 23% higher, in leached - for 29%. In chernozemic soils ordinary the return ratio is observed. In a profile of the virgin soil the total activity of enzymes is lower, than in arable for 22%. The high activity of urease and a dehydrogenase in a middle part of a profile and also the big power of the agrochernozem ordinary is the reason of the received result.

The provided data say that influence of arable impact on activity of soil enzymes has ambiguous character. In general, processes of decrease of the activity of enzymes, both in arable, and in the underlying horizons of the processed soils prevail. However, in some cases activation of separate enzymes is observed which reasons it is difficult to establish within this work. The numerous materials of various authors analyzed by Haziyevev and Gulko [30] specify that influence of agroecological factors on processes of biological circulation in the soils-plant-micro-organisms system possesses multidirectional action. In particular, it is noted that application of fertilizers leads to activation of hydrolysis of carbohydrates thanks to temporary creating favorable conditions for release of the enzymes connected with receipt and processing of a substratum. Despite a difficult picture of manifestation of various enzymes activity in profiles of natural and arable mountain chernozemic soils, this part of a research is necessary for determination of the general level of their biological activity and its change under the influence of a complex of agrogene factors.

The enzymatic activity of soils is very closely connected with functioning of soil microbic biomass therefore determination of microbiological parameters of the explored soils was a part of a research. The efficiency of use of respiratory indicators of microbiological activity when comparing of the natural and anthropogenic changed soils is confirmed by many authors [21, 2, 31, 32]. Application of the approach recommended by them allows defining extent of change of physiological activity of soil microbic biomass, relying on comparison of indicators of a BR and SIR rate of the explored soils [Table 5]. The indicators of intensity of BR characterizing the course of background breath of soil microbic biomass in profiles natural typical and leached chernozemic soils are quite close. The maximum values are typical of the for upper horizons, however a certain makes 62-53% respectively respiratory activity of a soil microbiota remains also upon transition to maternal breed, and decrease, in comparison with the most biogenous horizon A0. The profile of the natural mountain chernozem ordinary is allocated with the highest values of speed of BR up to horizon BCa. The considered indicators of this soil (a BR, SIR, Cmic) are significantly higher, than similar parameters of other subtypes of natural mountain chernozemic soils. Possibly, the submitted data reflect features of the concrete soil, but not this subtype in general. Average values of speed of BR in the top horizons (0-20 cm) of various subtypes of natural mountain chernozemic soils calculated on the basis of volume selection say that the distinctions established at the level of a subtype are not statistically significant ( $t < 1,53$ ;  $p > 0,16$ ) for mountain chernozemic soils. Chernozemic soils ordinary are characterized by BR rate =  $11,5 \pm 1,3$  mkg CO<sub>2</sub>/1r/h; chernozemic soils typical -  $13,9 \pm 1,9$  mkg CO<sub>2</sub>/1r/h; chernozemic soils leached -  $8,6 \pm 1,4$  mkg CO<sub>2</sub>/1r/h.



Values of rate of BR in profiles of arable mountain chernozemic soils are quite comparable: indicators gradually decrease down a profile, but a certain respiratory activity remains also in horizon BC. The maximum decrease, by comparison of absolute measures of the humic accumulative and arable horizons, is established for the ordinary chernozem (77%) that is explained by the BR high absolute values in the virgin soil. Easing of a BR in of intensity the similar horizons of typical and leached agro chernozemic soils makes according to 26% and 37%. As shows a detailed research of the top horizons, these values more reflect the extent of change of the considered parameter of biological activity in arable soils.

Determination of average values of BR rate in the arable horizons on the basis of volume selection showed statistically significant decrease in this indicator ( $t > 3,8$ ;  $p < 0,001$ ) for 29-52% in agrogene soils. BR rate in the arable chernozem ordinary is  $5,5 \pm 0,8$  mkg CO<sub>2</sub>/1r/h; typical  $5,8 \pm 0,7$ ; leached  $6,1 \pm 0,8$  mkg CO<sub>2</sub>/1r/h. The submitted data indicate essential decrease in background respiratory activity of the soil microbial biomass which resulted from under agricultural influence.

SIR rate characterizing the potential of physiological activity of microbial biomass of the soil with surplus of a substratum and optimum conditions of temperature and humidity also shows the highest values in a profile of the virgin chernozem ordinary that, is possibly feature of the considered profile as other subtypes of natural mountain chernozemic soils are characterized by lower and close profile indicators. Aar., in comparison with the horizon A, makes decrease in intensity of SIR in the horizon: in the ordinary chernozem of 54%, in typical - 49% and in leached - 41% that confirms reduction of potential physiological activity of microbial biomass in arable soils, in comparison with natural.

**Table 5:** Profile microbiological indicators of arable and virgin mountain chernozemic soils of Central Caucasus (in borders of Kabardino-Balkaria)

Depth of sampling, cm	Rate of BR, mkg CO <sub>2</sub> /1g/h	Rate SIR, mkg CO <sub>2</sub> /1g/h	Cmic, mkg C / 1h	Cmic reserves, g/m <sup>2</sup>
Arable chernozem ordinary				
Aar. 0-20	4,4	37,1	1487	309
A 20-37	3,8	35,8	1434	254
AB 37-57	3,6	31,2	1250	295
B1 57-76	3,7	30,3	1212	288
Bca 76-104	3,1	23,4	937	338
BC 104-140	3,1	9,6	386	183
Virgin chernozem ordinary				
A <sub>0</sub> 0-5	18,2	121,9	4882	215
A 5-18	16,2	79,8	3193	374
AB 18-33	13,8	71,5	2863	395
B1 33-47	8,7	53,2	2129	286
Bca 47-84	9,2	45,8	1834	747
BC 84-140	2,8	32,0	1282	825
Arable chernozem typical				
Aar. 0-20	5,1	23,1	925	222
A 20-46	3,4	13,8	496	146
AB 46-67	2,4	12,4	551	126
B1 67-90	3,0	5,5	221	60
B2 90-140	2,5	2,8	111	70
BC 140-180	1,0	2,0	81	16
Virgin chernozem typical				
A0 0-6	7,8	68,8	2755	134
A 6-26	6,9	45,4	1818	302
AB 26-50	5,3	44,0	1762	364
B1 50-73	5,4	26,5	1061	131
B2 73-110	4,1	18,3	733	317
BC 110-140	3	15,0	601	216
Arable chernozem leached				
Aar. 0-20	4,9	25,4	1817	223
A 20-38	4,6	28,9	1157	246
AB 38-64	4,0	27,5	1102	344
B 64-88	3,0	24,8	1016	297
BC 88-120	2,9	11,0	441	181
Virgin chernozem leached				
A0 0-5	9,8	52,3	2093	108
A 5-30	7,8	43,0	1722	460
AB 30-50	6,4	26,6	1065	230
B 50-84	5,5	16,0	643	243
BC 84-130	4,6	13,1	523	270

Content of carbon of microbial biomass (Cmic) is calculated on the basis of data of SIR and is the reliable indicator serving as the standard index when determining quality of the soil [33]. Smik is a live and

functioning part of carbon of the soil thanks to which there is a transformation of all complexes of organic substances of the soil. High content Cmic (> 1000 mkg C/g of the soil) is observed in all horizons of the virgin chernozem ordinary (up to maternal breed) and in the top half of a profile typical and leached. These contents Cmic in a profile of typical and leached agrochernozemic soils, though are inferior to the natural analogs on absolute values, belong to the category high, up to the lower part of a profile where they correspond to average and low values.

To establish degree of difference between virgin and arable soils according to contents Cmic in a layer 0-20 cm allow the average sizes calculated on the basis of data of volume selection. In natural mountain chernozemic soils ordinary Cmic makes 1926±358 mkg C/g, in arable - 1239±142 mkg C/g; chernozemic soils typical according to 1660±96 mkg with head and 1150±91; chernozemic soils leached - 1681±146 mkg C/g and 1210±121 mkg C/g. Average values speak about high content Cmic in all studied soils, nevertheless, it is established statistically significant ( $t > 2,65$ ;  $p < 0,001$ ) decrease in a microbic indicator in the arable horizons for 28-36%.

The data characterizing the stocks of Cmic calculated for all profile of the explored mountain chernozemic soils give the chance to compare the studied soils by this quantitative microbic index. Among natural mountain chernozemic soils the chernozem is in the lead (2842 g/m<sup>2</sup>), follow it typical (1543 g/m<sup>2</sup>) and leached (1311 g/m<sup>2</sup>). Among mountain agrochernozemic soils: ordinary (1667 g/m<sup>2</sup>); leached (1290 g/m<sup>2</sup>) and typical (644 g/m<sup>2</sup>). Thus, the greatest decrease Cmic (58%) is established for the typical mountain chernozem, the difference between chernozemic soils ordinary (decrease by 42%) and the minimum change of profile contents Cmic in the leached agrochernozem (18%) is slightly less. Change of profile indicators is connected with essential decrease in intensity of SIR (and as a result of contents and stocks Cmic) in the arable horizons, in comparison with humus-accumulative. These indicators decreased on average by 48%.

As appears from the submitted data, formation of biological activity in profiles of both natural, and arable mountain chernozemic soils - difficult and multidirectional process. The considered components of biological activity of mountain chernozemic soils show various profile dynamics and ambiguously react to a complex of agroecological factors. The arable horizons bear the maximum agrogene load, and extent of change of their biological indicators can be tracked on the basis of bigger selection, based on average values of the considered parameters. Apparently from the obtained data [Table 6], in the arable horizons of mountain chernozemic soils all controlled indicators in a varying degree decreased.

To establish the general level of biological activity of the explored soils and to estimate its change in result of long-term arable influence, it is necessary to integrate all studied parameters of biological activity into uniform estimated criterion. For performance of this task the profile IIEBSS of virgin and arable chernozemic soils are defined. Besides by IIEBSS which characterize biological activity of the arable and humus and accumulative horizons (0-20 cm) of the processed and natural soils are calculated. At calculations data of humus stocks (which consider also density of various horizons of the studied soils), rate of BR, reserves Cmic (SIR considering rate, contents Cmic and density of soils) and activity of five studied enzymes were used. The IIEBSS profile values of various subtypes of natural and agrogene mountain chernozemic soils are presented in the [Fig. a].

**Table 6:** Decrease in average values of biological activity (for % of rather natural analogs) in the arable horizons (0-20 cm) of various subtypes of mountain chernozemic soils of Central Caucasus (in borders of Kabardino-Balkaria)

Content of humus	BR rate	Rate SIR and content Cmic	Dehydrogenase	Catalase	Invertase	Urease	Phosphatase
Ordinary chernozemic soils							
34	52	36	51	20	67	63	45
Typical chernozemic soils							
26	58	31	28	27	51	51	48
Leached chernozemic soils							
25	29	28	44	20	57	72	41

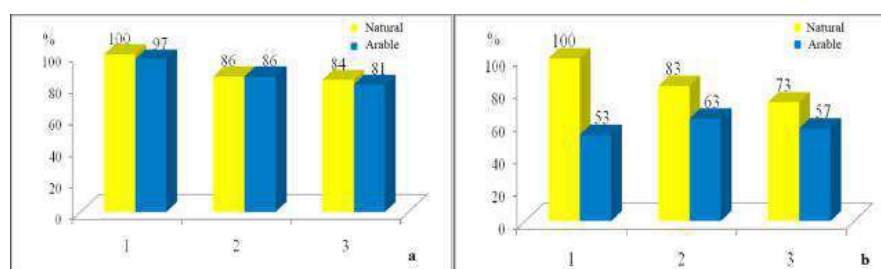


**Fig. IIEBSS (%):** a) profiles of natural and arable mountain chernozemic soils; b) natural and arable mountain chernozemic soils in a layer of 0-20 cm: 1. mountain chernozemic soils ordinary; 2. mountain chernozemic soils

typical; 3. mountain chernozemic soils leached. Scale of assessment of the IIEBSS level (%): up to 20% - very low, 21-40% of low, 41-60% average, 61-80% of high, 81-100% very high [22].

The chart reflects rather equal and high values of IIEBSS (> 80%) for all studied soils. Differences in IIEBSS values between profiles of agrogene and natural soils are practically absent. Essential differences at the level of a subtype between the explored soils are also not shown.

Noticeable easing of biological activity (for 16-43%) is established in the arable horizons (0-20 cm) of all subtypes of mountain chernozemic soils [Fig. b]. Comparing the data characterizing biological activity in the top horizons and in all a profile of natural and agrogene mountain chernozemic soils it is possible to come to a conclusion that the main changes of biological properties happen in the arable horizons, and down a profile indicators are gradually leveled. Therefore by consideration of total profile biological activity the differences between its level in arable and natural mountain chernozemic soils are leveled and the IIEBSS profile values practically do not differ.

The research of indicators of biological activity of various subtypes of mountain chernozemic soils allows tracking their profile dynamics in the conditions of natural and agricultural biogeocenoses. It is established that the compared virgin and arable chernozemic soils have common features of change of indicators of biological activity. The most biogenous are the top horizons, the horizon of A0 are in the lead in natural soils on the content of humus, microbial indicators, enzymatic activity. Down a profile absolute values of indicators decrease, but also upon transition to maternal breed the biological activity remains both in natural, and in agrogene soils. In spite of the fact that in a profile of the natural chernozem ordinary a number of indicators are higher, than in other subtypes of natural soils, the level of profile biological activity expressed through IIEBSS differs slightly (for 14-16%). The profile biological activity of various subtypes of arable mountain chernozemic soils also is approximately at one level.

The most essential distinctions of controlled parameters and the general level of biological activity are established for the top horizons of natural and arable soils. This conclusion is based not only on results of profile researches, but also on the average values characterizing the top horizons (0-20 cm) of virgin and the processed mountain chernozemic soils received on the basis of selection of 16-18 samples for each subtype. It is revealed that in the arable horizons there was a decrease in all studied indicators by 23-67%. The established distinctions (except catalase activity ( $t < 1,57$ ;  $p > 0,13$ ) are statistically significant ( $t > 2,07$ ;  $p < 0,03$ ). On sensitivity to arable influence the considered parameters of biological activity can be built in the following row: activity of urease (decrease on average by 62%)> activity of invertase (for 58%)> BR rate (for 46%)> activity of phosphatase (for 45%)> activity of dehydrogenase (for 41%)> the SIR rate and contents Cmic (for 32%)> the humus content (for 28%)> activity of catalase (for 22%).

## CONCLUSION

Comparing the data characterizing biological activity in the top horizons and in all a profile of natural and agrogene mountain chernozemic soils it is possible to come to a conclusion that the main changes of biological properties happen in the arable horizons, and down a profile indicators are gradually leveled. Therefore, by consideration of total profile biological activity the differences between its level in processed and natural mountain chernozemic soils are leveled and the IIEBSS profile values practically do not differ. At the same time IIEBSS, characterizing biological activity of the top horizons, decreased in arable soils on average by 28%. A conclusion follows from all aforesaid that despite long-term arable use, the mountain chernozemic soils created in a belt of meadow steppes and steppe meadows under the influence of bioclimatic conditions of the Elbrus option of zonation keep the high natural potential and remain highly productive soils. The established decrease in biological activity of the arable horizons indicates the need of continuous monitoring of the state of arable mountain chernozemic soils allowing controlling intensity and the direction of processes of their change under the influence of a complex of agrogene factors.

### CONFLICT OF INTEREST

Authors confirm that the submitted data do not contain the conflict of interests.

### ACKNOWLEDGEMENTS

None

### FINANCIAL DISCLOSURE

None

## REFERENCES

- |  |  |
|--|--|
| <p>[1] Makiyev AD. [2005] Agrogene transformation of chernozemic soils of the typical foothills of Central Caucasus Mountains: Bio Sci PhD Thesis Vladikavkaz. 145.</p> <p>[2] Anderson TH. [2003] Microbial eco-physiological indicators to assess soil quality. <i>Agric Ecosys Environ.</i> 98:285-293.</p> | <p>[3] Galstyan AS. [1974] Enzymatic activity of soils of Armenia. ASh Galstyan Ayastan. Yerevan. 275.</p> <p>[4] Kazeev KS. [2003] Biological diagnostics and indication of soils: methodology and methods of researches. KS Kazeev, SI Kolesnikov, VF Valkov Rostov-on-Don. 204.</p> |
|--|--|

- [5] Mirkin BM. [2002] Management of fertility of soils: agroecosystem approach BM Mirkin, FH Haziyeu, YT Suyundukov etc. *Soil science*. 2:228-234.
- [6] Sokolov VE. [1989] Vertebrata of the Caucasus. Mammals. Insectivorous. VE Sokolov, AK Tembotov M.: *Science*. 547.
- [7] [An electronic resource] - (reference date: 30.05.2017).
- [8] Valkov VF. [2002] Soils of the South of Russia: classification and diagnostics VF Valkov, SI Kolesnikov, KS Kazeev Rostov-on-Don: SKNTs VSh.349.
- [9] [1984] Soils Kabardino-Balkarian ASSR and recommendations about their use. Nalchik the State design institute on land management Sevkaivniiprozem. Nalchik. 201.
- [10] [2015] Interstate GOST 5180-2015 standard Soil. Methods of laboratory definition of physical characteristics (entered by the order of Federal agency on technical regulation and metrology as of November 3, No. 1694 of St).
- [11] Molchanov EN. [1990] A soil cover Kabardino-Balkarian ASSR. EN Molchanov the Explanatory text to the Soil card Kabardino-Balkarian the ASSR. M.: GUGK at CM of the USSR. 19.
- [12] Classification and diagnostics of soils of the USSR. MK 47 "Ear". [1977].
- [13] Tsepikova NL. [2008] Some associations of ruderal vegetation of Nalchik (Kabardino-Balkaria) NL Tsepikova, IT Kuchmezova, LM Abramova *Vegetation of Russia*. 12:97-103.
- [14] Haziyeu FH. [1986] Enzymatic activity of soils. FH Haziyeu M *Science*.
- [15] Gaponyuk EI. [1985] Complex system of indicators of environmental monitoring of soils. EI Gaponyuk, SV Malakhov. Works of the 4th All-Union meeting. Obninsk, June, 1983. L: *Gidrometeoizdat*. 3-10.
- [16] Zvyagintsev DG. [1980] Methods of soil microbiology and biochemistry DG Zvyagintsev. M.: MSU publishing house. 224.
- [17] Creamer RE, Schultea RPO, Stonea D, Gal A, Kroghc PH, et al. [2014] Measuring basal soil respiration across Europe: Do incubation temperature and incubation period matter. *Ecological Indicators*. 36:409-418.
- [18] Ananyeva ND. [2003] Microbiological aspects of self-cleaning and stability of soils. ND Ananyeva M.: *Science*. 222.
- [19] Ananyeva ND. [2011] Features of definition of carbon microbic biomass of the soil by method a substratum - the induced breath. ND Ananyeva, EA Susyan, EG Gavrilenk *Soil science*. 11:1327-1333.
- [20] Galstyan ASH. [1961] Breath of the soil as one of indicators of its biological activity Ash Galstyan *Message of laboratory of agrochemistry AN ARMSSR. Biological sciences*. 5:69-74.
- [21] Anderson TH, Domsch KH. [1986] Carbon links between microbial biomass and soil organic matter Eds: F Megusar, M Gantar. *Perspectives in microbial ecology*. Slovene Society for Microbiology Ljubljana. 467-471.
- [22] Kazeev KS. [2004] Biology of soils of the South of Russia KS Kazeev, SI Kolesnikov, VF Valkov Rostov N/Dona: TsVVR publishing house. 350.
- [23] Kolesnikov SI. [2002] Ecological functions of soils and influence of pollution on them heavy metals. SI Kolesnikov, KSh Kazeev, VF Valkov. *Soil science*. 12:1509-1514.
- [24] Gedgafova FV. [2015] Biological activity of chernozem soils of Central Caucasus (within tersky option of zonation of Kabardino-Balkaria) FV Gedgafova, TS Uligova, ON Gorobtsova etc. *Soil science*.12:1474-1482.
- [25] Gorobtsova ON. [2017] Assessment of level of biological activity of agrogene and natural chernozemic soils of Kabardino-Balkaria. ON Gorobtsova, TS Uligova, RH Tembotov etc. *Soil science*. 3:1-10.
- [26] Gorobtsova ON. [2015] Ecology-geographical regularities of change of biological activity of automorphic soils of flat and foothill territories of a northern macroslope of Central Caucasus Mountains (within Kabardino-Balkaria). ON Gorobtsova, FV Hezheva, TS Uligova etc. *Soil science*. 3: 347-359.
- [27] Gorobtsova ON. [2016] Ecophysiological indicators of a condition of microbic biomass of chernozemic soils of Central Caucasus (within tersky option of zonation of Kabardino-Balkaria). ON Gorobtsova, FV Hezheva, TS Uligova, etc. *Ecology*.1:22-29.
- [28] Speir TW, Ross DJ. [2002] Hydrolytic enzyme activities to assess soil degradation and recovery. *Enzymes in the Environment: Activity, Ecology and Applications*. New York. 407-431.
- [29] Badiane NNY, Chotte JL, Pate E. [2001] Use of soil enzyme eactivities to monitor soil quality in natural and improved fallows in semiarid tropical regions *Applied Soil Ecology*. 18(3):229-238.
- [30] Haziyeu FH. [1991] Enzymatic activity of soils of agrotsenoz and prospect of its studying FH Haziyeu, AE Gulko. *Soil science*. 8:88-103.
- [31] Insam H, Domsch KH. [1988] Relation between soil organic carbon and microbial biomass on chronosequences of reclamation sites. *Microbial Ecology*. 15(2):177-188.
- [32] Murugan R, Loges R, Taube F, Sradnick A, Joergensen RG. [2014] Changes in soil microbial biomass and residual indices as ecological indicators of land use change in temperate permanent grass land. *MicrobEcol*. 67:907-918.
- [33] Gavrilenko EG. [2011] Spatial variation of content of carbon of microbic biomass and microbic breath of the southern Moscow area. EG Gavrilenko, EA Susyan, ND Ananyeva etc. *Soil science*.10:1231-1245.

## ARTICLE

## EFFECTIVE METHODS TO TREAT HUMAN PAPILLOMA VIRUS

Huynh Tan Hoi\*

Department of Education, FPT University, VIETNAM

## ABSTRACT

The society is growing and leading to increasing demand for relations between people and people. However, genital warts is one of many social diseases have been caused by deviant lifestyles or some unavoidable reasons. It is said that this is the disease that the patients have to suffer and quietly seek for themselves a good place to treat or an effective therapy to cure the symptoms of genital HPV infection. In addition to the modern therapies, traditional ones have been applied as a savior of many pieces of life and have brought to bear this annoying disease. The paper is based on research paper as well as the survey data of 50 patients who are living in Ho Chi Minh City. Thanks to the analysis method of Hancock by the time of September up to November of 2018, this research found out some great ways that can help to improve people's health. From then on, some implications have been recommended with the purpose to make our life a better place and to contribute to the development of the country.

## INTRODUCTION

Human papillomavirus or HPV is an infection that is passed between people since it is a sexually transmitted virus through skin-to-skin contact. Over one hundred varieties of HPV have been passing through sexual contact and can affect people's health. Nowadays, with the development of science and technology, this disease has been treated by many different measures. Health facilities can use a variety of treatments such as laser burns, surgery, chemotherapy, etc. to remove papillae. However, there are patients who do not have recurrent but some papilloma will grow back [1,2].

## KEY WORDS

Effective methods,  
papilloma virus,  
traditional therapy.

## HPV AND ITS MECHANISM OF SPREAD

Rather different from HIV and HSV (herpes zoster), HPV is the most common sexually transmitted infection. It is so common that almost all sexually active men and women get sick at some point in their lives. About 15 types of viruses are listed as being at risk for human health. The two most common types are HPV-16 and HPV-18, which can penetrate deep into the cervix (3-10%), changes the uterine tissue and causes cervical cancer. In addition, HPV can also cause vaginal cancer, vulvar cancer, anal cancer or penile cancer. Less toxic, HPV-6 and HPV-11, can cause 90% of genital warts. The mild type of warts on the hands are (HPV-2) and the feet are (HPV-1) [2].

Nowadays, there are vaccines that can prevent health problems that people are concerned about. In sexually transmitted diseases diagnosed in public health facilities, Human Papilloma Virus accounts for the highest proportion. The highest incidence is from 15 to 49 years old. After each year, the number of new cases increases by about 10%. There are many causes for this including the sense of prevention in the community, personal neglect in sexual intercourse with new partners, improper use of condoms since condoms cannot completely prevent sexual diseases. In addition, there is an increase in cases of oral sex and anal sex without condoms, some people are infected with latent disease and often go to doctors in the low quality facilities in order to achieve effective treatment thoroughly [3].

A person can get HPV during oral, vaginal, or anal sex with a person since it usually spreads during vaginal or anal sex without any signs or symptoms. Anyone who has sex can get HPV, even if they have sex with only one person. They can get the symptoms many years after having sex with an infected person so it is difficult to know when they first got infected. Currently, some clinics do not usually tell the truth about the disease and even after the treatment. There are a number of sites on the network advertising the traditional medicine to cure HPV within a few days to a week out, they advised patients should consider carefully before the examination or treatment. Because the effect of traditional medicine is not so fast and does not have a cure for HPV completely. So, patients should not be so bewildered, hurry, but find themselves a reliable "gold" address, listen to the doctor's advice to understand and peace of mind in the treatment. But this disease will not be a concern for many people. It is just a common disease in the world although it has rapid spread and can develop into cancer [2].

Vietnam has a very high population. The anal and oral sex of many people can lead to the appearance of HPV which appear in these two positions. Accordingly, for men, the location usually occurs in the foreskin, the penis and the scrotum. For females, the appearance of the lips often occurs on the sex organs, the hooves, around the urethra, the perineum, the vagina. In addition, both sexes may be at the bottom of the pelvis, anus, rectum, urethra, bladder and pharynx. Doctors recommend that oral sex can cause other sexually transmitted diseases such as gonorrhoea, syphilis, hepatitis B, HIV, and other infections. Although the disease can be cured properly but experts say that HPV disease is easy to relapse and cannot be cured completely. If it is not detected and treated promptly, or if it is not treated properly, the disease will become more severe, causing ulcers, bleeding, or even severe illness that can lead to infection, sexual intercourse or other conditions.

## \*Corresponding Author

Email:  
hoiht@fe.edu.vn  
Tel.: 0084-0965460459

Received: 26 Dec 2018  
Accepted: 11 Feb 2019  
Published: 17 Feb 2019



For this disease, the patient usually has no symptoms unless the masses make the patient feel uncomfortable feeling or when the infection is causing minor pain, because HPV has time. The incubation may last from 2 to 9 months. Initially, the disease is characterized by small papules, pink papule or pinkish white. They grow progressively, are like flowers of cauliflower or a strawberry, initially only small with the tip of a pin, later it can be apple size, soft density, rugged surface. The rash may be dry or slippery, with foul odor due to rubbing and superinfection. The number of papules is sometimes only a few lesions, but is usually concentrated in clusters.

In most cases, HPV will cure itself and not cause any health problems. When HPV does not heal, it can cause health problems like herpes and cancer. Herpes is usually like a small lump or a group of lumps in the genital area. These lumps may be small or large, prominent or flat, or shaped like broccoli. Regular caregivers can diagnose herpes by examining the genital area.

“Does HPV cause cancer?” may be a question many patients like to know the right answer. Yes, it can cause cervical cancer and other cancers including vulvar, vaginal, penis, or anal cancers. It can also cause cancer in the back of the throat, including under the tongue and tonsils (called oral cancer of the mouth). It usually occurs every year, including decades, after being infected by HPV. However, there is no way to know who is infected with cancer or other health problems. People with weakened immune systems may be less likely to get rid of HPV and may have health problems, including those with HIV / AIDS [2].

## COMPARISON OF TRADITIONAL METHODS AND MODERN METHODS

Viet Nam is a country where many patients are suffering from this disease, people still do not have much knowledge related although Western medication is widely used by many people for their effective treatment and prevention of re-infection by its prominent advantages. Advanced techniques to accurately assess the level of inflammation and provide a good basis for treatment. The first benefit is painless, leaving no scar with the combination of anesthetic.

With traditional healing remedies for this difficult disease, it is said that the patients are wise to take the traditional one because of its high therapeutic potential and it takes less side effects for the body. This is a method that many people consider effective when treated with Western medicine. Very trivial items such as banana peel, apple cider vinegar or turmeric can also be treated [4].

The first is the use of banana peels. It contains a lot of antibacterial, inflammatory, acne boil so it is quite suitable for treatment of the disease. This method has been applied and has its unexpected effects before Western medical therapy is applied in modern society. Although the effectiveness of this method requires patience because the patient takes a lot of time to treat, but if persist, the effect is very positive. Every day, just rub the banana peel into the affected area, the nodules will disappear after a few weeks onwards.

Apple cider vinegar is also mentioned as containing a therapeutic method because it contains a high level of natural acidity, which is worn down and worn off after a period of treatment. Patients also have to be patient and not hurriedly rushed. The disadvantage of apple cider vinegar is its ability to erode the skin if used for too long and potentially damage the diseased skin.

Considered as a spice, garlic is very familiar but is also a very effective herbal treatment. With abundant antibiotic allicin, garlic can inhibit the HPV virus very well. Just take a small amount of garlic, beat out and put in the right position, the nodules will gradually disappear.

Turmeric is also considered as a very good spice and a relief for the sick. When turmeric powder mixes well with the coconut oil to form a paste mixture and apply to the nodules for a certain time, the nodules will fall off. This is a folk remedy to cure HPV at home for patients. It is quite effective and very safe since it can limit the damage to the skin and especially not cause side effects such as the use of drugs to treat the disease.

However, it is said that the traditional remedy is just a way to limit the development of the disease and can prevent it from growing worse, but cannot definitely have good result because the disease can recur after a certain time. Yes, we understand that it is not easy to treat the disease, but traditional methods today are widely believed and applied. However, depending on the severity of the disease, there are different treatments. Besides, patients can apply directly to nodules, or they can apply a thin aloe leaf to the skin. It should be noted that each of the skin should cover a different piece of aloe vera, avoid rubbing back and forth to spread disease.

What does science say about tips to cure genital warts? More and more people choose to treat the genital warts with traditional therapy because it is confidential, simple, safe and can fit many people. However, many experts say that these tips cannot cure genital warts thoroughly. Because this disease may develop from the inside so the patients need to go to a reputable clinic or medical institution to treat the underlying disease.

The treatment of genital warts with traditional medicine can only limit the nodules on the skin while the germs that grow silently inside cannot be destroyed. In addition, we can now treat genital warts with



Oriental medicine since it brings amazing results. The more advanced the human, the more hopeful it is for modern methods of curing genital warts (Western medicine, electricity, laser ...), but then many people have to be disappointed. There are people who use only Oriental medicine in a couple of weeks have cured the genital warts. They began to doubt and wondered: "What is the better method?"

Yes, all comparisons are limp, we cannot say if Oriental medicine is good or Western medicine is not good. However, we can only say that it depends on your health condition.

Although the cure of this disease by Oriental medicine or Western medicine, the general rule should be that what we need is to thoroughly destroy the HPV. Causes of the disease are many, but the common cause is caused by HPV. Therefore, if we want to treat the root of genital warts, we must destroy this virus rather than reduce the swelling, flaking the acne.

In general, most Western methods now treat necrotic and osteoarthritis, and at the same time inhibit the growth of pustules. Eastern medicine, in turn, focuses on in-house treatment, which means that it excretes HPV out of the body, helping to cure it. That is why more and more people believe and turn to cure this disease with Oriental medicine.

Oriental medicine from the past to focus on the root cause while improving the health of people, so it is considered a safe choice for patients. Oriental herbs (specifically Oriental herbs) are not for the purpose of destroying the HPV virus, effectively treating it and its origin.

If the patient has fully applied the Western medicine methods but still has not survived, or fear of suffering the modern methods can completely believe in Eastern medicine can cure HPV. Oriental medicine does not cause pain, simple treatment and especially bring long-term effectiveness, if the patient has the appropriate treatment will cure in a short time [5].

## COMBINATION OF TRADITIONAL METHODS AND MODERN METHODS

By combining both Eastern and Western approaches, this treatment takes good effect but still ensures that the patient minimizes the risk of side effects from Western medicine, then increases the resistance and immune system to the body. The patients should go to the clinic to know what treatment should be treated. Scientists believe that the use of drugs is the first treatment of this disease. Patients may use gel or water-based medication to spot the nodules, combining the use of antiretroviral drugs [1].

Because the level of injury in each person carrying the disease is not the same, the drug and the dosage used are not the same. Therefore, the sick person must abide by the treatment regimen of doctors, take the right medicine, the right dose, absolutely do not buy drugs or use other people's medications.

Opposite to traditional therapy, there is debate and skepticism about how to cure HPV by traditional methods because it can only limit the signs of disease. With this method, the nostrils only fall away, not to prevent the virus root. And to avoid that pain, the method of treating HPV by laser therapy is considered as an effective solution because the advantage is to prevent the skin from scratches with the disadvantages that the nodules are still possible to reappear [3].

In addition to the Western methods, people still believe in the Oriental medicine because it is easy to apply, simple and capable of home treatment. However, medical investigators have found that the treatment of papilloma with Oriental medicine is not possible [4]. All of these methods use detoxification medication, only the ability to avoid swelling inflammation, edema, decrease the intensity of the nostrils. Moreover, this method requires patients to be patient, if left unmatched, the disease will have a high risk of recurrence. Patients can use natural materials such as aloe leaf, banana peel, apple cider vinegar, potato, etc. for treatment Human Papilloma Virus [2].

## RESULTS

The first question addressed in the survey is to determine the importance of applying the traditional ways in order to treat this virus [Fig.1]: "What do you think about the new methods?". Only 8 respondents selected "Very good" (16%), 22 chose "Good" (44%), and 20 (40%) chose "Not good". This shows the patients' points of view while they are using this modern methods, and some of them (40%) still didn't recognize this as a good choice.

On the contrary, the result of the second question is rather different from the first one. The importance of the traditional method once again confirms its vital role when treating this kind of virus [Fig.1]: "What do you think about the traditional methods?". There were 17 respondents who selected "Very good" (34%), 33 chose "Good" (66%), and no one (0%) chose "Not good". This result, again shows the patients' passion on using this traditional ways or Eastern methods.

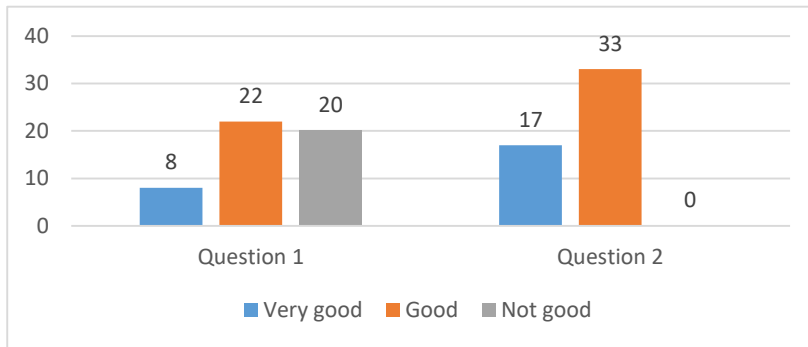


**Fig. 1:** Comparison between the traditional methods and the modern ones.

And to clarify this, the interview questions directly with the patients have shown that most of them understood the hard time they had to wait. That means, the patients should be patient since they can't see the good result immediately. To get rid of the genital warts, they have to wait for a few months depending on their symptoms. It may take one month, but I may take four or five months. However, they don't have to worry so much about their disease and feel happy to come back to their daily life as usual [4].

When interviewed some respondents, they showed their disappointment about the new methods since the warts came back after treatment [3]. At first, they felt so much happy and safe but after a few months (about three or four months), they had to go back to the hospital [Fig.2]. Even though, they were satisfied with the good services and professional doctors, the big matter is that they don't want to have the surgery many times. They don't want to wait in the stuffy rooms and be asked some questions (even polite questions) related to their symptoms.



**Fig. 2:** Genital warts caused by HPV virus.

### SOME GOOD METHODS TO CURE HUMAN PAPILOMA

According to Oriental Medicine, not only genital warts but all other diseases in general, if we want to treat effectively, we must combine a remedy for external medicine with an internal remedy. However, nowadays traditional medicine is much more modern. One can take an independent medicine (in or out) for mild illness, and combining two of them only if the disease is in severe stage. Depending on the degree of disease of each person and the physician will give medicine or use drugs outside [4].

Combining Southern therapy (therapy of the Vietnamese) and Northern therapy (therapy of the Chinese) together will become the most effective Oriental medicine (also called traditional therapy). However, in some cases, the patient can effectively treat the disease with only one medication. Here is how to cure the disease with drugs used by many men:

- Portulaca oleracea is spicy, welded, non-toxic. It can treat swelling, tumor and has certain uses in the treatment of HPV virus. It can be used for drinking.
- Chrysanthemum indicum is bitter, slightly welded, poisonous, detoxifying, detoxifying, sterilizing. Drugs for drinking.
- Sophora tetraptera is a little bitter, non-toxic and can be used for treating itching, human papilloma.

• *Plumbago zeylanica* can increase immune system, anti-inflammatory, dive tumors, be suitable for treatment of human papilloma.

As one of the sexually transmitted diseases caused by Human papilloma bacteria, HPV virus makes many patients suffer since the most effective treatment have not been found. As a result, the Western treatment is the first choice of many people but not completely resolved. Traditional methods such as the use of traditional medication can help to support patients with cataracts quite effectively. The plants are often referred to as the notion that not all people including, *astragalus propinquus*, *phellodendron amurense* or *sophora tetraptera* have a lot of special effect [5].

Most people who are infected with HPV do not know they have this disease because they have no obvious symptoms or have significant health effects. According to statistics, about 14 million new people are infected each year. How to reduce the risk of getting or to avoid HPV and the health problems that this disease causes is perhaps the question that many people are concerned about [3].

The first is to vaccinate against HPV virus since the vaccine is safe and effective. This type of HPV vaccine is given three times in six months at the physician's request and should not miss any dose. Probably many people think that the disease is only sexually transmitted, which is not wrong. However, prevention is better than cure, so that people need to be vaccinated at the appropriate age of 10 years or older. Particularly for the homosexuals, vaccines are needed to make life better [2].

Having safe sex is a must. This can reduce the risk of HPV quite effectively. Should only be associated with trustworthy people such as spouses to reduce the possibility of high spread of the disease.

The next recommendation is not related to preventive measures, but rather the cure of the disease caused by HPV virus, and traditional methods still have very great values [1].

## CONCLUSION

Modern methods have not yet completely cured the disease, but the medicine of some herbalists is rather effective. After many years of successful research and treatment for over a thousand people, traditional therapies have shown that HPV that causes this disease is a "parasitic" parasite exist under closed skin, and at an appropriate time, they will develop into the nodules. The nodules have very deep roots, so after acid or burning, they can only be applied on the mucosal surfaces, the roots are still and the roots are back. So, choosing which therapy depends on the patients' acknowledgement, depends on their health condition and their decision.

### CONFLICT OF INTEREST

None

### ACKNOWLEDGEMENTS

None

### FINANCIAL DISCLOSURE

None

## REFERENCES

- [1] Hadeel K, Agnieszka G, Angelika R. [2014] Therapeutic vaccine strategies against HPV. *Vaccines*. 2:422-462.
- [2] Stina S, Nicoletta T, Giuseppa C, Carlo P, Vera P, Campisi G. [2012] Oral HPV Infection: Current Strategies for Prevention and Therapy. *Current Pharmaceutical Design*, 18: 5452-5469.
- [3] Mamas N, Sourvinos I, Demetrios D. [2009] Human papilloma virus (HPV) infection in children and adolescents. *European journal of pediatrics*. 168: 267-273.
- [4] Lin J, Chen L, Qiu X, et al. [2017] Traditional Chinese medicine for human papillomavirus (HPV) infections: A systematic review. *Bioscience trends*. 11(3):267-273.
- [5] Wang SX, Zhang XS, Guan HS, Wang W. [2014] Potential Anti-HPV and Related Cancer Agents from Marine Resources: An Overview. *Mar. Drugs*, 12(4):2019-2035.

## ARTICLE

# FRICIONS STIR WELDING OF MAGNESIUM AND ALUMINIUM ALLOYS: A REVIEW

Sahil Verma\*, Ayush Chaudhary, Isha Sharma, Pradeep Mouria

Department of Mechanical Engineering, Manav Rachna University, Faridabad, INDIA

## ABSTRACT

On account of the global warming problem, the emphasis is given on reducing the consumption of fuel in various industries. This problem can be reduced to a greater extent by using light weight Al and Mg alloys. It is essential to weld them properly to extract the specific properties of both the alloys. The evolution of the welding techniques of dissimilar materials is an advanced research topic that has drawn much attention in the recent past. Among many welding methods, friction stir welding (FSW) was considered to be feasible for adequate welding of dissimilar alloys. In this article, a comprehensive review of the FSW process used for adding Al alloy plates to Mg alloy plates and the strength of weld is presented. The effect of process parameters like tool rotational speed, traverse speed, tool inclination etc. on the weld microstructure and strength is also summarized. For the welding of Al/Mg plates, the development and innovative modification of FSW has also been addressed.

## INTRODUCTION

Recently, the focus has been shifted from traditional metal components to light metal components in several industries for weight saving purpose. The weight saving in the automotive sector might provide better fuel economy as the fossil fuel reserves are depleting with time, and alternative energy resources are not fully operational. In the construction of a lightweight structure, dissimilar lightweight materials have been extensively used as per requirement. The most frequently used materials are aluminium (Al) and magnesium (Mg) alloys. There is a significant amount of weight saving with considerable strength of a structure if these alloys are utilized in an adequate proportion. The joints of dissimilar alloys must be strong enough to bear the applied load. This could be ensured by the use of a suitable welding technique in conjunction with appropriate materials. In fusion welding techniques, the energy density is very high, which creates challenges in the joining of low melting point metals like Al or Mg. Near precise welding of Al to Mg alloys were achieved using TIG welding, which is expensive, slow and difficult to control process for the said materials. Additionally, the joint strength is marginal due to high process temperature, accelerated mixing and formation of brittle intermetallic compounds (IMCs) in the fusion region [1]. In view of these challenges, FSW is considered as an appropriate alternative for high strength welding of these alloys. Because of solid state processing and low operational temperature in FSW, the shape and size of brittle IMCs are almost insignificant. The applicability of FSW for different Al/Mg alloy joints was studied extensively [2–6].

The present review aims to provide a lucid and systematic review of different Al/Mg alloy welding using FSW. The influence of the processing parameters on the weld strength as well as on weld quality was also incorporated.

## SOLID STATE WELDING

In solid-state welding, a sound joint is established between two materials by the coalescence achieved in the solid state using pressure or temperature. However, the temperature must always be below the melting temperature of both the materials. The processes involved in this technique are providing localized plasticization effect, which is responsible for this type of joint. Solid state welding could be accomplished by friction welding, roll welding, forge welding, hot pressure welding, diffusion bonding, explosion welding, cold welding, and ultrasonic welding [7].

## FRICION STIR WELDING (FSW)

FSW is a type of solid state welding. It was invented in 1991 by the researchers of The Welding Institute (TWI), UK, especially for Al alloys [8]. They named it friction stir butt welding. The tool used in FSW has a particular geometrical design consisting of pin and shoulder, as shown in [Fig. 1]. It must be made from the non-consumable and hard material so that it cannot be deformed or worn out during the process. The rapidly moving tool is inserted into the joint of two materials by applying a downwards force. After this operation, the quick rotating tool moves forward in the direction of the joint. In the contact area of materials and tool, heat generation will take place by friction locally, which will stimulate the plastic deformation in materials. Owing to the localized heating, the material around the pin becomes soft, and due to the rotation and horizontal motion of the tool, the material in front of the pin starts moving in the rear direction. This action occurs in the solid state, and the bond will be established on cooling. As the material comes under the intense plastic deformation in this process, the welded region consists of fine

### KEY WORDS

Aluminium, Magnesium,  
FSW, Alloys

Received: 23 Mar 2019  
Accepted: 28 April 2019  
Published: 11 May 2019

\*Corresponding Author  
Email:  
vsahil307@gmail.com  
Tel.: +91 8826131032

and equally distributed recrystallized grains [9, 10]. As per the Hall-Petch relationship, finer the grains better the mechanical properties [11]. Therefore, a joint established using FSW has better mechanical properties than its counterparts. FSW is considered as energy efficient, environment-friendly and a versatile material joining technique with comparison to traditional joining methods. As there is no need for filler material in FSW, almost all Al alloys can be joined using this technique irrespective of their chemical composition [12]. In this welding, there is no emission of harmful fumes, nor is the presence of solidification cracks in the welded region. Therefore, improved weld quality can be obtained by this method on the proper selection of process parameters. Additionally, this process makes less noise than other welding processes. The FSW processes are broadly classified into two groups, i.e., conventional and self-reacting FSW. The conventional FSW follows the same procedure explained beforehand. It is an advanced, high quality and efficient welding technique for longitudinal, circumferential and varied thickness (butt and lap) joints and commonly utilized in Al, Mg, Cu, Ti and steel alloys. The design of self-reacting FSW tool is unique [Fig. 2]. Unlike conventional FSW, the tool of self-reacting FSW consists of a pin, linked with top and bottom shoulders. It is also named as bobbin tool FSW. The self-reacting FSW tool can be designed for variable pin height as well as for constant force during the entire welding incident [13]. The advantages of self-reacting FSW over conventional FSW are negligible weld roots/root defects, fixture and machine experiences low Z force, no need of backing bar, minimum distortion owing to uniform heat input, and tolerance for thickness variation [14].

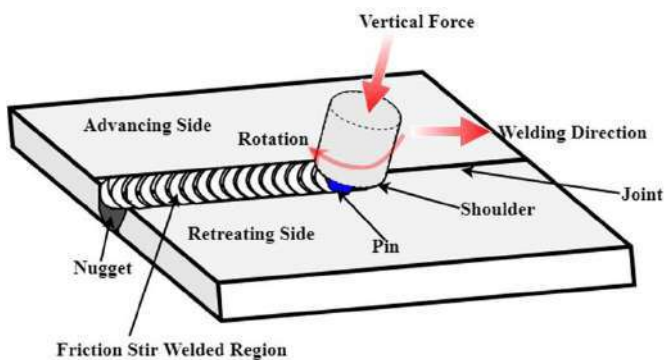


Fig. 1: Schematic drawing of the FSW technique [9].

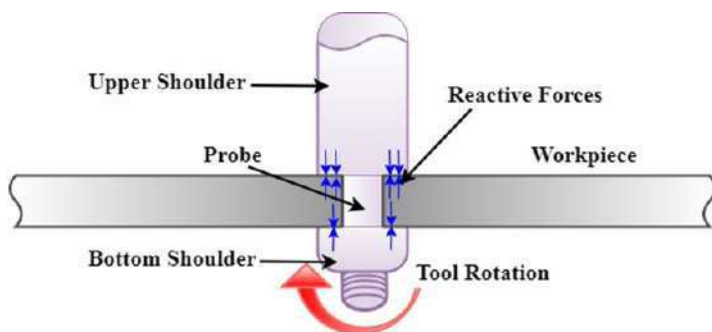


Fig. 2: Schematic of self-reactive or bobbin tool FSW [14].

## COMMON CHALLENGES IN DISSIMILAR METAL WELDING USING FSW

It is an arduous task to successfully weld two dissimilar materials using FSW because the thermal characteristics, coefficient of friction and softening behavior of both materials will be different. Therefore, the production, distribution and dissipation of heat will vary in both materials and an unwanted temperature gradient will establish between the materials. Due to this uneven thermal distribution, bonding between the materials will affect, and undesirable defects will introduce in the central region of the weld. Additionally, selection of improper welding parameters will hamper the joint strength to a great extent. Another major issue which affects the welding strength is the formation of IMCs during dissimilar metal welding. The composition, size and shape of IMCs impose a more significant impact on weld quality. As the temperature is involved in the FSW, it cannot be avoided completely during the process. However, it can be mitigated by carefully chosen process parameters for FSW [15].

## AL-MG DISSIMILAR ALLOY WELDING USING FSW

The utilization of lightweight metals and alloys like Al, Mg etc. has been extensively increased in several industries due to their specific properties, lightweight and die-castability. Using these light metal and



alloys, designers get the freedom to build complicated, intricate and amazing yet strong structures. In the creation of complex structures, similar or dissimilar materials need to be fastened together. The requirement of joining two dissimilar materials is essential when two parts of the same structure exposed to different loading conditions or environments. Al and Mg alloys are wonderful materials with marvelous properties, and it is being successfully used in many industries. It has also been cited that they will be abundantly used in the future in automobile, aerospace and marine ventures. To date, their use in many industries is limited because the welding methods have not yet been fully developed. Fusion welding techniques are utilized to serve the purpose, but the joint made is undermined in strength. Usually, the strength of the joint made by fusion welding was reported well below the yield strength of the Al and Mg alloys. The formation and growth of brittle IMCs during this process is considered to be the main reason for the weakness of the joint. To avoid the formation of brittle IMCs in the welding zone, low-temperature pressure welding methods are gaining attention as an alternative to fusion welding techniques. FSW is an attractive welding method of this group and widely used for the welding of lightweight metal sheets. In Al/Mg hybrid structure, the control over brittle IMCs can provide improved welding strength. The temperature generated in FSW is well below the melting temperature of Al and Mg alloys, which effectively minimizes the formation of IMCs in the welding zone. The detailed research progress and parametric optimization of welding of Al and Mg alloys using FSW are reviewed and listed in [Table 1].

**Table 1:** An overview on research on Al and Mg alloys using FSW

S. No.	FSP Parameters	Material	Outcomes	Year	Ref
1	Plate thickness (PT): 12 mm Weld Length (WL): 160 mm Rotational speed (RS): 300-400 rpm Traverse speed (TS): 1-1.67 mm/s	AZ31B+5083	Sound weld but weld region has virtually no ductility	2003	[16]
2	PT: 2 mm RS: 800 rpm TS: 1.5 mm/s Tilt angle (TA): 1°	AZ31B-H24+6061-T6 AZ91D+6061-T6	Weld region consists of lamellar shear bands.	2004	[5]
3	PT: 6 mm RS: 2450 rpm TS: 1.50 mm/s TA: 3°	1050 (Al)+AZ31	The presence of Mg <sub>17</sub> Al <sub>12</sub> IMCs increased the hardness of the weld region.	2004	[3]
4	PT: 4 mm RS: 200-1000 rpm TS: 0.32-1.25 mm/s	AZ31 (Mg)+1060 (Al)	Highest strength of the welded joints: 82.4 MPa Failure Mechanism: Cleavage Type	2005	[6]
5	PT: 2 mm RS: 800-1600 rpm TS: 5 mm/s	Annealed (AZ31B+A5252P)	Defect free weld were reported for 1000, 1200, 1400 rpm. Maximum tensile strength: 132 MPa at 1000 rpm Maximum ductility: 2%	2008	[2]
6	PT: 1.5 mm RS: 1400 rpm TS: 3.75 mm/s	AZ31+AA6040	The interface of FSW exhibited the presence of fine-grained Al <sub>12</sub> Mg <sub>17</sub> and nanosized-grained Al <sub>3</sub> Mg <sub>2</sub> IMCs.	2009	[4]
7	PT: 6 mm RS: 600 rpm TS: 0.67 mm/s	5052 (Al)+AZ31 (Mg)	Microhardness of weld region was almost double than the base Al and Mg alloys.	2010	[17]
8	PT: 1.2 mm (AA 5083) & 1.3 mm (AZ31) RS: 1500-2250 rpm	AA5083+AZ31	In friction stir spot welding (FSSW), lap share stress was higher when IMCs were mixed with α-Mg+Mg <sub>17</sub> Al <sub>12</sub> eutectics.	2010	[18]

9	PT: 4 mm RS: 800 rpm TS: 0.58 mm/s	Al 6061-T6+AZ31	Weld tensile strength (max): 95 MPa	2011	[19]
10	PT: 3.25 mm RS: 900-2700 rpm TS: 1.69-6.4 mm/s Force: 14-30 kN TA: 1° or 3°	6065-T5 (Extruded)+AZ31B- H24 (Rolled)	Best mechanical strength were reported when rotational speed varied in between 900-1680 rpm and welding speed 1.69-4 mm/s	2012	[20]
11	PT: 3 mm RS: 300 rpm TS: 0.83 mm/s TA: 3°	5083 Al+AZ31C-O	Formation of IMCs was low in underwater welding due to less intermixing resulted in smooth surface.	2012	[21]
12	PT: 2 mm RS: 2000 rpm Tool shoulder plunge depth (TSPD): 0.2 mm TS: 3 mm/s	AZ31B-H24 (Mg)+5754-O (Al)	FSW of similar alloys (Mg-Mg) had better lap shear strength, failure energy and fatigue strength than dissimilar alloys weld (Al-Mg) due to the presence of IMCs like Mg <sub>17</sub> Al <sub>12</sub> and Al <sub>3</sub> Mg <sub>2</sub> in the dissimilar weld.	2012	[22]
13	PT: 2.5 mm RS: 1200 rpm TS: 1.33 mm/s	AA6013+AZ31	Sound joint is obtained using underwater FSW. Maximum Tensile strength: 152.3 MPa Maximum Hardness: 142 HV	2015	[23]
14	PT: 3 mm RS: 600-800 rpm TS: 0.5-1.0 mm/s	6061-T6+AZ31B	Sound and defect free joint, Tensile strength of the weld is 70% of Mg alloy	2015	[24]
15	PT: 3.1 mm (AZ31B) & 2.3 mm (6061) RS: 560-1400 rpm TS: 0.27-0.67 mm/min TA: 3°	AZ31B+Al 6061	Maximum mechanical interlocking and optimum tensile strength of the weld was obtained when rotation speed was 1400 rpm and welding speed 40 mm/min.	2015	[25]
16	PT: 3.1 mm (AM60B) & 1.5 mm (AA6022) RS: 1000-2500 rpm TSPD: 0.2-0.6 mm TS: 0.2 mm/s	AM60B (die-cast)+AA6022-T4 (Rolled)	Welded region was able to bear 2.5 kN shear force when welded at the rotational speed of 1000 rpm and shoulder depth of 0.9 mm.	2015	[26]

## CONCLUSION

This manuscript represents the recent progress and research activities of dissimilar aluminum and magnesium alloys welding using FSW. Although the FSW is successfully being used in the welding of hard to weld materials, still its full potential is not being utilized commercially. This review will assist in understanding the use of FSW in the welding of dissimilar materials, especially the welding of Al and Mg alloys. The attributes of the FSW of Al alloys to Mg alloys are discussed. Other than this, the effect of various parameters on the strength of Al/Mg joints is also reviewed. It was noticed that even today, FSW is not widely used in Al-Mg welding because the strength of the joint is reduced due to the presence of IMCs. Owing to the presence of these IMCs, high hardness of the joints was reported. By selecting some process parameters, fragmental defects, voids, pores and cracks were also found in the weld region. The high hardness of the joint is also considered responsible for its brittle behavior and poor ductility. It is difficult to establish an appropriate analytic relationship among the various parameters to achieve the desired qualities from the joint. It was found that the quantity and size of IMCs are less in FSW than fusion welding. Finer grains were detected in the welded portion owing to dynamic recrystallization. At the same time, the joint hardness in fusion welding is much higher than that of FSW, which impairs the flexibility and strength of the joint. Consequently, FSW is a much better process than fusion welding to weld Al/Mg alloys.

## CONFLICT OF INTEREST

None.

## ACKNOWLEDGEMENTS

The support extended by Accendere Knowledge Management Services, CL Educate, New Delhi during the manuscript preparation is greatly acknowledged.

## FINANCIAL DISCLOSURE

None.

## REFERENCES

- [1] Liu L, Ren D, Liu F. [2014] A review of dissimilar welding techniques for magnesium alloys to aluminum alloys. *Materials*. 7:3735–3757.
- [2] Kwon YJ, Shigematsu I, Saito N. [2008] Dissimilar friction stir welding between magnesium and aluminum alloys. *Materials Letters*. 62:3827–3829.
- [3] Sato YS, Park SHC, Michiuchi M, Kokawa H. [2004] Constitutional liquation during dissimilar friction stir welding of Al and Mg alloys. *Scripta Materialia*. 50:1233–1236.
- [4] Kostka A, Coelho RS, Dos Santos J, Pyzalla AR. [2009] Microstructure of friction stir welding of aluminium alloy to magnesium alloy. *Scripta Materialia*. 60:953–956.
- [5] Somasekharan AC, Murr LE. [2004] Microstructures in friction-stir welded dissimilar magnesium alloys and magnesium alloys to 6061-T6 aluminum alloy. *Materials Characterization*. 52:49–64.
- [6] Yan J, Xu Z, Li Z, Li L, Yang S. [2005] Microstructure characteristics and performance of dissimilar welds between magnesium alloy and aluminum formed by friction stirring. *Scripta Materialia*. 53:585–589.
- [7] Guo J. [2014] Solid-State Welding Processes in Manufacturing. In: *Handbook of Manufacturing Engineering and Technology*. Springer. 1–21.
- [8] Thomas WM, Nicholas ED, Needham JC, Murch MG, Temple-Smith P, Dawes CJ [1995] Friction welding
- [9] Liu G, Murr LE, Niou CS, McClure JC, Vega FR. [1997] Microstructural aspects of the friction-stir welding of 6061-T6 aluminum. *Scripta materialia*. 37:355–361.
- [10] Jata KV, Semiatin SL. [2000] Continuous dynamic recrystallization during friction stir welding of high strength aluminum alloys. *Scripta Materialia*. 43:743–749.
- [11] Smith WF, Hashem J. [2011] *Foundations of Materials Science and Engineering*, 5th ed. McGraw-Hill.
- [12] Li Y, Trillo EA, Murr LE. [2000] Friction-stir welding of aluminum alloy 2024 to silver. *Journal of Materials Science Letters*. 19:1047–1051.
- [13] Thomas WM, Wiesner CS, Marks DJ, Staines DG. [2009] Conventional and bobbin friction stir welding of 12% chromium alloy steel using composite refractory tool materials. *Science and Technology of Welding and Joining*. 14:247–253.
- [14] Threadgill PL, Ahmed MMZ, Martin JP, Perrett JG, Wynne BP. [2010] The use of bobbin tools for friction stir welding of aluminium alloys. In: *Materials Science Forum*. Trans Tech Publ. 1179–1184.
- [15] Unnikrishnan MA, Raja DJE. [2017] A Survey on Friction Stir Welding Of Dissimilar Magnesium Alloys. In: *IOP Conference Series: Materials Science and Engineering*. IOP Publishing. 012009.
- [16] McLean AA, Powell GLF, Brown IH, Linton VM. [2003] Friction stir welding of magnesium alloy AZ31B to aluminium alloy 5083. *Science and Technology of Welding and Joining*. 8:462–464.
- [17] Yong YAN, Zhang D-T, Cheng QIU, Zhang W. [2010] Dissimilar friction stir welding between 5052 aluminum alloy and AZ31 magnesium alloy. *Transactions of Nonferrous Metals Society of China*. 20:s619–s623.
- [18] Sato YS, Shiota A, Kokawa H, Okamoto K, Yang Q, Kim C. [2010] Effect of interfacial microstructure on lap shear strength of friction stir spot weld of aluminium alloy to magnesium alloy. *Science and Technology of Welding and Joining*. 15:319–324.
- [19] Chang WS, Rajesh SR, Chun CK, Kim HJ. [2011] Microstructure and mechanical properties of hybrid laser-friction stir welding between AA6061-T6 Al alloy and AZ31 Mg alloy. *Journal of Materials Science & Technology*. 27:199–204.
- [20] Venkateswaran P, Reynolds AP. [2012] Factors affecting the properties of Friction Stir Welds between aluminum and magnesium alloys. *Materials Science and Engineering: A*. 545:26–37.
- [21] Mofid MA, Abdollah-Zadeh A, Ghaini FM. [2012] The effect of water cooling during dissimilar friction stir welding of Al alloy to Mg alloy. *Materials & Design (1980-2015)*. 36:161–167.
- [22] Chowdhury SH, Chen DL, Bhole SD, Cao X, Wanjara P. [2012] Lap shear strength and fatigue life of friction stir spot welded AZ31 magnesium and 5754 aluminum alloys. *Materials Science and Engineering: A*. 556:500–509.
- [23] Zhao Y, Lu Z, Yan K, Huang L. [2015] Microstructural characterizations and mechanical properties in underwater friction stir welding of aluminum and magnesium dissimilar alloys. *Materials & Design (1980-2015)*. 65:675–681.
- [24] Fu B, Qin G, Li F, Meng X, Zhang J, Wu C. [2015] Friction stir welding process of dissimilar metals of 6061-T6 aluminum alloy to AZ31B magnesium alloy. *Journal of Materials Processing Technology*. 218:38–47.
- [25] Mohammadi J, Behnamian Y, Mostafaei A, Izadi H, Saeid T, Kokabi AH, Gerlich AP. [2015] Friction stir welding joint of dissimilar materials between AZ31B magnesium and 6061 aluminum alloys: Microstructure studies and mechanical characterizations. *Materials Characterization*. 101:189–207.
- [26] Rao HM, Yuan W, Badarinarayan H. [2015] Effect of process parameters on mechanical properties of friction stir spot welded magnesium to aluminum alloys. *Materials & Design (1980-2015)*. 66:235–245.

## ARTICLE

# ENGINEERED CEMENTITIOUS COMPOSITES - A REVIEW

Mudit Mishra\*, Gift Pon Lazarus D, Rajat Kumar Tomar

Department of Civil Engineering, Manav Rachna International Institute of Research & Studies, Faridabad, INDIA

## ABSTRACT

This study presents a short summary on the recent progress within the analysis, growth and specific use of Engineered Cementitious Composites (ECC). The use of ECC as a replacement to conventional concrete will contribute to safer, more durable and sustainable concrete infrastructure. The material properties such as tensile and flexural characteristics, compressive strength, durability, permeability, self-healing capacity and seismic performance have been reviewed here. The material constituents and mix design used to achieve the unique properties of ECC concrete have been listed out and discussed. The potential structural applications such as Earthquake Resistant Structures (ERS), Bridge deck and link slabs, Pavements, Repair and Retrofitting works, which utilize the special qualities of ECC are included in this paper. A comparison between ECC and conventional concrete in terms of feasibility and cost efficiency has been made. The concept of green ECC for sustainable infrastructure and the scope for future research work has been addressed.

## INTRODUCTION

In civil engineering applications like buildings, bridges, pavements, retaining wall structures, tunnel linear, etc are developed by the use of cement concrete. In recent decades, high compressive strength concrete is being used in various applications. Concrete is brittle in nature and as the compressive strength increases its brittleness increases. Higher brittleness can increase the chance of sudden failure/collapse during earthquake and impact loading [1]. If by some method the ductility is introduced into the concrete, it can reduce the sudden collapse or failure. In such cases concrete material is needed to improve its power and tensile capacity. To make the concrete ductile concept of Engineered Cementitious Composites (ECC) is introduced. ECC has ultra-fibres mixed with concrete. The ultra-fibres having reinforcement and ductile properties and it makes the mix ductile and more workable. The first use of ECC was found at the University of Michigan by Victor C Li. ECC is strong resistance against impact and earthquake loading [2]; also it reduces the total amount of reinforcement used in concrete. Ultra-fibres present in the ECC makes the flexible bond with cement-sand and aggregates which makes it more deformable against external forces [3]. It has higher resistance against vibration and heat. It is bendable with respective forces (moving loads, wind load, earthquake forces etc.) and absorbs the shocks. It can sustain higher loads with small amount of deformation; in other words, stiffness of ECC is huge as compared to conventional concrete. Further, ECC has, self-healing properties and improved durability. Apart from its use in structural elements, ECC is finding its way into repair and retrofitting of structures. In the present paper a deep review of various properties of ECC and its applications is presented.

## CHARACTERISTICS OF ECC

The application of precast building material composite as a construction material is different from standard concrete being used now- a- days thanks to better properties of the former. Level of excellence is based upon its mineral composition to produce a new effect with the surrounding environment shown by it. ECC has self-healing property when it gets damaged from physical and chemical reactions. Tensile strength and ductility gets improved due to its improved physical characteristics. The tensile strength within a very low degree of permeability considerably decreases the micro cracking. This low permeability degrades the trend related to the assimilation of chemicals that include the corrosion of steel reinforcement and erosion of the concrete itself. These above characteristics are used to increase the lifespan and repair cycle of the concrete and the structure as a whole, whereas also making the requirements that permit certain chemical reactions to occur which will help bring about healing of the cracks of the concrete [4].

### Tensile and flexural characteristics

ECC has the tensile strain capacity up to 3-5% (300-500 times varies from normal concrete) because the conventional concrete has tensile strain capacity up to 0.01% only. ECC can attain high ductility with comparatively low fibre content (2%) through methodical modification of the fibres, matrix, interface characteristics and guided by micromechanics properties. Micromechanics is the study of heterogeneous or composite materials on the extent of the individual constituents that represent the materials. Micromechanics theory affords a systematic approach in selecting the type, size and amount of the constituents and their combinations [5]. The principle of micro cracking is responsible for the distinctive tensile properties of ECC when compared with conventional concrete. ECC flexes without fracturing, due to the interaction between fibres, sand, and cement working in a matrix that binds everything together within the material. Where ordinary concrete and fibre-reinforced concrete (FRC) are designed to resist cracking, ECC is designed to develop cracks only in a controlled manner. The cracks that appear in ordinary concrete

### KEY WORDS

Engineered  
Cementitious  
Composites; Concrete;  
Seismic resistance; PVA  
fibres; Structural

Received: 23 Mar 2019  
Accepted: 24 April 2019  
Published: 12 May 2019

### \*Corresponding Author

Email:  
mudit.mishra2607@gmail.com  
Tel.: +919971898822

and FRC increase in width as they grow longer, these are termed Griffith-type cracks. Whereas the width of cracks that are designed into ECC remains constant regardless of the length, these are known as steady state (or flat) cracks [6]. A direct application of pure tensile stress is difficult and hence an indirect way is adopted by measuring the flexural strength of beam. The flexural reaction of ECC reacts with its tensile ductility. Underneath flexure, at the bottom of the beam multiple micro-cracks are formed, consequently it leads to tolerate a remarkably massive curvature growth, an occurrence that has provided it the name of bendable concrete. A flexural strength of regarding 10 to 15 MPa may be achieved. Deflection hardening is an essential property of ECC based on geometry. ECC has notable enhancements in fatigue strength compare to standard concrete and FRC. ECC was developed based on flexural fatigue tests where it shows high fatigue durability and ductility when compared with standard cement mortars widely utilized in repair and retrofitting applications [7].

### Permeability and freeze-thaw durability

The Permeability Crack provides an easier access for the water, oxygen and other aggressive agents to pass through the concrete cover and come in direct contact with the steel reinforcement, therefore resulting in the beginning and proliferation of steel corrosion. Since cracks inevitably exist in concrete elements, the influence of crack width on the water permeability is of great interest from academic and practical point of view. Therefore, the micro-cracked ECC should definitely have better corrosion resistance in comparison with the normal concrete. Accelerated corrosion test has been conducted on steel-reinforced ECC beams, where mortar specimens of an equal compressive strength were used as reference. The results showed that due to its micro-cracking behavior and high ductility, ECC prolonged the corrosion propagation stage and retained much higher level of the loading capacity. These results are expected to contribute substantially in increasing concrete structures durability and sustainability by minimizing the needs of maintenance during the life span of ECC structures [5].

### Self-healing capacity

Formations of cracks are inevitable during the lifetime of concrete infrastructure. Cracks are often shaped thanks to progressively high loading, volumetric modification thanks to temperature changes, plastic settlement, restrained shrinkage, creep, chemical actions like alkali-silicate reaction and freeze/thaw cycles. Cracks on concrete structures will have undesirable effects in various ways. It should cut back the sturdiness by making sequence for corrosive sources to perceive the concrete cover and affect the inside steel reinforcement. It can cause a rise in the maintenance cost and reduce the service life. Thus it's extremely desirable to develop concrete which will automatically recapture this loss of capability due to cracking. Theoretical and experimental results have exhibited that once cracked concrete is exposed to water, the un-hydrated cement gets hydrated thereby having the potential to cure itself over time by decreasing the crack width and this development is referred to as self-curing of cracks. The range of self-curing of cracks is especially based on the crack size. Compare to larger width cracks the smaller width cracks cure fully and at a quicker rate [10]. Thereby, the event of a cementitious composite that may autogenously counter the results of cracking by self-healing is extremely desirable. Self-healing results in crack-closing, therefore improving sturdiness, permeability, mechanical properties and therefore prolonging the service lifetime of infrastructure [11]. The long lifespan of ECC is not only attributed to its low permeability, high tensile and compressive strength, but also to the chemical action of self-curing that happens within the small size cracks formed. Thus it's needed to see up to what extent an ECC specimen will cure itself fully when susceptible for daily environmental situations. ECC specimens were observed up to one-year for mistreatment mechanical and resonant frequency (RF) loading for study the speed and range of self-curing within the inherent atmosphere. It was discovered based on the resonant frequency (RF) range, initial cracking influence improvement and stiffness enhanced with the rise in period of exposure to natural environment. Experimental results have shown that ECC samples kept under tensile strain and subjected to damp dry cycles, successfully healing the 100 micrometer cracks. Further testing during this study has exhibited that the addition of fly ash can reduce the average crack dimension up to 10 micrometers, therefore providing a faster and completely filled self-healing specimen.

## MATERIAL CONSTITUENTS AND MIX DESIGN

ECC concrete constitutes of cement, sand, fly ash, water, admixtures and an optimum amount of fibers. Coarse aggregates aren't employed in the mix as they have an inclination to adversely have an effect on the distinctive ductile behavior of the composite. Ordinary Portland cement of desired grade can be used. Blast furnace slag can be used as adhesive if required. The fine aggregate to be used can be river sand or manufactured sand based on availability. To improve the fresh concrete workability without increasing the water cement ratio by adding super plasticizer is possible. The use of super plasticizers will avoid the need for compaction as they add on to the self-consolidating property of ECC concrete. Fly ash is a pozzolanic material which will be used as a partial replacement for cementitious material. The use of fly ash can reduce heat generation without considerable loss in strength. Unlike some High Performance Fiber Reinforced Concrete (HPFRC), ECC doesn't utilize great quantity of fiber. usually 2% or less by volume of intermittent fiber is sufficient, albeit the combined is meant to significant structural benefits. Based on the comparatively less quantity of fibers used, the mixing method of ECC concrete is kind of the same as that used for mixing standard concrete. The most common type of fiber used in ECC is Poly Vinyl Alcohol (PVA) fiber. High Young's modulus, bonding strength, durability and tensile strength are some of the properties that make it suitable for reinforcing cementitious composites. Water free from alkalis, oils, acids or any



other organic Impurities should be used for mixing concrete. In short water used for making concrete should be of consumable standards. The main purpose of adding water to concrete is for it to react with cement to form a cement paste adhesive until it hardens. Water cement ratio engages a critical part for determining the potential of hardened concrete. Optimum water cement ratio has to be used to maintain perfect balance between workability and strength of concrete [8].

## STRUCTURAL APPLICATIONS

The special characteristics of Engineered Cementitious Composites that have been repeatedly tested in laboratories, pose several benefits to the construction industry through application. ECC's will make way for several potential enhancements to the present standing of typical concrete, and in some places, they have already been used as a construction material in projects. ECC structures shows more durability and less possibility to damage. Since feasibility is the capability to sustain, the additional study and long-lived structures related to the utilization of ECC's not provide solely for the feasibility of infrastructures in the world, however additionally for conjointly in preservation and renovate prices, as far as good environmental influence, and an overall development for the invulnerability of structures created by concrete [4]. Structural applications where ECC can be used are as impact resistant panels, strengthening of unreinforced masonry walls, repair and corrosion resistance for RCC beams and columns. Due to its ductility and tensile strength, ECC is suitable for members that take high loading and shock absorption like bridge surface decks, link slabs in bridges, pavements and seismic structures.

### Bridge deck and link slab

ECC's mechanical properties and durability factors are its tensile behavior, crushing strength (350 times that of concrete and FRC) [12] and tight crack width control. The micro crack width of ECC formed is below 100  $\mu\text{m}$  and can be independent of structural geometry and loading. Since steel reinforcement is not required to control crack width which is a cost effective advantage. Flexural Behavior of ECC helps to absorb shocks during transport and it also possess superb abrasion and wear protection. When the tensile strain is loaded to 15%, it is found that micro-cracked ECC displayed roughly the similar permeability as that of sound concrete. ECC has less water permeability by virtue of controlled formation of cracks, crack width is less. ECC also does not have dependency on the properties steel reinforcement and does not rely on applied strain level when strain capacity of ECC is not exceeded [12]. Rate of Chloride diffusion in ECC is comparatively lower. As a result, corrosion resistance is good. This signifies that the lifetime under service of reinforced ECC will be close to 15 times compared to reinforced mortar. Fatigue loading has no effect on the crack formation and fatigue resistance is fairly high. There is less reflective cracking in repairs due to formation of micro cracks.

### Bridge deck patching

In 2004, ECC pavement patching test was done by MDOT in a two-lane bridge overpassing. Patch repair ECC was used in Southern Michigan on the bridge deck of Curtis Road over M-14 in October 2002. The mentioned bridge built in 1976, has simply supported four span along with a nine inches thick reinforced concrete deck and steel girder. Traffic survey conducted by the Washtenaw County Road Commission was measured average daily traffic (ADT) for this bridge around 3000 vehicles per day. In this experiment one part was patched using ECC while other part was patched using OPC for comparative study.

Over a long duration both patches were observed during site visits and pictures were taken to study day by day progress of crack development and patterns. After two days patching in concrete had a distinctly visible crack, around 300mm wide had been formed possibly due to shrinkage deformation whereas there were no visible cracks in ECC. After four months, during winter, small micro cracks, 50mm wide, created in the ECC patch. Concrete crack observed shortly after casting the concrete had widened to 2mm and showed signs of deterioration due to spalling. A crack of 50mm was revealed after 10 months of the patch work, whereas concrete had serious deterioration. Thus ECC survived the best under severe environmental and mechanical factors.

### Bridge deck link slab

Between adjacent bridge decks, failure of mechanical expansion joint is a major issue, which could eventually lead to leaks and thermal deformations leading to failure of entire super structure. At the bridge deck water was discharging and fully soaking wet with de-icing salts used through cold weather, finally leaks through the damaged joints is the cause to corroding the steel girders, also penetrating moisture into the precast concrete girders moreover corroding the steel reinforcement [13]. Experiments showed that ECC had 4% strain in uni-axial tension unique capability to buckle close to while preserving small crack widths, this permits the ECC link slab to contain the distortion placed on the adjoining bridge decks during the contraction and thermal expansion, all the period the superstructure is protected from the action of corrosion. ECC had large tensile strain capacity as a link slab and saturated micro cracking (width 60 mm). This is sufficient to take care of all structural applications in link slabs. Also reduction in reinforcement is an added advantage in terms of cost.

## Seismic applications

ECC Applications are considered mainly in structures where good energy absorption and high failure tolerance is required during performance. ECC can be opted to reduce seismic action and damage of structural members. Normal concrete simply as a brittle material is susceptible to collapse. Basic concept in earthquake engineering is based on the fact that when a building absorbs seismic waves from the earth it is transferred thorough out the buildings components like beam and columns. The Joints and structural members need to be ductile enough to absorb the vibration created without formation of cracks, which occurs at a faster rate in brittle material due to lack of elasticity. ECC having higher ductility and tensile strength is a suitable material for seismic resistance. Particularly the joints and structural members of the building need to be ductile, since it is the basic skeleton of the building and its failure could lead to complete collapse. To find out the seismic resistance of ECC a cyclic loading alternatively of tension and compression was given to beam members. The test outputs done with PVA-ECC showed that the brittle and shear failure seen in RCC can be prevented using ECC and it gave good ductile capacity. The PVA (polyvinyl-alcohol) fibers also helped confine the concrete after fracture. [14] The beam-column connections were also tested [15] using reverse cyclic load capable of producing seismic action using a 500KN hydraulic actuator. From the corresponding hysteresis loop diagram generated, ECC proved to have higher energy dissipation than other material. Also multiple small cracks were created in the plastic zones and joint cores allowing ECC joint to maintain its structure. As a result of these findings, ECC has massive potential in seismic resistance development of buildings where ductile material that are capable of withstanding seismic shocks are required.

## Repair and retrofitting

Retrofitting is the process of modifying a finished structure by changing structural components to improve its performance and amenities. Some structures over time may need extra elements like columns or beams to undertake changes over years due to age and tectonic movement. It is uneconomical to demolish and rebuild old structures from scratch. In such case structural elements can be added using repair and retrofit techniques Properties of material that are particularly required for retrofit techniques are high efficiency, durability, Isotropic properties, easy flexible processing and shorter fibers at moderate volume fractions [16]. Isotropic property helps when the stress field has changing load conditions or the stress is multi-directional. Retrofits are designed by analyzing ECC established on its synergy between the fibers, interface and matrix components under load. To test its capacity as a retrofit material pre-cast ECC and FRC were analyzed under simplified boundary and loading conditions. The observations made were that ECC had three times the shear capacity of FRC. Also the strain distribution method is ease to finding the stress concentration for the ECC specimen. ECC thus has good shear absorbing capacity and tends to be isotropic in nature due to equivalent distribution of micro cracks formed. Repair-where a repair material is laid over a defective material. The repair material is required not to carry the stress from the defective material and develop cracks in itself. Repair factors that need to be taken into consideration is the lifecycle of repair, cost and durability. This durability can be created when the bond between the substrate material and repair material is at its best. Based on the bonding between these two layers, failure can occur in the form of “de-lamination” where weak bonds cause an internal defect. It can also occur if the bonding is too strong and if the repair material is brittle compared to the substrate. This failure is called “spalling”. Bond tests need to be conducted to analyze how the behavior or repair and substrate material is. Sometime difficulty in bond test occurs when there is a change in environmental conditions from the laboratory to the actual field performance. This is caused due to the mechanics of failure and material reaction under different conditions. In case of the mechanics, failure of bond is predominately due to fracture process variation for similar specimen of shape and geometry under different field conditions. ECC thus produces a solution to the bond failure problem. This is proved by a test where a substrate specimen already having a notch is coated with three different repair material-plain concrete, FRC and ECC. For ECC Overlay, a series of minute interface micro cracks occur under increasing applied loading. This makes it suitable as a repair material since there is no sudden failure, thus increasing lifetime of the repair component.

## Pavements

Transportation is an important facility which determines the mobility of goods between places thus improving the overall development of a country. As a result, pavements are important transportation components required for a country also cost, durability, life time and maintenance criteria are some factors to be considered for effective and efficient pavement systems. Pavement Overlays- are materials used to rehabilitate and fix surface defects on a pre-existing pavement and to create a durable rigid surface with a long life-time and least maintenance. Types of Pavement Overlay (i) mixed asphalt with high temperature (HMA) (ii) an unconstrained concrete overlay. From these mentioned overlay systems, cause of the ultimate failure system is reflective cracking which decrease the life of surface of the overlay [17]. This reflective cracking is caused when an overlay also tends to develop cracks due to transfer of pre-existing cracks in substrate layer during differential loading caused by moving traffic. Extra Info-Modern methods to minimize reflective cracking contain the implementation of a bond disintegrate layer (i.e. HMA) beneath concrete overlays that reduce stress concentration at the origin of reflective cracking, full rubblization (In situ broken concrete into particles like aggregate) of pair deterioration of remaining

pavement before overlaying or surface of the concrete. Presently, reflective overlaying cracking has not been effectively eliminated in rigid pavement overlays.

### Need for ductile rigid pavement overlay

A ductile material would be a solution to the formation of cracks which is due to brittleness of a material. Whereas a tensile material could help overwhelmed the fracture based phenomena caused by reflective cracking. This is where ECC comes into play. Based on mix proportions having 3% to 5% for the ultimate tensile strain capacity. This strain capacity is 300 times normal Ordinary Portland Cement and is created by many closely spaced micro cracks under load. These cracks carry increased load after formation causing materials strain hardening to be similar to ductile material. Inelastic strain is created in material due to distribution of micro-cracks along gauge length instead of single localized crack like in FRC. In FRC cracks are caused due to dislocation slip on crystallographic plane and the cracks open wide due to slow loading showing tension softening behavior by rupture of fibers. Conducting tests on these models overlay thickness were determined and a relationship between the highest stress developed in the appropriate edge loading of a one equivalent single axle load (ESAL) (80kN) dual axle load. Subgrade parameters and existing block were remaining constant ( $E_{existing} = 20.7\text{GPa}$ ,  $k_{subgrade} = 27.1\text{MN/m}^3$ ). For all combine designs in ECC overlay the coefficient of elasticity was additionally kept constant at  $20.7\text{GPa}$ . But the coefficient of elasticity was magnified to  $34.5\text{GPa}$  for the design of a concrete overlay. Based on the FEM model, subsequent overlay design chart was formed, concerning within the overlay design thickness with the highest stress level.

### COST ANALYSIS

Engineered Cementitious Composites are around three times more expensive than conventional concrete, but when comparing costs, it is necessary to take into consideration the cost over the entire life span of the structure rather than taking into account only the initial costs. The financial benefits in the long run favor ECC as it saves up on the service costs. The use of high cement in ECC and expensive Poly Vinyl Alcohol (PVA) Fibers is responsible for the price difference when compared to regular concrete. PVA fibers weigh much less when compared to other fibers and steel used in FRC's and normal concrete. It is to be noted that ECC has a very low fiber volume when compared to other FRC's. The use of cheap pozzolanic alternatives such as fly ash as partial replacement for expensive cement will help in lowering the price of ECC without causing much changes in its properties. Since ECC is less brittle, more ductile and durable and also possesses self-healing property, it can cut down on frequent maintenance costs. In short, ECC is a cost effective construction material alternative to conventional concrete [4].

### ENVIRONMENTAL SUSTAINABILITY

ECC by itself is not sustainable without the combination of industrial wastes. Green Engineered Cementitious Composites (ECC) where industrial wastes are used as constituents can be used to give more sustainable, eco-friendly, durable and rigid structure. It reduces pollution due to cement production and can use industrial waste as its constituents thus giving a greener alternative to ordinary cement. Use of industrial waste up to 70% in ECC has no reduction in its mechanical performance and there is 50% reduction in thickness of overlays reducing spacing. Furthermore "Green" ECC has been attempted to be formulated for sustainable development and environmental protection. The development of green ECC material is based on certain indicators called Material Sustainability Indicators (MSI). These indicators include the environmental factors like total production of energy; resulting amount of solid waste, carbon dioxide levels during production, water pollution caused by chemicals in ECC. Comparatively ECC has good mechanical performance but its environmental effects due to its manufacture are adverse in nature because of the proportionately of standard ECC has more cement content, also the addition of polymeric fibers is necessary. In terms of solid waste production, fly ash material usage reduces solid wastage. Fly ash is a waste that is created in from power plants where coal is used. We can infer from the table that by reducing cement and use of PVA fibers without compromising the ductility and other mechanical properties; we can reduce the environmental burden caused by ECC and increase its sustainability in comparison to concrete. The replacement of the components of ECC like cement and fiber with industrial wastes without compromising its mechanical properties is important. Few potential alternatives like fly ash and bottom ash can be used since they affect the environment and this can be reduced by using them to create green ECC. Other different materials need to be tested to find suitable alternatives. Experiments suggest inclusion of fly ash lead to improvement in the materials strain-hardening. When high volumes of fly ash were used. The results of the composites show 3% to 4% of the tensile strain capacity and while the material sustainability ratios significantly improved then the tensile strength becomes more than 4.5 MPa (653 psi) [19], Thus by using the concept of micromechanics, high performance criteria can be achieved using industrial wastes provided that the parameters are carefully designed.

### CONCLUSION

ECC shows a number of special characteristics that look appealing to the construction industry and its engineers. Experimental studies show that ECC can perform remarkably better than conventional concrete when subjected to all forms of severe environmental and mechanical conditions. After a long stretch of

research and development of ECC, it is now not just confined to research laboratories but is making its way into real life applications in the construction industry through precast elements, conventional in-situ casting and repair and retrofitting works. ECC also has demonstrated to possess flexibility in the processing route, which include in-situ self-consolidating casting, spraying in form of shotcrete and also in precast and extrusion elements. The application of ECC in the commercial market may benefit many, established consequently on the fact that the life span of the concrete infrastructure gets increased exponentially. The fields of application of ECC are forever expanding. The use of green ECC makes way for significant reduction of energy resource consumption, material consumption and emission of pollutants. Engineered Cementitious Composites anticipated in future become more ubiquitous in all concrete infrastructure construction works worldwide. Despite the advancement in the improvement of ECC and real life use accessible, a large amount of experimentation and more number of research are still needed. On further research, more favorable characteristics of ECC might be discovered that will make way to modern infrastructure applications [20]. As research advances more laboratory work and investigations can be done to determine the shear resistance and Poisson's ratio of ECC. Another space for analysis is an examination of the fiber distribution and orientation within the materials, and also the development of strategies to gauge the orientation and effect of fiber distribution on the tensile response of the materials. Applied mathematics strategies will be used to develop representative samples of the fiber orientation, and surface bond strength of the fibers [21]. Continued research will maintain the materials-structure interaction approach and will focus on filling in knowledge gaps in material properties and design [13]. The use of pozzolanic industrial wastes as partial substituents to cement has to be studied in detail to develop eco efficient green Engineered Cementitious Composites.

#### CONFLICT OF INTEREST

There is no conflict of interest.

#### ACKNOWLEDGEMENTS

The authors express their deepest gratitude towards the help of Accendere Knowledge Management Services, New Delhi, India for giving the valuable suggestions for preparing the manuscript.

#### FINANCIAL DISCLOSURE

None.

#### REFERENCES

- [1] Sahmaran M, Li VC. [2010] Engineered Cementitious Composites: Can it be Accepted as a Crack-free Concrete?, TRB Transportation Research Record, No. 2164, Transportation Research Board of the National Academies, Washington DC.1-8.
- [2] Li, Victor C, Kanda T. [1998] Engineered Cementitious Composites for Structural Applications ASCE Journal of Materials in Civil Engineering, ASCE J Materials in Civil Engineering. 10(2):66-69.
- [3] Li, Victor C. [2003] On Engineered Cementitious Composites (ECC) - A Review of the Material and its Applications Journal of Advanced Concrete Technology, J Advanced Concrete Technology. 1(3):215-230.
- [4] Marks, Jayne, Jon Conklin. Engineered Cementitious Composites: Applications and Impact Of High Tensile, Self-Healing Concrete.
- [5] Qian, Shunzhi, Victor C, Li. [2011] Ductile Concrete-Engineered Cementitious Composites (Ecc) For Durable Bridge Deck Repair and Rehabilitation 2. rehabilitation. 26.27:28.
- [6] Li, Victor C. Bendable Concrete Provides Insight into Sustainable Material Development Process.
- [7] Li, Victor C. [2008] Engineered Cementitious Composites (ECC) Material, Structural, and Durability Performance.
- [8] Dhawale AW, Joshi VP. [2013] Engineered cementitious composites for structural applications. International Journal of Application or Innovation in Engineering & Management. 2:198-205.
- [9] Kanakubo, Toshiyuki. [2006] Tensile characteristics evaluation method for ductile fiber-reinforced cementitious composites. Journal of Advanced Concrete Technology. 4.1:3.
- [10] Herbert, Emily N, Victor C, Li. [2013] Self-healing of microcracks in engineered cementitious composites (ECC) under a natural environment Materials. 6.7:2831-2845.
- [11] Kan, Li-Li, et al. [2010] Self-healing characterization of engineered cementitious composite materials. ACI Materials Journal. 107.6.
- [12] LI M. [2014] Engineered cementitious composites for bridge decks." Advanced Composites in Bridge Construction and Repair. 50:177.
- [13] Lepech, Michael D, Victor C, Li. [2010] Sustainable pavement overlays using engineered cementitious composites. J Pavement Res Technol. 3.5: 241-250.
- [14] Fukuyama, Hiroshi, et al. [2000] Ductile engineered cementitious composite elements for seismic structural applications. CD Proceedings of the 12 WCEE. 1672.
- [15] Qudah, Salahuddin, Mohamed Maalej. [2014] Application of Engineered Cementitious Composites (ECC) in interior beam-column connections for enhanced seismic resistance. Engineering Structures. 69:235-245.
- [16] Li, Victor C, et al. [2000] Repair and retrofit with engineered cementitious composites." Engineering Fracture Mechanics. 65.2:317-334.
- [17] Lepech MD, et al. [2008] Design of green engineered cementitious composites for pavement overlay applications. Proceedings of the First International Symposium on Life Cycle Civil Engineering.
- [18] Li, Victor C, et al. [2004] Development of green engineered cementitious composites for sustainable infrastructure systems. Proceedings of the International Workshop on Sustainable Development and Concrete Technology, Beijing, China, May 20-21. Center for Transportation Research and Education low.
- [19] Wang, Shuxin, Victor C, Li. [2007] Engineered cementitious composites with high-volume fly ash. ACI Materials Journal. 104.3.
- [20] Akkari, Alexandra. [2011] Evaluation of a Polyvinyl Alcohol Fiber Reinforced Engineered Cementitious Composite for a Thin-Bonded Pavement Overlay. Report No. MN/RC 2011-11. Minnesota Department of Transportation, Research Services Section, 1-48.
- [21] Kesner, Keith, Sarah Longstreth Billington. [2004] Tension, compression and cyclic testing of engineered cementitious composite materials. Technical Report No.MCEER-04-2002, Cornell University, School of Civil & Environmental Engineering, Ithaca, New York, 1-125.



## ARTICLE

# MAXIMUM POWER POINT TRACKING- EFFICIENCY AND ITS FUTURE SCOPE

Rohit Jain\*, Aadil, Richa Khara, Rajat

Department of Electrical and Electronics Engineering, Manav Rachna International University,  
Faridabad, Haryana, INDIA

## ABSTRACT

As the fossil fuels are depleting it is desirable to use the renewable energy source. There are different sources of energy available like Sun, Wind, Fuel, but the solar energy is available in abundance. It is desirable to use this energy. This solar radiations change with the course of time in a day. So to maximize the solar output the point of maximum energy has to be calculated. There are different methods for this which is known as MPPT (Maximum Power Point Tracking). The advantages and implications of the Maximum power point technique is compared. The DC-DC converters are used to boost the voltage level obtained from the photovoltaic source. The switching devices of the converters are energized in way to track the maximum power point. The MPPT algorithms are applied to obtain the required switching. The association between the MPPT solar charge controllers and pulse width modulation solar charge controller is discussed in the paper.

## INTRODUCTION

Increasing demand of Electricity in today's world, efficiency of Electricity enhancement and for making eco-friendly environment, necessitates the production of electricity in a very effective manner. MPPT is one of the smart ways of electricity generating with high efficiency. As, MPPT is already associated with the solar power & this technique has the ability to use directly for several purposes such as heating and lighting the facilities, producing electricity, for temperature treatment (heating or cooling), and various other uses related to manufacturing, engineering or money-making [1].

Advantages of Solar Power:

- This energy source is renewable/ regenerative.
- This source has high impact on the reduction of the Electricity bills.
- The maintenance cost of this source is low.

Nowadays, the electricity is mainly generated by non-renewable energy resources such as coal, petroleum, nuclear energy etc. which is limited and also harms the environment badly. Therefore, researchers from all over the world are now working to find out an alternative way to produce the electricity from unlimited resources. Solar electricity is one of them. Unfortunately, the reliability of solar electricity in terms of its efficiency and consistency is not appropriate [2]. To resolve these issues, some innovative techniques are required. MPPT is one of them new techniques, which can be playing an important role for efficient generation of electricity in eco-friendly environment. Solar power is an important resource for generating electricity, because it is cheap and saves environment as well. MPPT is a charge controller, which directs to extract the maximum power from the PV system. Earlier using MPPT is difficult because it can damage the battery due to its fast charging or discharging process. This charge controller enables the facility of generating energy with high efficiency and charges the battery in efficient way. MPPT is designed in such a way that it can extract maximum power from PV panels in a smarter way in order to enhance its reliability, efficiency, reducing cost, and to meet the needs of the future demands of consumers.

## MAXIMUM POWER POINT TRACKING (MPPT)

MPPT is a type of charge controllers which extract maximum power from PV system, boosting up the current, by which one can get the maximum power. Generally, it converts high voltage DC from PV panels into low voltage needed for charging the battery in efficiently way as shown in [Fig. 1]. As the recent technologies are much better and efficient as compared to the old ones, therefore, the up gradation plays an important role for producing more energy in low cost. But few challenges are faced in MPPT.

Here are the few challenges where MPPT works:

- Cold weather- At the time of cold temperatures, the timing of sun hour is low, then it needs power for charging the batteries. MPPT works better at low temperatures, but without the use of MPPT we cannot extract maximum power [2].
- Basic working of MPPT- In MPPT technique, at first the ability of the PV module for producing output power is determined then this power is compared with the available voltage if the battery. After the comparison, the amount of power (extract from the PV panel and go to the battery for charging) is fixed in order to provide the optimum voltage for getting maximum current into the

### KEY WORDS

MPPT, PWM, P&O method, Incremental conductance technique

Received: 29 Mar 2019  
Accepted: 2 May 2019  
Published: 14 May 2019

\*Corresponding Author

Email:

rohit.mriu.eee@gmail.com



battery. It can also work as on-grid system, i.e. supply power directly to the DC load bypassing the connection with the battery according to the requirements.

- Low Battery Charge- Sometimes, the battery power is too low and it requires more power to charge. In this condition, the MPPT puts more current into them in order to charge such batteries.
- Long wire runs- If panels are 200 feet away, the voltage drop and losses are more. Although using large wires are expensive. In MPPT, a DC to DC converter is used, which determine the optimum point where the solar array (PV panels), and the battery bank or utility grid are matched in order to reduce the losses.

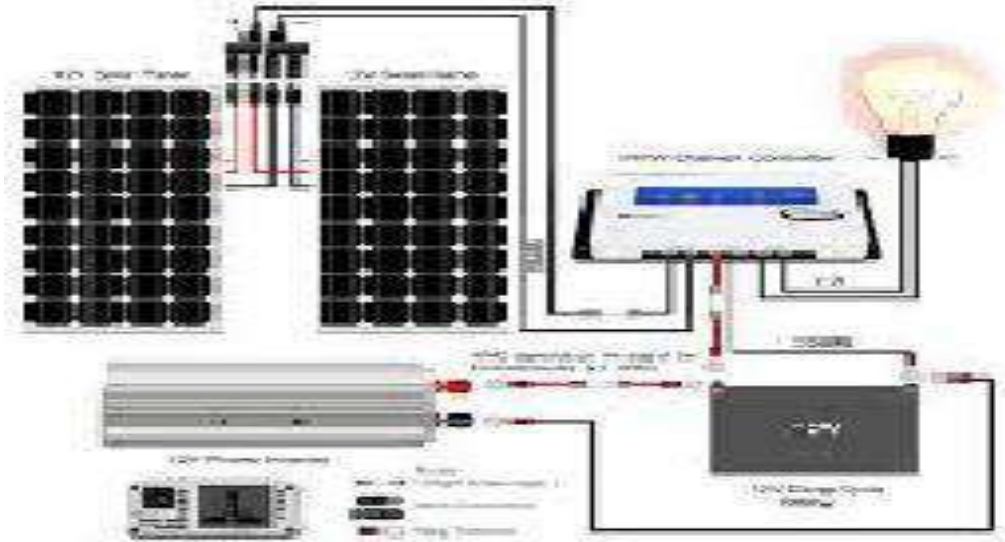


Fig. 1: Set-up for MPPT. [3]

But PV system should be keep at much angle so that it can achieve good sunlight. PV system should be keep at longitudinal degree of that area where the PV system is set-up.

**Block diagram of MPPT**

The mechanism based on maximum power tracking uses the algorithm and in surplus makes use of the electronic circuitry. The mentioned mechanism works on the principle of impedance matching between load and PV module, which is mandatory for the maximum power transfer as shown in [Fig. 2]. In general scenario, the MPPT termed as an adaptation of direct current (DC) to direct current switching voltage regulator. The impedance matching is executed by varying the duty cycle of the switch.

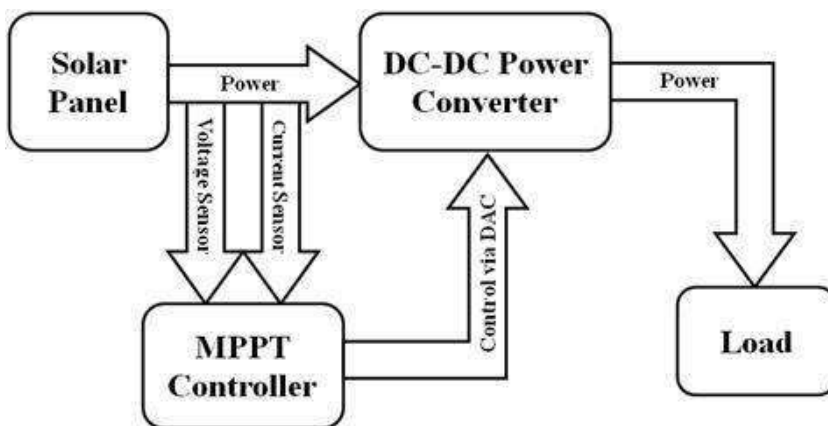


Fig. 2: Block diagram of MPPT [4]

## ADVANTAGES OF MPPT

MPPT have several advantages over the traditional techniques. the comparative study in between MPPT enabled sources and traditional sources in terms of efficiency, cost, power etc. is depicted in [Table 1].

**Table 1:** Comparative study between MPPT and traditional sources [5]

S. No.	Related terms	Traditional	MPPT
1.	Transmission of electricity	It needs long wire to transmit the power	It does not require long wire.
2.	Efficiency	Less	More than 95%
3.	Cost of energy	High cost	Less cost
4.	Planning time	Planning time is large	Less planning time
5.	Area required	Large	Less
6.	Eco-friendly	It is not eco-friendly as it radiates radiations, pollutions etc.	Eco-friendly
7.	Back up	It doesn't provide backup	Provides backup
8.	Quick supply	Since they are installed far away, so doesn't have quick power supply	Not far, so quick supply
9.	Electricity at remote areas	It doesn't provide electricity at remote areas.	It provides electricity everywhere
10.	Reliability	Less reliable	Reliability is high

## MPPT V/S PWM

The other technique named as Pulse Width Modulation (PWM) is mainly known for its ability to attain constant voltage throughout the entire session of battery charging by controlling and switching the solar system power devices. When the entire system is following the PWM regulation mode, at first the condition of the battery and its recharging requirements are observed and then according to this the current from the solar array tapers. The comparison is shown in [Table 2].

**Table 2:** Comparison between MPPT and PWM

S.No.	MPPT solar charge controller	PWM solar charge controller
1	Having ability to extract maximum amount of power from solar panel for charging purpose	Using whatever the power producing from solar panels for charging battery
2	Highly efficient (up to 96%)	Efficiency is low as compared to MPPT technique (up to 70%)

## CHARACTERIATICS OF TECHNIQUES OF MPPT

As there are many types of MPPT techniques are available, but three major MPPT techniques are discussed here:-

- P&O method- In perturb and observe (P&O) technique; the photovoltaic output voltage is continuously varying from the minimum to maximum level in order to track the maximum power point (MPP). This is very simple technique and easy to implement. Although, it can't be able to track/retain the MPP, if the variation in irradiance is rapidly fast with time.
- Incremental conductance- This is very interesting property of PV, which is used to optimize the operating current in order to get the output power at maximum level.
- Parasitic Capacitance- As general the parasitic capacitance is defined as the unwanted capacitance present between the various electronic components. It is an unavoidable effect but can be used in MPPT for charge storage purpose.

The [Table 3] represented the comparative analysis between the various characteristics of techniques of MPPT and concluded that the dominance of Parasitic Capacitance technique among the others in terms of output power achieved. Although, it has also getting the maximum ripple amplitude and time responses.

## APPLICATIONS

Different users having dissimilar requirement of power. Like Hospitals need premium power because regular use of different types of equipment. Industrial Plants need more electricity because the long

production hour, and hence seek MPPT applications that give free energy from solar with good efficiency. Indian Railways require more electricity, steady, uninterrupted premium power because running of trains 24 hours. Therefore MPPT plays an important role to achieve these goals with low cost and good efficiency.

Some implementation of solar power and MPPT in different areas and fields are:

1. Electric Rickshaw from Sukam runs by the solar power. Ordinary battery rickshaw uses electricity from conventional form to charge the battery (takes 2-3 hours), but Solar rickshaw runs by the Sun. It gives 20km more average than an ordinary rickshaw [7]. Using MPPT technique, at first the MPPT Controllers converts the achieved voltage into regular voltage of need, and then the remaining excess/extra amount of voltage is converted into Amp. Due to this, the level of charged voltage in the battery is kept at an optimal point, which helps to reduce the required time for charging.

2. Envision Solar, California, has been awarded contract in California to provide portable EV (electric Vehicle) chargers. They made the PV panels in upper side of parking area where the Vehicles can be charged and provides 150miles of range in a day. [8] MPPT used in electric vehicles for fast charging as compared to others.

**Table 3:** Comparison between various characteristics of techniques of MPPT [6]

Related terms	P & O Method	Incremental Conductance	Parasitic Capacitance
Benefits	Very simple and easy to implement.	Power of the entire system can be controlled by varying voltage value	This system is able to store the charge with in solar cell itself by adding the capacitance with the lighted diode equation.
Drawbacks	It fails under rapidly changing environment condition.	Time response, average power is low.	No such drawbacks.
Time response	1.758	0.55792	2.558
Average power	279.7	280.7	283.7
Ripple Amplitude	88.23	88.73	89.17

### FUTURE VISION

It is well known that various types of methods is used for generating the electricity like Thermal Power plants (Nuclear, Coal, petroleum etc.), Hydro (water) power plants, but it is non-renewable resources and also harmful for humans as well as environment. [9]

As many types of other charge controllers like PWM etc. also available, but due to low efficiency it cannot be used completely by the consumers. Hence there is need to develop more other cheap and effective MPPT algorithms [10], so that almost 100% efficiency can be achieved.

Here are the some that can be future research papers:

1. MPPT operating APP: An application of operating MPPT by the help of smartphones can so be made operate from whenever via the Internet.
2. DC-DC running loads: DC from MPPT can be taken directly and DC load can be run. DC loads helps to consume low electricity. [1]
3. Energy Management: There is need to manage energy when these algorithm are developed. [11]

### CONCLUSION

By seeing the world population and demand of electricity, it is necessary to use solar power and extract more power from it, MPPT is one of the technique to done efficiently. As it is discussed that parasitic capacitance technique is good from both P&O and Increment conduction method by power output. So as the population is increasing, there is need to use the renewable energy source. Therefore, solar energy is gaining the popularity. To extract maximum power, it is desirable to use MPPT algorithm, therefore to develop different types of algorithms of MPPT, so that maximum power can be extracted from solar energy with good efficiency. Comparative analysis on the basis of the advantages & disadvantages, voltage ripple, average power obtained, time response is done. The case study of the applying the MMT techniques on the Electric Rickshaw has been depicted in this paper

### CONFLICT OF INTEREST

There is no conflict of interest.

### ACKNOWLEDGEMENTS

Authors would like to express the gratitude to the Research Mentors of Accendere Knowledge Management Services Pvt. Ltd. for their comments on an earlier version of the manuscript. Although any errors are our own and should not tarnish the reputations of these esteemed persons.

### FINANCIAL DISCLOSURE

None.

## REFERENCES

- [1] Lal S, Dhiman R, Sinha MS. [2012] Analysis different MPPT techniques for photovoltaic system. International Journal of Engineering and Innovative Technology (IJEIT). 2(6):1-3.
- [2] Gaga A, Errahimi F, Es-Sbai N. [2014] Design and implementation of MPPT solar system based on the enhanced P&O algorithm using Labview. In 2014 IEEE International Renewable and Sustainable Energy Conference (IRSEC). 203-208.
- [3] <http://4.fgrw.dolmetscherbuero-ilyas.de/yuo/wiring-diagram-for-a-solar-panel.html>
- [4] <https://www.ijser.org/paper/Comprehensive-Overview-of-Basic-Photovoltaic-PV-Power-System.html>
- [5] Gupta AK, Saxena R. [2016] Review on widely-used MPPT techniques for PV applications. In 2016 IEEE International Conference on Innovation and Challenges in Cyber Security (ICICCS-INBUSH). 270-273.
- [6] Joshi S, Pandya V, Bhalja B. [2014] Maximum Power Point Tracking and MPPT efficiency for wind and solar energy conversion standalone system. In [2014] Annual IEEE India Conference (INDICON). 1-6..
- [7] Wan C, Zhao J, Song Y, Xu Z, Lin J, Hu Z. [2015] Photovoltaic and solar power forecasting for smart grid energy management. CSEE Journal of Power and Energy Systems. 1(4):38-46.
- [8] Sher HA, Addoweesh KE, Al-Haddad K. [2018] An efficient and cost-effective hybrid MPPT method for a photovoltaic flyback micro inverter. IEEE Transactions on Sustainable Energy. 9(3):1137-1144
- [9] Yi J, Su F, Lam YH, Ki WH, Tsui CY. [2008] An energy-adaptive MPPT power management unit for micro-power vibration energy harvesting. In 2008 IEEE International Symposium on Circuits and Systems. 2570-2573.
- [10] Olteanu S, Torous C, Miron C, Popescu D. [2017] Model based MPPT control of a small photovoltaic panel. In 2017 21st International Conference on System Theory, Control and Computing (ICSTCC). 524-528.
- [11] Alajmi BN, Ahmed KH, Finney SJ, Williams BW. [2011] Fuzzy-logic-control approach of a modified hill-climbing method for maximum power point in microgrid standalone photovoltaic system. IEEE Transactions on Power Electronics. 26(4):1022-1030.

## ARTICLE

# BRAIN MACHINE INTERFACE USING ELECTROENCEPHALOGRAPHY

Siddhartha Suman Rout, Vasudha Arora\*

*Faculty of Engineering & Technology, Department of Computer Science Engineering, Manav Rachna International Institute of Research and Studies, Faridabad, INDIA*

## ABSTRACT

Machine Learning a very popular and extremely useful technique in Brain Machine Interface. We explore the use of BMI for implementing electroencephalography for recording electrical activity of the brain. In this paper, we focus on developing a prototype that uses BMI to extract the current mood of the human brain. A BMI/BCI system provides a new method of communication to the brain through the computer. The brain consists of billions of neurons and these neurons communicate via minute electrochemical impulses which generate movement, expressions, emotions and words. Mental activity leads to changes of electrophysiological signals. Brain-computer interface (BCI) takes the input through the brain and link it to the device for some external activity, such as body movement, intelligence. The system opens a pathway for connecting the human brain and the matter that to be inhabited and is also helpful for treatment of severely paralyzed or locked-in people.

## INTRODUCTION

Machine Learning is a field of Computer Science, which enables the computer to work according to its own intelligence without being explicitly programmed.

A BCI machine sometimes called a mind-machine interface, direct neural interface or brain-machine interface (BMI), these are gates for communicating and for the controlling the systems which translate the input received from the brain and send it in order communicate with the devices.

Using of computers had always struck the question of interfacing. The ways by which human has been interacting with computers has advanced from last few decades. The new designs of technologies and systems appear more and more every day.

The growth in Human-Computer Interaction (HCI) field has not only been in quality of interaction, it has also experienced different branching in its history. Instead of designing regular interfaces, the different research branches have had different focus on the concepts of multimodality rather than unimodality, intelligent adaptive interfaces rather than command/action based ones, and finally active rather than passive interfaces.

This paper provides an impact on the HCI systems and cover most important branches as mentioned above. In the next section, basic definitions and terminology of HCI are given. This is a description on the different architectures of HCI designs. The final sections give the description on some of the applications of HCI and future directions in the field.

Electroencephalography (EEG) is a method for translating and recording the data received from the brain as the source of the input.

Further to study the method electroencephalography and to implement how EEG signals are different for different subjects to another furthermore, the concept of transferring of data between subjects is examined.

The non-invasive technique works by placing the twenty-four electrodes all over the head; It measures voltage fluctuations coming from the neurons of the brain.

The main focus is of developing a prototype which uses available EEG signals from brain as a input, and do certain task –

1) Receiving the EEG signal 2) process with the EEG signal and 3) uses the signal to classify and control the playlist of the music.

The focus is in developing a prototype of a headphone, which changes the music in reference to the current mood of the listener.

This draft focuses on the doorway of the EEG signals from the brain and to be implemented for testing purpose for the model, and the output is a functional prototype that can use user brain signals to control the music in the headphone through the application with over 90% accuracy.

### KEY WORDS

Machine Learning, Brain Machine Interface, EEG

Received: 21 Mar 2019  
Accepted: 6 May 2019  
Published: 14 May 2019

\*Corresponding Author  
Email:  
Vasudha.fet@mriu.edu.in



### Anatomy of brain

Human brain being the most complicated machine consists of neurons as many in number as there are stars in the galaxy [1]. It controls and regulates all functions and tasks performed by body. Our brain mainly consists of three, 1.cerebrum Cortex, 2.cerebellum cortex and 3.pons. Human mind consisting different lobe, the largest part of the brain is known as cerebrum see in the [Fig. 1]. [2]

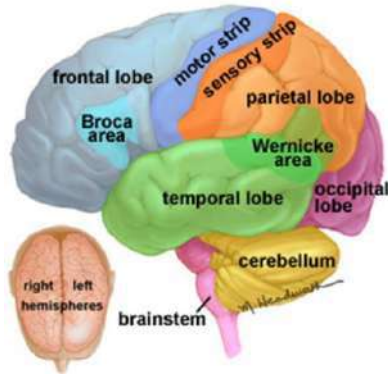


**Fig. 1:** Parts of Human Brain [2].

Cerebral Cortex is further branched into four lobes, which are: frontal, temporal, parietal, and occipital. Functions performed by each lobe are explained in [Table 1]. Further the lobes are again divided to the section that performs some particular functions. These brain cells are very complex in nature. Each lobe of the brain doesn't function alone.

Notice two important areas in cerebrum called sensory strip and motor strip. The sensory strip is in the parietal lobe, near the border of the frontal lobe. The strip is involved in registering sensation that is connected to specific body parts or body functions. Motor strip is located at the frontal lobe and controls all muscle movements including the ones that are necessary for speech.

**Table 1:** Functions performed by different Lobes of Cerebrum

Lobe	Function
Gyrus Lobe	Personality of the user, Behavior of the user, Emotions of the user, Judgment capability, Planning and strategy, Problem Solving capacity.
Parietal Gyrus gland	Interprets the language, Sensitivity, Temperature ( <i>Sensory strip</i> ), Interprets signals from Vision, Hearing capacity etc.
Temporal gyrus Lobe	Memory storing, Hearing capacity, Sequencing and Organization ability
Occipital gyrus Lobe	Memory Storing, Hearing capacity, Sequencing and Organization ability

## ELECTROENCEPHALOGRAPHY

### Basic of EEG

Electroencephalography (EEG) is a technique for continuously monitoring brain's activity. German psychiatrist Hans Berger first observed it in 1924. It involves placing electrodes on the scalp and measuring the electrode potential of each electrode.

Neurons, which are basic building blocks of our nervous system, send their energy or "talk" to one another through tiny spaces called synapse. Whenever a neuron receives a signal, its membrane generates electric potential changes. Generating action potentials along the neuron passes along these signals. This electrical activity always occurs inside a live brain that is whenever there is any sensory, imagery or motor action happening or even during sleep. The electrodes of EEG on scalp detect the weighted effect of this electrical activity of pyramidal cells (i.e. neurons just under the scalp). Being a weighted measurement of many nerve cells, EEG has lower spatial resolution but good temporal resolution.

Measurement system (international 10-20 system)

There are many methods which EEG places electrodes. The standard 10-20 system is usually used to collect the instant EEG. In this method 21 electrodes are specified on the scalp, as shown in [Fig. 4A, 4B]. The positions are as follows: Source points are mansion, that is an apparatus on the nose, aligned with the eyes; and inion. From these references, the skull specifications are calculated in the transverse and median planes [3]. Electrode positions are known by separating these values into 10% and 20% breaks, this is the reason it is called 10-20 systems. Tracing this pattern, we will get the electrode layout as shown in [Fig. 2]

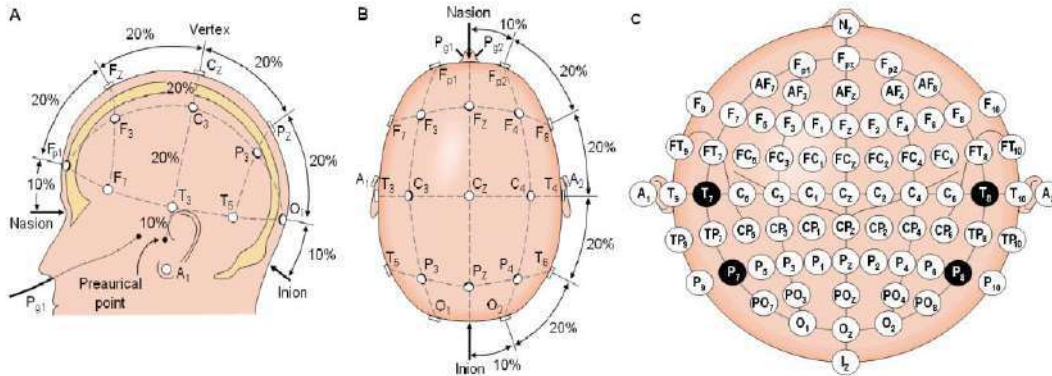


Fig. 2: International 10-20 system Electrode Placement [4].

All the positions and specifications of these electrodes are specified and standardized by the American Electroencephalographic Society. In this diagram the circles containing numbers and letter represent the electrodes. Letter represents the region of brain like F for frontal and C for central and numbers indicate the place. The numbers, which are odd, are on left side and even numbers are on right side. Lower the number means it is close to centerline and center line is represented by letter 'z' indicating zero.

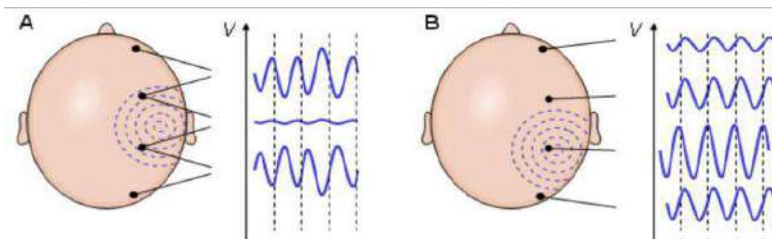


Fig. 3: EEG measurement (A) Bipolar (B) Unipolar [5].

EEG signal strength is very small, in the order of microvolts. Therefore, to increase the signal and noise ratio, we take differential measurement of two electrodes using differential amplifier with high input impedance to remove the common-mode noise. Thus, EEG is relative measurement. The measurement can be bipolar [Fig. 3A] in which the potential drop between a pair of electrodes is mapped or it can be unipolar as shown in [Fig. 3B] in which potential of each electrode is compared either to a neutral electrode or to the average of all electrodes. Frequency spectrum of EEG reveals frequency content of signal. It has bandwidth about 50Hz.

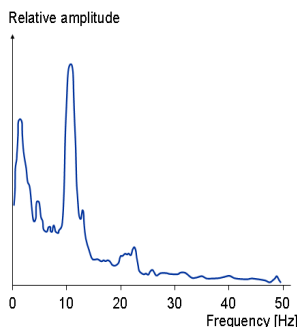


Fig. 4: Frequency Spectrum of typical EEG signal [6].

The bandwidth is further divided to more commonly observed frequency beats, which is further explained in [Table 2].

For example, if we take EEG measurement of person sleeping we will see most of the frequency content will be less than 4 Hz, which is called Delta band. Likewise, we have Theta, Alpha, and Beta mu bands. Note that Mu waves diminish with movement or imagination of movement. We will see later that this property is used in control applications.

**Eeg based bmi system architecture**

Architecture is converted into statement that operates a command in the device. The important point to notice here is that this whole system involves two adaptive controllers i.e. Brain and BMI machine. It is the responsibility of the user to create and maintain a well co-relation between his/her intent and the frequency signal featured employee by the BCI, and the BCI should select and extract the features that the user can control efficiently. [7]

**Table 2:** EEG wave bands [8]

Frequency Location Uses			
Delta ( $\delta$ )	0.5-4 Hertz	Common	Sleeping / coma
Theta ( $\theta$ )	4-8 Hertz	Temporal-lobe & parietal-lobe	All kind of Emotional Stress (Anger, Sadness)
Alpha ( $\alpha$ )	8-13 Hertz	Cerebral-cortex	Visualizing Problem(Hearing, Imagining)
Beta ( $\beta$ )	13-30 Hertz	Parietal and frontal	Increases the amplitude at the time Of intense mental activity
Mu ( $\mu$ )	8-13 Hz	Frontal-lobe (motor cortex)	Diminishes to the behavior that Is preparatory to another behavior

**Output**

Output device can be any controllable machine. The system can be used to answer the yes/no questions or for type processing. It is being used for control objects like wheelchair or can be channel of communication in games or virtual reality. Usually, computer screen is used for visual feedback and the output is the selection of target.

**PRESENT-DAY BMI SYSTEM**

BMI is a highly multidisciplinary field. After its first successful implementation in 1999, that enables the cortical neurons that could directly control a machine manipulator, the field has shown remarkable progress. Given below are few present-day applications and current research trends in BMI technology.

**Visually evoked potentials**

Visually Evoked Potentials (VEP) is type dependent BCI system and uses the concept of evoked potentials. The system detects the EEG patterns in primary visual cortex. Example of such system involves stimulating the user with a light having certain frequency. The EEG signals around visual cortex will have peaks in spectrum at that frequency component and its harmonics. [Fig. 5] shows one implantation. In this application, user faces a screen displaying several virtual buttons that are flashed at different rates. Once the user directs his/her gaze at screen.



**Fig. 5:** Visual Evoked Potentials [9] (Left) EEG Spectrum (Right) Application [10].

THE IIOAB3 JOURNAL

P300 evoked potentials follows the concept of independent BMI. The P300 is a (+ve) deviation on the (EEG).  
Neural Interface Engineering Brain Machine Interface using EEG

FLOW CHART

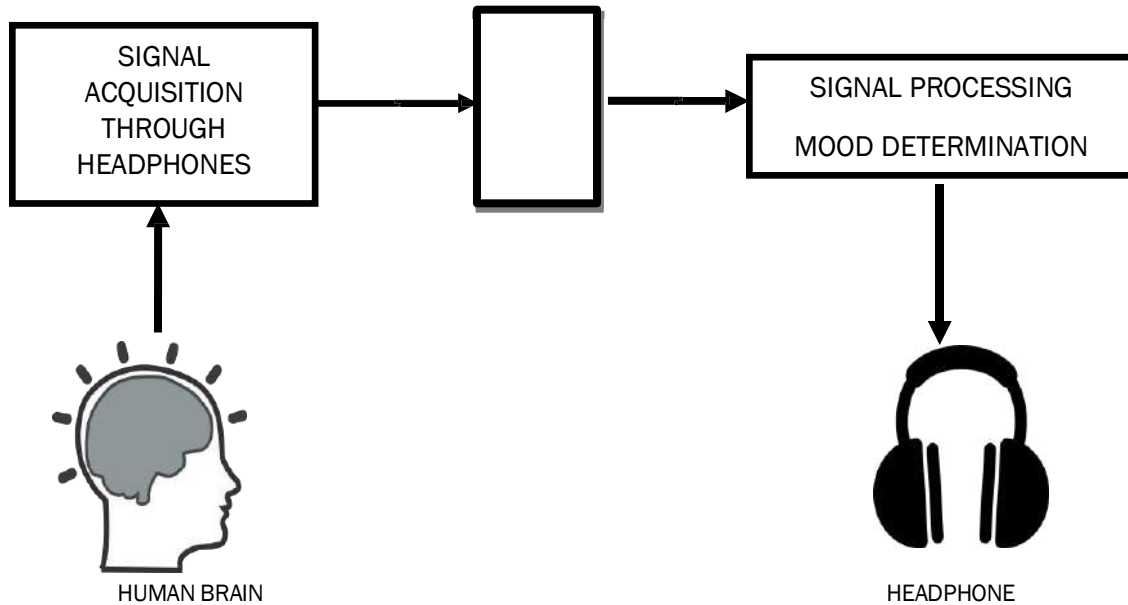


Fig.6: Signal acquisition and processing

As described in Fig-6, the process begins with ‘Signal Acquisition’; the brain electrodes connected to the head of the person through headphones capture the electrical activity from the brain. Signals from the brain once collected are then sent to the ‘Signal Processing’ phase of the process in the mobile application where, the system developed by K. Ishino and M. Hagiwara [12] applying FET, Once the mood of the person is identified it is then compared to the music database, where it determines which type of music would best suited the person’s current mood based on Thayer’s mood classifications.

Algorithms used:

**Principal component analysis:** This idea of the (PCA) Principal component analysis is to reduce the chance of the variables and the data sets, which co-relates, (high or low), assessing the data from the data sets, it is extent to the maximum. This can be done by the transforming the data sets into variables, which are known as the principal components (or simply, the PCs) and are orthogonal. This is the way to retain the data sets and to use it. The principal are components are the Eigen-vectors of a co-variance matrix, and hence they are orthogonal. The results are also sensitive to the relative scaling. The PCs are essentially the linear combinations of the original variables, the weights vector in this combination is actually the Eigen-vector found which in turn satisfies the principle of least squares.

- PCs are already discussed.
- As we move to the 1st PC to the last PC the variation present at it decreases and with it the importance, the unwanted PCs are sometime important in the regression, outlier and detection.

Wavelet transform:

**CWT:** The Continuous Wavelet Transform transforms a continuous signal into highly redundant signal of two continuous variables: 1. translation and 2. Scale. The resulting is the transformed signal, the signal is easy to interpret and valuable for time frequency analysis.

**DWT:** The Discrete Wavelet Transform has become a powerful technique in biomedical signal processing. It can be written on the same form as (1), which emphasizes the close relationship between

CWT and DWT. The most obvious difference is that the DWT uses scale and position values based on powers of two.

**Table 3:** Moods classifies according to musical components [13]

Feeling	Power	Sound	Tone	Rhythm
<b>Cheerful</b>	Average	Average	Extreme	Extreme
<b>Exuberant</b>	Excessive	Average	Excessive	Excessive
<b>Energetic</b>	Extreme	Average	Average	Excessive
<b>Frantic</b>	Excessive	Extreme	Little	Extreme
<b>Depressed</b>	Average	Extreme Low	Extreme Low	Little
<b>Sorrow</b>	Little	Little	Little	Little
<b>Calm</b>	Extreme Low	Extreme Low	Average	Extreme Low
<b>Contentment</b>	Little	Little	Excessive	Little

Many other algorithms and technique can be used to make this system more accurate and efficient. At last the songs are played from a large library of songs matching the mood of the person and making him feel better.

### CONCLUSION

Brain Machine interface is very interesting field which gives us chance to expand the capabilities of human brain, potential to bring science fiction into reality. EEG based BMI systems are the hope for severely and partially paralyzed patients in that one day they do the basic communications and the motor control, it helps in the communication process with the brain. It holds the promise of bringing sight to the blind, hearing to the deaf and words to unspoken emotions, even increasing the level of interaction between human and machine. We will add more features like changing the color of headphones depending on the state of the user in addition to that we can also try to determine the type of music which helps the human brain to lessen the effect of stress.

### CONFLICT OF INTEREST

There is no conflict of interest.

### ACKNOWLEDGEMENTS

We would like to sincerely bring our kind gratitude to the Research Co-coordinators of Accendere CL Educate Ltd. for helping and guiding us in this paper formation.

### FINANCIAL DISCLOSURE

None.

### REFERENCES

- [1] Kaku M. [2015] The Future of the Mind: The Scientific Quest to Understand, Enhance, and Empower the Mind, New York: Anchor Books. 722.
- [2] Mayfield Brain and Spine, Anatomy of Brain, [Online]. Available: <https://www.mayfieldclinic.com/PE-AnatBrain.html>.
- [3] Advanced Biometric Research Center, EEG for Noninvasive BCI, [Online]. Available: <http://abrc.snu.ac.kr/korean/files/bci02.pdf>.
- [4] Brain-Computer Interfaces: A Gentle Introduction ll Bernhard Graimann, Brendan Allison, and Gert Pfurtscheller.
- [5] Malmivuo J, Plonsey R. [1995] Bioelectromagnetism - Principles and Applications of Bioelectric and Biomagnetic Fields, New York: Oxford University Press.
- [6] Wolpaw JR, Birbaumer N, McFarland DJ, Pfurtscheller G, Vaughan TM. [2002] Brain-computer interfaces for communication and control, Clinical Neurophysiology. 113:767-791.
- [7] Lotte F, Bougrain L, Clerc M. [2015] Electroencephalography (EEG)-based Brain- Computer Interfaces, in Wiley Encyclopedia of Electrical and Electronics Engineering, Wiley. 44.
- [8] Pfurtscheller G, Silva FLD. [1999] Event-related EEG/MEG synchronization and desynchronization: basic principles, Clinical Neurophysiology. 110:1842-1857.
- [9] ASPEN Lab (Old Dominion University), BCI Control of a Motorized Wheelchair for Disabled Individuals using a calibrationless [Online]. Available: <https://www.youtube.com/watch?v=qhK572LJhSc>.
- [10] Dornhege G, Millán JDR, Hinterberger T, McFarland DJ, Müller KR. [2007] Toward Brain-Computer Interfacing, Cambridge MA, MIT Press. 14-15.



- [11] Cobb WA. [1983] Recommendations for the practice of clinical neurophysiology., Elsevier.
- [12] Ishino K, Hagiwara M. [2003] A Feeling Estimation System Using a Simple Electroencephalograph, Proc. of the IEEE, International Conference on Systems, Man and Cybernetics. 4204-4209.
- [13] Bhat ASVSAS, Prasad N, Mohan DM. [2014] An efficient classification algorithm for music mood detection in western and hindi music using audio feature extraction. 2014 Fifth International Conference on Signal and Image Processing. 359-364. DOI: 10.1109/ICSIP.2014.63.

## ARTICLE

## A NOVEL SMART GARBAGE SYSTEM FOR SMART CITY

Vaishnavi Gupta<sup>1</sup>, Divyanshu<sup>1</sup>, Shweta Sharma<sup>1</sup>, Prateek Jain<sup>2\*</sup><sup>1</sup>Faculty of Engineering & Technology, Department of Computer Science, Manav Rachna International Institute of Research & Studies, Faridabad, INDIA<sup>2</sup>Accendere CL Educate. Ltd, New Delhi, INDIA

## ABSTRACT

This is generally seen that garbage bins are placed at various public places in the cities to reduce the amount of garbage thrown on the streets, due to increase in the waste every day; it creates unhealthy condition for the people and creates bad smell around the surroundings. It also leads to many diseases and human illness. So to avoid this, smart bin system is proposed in this paper which will intimate the amount of garbage level through the tags placed on the smart bins called as RFID technology. RFID is used to intimate the storage capacity of smart bin. It may also be responsible for the type of waste to be managed either biodegradable or non-biodegradable. Garbage management system is the main issue in the field of Internet of things. The absence of efficient waste management has caused serious environment problems and cost issues. Smart bin includes plasma decomposition process, in which plasma decomposes all the waste and converts it into syngas. This is new technology of decomposing waste when the smart bin is full of garbage and reaches its threshold value then the sensors will send the notification to the lid to close and it will notify plasma to start its functioning and starts decomposing the waste and then gasoline air converter further converts the syngas into fuel (natural gas). Plasma torches are used in many machines works. This paper includes the new garbage management system.

## INTRODUCTION

The improper disposal of waste has a serious and dangerous impact on many areas. Garbage thrown in the street or in open spaces creates a problem for the people to survive; it stinks and also spread diseases. Non-biodegradable materials thrown into open drains make their way into the sewerage system, it clogs pipelines and damages infrastructure. The hazards posed by the removal of industrial waste are even greater, with the release of pathogens and toxic compounds harmful not just to human life but also to plants and animals. Garbage dumped in the countryside ruin the landscapes and unique habitats of flora and fauna are lost. [1]. The traditional way of manually monitoring the wastes in waste bins is a complex, cumbersome process and utilizes more human effort, time and cost which is not compatible with the present-day technologies. So new methods are required to introduce to reduce garbage waste and this can be done technically.

In this paper analytics is integrated in order to create optimal changes in the conventional methodology of waste collection with the large amount of data that is being produced by the smart bin networks. The movement of waste across the whole city can be tracked and thus can be monitored by a system efficiently and concretely. This system can prove to be a revolution for the whole urban waste management system of upcoming smart cities. A technology named Zigbee GSM (), that enables the remote monitoring of solid waste bin in real time and which will inform the authorized person when the garbage bin is about to fill. These technologies are good enough transport monitoring management facilities and storage waste collection. It does not have any user interaction site like websites and android application, and that's why RFID is used to detect the tags and aware the people in their android application. [2].

Smart bin also describes the application of managing waste collection system of an entire city. The sensors enabled smart bins generate a large amount of data, which is further analyzed to see the condition of waste disposal and notify when the garbage is at its threshold value. It is difficult to implement in large cities. The IR sensor placed inside the trash sense the level of trash and there are another sensor will sense the amount of toxic gases. Once the trash is filled, notification is send. The RFID placed inside the trash will intimate about the overflowing of trash. Some researchers proposed that there are many dustbins located throughout the city or the campus, these dustbins are provided with which helps in tracking the level of the garbage bins and a unique ID will be provided for every dustbin in the city so that it is easy to identify which garbage bin is full. Tags are placed to detect the dustbins. When the level reaches the threshold limit, the device will transmit the level along with the unique ID provided [3, 7]. The concerned authorities can help us in making the people aware about the smart bin.

Problems with existing smart bins: -

- Overflowing of bins
- Bacteria, insects and vermin thrive from garbage Air pollution and respiratory diseases
- Contaminates surface waters, which affects all ecosystems

Direct handling of overflowing waste exposes for health risks inefficient waste control is bad for municipal well being

Received: 24 Mar 2019  
Accepted: 13 May 2019  
Published: 16 May 2019

\*Corresponding Author

Email:  
prateek.jain@accendere.co.in

## INTERNET OF THINGS

The internet of things is the network of devices, which allows things to connect, interact and exchange data. Internet of things (IOT) involves extending internet connectivity beyond standards devices, such as desktops, laptops, smart phones and tablets, to any range of traditionally dumb or, non- internet- enabled physical devices and everyday objects, these devices can communicate and interact over the internet, and they can be remotely monitored and controlled. It connects things with internet and data can be exchanged within the systems. The entire network-based technologies need IOT to share information required.

### Architecture of IOT

The bottom most layers consist of your devices and things which include the plasma torches which can be used to decompose all the waste material and converts it into syngas. The functioning of garbage bin starts from here, on the top of the device there is a layer called device communication layer, devices can communicate with each other or upper layers using this layer. This communication layer communicates in the way it sense the amount of garbage present in the garbage bin. And when it crosses its threshold value it starts its functioning. It warns plasma torches to function and decompose as fast as possible. The third layer is the aggregation layer. A message will be sent here. There is an aggregation layer between the garbage waste which is not decomposed and the garbage waste which is decomposing and which is in the process. And event processing layer is very important component and this is generally cloud. The data can be stored, analyzed and processed here. So in garbage system the event processing layer will the RFID (Radio frequency identification), which is used to track various objects. So it is used in tracking the garbage bins at what distance the garbage bin is placed and it is connected through an android application which will help us in tracking the bin by code which is placed on the garbage bin. It also ensures at what level the garbage bin is full and the storage capacity of the garbage bin [4] [8]. And these are how human can be connected through applications. The top most layers are the external communications layer, a human being can communicate with the devices using this layer, and this may be with the help of dashboard and apps. In this how human being can communicate with the devices through their mobile phones and by throwing garbage in the dustbins. This is to identify who all hare accessing the data and if they have the permission to do so. Management needs to check whether the device is working properly or not. And the syngas which is produced can be reformed and converted into fuel so that it can be used further by many industries. The gas is transferred into another chamber in which gasoline air converter helps in converting the syngas into fuel (natural gas) [5]. An IOT architecture has been shown in Fig 1.

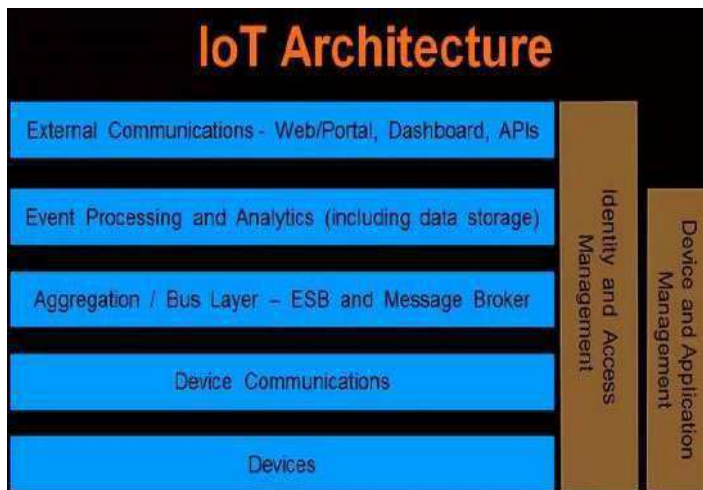


Fig. 1: IOT architecture

### Advantages of IOT

**Environmental monitoring-** It measures the amount of water and the soil which is required for the better plant growth. It warns the people about the disasters and prevent damages and can helps in pre-precautions need to be taken. It can also detect the amount of garbage thrown and can reduce it. It helps in maintaining the environment clean.

**Infrastructure management-** It is useful for tracking if there is any problem in urban or rural infrastructure such as bridge, railway to reduce risk of danger and any failure in strength would be cured.

**Industrial applications-** They investigate the quality of product in order to check whether product fulfil the demands of the customer and is gaining much in the market.

**Energy management-** Energy management is how the energy consumption can be reduced when connected with the internet and reduce power consumption such as cloud based, remote control for oven, lamp and etc. [6].

**Medical and healthcare Systems-** Healthcare systems help to improve patient state better by monitoring and controlling their heart rate or blood pressure or even for their diet. IOT helps in improving health of the patient as soon as possible.

**Building and home automation-** It maintains the appliances such as air condition, security lock lightening, heating, ventilation, telephone system, TV to make a comfort, secure, with low energy consumption [11].

## APPLICATIONS OF IOT

**Smart home:** Smart Home has become the revolutionary ladder of success in the residential spaces and it is predicted Smart homes will become as common as smartphones. The cost of owning a house is the biggest expense in a homeowner's life. Smart Home products are promised to save time, energy and money. With Smart home companies like Nest, Ecobee, Ring and August, to name a few, will become household brands and are planning to deliver a never seen before experience. For example, Amazon Cloud Cam, LixMini Wi-Fi Smart Bulb, Ecobee4 etc. Fig 2 depicts the smart home.

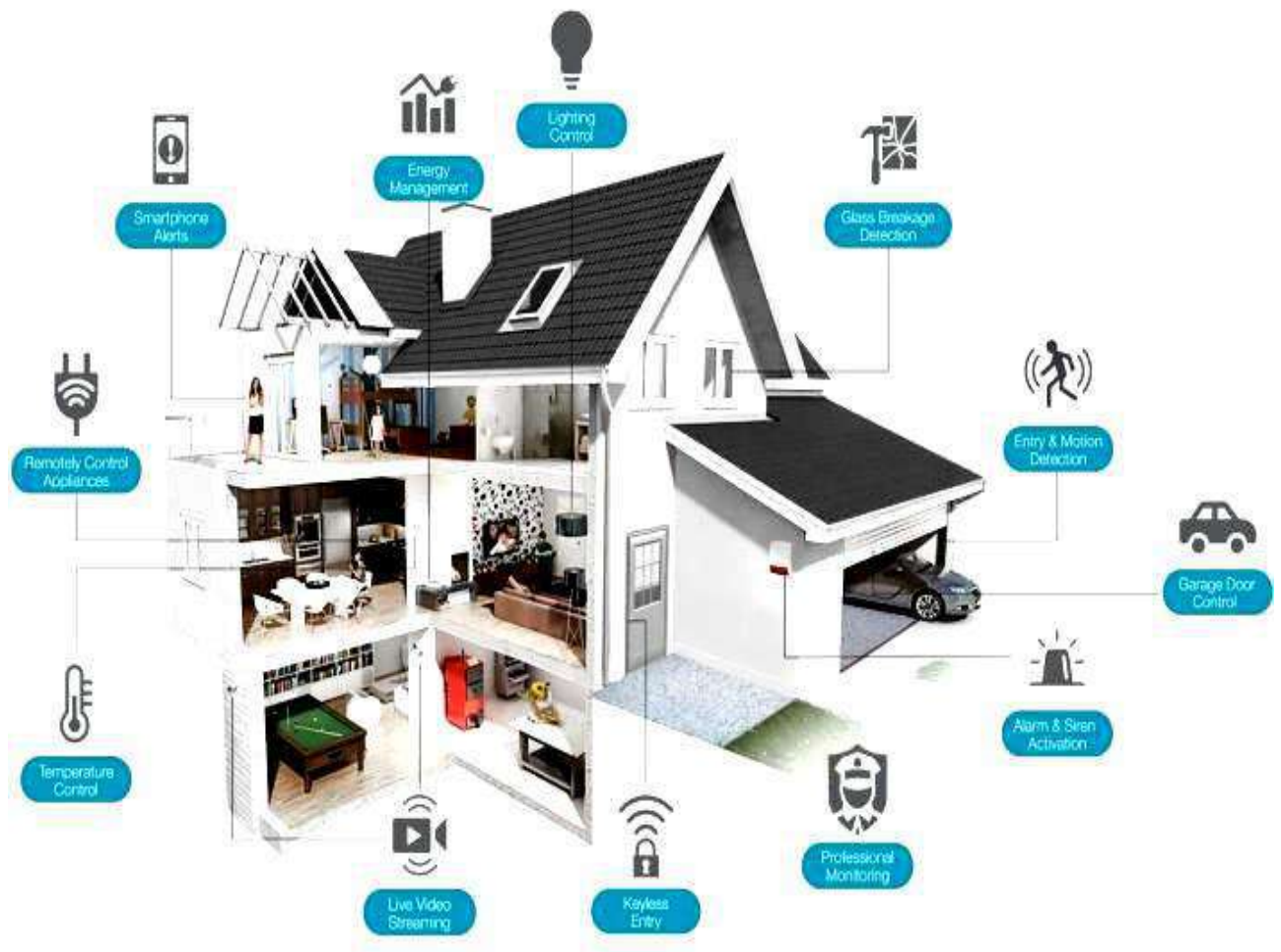


**Fig. 2:** Smart Home

**Wearables:** Wearable devices are installed with sensors and software's which collect data and information about the users. This data is later pre-processed to extract essential insights about user. These devices broadly cover fitness, health and entertainment requirements. The pre-requisite from internet of things technology for wearable applications is to be highly energy efficient or ultra-low power and small sized. For example, Samsung Gear Fit2. Fig 3 shows the typical smart watch based on an IoT mechanism.





Fig. 3: Smart Watch

**Connected cars:** The automotive digital technology has focused on optimizing vehicles internal functions. But now, this attention is growing towards enhancing the in-car experience. A connected car is a vehicle which is able to optimize it's own operation, maintenance as well as comfort of passengers using onboard sensors and internet connectivity. Most large auto makers as well as some brave startups are working on connected car solutions. Major brands like Tesla, BMW, Apple, Google are working on bringing the next revolution in automobiles. Fig 4 denotes the concept of smart cars.



Fig. 4: Smart cars

**Industrial internet:** Industrial Internet is the new buzz in the industrial sector, also termed as Industrial Internet of Things (IIoT). It is empowering industrial engineering with sensors, software and big data analytics to create brilliant machines. According to Jeff Immelt, CEO, GE Electric, IIoT is a “beautiful, desirable and investable” asset. The driving philosophy behind IIoT is that, smart machines are more accurate and consistent than humans in communicating through data. And, this data can help companies pick inefficiencies and problems sooner. IIoT holds great potential for quality control and sustainability. Applications for tracking goods, real time information exchange about inventory among suppliers and retailers and automated delivery will increase the supply chain efficiency. According to GE the improvement industry productivity will generate \$10 trillion to \$15 trillion in GDP worldwide over next 15 years. The traditional usage of industrial internet is being shown in Fig 5.



Fig. 5: Industrial Internet



**Smart cities:** Smart city is another powerful application of IoT generating curiosity among world's population. Smart surveillance, automated transportation, smarter energy management systems, water distribution, urban security and environmental monitoring all are examples of internet of things applications for smart cities. IoT will solve major problems faced by the people living in cities like pollution, traffic congestion and shortage of energy supplies etc. Products like cellular communication enabled Smart Belly trash will send alerts to municipal services when a bin needs to be emptied. By installing smart sensors and using web applications, citizens can find free available parking slots across the city. Also, the sensors can detect meter tampering issues, general malfunctions and any installation issues in the electricity system. A typical smart city mechanism/design is being depicted in Fig 6.



Fig. 6: Smart cities

**Smart retail:** The potential of IoT in the retail sector is enormous. IoT provides an opportunity to retailers to connect with the customers to enhance the in-store experience. Smartphones will be the way for retailers to remain connected with their consumers even out of store. Interacting through Smartphones and using Beacon technology can help retailers serve their consumers better. They can also track consumers path through a store and improve store layout and place premium products in high traffic areas. Fig 7 shown the concept of Smart Retail chain.



Fig. 7: Smart Retail

### PROPOSED WORK

The problem nowadays is about litter of garbage around the streets when the garbage is full. And due to this there are many diseases that occur, so to prevent the losses Smart bin is introduced. The proposed system is about smart garbage in which the garbage gets decomposed by using plasma and gets converted into syngas which further purified as natural gas and released in atmosphere. To deal with the

problem of waste disposal a system was proposed to identify the waste products to be thrown and these could be differentiated as, plastic garbage bags, chips and stickers. The followings are used in the proposed system.

### RFID- Radio frequency identification

RFID is used to identify and track tags attached to objects. The tags contained information stored in it. Active tags have a local power source and RFID can be operated from a distance from the RFID reader. RFID is one method for automatic identification and data capture, RFID is used to aware the person that the smart bin is at its threshold value and cannot store more garbage and storage capacity is limited.

RFID system is made up of two things- a tag and a reader. RFID tags include a transmitter and a receiver. The RFID component on the tags has two parts- a microchip that stores information, and an antenna to transmit a signal. To read the information encoded on a tag, a two-way radio transmitter-receiver called an interrogator emits a signal to the tag using an antenna. The interrogator will then transmit the read results to an RFID computer program [9, 10].

There are two types of tags- passive and battery powered. A passive RFID tag will use the interrogators radio wave energy to interrogate. A battery powered RFID tag is embedded that powers the relay of information. In an RFID- based garbage collection system, an RFID collection bin includes a communication module to communicate with a central server, automatic garbage entrance, and a scale function to measure the weight of the food waste. However, the collection bin communicates only with a server [15].

### Plasma

Plasma is a state of matter. Plasma is created by ionization process by adding energy to a gas so that some of its electrons leave its atoms. The results are negatively charged (electrons), and positively charged (ions). The charged particles in plasma react strongly to electric and magnetic fields. If plasma loses heat, the ions will re-form into a gas, and emits the energy which had caused them to ionize. Plasma is found in stars. It requires very high temperatures to break the bonds between electrons and the nuclei of the atoms.

A plasma waste converter is a plasma torch applied to garbage which converts the garbage waste into syngas and the syngas can be used further in the form of fuel in the industries. A plasma torch uses a gas and powerful electrodes to form plasma. The temperatures generated by a plasma torch are hotter than the surface of the sun. Molecules break down in molecular dissociation. When molecules are exposed to intense energy, the molecular bonds holding them together break apart. Only elemental components of the molecules are left [13].

Organic molecules become volatilized, or turn into gases. This syngas can be used as a fuel. Inorganic compounds melt down or converted into a glassy substance. Metals melt down and combine with the inorganic matter called as slag. The heat evolved from plasma converters causes pyrolysis. It is a process in which organic matter breaks smaller compounds and decomposes. Plasma torches can operate in airtight vessels also. [12].

Plasma waste converters can convert almost any kind of waste. It can treat medical waste or contaminated waste and gases and slag are left as residue. The waste breaks down in basic elements; they can be disposed of safely. A plasma converter can break down every type of waste but can't break down heavy radioactive material, such as the rods used in a nuclear reactor. If you put such material in a plasma furnace, it would catch on fire or even explode.

### Workstation

Conveyor system- garbage is loaded on the conveyor and is pushed into the furnace

Pre-treatment mechanism- Pre-treatment process is required for efficient working of plasma torch.

Furnace- furnaces have an airlock system which allows garbage to come in and prevent the hot gases in the furnace from escaping into the atmosphere.

Plasma torch- the plasma torches used in these facilities are custom-built.

Slag drainage and afterburners- molten slag pools at the bottom of the furnace and it maintains the high temperature inside the gasification chamber.

Gas ventilation- the furnace also has a vent system to allow gasifier components to pass into another part of the system.

Afterburner- gases can pass through a secondary chamber [14]. These extremely hot gases then pass through a heat recovery steam generator system where they heat water to form steam.

Syngas cleaning- e gases from the furnace enter a chamber where they are cooled. The gases pass through a spray of water, which scrubs the gases of pollutants.

#### Components of smart garbage bin:

- Bottom layer at which lid is placed which collects all the waste required for decomposing and plasma torches are placed in the same layer which decompose the same waste side by side. The devices are found in this layer.
- Another component is layer which is present at the top called as device communication layer, at this layer sensors are present used to detect the amount of garbage stored, and it ensures when the garbage cross its threshold value the sensors sends the notification to close the lid and starts functioning of plasma.
- There is another chamber where decomposition of garbage takes place and plasma converts it into syngas and then gasoline air converter converts syngas into fuel.
- Aggregation layer is the third component which separates the waste which is yet to be decomposed and the waste which is being decomposed by plasma.
- The topmost layer is the garbage collection layer. It is the external communication layer, where humans can communicate with the device through the app. It notifies them about the storage capacity of the bin.
- Then is one more layer named as event processing layer, ensures about the usage of RFID. The tags placed on the smart bin can easily track the bin and notify about the bin [17].
- Another chamber attached to the dustbin is gasoline air converter which converts syngas into fuel (natural gas) which can further be used in industries.

#### Tools/equipment required:

- Garbage container in which garbage is thrown
- Two Sensors (one at upper lid one at lower lid) are used to detect the threshold value up to which garbage bin is full
- RFID is used to detect the dustbin with the help of tags placed on the bin and notify about the amount of garbage stored in it.
- Two lids are used. (One on the top of the bin which is half open and half closed, and another on the third most layer of the garbage bin to open and start functioning [16].
- Plasma torches
- Gasoline air converter

### SYSTEM DESIGN OF PROPOSED SMART DUSTBIN

A smart bin is created which works on RFID technology and also made up of high-tech materials which do not get melt through plasma. The waste is decomposed and converted into natural gas. This has been introduced before but now this can be used in the form of smart bin [18]. Garbage thrown in the smart bin can be toxic and non- toxic, plasma convert all types of waste into gas and also helps in decrease of diseases. Smart bin is automatic and works on neural networks technology. An app is created which can function all the automatic operations of smart bin. Sensors can be introduced which can sense the amount of garbage around the surrounding. The automatic functioning of the smart bin makes sure when the lid is open or closed. The proposed mechanism/idea of smart garbage bin in shown in Fig 8 in the form of flowchart and its corresponding parts/components is shown in Fig 9.

#### WORKING

The bottom most layers consist of the devices and things which include the plasma torches which can be used to decompose all the waste material and converts it into syngas. The functioning of garbage bin starts from the top most layer where there is a cover lid present on the top of the dustbin which usually remains closed so that it does not stink. There will be a small opening on the cover so that the garbage should be thrown from that. When the bin gets full and as the garbage gets above the marked level the sensor attached to the upper lid sends signal to lower lid and the lower lid gets open, the garbage from the upper chamber moves to the lower chamber where decomposition takes place through plasma beam which is attached in the lower most level [19]. The decomposed garbage gets converted into syngas which flows to the third chamber in which the gas is transformed into fuel. Syngas is composed of hydrogen and carbon monoxide and gasoline air converter converts the syngas into fuel which can be used for further purposes in many industries.

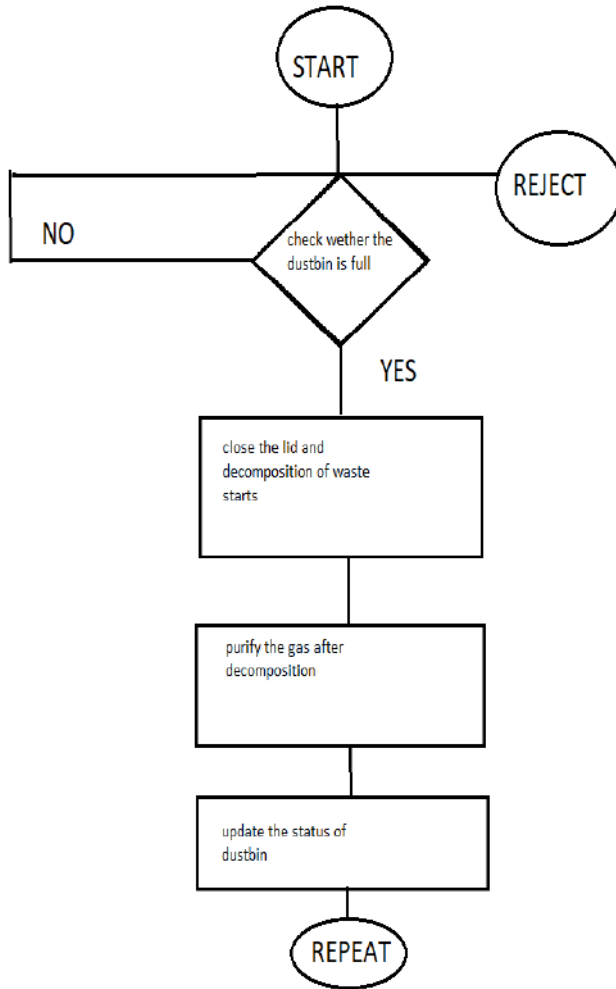


**Fig. 8:** Flowchart of Smart garbage bin

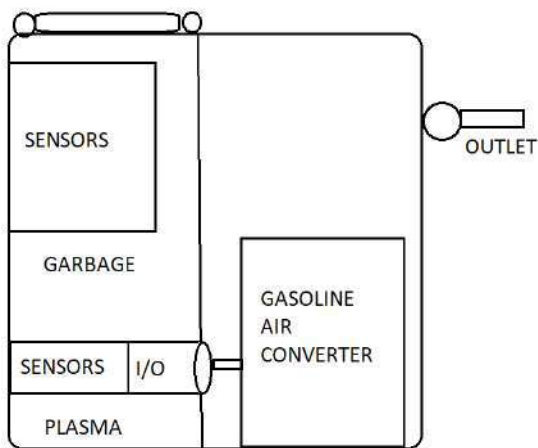


**Fig. 9:** Smart Garbage Bin

### BENEFITS OF PROPOSED DUSTBIN

- Keeps the environment clean and fresh: The greatest advantage of waste management is keeping the environment fresh and neat.
- Reduces environmental pollution: Waste management not only eliminates the surrounding waste, but also will reduce the intensity of the greenhouse gases which is emitted from the wastes accumulated. The gas converter will convert these gases into non-toxic gases.



- Reduces human workload: As everything is automatic the human effort in waste disposal is reduced and burning of waste is avoided which in return affects the environment.
- Time saving: It takes only few minutes to decompose the garbage present in the dustbin
- Reduces cost: So much money wasted in waste disposal and still not disposed of correctly is reduced with our smart dustbins as it is only one time investment.
- Conserves land: The large acres of land wasted and destroyed in just for waste disposal can be conserved using smart bins [20, 21, 22].

## CONCLUSION

As we know that India comes at third position in pollution and garbage mismanagement, so to avoid this we introduce smart bin which on sensing the threshold value of garbage decompose it automatically and can reduce littering of waste products and materials. The data collected from various surveys noticed that most of the garbage waste do not get decomposed and left as a residue which cannot be recycled. Plasma converters may be used to convert the garbage waste into syngas. The syngas is evolved in the form of hydrogen and carbon monoxide. As in various industries gasoline air converters are used which converts syngas into fuel (natural gas). The smart bin also does have the capability to sense the amount of garbage present in the surroundings. This may have great impact in the environment, diseases can be reduced to an extent and this can be used in routine purposes. Having such a huge mountain of garbage collected from various places in Delhi can also have the solution to the problem. And the gas which is evolved gets converted by the gasoline air converter into fuel which can also be used in the environment. This would also help in reducing the amount of diseases.

### CONFLICT OF INTEREST

There is no conflict of interest.

### ACKNOWLEDGEMENTS

None.

### FINANCIAL DISCLOSURE

None.

## REFERENCES

- [1] Shrivastava A, Harshitha R. [2017] Smart Parking: Green IoT for Smart City. Asian Journal of Applied Science and Technology (AJAST) 1.5: 86-90.
- [2] Hong, I, et al. [2014] IoT-based smart garbage system for efficient food waste management. The Scientific World Journal.
- [3] Kalpana M, Jayachitra J. [2017] Intelligent Bin Management System for Smart City using Mobile Application. Asian Journal of Applied Science and Technology (AJAST) 1.5:172-175.
- [4] Sharma N, Singha N, Dutta T. [2015] Smart bin implementation for smart cities. International Journal of Scientific & Engineering Research 6.9:787-791.
- [5] Cuff D, Hansen M, Kang J. [2008] Urban sensing: out of the woods. Communications of the ACM. 51(3):24-33.
- [6] Kalpana M, Jayachitra J. [2017] Intelligent Bin Management System for Smart City using Mobile Application. Asian Journal of Applied Science and Technology (AJAST) 1.5:172-175.
- [7] Chowdhury B, Chowdhury MU. [2007] RFID- based real-time smart waste management systems, in processing of the Telecommunication Networks and Applications Conference. 175-180.
- [8] Kelly SDT, Suryadevara NK, Mukhopadhyay SC. [2013] towards the implementation of iot for environmental conditions monitoring in homes, IEEE sensors journal. 13(10):3846-3853.
- [9] Li X, Lu R, Shen X, chen J, Lin X. [2011] Smart community: an internet of things application, IEEE communications Magazine. 49(11):68-75.
- [10] Vakali A, Leonidas A, Srdjan K. [2014] Smart Cities Data Streams Integration: experimenting with Internet of Things and social data flows. Proceedings of the 4th International Conference on Web Intelligence, Mining and Semantics (WIMS14). ACM.
- [11] Gama K, Touseau L, Donsez D. [2012] Combining heterogeneous service technologies for building an internet of things middleware, Computer communications. 35(4):405-41.
- [12] Foschini L, Taleb T, Corradi A, Bottazi D. [2011] M2M-based metropolitan platform for IMS-enabled road traffic management in IOT, IEEE communications magazine. 49(11):50-57.
- [13] Jara AJ, Zamora MA, Skarmeta AFG. [2011] An internet of things- based personal device for diabetes therapy management in ambient assisted living (AAL), personal and ubiquitous computing. 15(4):431-440.
- [14] Tozlu S, Senel M, Mao W, keshavarzian A. [2012] Wi-Fi enabled sensors for internet of things: a practical approach, IEEE communications magazine. 50(6):134-143.
- [15] Touafek K, Haddadi M, Malek A. [2011] Modeling and experimental validation of a new hybrid photovoltaic thermal collector, IEEE transactions on energy conversion. 26(1):176-183.
- [16] Muller I, De R, Brito, Pereira CE, Brusamarello V. [2010] Load cells in force sensing analysis- theory and a novel application, IEEE Instrumentation and measurement magazine. 13(1):15-19.
- [17] Pratheep P, Hannan MA. [2011] Solid waste bins monitoring system using RFID technologies, Journal of applied sciences research. 7(7):1093-1101.
- [18] Zanella A, et al. [2014] Internet of things for smart cities." IEEE Internet of Things journal 1 (1): 22-32.
- [19] Postscape: www.postscapes.com/smart-trash/
- [20] Ashton, Kevin. [2009] That 'internet of things' thing. RFID journal 22.7:97-114.
- [21] Dubey A, et al. [2018] A Detailed Study of Digital Image Processing. The IIOAB Journal, Vol 9(2):33-42.
- [22] Sagar D, et al. [2018] Studying open source vulnerability scanners for vulnerabilities in web applications, The IIOAB journal Vol 9(2): 43-49.



## ARTICLE

# TOWARDS THE MODERNIZATION OF SMART TRAFFIC LIGHTNING USING IOT

Megha Verma<sup>1</sup>, Ridhima Ohri<sup>1</sup>, Simran Kaur<sup>1</sup>, Sunita Virmani<sup>1</sup>, Prateek Jain<sup>1,2\*</sup>

<sup>1</sup>Faculty of Engineering and Technology, Department of Computer Science & Engineering, Manav Rachna International Institute of Research & Studies, Faridabad, INDIA

<sup>2</sup>Accendere CL Educate Ltd, New Delhi, INDIA

## ABSTRACT

In the present scenario of smart city, explicitly in the modern and market zones, the traffic situation is much clogged more often especially at the pinnacle time of business hours. Because of expanding development of populace and vehicles in smart and metropolitan urban areas individuals are confronting a ton of issue at the significant traffic purposes of the business towns. It causes delays as well as it adds to ecological contamination just as different well-being perils because of contamination brought about by vehicle speeding. To avoid such extreme issues numerous brilliant urban networks are connect presently executing keen traffic control structures that chip away at the benchmarks of traffic computerization with counteractive action of the recently referenced issues. In this paper, we have contemplated and thought about the conventional and the sharp traffic control framework, their different favorable circumstances and impediments. We likewise did some examination into different urban communities worldwide where the sharp traffic control framework has been embraced and their prosperity proportions. Moreover, we investigated the urban areas in India where this idea is a generally new one with more accentuation and contextual investigation on the smart traffic control framework received in Bhubaneswar, the parts utilized, the deformities in it and based on this paper, we mean to amend the imperfections in this rush hour gridlock control framework.

## INTRODUCTION

The conceptualization of Smart City varies from city to city and country to country, depending on the level of development, willingness to change and reform, resources and aspirations of the city residents. In the imagination of any city dweller in India, the picture of a smart city contains a wish list of infrastructure and services that describes their level of aspiration. The urban planners aim at developing the entire urban eco-system, which is represented by the four pillars of comprehensive development-institutional, physical, social and economic infrastructure. The core infrastructure elements in a Smart City would include: sufficient water supply, guaranteed power supply, sanitation, including strong waste administration, effective urban versatility and open transport, reasonable lodging, particularly for poor people, vigorous IT availability and digitalization, great governance, particularly e-Governance and native cooperation, feasible condition, well-being and security of residents, especially ladies, kids and the old, and wellbeing and training. As needs be, the motivation behind the Smart City Mission is to drive economic growth and improve the personal satisfaction of individuals by empowering neighborhood and tackling innovation that prompts smart results.

## INTERNET OF THINGS

### Evolution of IoT

IOT is a network of devices, buildings, vehicles and other physical objects embedded with sensors that transmit the valuable data between a company and the consumer. The purpose of all this communication between the two is to provide consumers smarter products and services, a better customer experience, and for businesses a competitive edge and ability to build revenue. The evolution of IOT took place since 1999 to till date. The evolution of an IoT has been shown in Fig 1.

## ARCHITECTURE OF IOT

With the use of IoT, things in the physical world (i.e. the IoT devices or objects) interact with the virtual world (cloud services, platforms and various applications) through a communication network which enables exchange and sharing of information with each other. So, an IoT system comprises of the physical world, virtual world and a communication network and these three are most importantly the basic blocks of an IoT system.

**Things** - With Internet of things, any item that has a special personality in the physical world or in the realm of data which can be coordinated in correspondence is called 'Thing'. The Things can be of two kinds' physical things and virtual things. The physical things are commonly the IoT devices and the virtual things can be the cloud administration arrangements like programming applications, APIs and application arrangements that trade and procedure information in their own position. The most well-known case of physical things can be a temperature sensor. A temperature sensor is associated with a correspondence organize through a controller and after that it is utilized for gathering and sharing the dynamic data about the ongoing temperature of the earth.

### KEY WORDS

IoT, Smart-cities, Censors, ATSC System

Received: 20 Mar 2019  
Accepted: 11 May 2019  
Published: 17 May 2019

\*Corresponding Author

Email:

prateek.jain@accendere.co.in

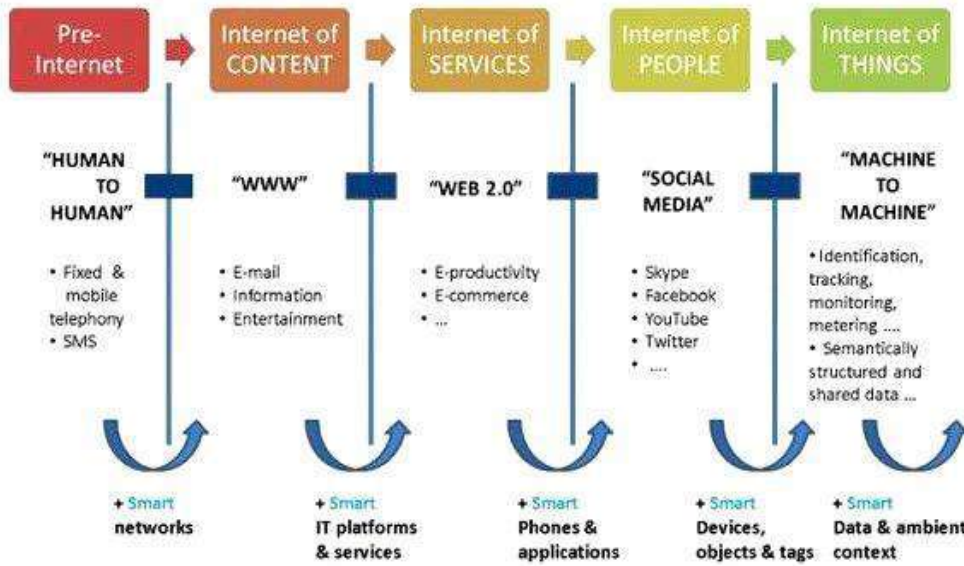


Fig. 1: Evolution of IoT

**The physical world** - The physical world in an IoT framework is an accumulation of physical things or devices. These physical things or devices are worked around controllers or processors with of include IOT sheets. These devices are fit for detecting, gathering, putting away, sharing and handling data and are likewise fit for working at least one actuators to affect in reality.

**The virtual world** - The virtual world in IoT alludes to the gathering of virtual things. These virtual things are by and large Internet, cloud or versatile applications, APIs or application stages. The virtual things additionally assume a noteworthy job in information logging, information mining and investigation in an IOT framework.

**Communication system:** The correspondence organizes a connection that permits communication between the physical world and the virtual world.

IoT has a basic four tier architecture and following are the layers as denoted in Fig 2:

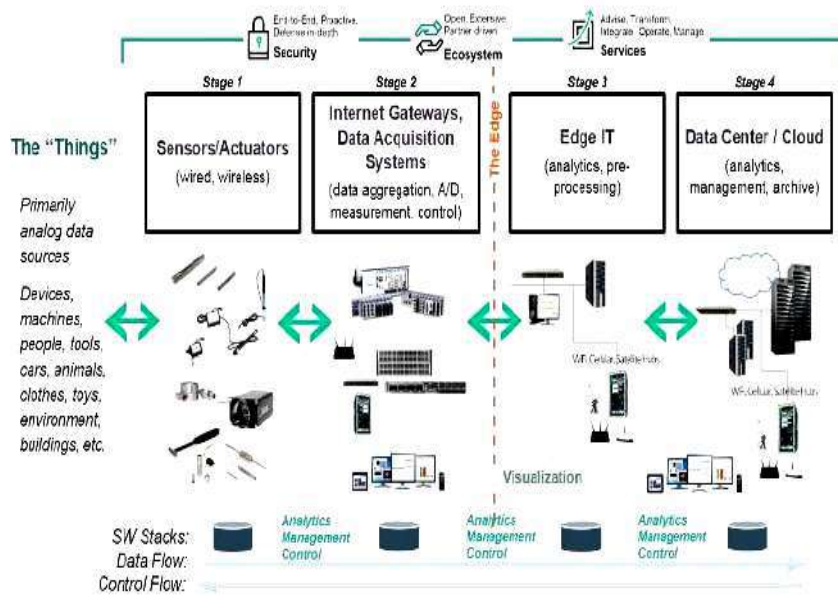


Fig. 2: Four Stages of IoT Architecture

## Advantages of IoT

- **Communication:** IOT empowers the correspondence between devices which is additionally prominently known as Machine-to-Machine (M2M) correspondence. Along these, the physical devices can remain associated and subsequently the all-out straightforwardness is accessible with a less wasteful aspects and improved quality.
- **Automation and control:** Because of physical articles getting associated and controlled carefully and midway with remote framework, there is a tremendous measure of robotization and control in the operations. Without human impedance, the machines can speak with one another which prompts a quicker and convenient yield.
- **Information:** It is clear whether there will be more data then it will enable us to detail better choices. Regardless of whether it is a minor choice as having to recognize what to purchase at the supermarket or if your organization has enough devices and supplies, information is power and more learning is better.
- **Monitor:** The IoT enables you to computerize and control the assignments that are done every day, keeping away from human impedance. Machine-to-machine correspondence keeps up straightforwardness in the procedures. It additionally prompts a consistency in the errands. It can likewise keep up the nature of administration. We can likewise make vital move if there should arise an occurrence of crises.
- **Time:** The machine-to-machine connection gives better effectiveness; consequently, exact outcomes can be acquired rapidly. This outcome in sparing profitable time. Rather than rehashing similar assignments consistently, it empowers individuals to do other imaginative employments.
- **Money:** The greatest preferred standpoint of IOT is setting aside extra cash. IOT on a very basic level ends up being an exceptionally supportive to individuals in their everyday schedules by influencing the machines to impart to one another in a powerful way subsequently sparing and moderating vitality and cost. Enabling the information to be conveyed and shared among devices and afterward making an interpretation of it into our required way, it makes our frameworks effective.
- **Better Quality of Life:** All the applications of this technology emphasize on increased comfort, convenience, and better management, thereby improving the quality of life.

## Drawbacks to IoT

- **Security:** With the majority of this IoT information being transmitted, the danger of losing protection increments. For instance, how very much encoded will the information be kept and transmitted with? Do you need your neighbors or managers to know what meds that you are taking or your money related circumstance?
- **Compatibility:** As devices from various makers will be interconnected, the issue of similarity in labelling and checking manifests. Although this disadvantage may drop off if all the manufacturers agree to a common standard, even after that, technical issues will persist. Today, we have Bluetooth-enabled devices and compatibility problems exist even in this technology! Compatibility issues may result in people buying appliances from a certain manufacturer, leading to its monopoly in the market.
- **Complexity:** The IOT is a different and complex system. Any disappointment or bugs in the product or equipment will have genuine outcomes. Indeed, even power disappointment can cause a ton of burden.
- **Lesser work of modest staff:** The incompetent specialists and partners may finish up losing their positions in the impact of robotization of every day exercises. This can prompt joblessness issues in the general public. This is an issue with the appearance of any innovation and can be overwhelmed with training. With every day exercises getting computerized, normally, there will be less necessities of HR, principally, laborers and less taught staff. This may make Joblessness issue in the general public.
- **Technology assumes responsibility forever:** Our lives will be progressively constrained by innovation, and will be reliant on it. The more youthful age is as of now dependent on innovation for each seemingly insignificant detail. We need to choose the amount of our everyday lives willing to automate and be constrained by innovation.

## APPLICATIONS OF IoT IN SMARTCITIES

**Smart car parking system:** Traffic congestion caused by vehicle is an alarming problem at a global scale and it has been growing at a large scale. Car parking is a major issue these days and has contributed immensely with increasing vehicle size in the luxurious segments and confined parking spaces in the urban cities. Searching for a parking space has become a routine task and often is a frustrating activity for many people in cities around world. With IOT based smart parking system, users will automatically find a free parking space in a particular geographic area and that too at a minimal cost [4]. IOT based smart parking system involves using low-cost sensors, real-time data collection, and mobile-phone-enabled automated payment systems that will allow people to reserve parking spaces in advance or very accurately

predict where they will likely find a parking spot. It also enables cities to carefully manage their parking space. Smart car parking has solved one of the biggest problems in urban areas for finding empty parking spaces and controlling illegal parking spaces and controlling illegal parking. As for example we have shown an IoT based smart parking system in below Fig 3.

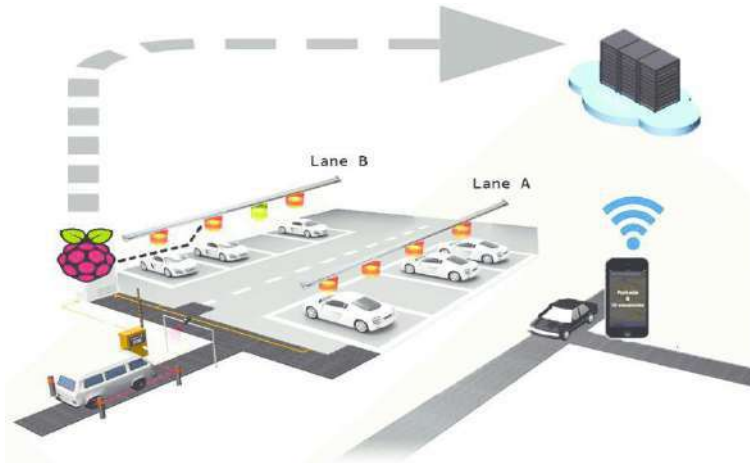


Fig. 3: IoT based Smart Parking system

**Waste management- (smart bin):** Sensor Based Waste Collection Bins are used to identify the status of waste bins if they are empty or completely filled so as to customize the waste collection schedule accordingly and also to make it cost effective. Real time waste management system with the use of smart dustbins enables to check the fill level of dustbins whether the dustbins are completely full or not, through this system the information of all smart dustbins can be accessed from anywhere across the globe and anytime by the concerned person [3]. It will also inform the status of each and every dustbin in real time so that the concerned authority can send the garbage collection vehicle only when the dustbin is full. It has been represented in Fig 4 below.

Benefits:

- It will stop the overflowing of dustbins along roadsides and localities as smart dustbins are managed at real time.
- The filling and cleaning time of smart bins will also be reduced thus making empty and clean dustbins available to the common people.
- It also aims at creating a clean and green environment.
- By using the route algorithm it will smartly find the shortest route thus it will reduce the number of vehicles used for garbage collection.
- It will send optimized routes directly to drivers.
- It will reduce the fuel Consumption.
- Less amount of fuel will be consumed by vehicles thus it will help in saving a large amount of money as well.
- It will stop overflowing of dustbins along roadsides and localities.

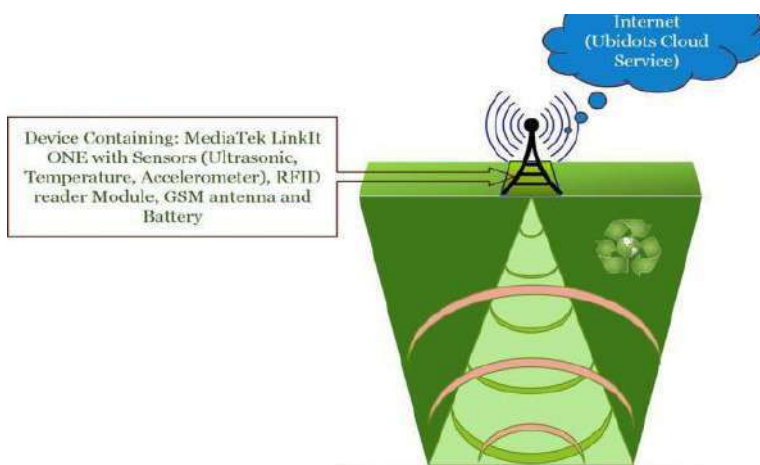
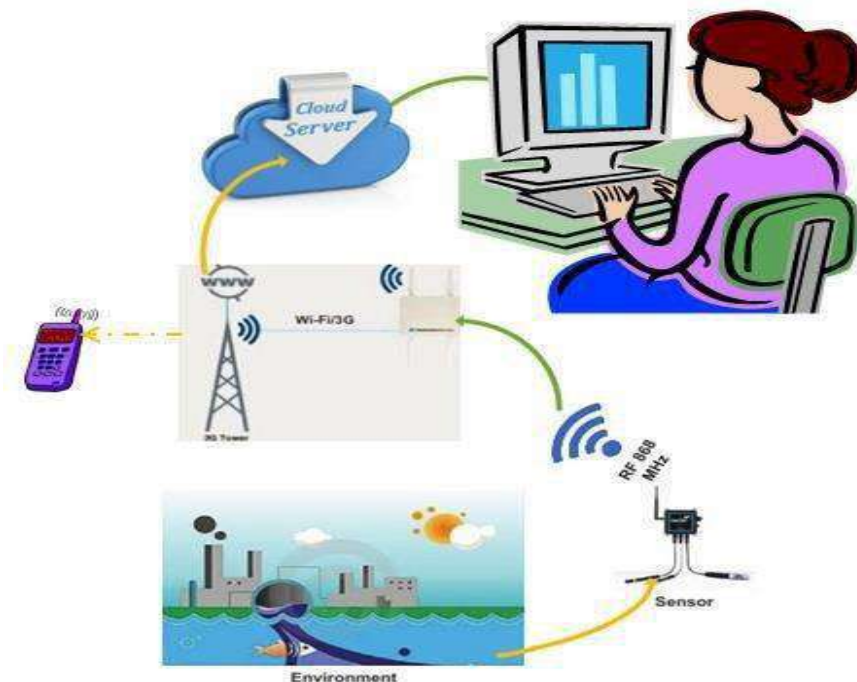


Fig. 4: IoT based Smart Dustbin



**Smart water quality checking framework:** Guaranteeing the security of water has turned into a testing undertaking because of the unnecessary wellsprings of poisons a large portion of which are brought about by human exercises. The primary driver for water quality issues is the over-abuse and over utilization of common assets. The quick development of industrialization, urbanization and more prominent accentuation on rural development joined with the most recent headways and mechanical improvement, rural composts and non- authorization of laws have added to water contamination to an expansive extent. The issue is at times disturbed because of the unpredictable circulation of precipitation. The Keen Water Quality Observing Framework which is IOT based will screen the nature of water continuously [3]. This framework comprises of certain sensors which measure the water quality parameter, for example, pH, turbidity, risky Gas, broke up oxygen, water level, and so on. It is planned and oversaw utilizing a Remote Sensor System (WSN) that screens the water quality with the assistance of data detected by the sensors submerged in water, in -order to keep the water asset inside a standard that is depicted for household use and to almost certainly take essential activities to re-establish and improve the soundness of the debased water asset. It has been represented in Fig 5 below.



**Fig. 5:** Schematic diagram of the Smart Water quality monitoring system

**Smart air quality checking frameworks:** The air quality in Delhi, as indicated by a WHO review of 1600 world urban areas, is the most exceedingly bad of any significant city on the planet. Air contamination in India is assessed to slaughter 1.5 million individuals consistently; it is the fifth biggest executioner in India. India has the world's most astounding demise rate from unending respiratory illnesses and asthma, as indicated by the WHO [2]. Significant poisons causing respiratory sicknesses are:

- I. Fine particles delivered by the consuming of non-renewable energy sources like coal, oil, and so forth.
- II. Noxious gases like sulfur dioxide, nitrogen oxides, carbon monoxide-CO, compound vapors, and so forth.
- III. Ground-level ozone (a receptive type of oxygen and an essential part of urban exhaust cloud) .
- IV. Volatile Natural Mixes having a high vapor weight at standard room temperature, formaldehyde-HCHO gas being significant segment.

Air quality Checking gives crude information comprising of estimations of gases and convergences of contaminations, which would then be able to be examined and deciphered. IOT Based Air Contamination Observing System screens the Air Quality over a Internet server utilizing Internet and it will trigger a caution when the air quality goes down past a specific dimension, implies when there are unreasonable measure of hurtful gases present noticeable all around like CO<sub>2</sub>, smoke, liquor, benzene, NH<sub>3</sub>, NO<sub>x</sub> and LPG. The framework will demonstrate the air quality in PPM on the LCD screen and just as on site page with the goal that it tends to be observed in all respects effectively. Temperature and Humidity(moisture)can additionally be identified and observed in the framework. It has been represented in Fig 6 below.





Fig. 6: IoT based Air Quality monitoring system

**Smart traffic control system:** Traffic light control frameworks are broadly used to screen and control the stream of vehicles crosswise over different intersections of a few streets. Their point is to acknowledge smooth movement of cars in the transportation courses. Be that as it may, the synchronization of various traffic lights frameworks at adjoining intersections is a confounded issue. Likewise, the common impedance between nearby traffic light frameworks, uniqueness of autos streams with time, different instances of mishaps, the entry of crisis vehicles, and the person on foot intersections are not actualized in the current traffic framework which prompts automobile overload and blockage. The ordinary traffic framework should be moved up to understand the extreme traffic blockage, ease transportation issues, diminish traffic volume and holding up time, limit generally travel time and advance vehicles wellbeing. IOT based traffic the executive’s frameworks for smart urban communities serves to effortlessly arrange with emergency vehicle driver to locate the flag status and pick the way where traffic stream can be progressively controlled and petty criminal offenses are been distinguished by on location traffic officers through halfway checked and controlled through Internet. A robotized miniaturized scale controller based traffic control framework utilizing sensors alongside live Internet updates can be a useful advance in enhancing the traffic stream design in occupied convergences. Keen Traffic The board is where halfway controlled traffic signs and sensors direct the stream of traffic through the city.

### TRADITIONAL TRAFFIC CONTROL SYSTEM

One of the serious issues looked in any metro city is traffic clog. Stalling out between substantial traffic is a migraine for every single individual driving the vehicle and even to the traffic police in controlling the traffic. One of the most established methods for taking care of traffic was having a traffic policeman conveyed at every intersection who physically controls the inflow of traffic through hand flagging. Anyway this was very bulky and afterward came the requirement for an alternate kind of control – utilizing Traffic signals, which is developed by Garret Morgan and J.P.Knight. Customary Traffic light controllers utilized a fixed foreordained calendar for traffic inflow for every bearing in the intersection. The controller was an electro mechanical controller which comprises of mechanical frameworks worked electrically. It comprises of three noteworthy parts-a dial clock, a solenoid and a cam get together. An engine and an apparatus gathering works the dial clock which thusly are dependable to empower or de-invigorate a solenoid which thusly works a cam get together which are capable to give current to each flag sign. The dial clock is utilized to give redundancy of fixed span interims. The issue with this conventional methodology is that it will in general be wasteful. Indeed, even arrangements that offer need to open and crisis transportation will in general miss the mark. This principally happens on the grounds that one key blemish stays with these frameworks that the control is brought together. It has been represented in Fig 7 below.



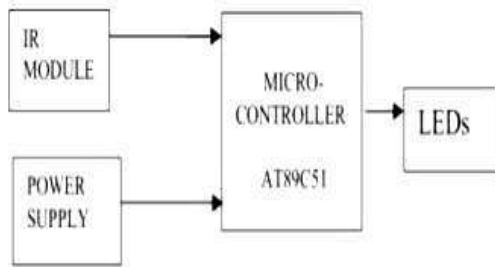
- Traditional signal timing process is time consuming and expensive
- Requires frequent maintenance and updates – i.e. 2-3 years
- Final Assessment is often based on anecdotal and observational judgment due to cost.

Fig. 7: Traditional signal timing process

### Working of traditional traffic lights

A traffic control system in general consists of traffic light heads, controllers and detectors.

**Block diagram:** It has been represented in Fig 8 below.



**Fig. 8:** Block Diagram of Traffic System

**Function of signal controller:** A controller is a device or group of devices that serves to govern in some predetermined manner the performance of an electric device. A controller might include a manual or automatic means for starting and stopping the motor, selecting forward or reverse rotation, selecting and regulating the speed, regulating or limiting the torque, and protecting against overloads and faults. Type of controllers used is:

**Centralized signal controllers:** These controllers use microchips and LSI particularly for traffic control in various leveled structure for improved unwavering quality.

Just as dealing with the different sensor controls, the chip additionally gain proficiency with the split controls, show changeovers and remotely controlled cycles, split controls. This forestalls flag control interruption by guaranteeing that the capacity is proceeded regardless of whether there is a break in the rush hour gridlock control focus circuits. This framework is intended to proceed with safe flag task even in case of breakdown where the microchips helpless to incite the traffic flag control LSI. It has been represented in Fig 9 below.

**Multistage signal controllers:** With an inherent widespread timetable, this device can adaptably program flag designs for some random schedule vacancy on weekdays, Saturdays and Sundays.

**Push-button signal controllers:** These controllers initiate green signs for people on foot wishing to cross fundamental streets all walkers need to do is to press the catch given at the street crossing point. Ordinarily the lights on the fundamental streets are set to green, enabling vehicles to pass.

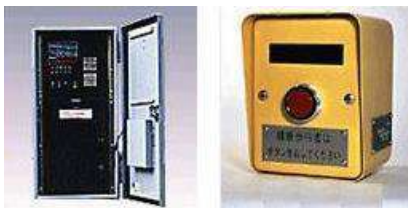


**Fig. 9:** Signal controllers

### Function of traffic light heads

Traffic lights, also known as traffic signals, traffic lamps, traffic semaphore, signal lights, stop lights, robots (in South Africa and most of Africa), and traffic control signals (in technical field), are signaling devices positioned at road intersections, pedestrian crossings, and other locations to control the flows of traffic. Traffic lights alternate the right of way accorded to users by displaying lights or LEDS of a standard color (red, amber (yellow), and green) following a universal color code. In the typical sequence of color phases:

- The green light enables traffic to continue toward the path meant, in the event that it is sheltered to do as such and there is room on the opposite side of the crossing point.
- The amber (yellow) light cautions that the flag is going to change to red. In various nations – among them the Unified Kingdom – a stage amid which red and yellow are shown together demonstrates that the flag is going to change to green. Activities required by drivers on a yellow light change, with certain wards expecting drivers to stop in the event that it is sheltered to do as such, and others enabling drivers to experience the crossing point if safe to do as such.

- A blazing golden sign is a notice flag. In the Unified Kingdoms, a blazing golden light is utilized just at pelican intersections, instead of the consolidated red- golden flag, and shows that drivers may pass if no walkers are on the intersection.
- The red flag restricts any traffic from continuing.
- A flashing red sign is treated as a stop sign.

#### Function of detectors:

Any traffic-responsive control system depends on its ability to sense traffic for local intersection control and / or system-wide adjustment of timing plans. A system accomplishes this by using one or more of the following detector types:

#### Pavement invasive detectors

- **Inductive circle:** It is the most widely recognized indicator innovation. It comprises of at least one turns of protected circle wire twisted in a shallow space sawed in the asphalt. Circle locators come in various sizes and shapes, and different arrangements can be utilized relying upon the zone to be recognized, the sorts of vehicles to be distinguished, and the goal, (for example, line identification, vehicle tallying, or speed estimations).
- (Such as queue detection, vehicle counting, or speed measurements).
- **Magnetometer:** It measures changes in both the horizontal and vertical components of the earth's magnetic field. Early magnetometers could only detect the vertical component, which made them unable to operate near the equator, where magnetic field lines are horizontal. Newer two-axis fluxgate magnetometers overcome this limitation. Magnetometers are useful on bridge decks and viaducts, where the steel support structure interferes with loop detectors, and loops can weaken the existing structure. Magnetometers are also useful for temporary installations in construction zones.
- **Magnetic:** It consists of a coil of wire with a highly permeable core. Measures the moving faster than a certain minimum speed, and therefore cannot be used as a presence detector. Useful where pavement cannot be cut, or where deteriorated pavement or frost activity break inductive loop wires.

#### Non-pavement invasive detectors

- **Microwave Radar:** It transmits microwave energy toward the roadway. CW (Continuous Wave) Doppler radar can only detect flow and speed. FMCW (Frequency Modulated Continuous Wave) radar can also act as presence detector. Certain bridges with large steel structures can cause problems with radar based systems.
- **Active infrared:** It transmits infrared energy from detector and detects the waves that are reflected back.
- **Passive infrared:** It does not transmit any energy; detects energy from vehicles, roadway and other objects, as well as energy from the sun that is reflected by vehicles, roadway, and other objects.
- **Ultrasonic:** It transmits ultrasonic sound energy waves, and measures the distance that the reflected wave travels. Can detect vehicle count, presence, and lane occupancy.
- **Acoustic:** It measure vehicle passage, presence, and speed by passively detecting acoustic energy or audible sounds produced by vehicular traffic.
- **Video image processor:** Video cameras detect traffic, and the images are digitized, processed and converted into traffic data. Can replace several loop detectors, and measure traffic over a limited area, rather than just a single point. The typical usage of Induction Loop Traffic Sensors has been shown in Fig 10.

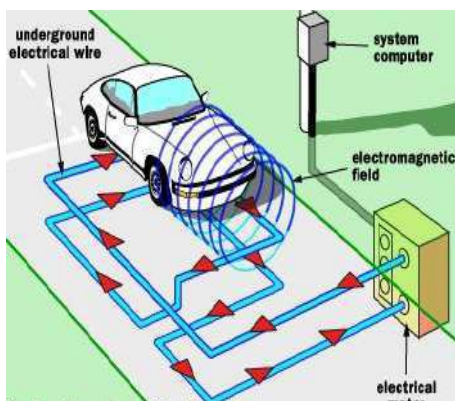


Fig. 10: Induction loop traffic sensors.

## PROBLEMS FACED BY TRADITIONAL TRAFFIC CONTROL SYSTEM

These limitations hinder the ultimate usefulness of traffic control systems. They become limited in terms of effectiveness and versatility. While this is a problem in any setting, it becomes worst in a city experiencing rapid growth. These traffic control systems will be unable to effectively direct traffic. Multiple redundant systems may employ conflicting control schemes, which in turn further diminish the effectiveness of these systems. The main problems with most traffic direction solutions are that they:

- **Increase in rear- end collisions:** When it comes to accidents, traffic signals are sort of a mixed bag. Traffic signals can reduce certain type of car accidents, most commonly broadside collisions. One of the primary disadvantages of traffic signals are that they lead to an increase in rear-ends collisions. Rear-end collisions occur more frequently when a driver abruptly stops at a yellow or red light, causing a distracted driver behind him to ram into the rear of his car. Rear-end collisions aren't typically as severe as broadside collisions, so this trade-off can be seen as worth it. However, in an intersection where broadside accidents are not a concern, installing traffic lights can mean an automatic increase in accidents at the intersection. Traffic engineers do a risk-benefit analysis as part of determining whether to install a traffic light.
- **Excessive delays:** While they do help manage the flow of traffic, one of the other disadvantages of traffic signals is that they can cause traffic delay. Waiting for a traffic light to turn or waiting for a car in a turn lane to safely cross an intersection can result in long wait periods. Excessive delays can translate to wasted fuel, air pollution and costs to motorists.
- **Aggressive driving:** Partially as a result of excessive delay and partially as a result of unwarranted or improperly functioning traffic signals, drivers can get impatient and aggressive when driving. When that happens, more red lights may be run, more traffic laws are broken and drivers may veer off onto neighborhood streets. Aggressive driving can mean increased accidents, congestion, and air and noise pollution. These are some of the many disadvantages of not following traffic rules.
- **Cost of traffic signals:** One of the other disadvantages of traffic signals is the cost, especially when a less expensive stop sign will do. The cost of installing and maintaining a traffic signal varies, depending on the state. In Missouri, it costs between \$100,000 and \$150,000 to install and about \$4,000 a year to maintain a traffic signal. It costs the taxpayer \$250,000 and \$500,000 to purchase and install a signal and about \$8,000 a year to maintain. A basic stop sign, on the other hand, can average around \$400 to manufacture and install. Maintenance costs of a stop sign are significantly lower than a signal, since there is no electrical system to maintain. Traffic engineers consider the advantages and disadvantages of traffic signals when determining whether to install them. Once they are installed, signals are monitored and adjusted on an ongoing basis to make sure they are as beneficial as possible.

## SMART TRAFFIC CONTROL SYSTEM

Keeping these challenges of traditional traffic lights in mind, the concept of intelligent traffic control system was introduced. Objective of this project is to provide traffic and transit management services to the traffic police in support of improving congestion and reducing delays in the cities. This traffic system will improve travel time reliability by progressively moving vehicles through intersections.

## BASIC MODEL OF A SMART TRAFFIC CONTROL SYSTEM

The traffic control framework planned in programmed mode and manual mode. In programmed mode relying on sensors yield the choice is taken. However, in manual mode we can have control on traffic; this is finished by approved individual in control room. The Raspberry Pi is utilized in framework takes controls on all. IR sensors are utilized to distinguish the thickness of traffic. What's more, to recognize the section of rescue vehicle and lost cars RFID is utilized. Camera utilized in framework takes still pics of traffic. By observing this image, approved individual in control room will take choice in manual method of activity.

**Raspberry Pi:** UK was first to create Raspberry Pi. It is a progression of little single board PC. There are three ages in Raspberry Pi for example Raspberry Pi 1, 2 and 3. In this age we can likewise discover diverse models like model A, B. The fundamental Raspberry Pi did not have Wi-Fi and Bluetooth in it, later it was included. Raspberry Pi 3 is utilized in our proposed framework. It has Broadcom SOC and GPU. CPU's speed is 700M Hz – 1.2G Hz.

RAM has 256MB – 1GB memory. SD card store OS in it. There are 4 USB slots. For camera to interface it has CSI. USB cable is used to power the raspberry pi. Raspberry Pi also have video or audio jack. And it has 40 GPIO pins. For monitor connection it has HDMI port.



**RFID:** RFID is a technology in which data will be transferred without any external connection of components. In RFID we have RFID Reader and RFID tag [5][6]. A unique number is allotted for every tag. The RFID tags are of two types:

- Active
- Passive

In traffic lights, passive RFID tags are used. The RFID system contains of a passive tag, an RFID reader, a micro- controller, a GPRS module, a high speed server with a database system and a user module. It has been represented in Fig 11 below.

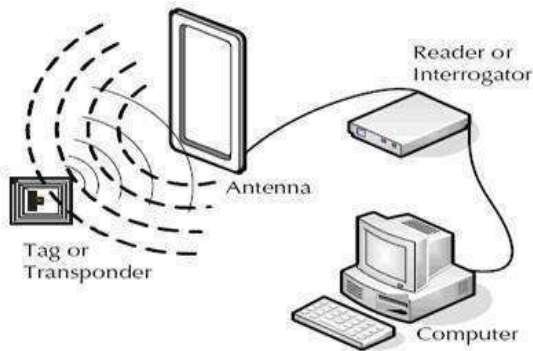


**Fig. 11:** RFID

**IR sensor:** An IR sensor contains a transmitter and a receiver. The transmitter emits the IR rays which strike the object, if present in front of the sensor. These rays will be reflected and thus sensed by the IR receiver. This will help in confirming the presence of an object and how far it is [7]. It has been represented in Fig 12 below.

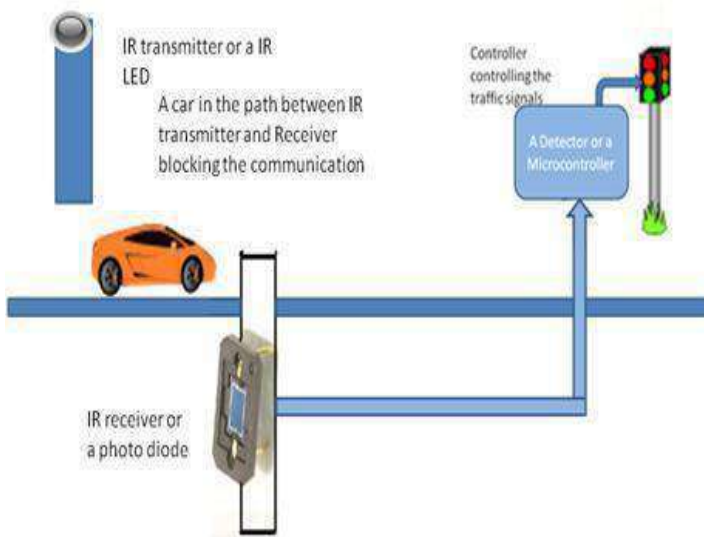


**Fig. 12:** IR Sensor

**Pi camera:** A Pi camera takes high definition pictures and videos. It has a flat cable which is used for connected to CSI port of the Raspberry Pi. The camera is a 5 Mega-Pixel which is generally used for surveillance purposes.

**LED lights:** The LED lights are used as traffic lights. These are diodes and when the p-n junction is forward biased, it emits lights in the form of photon. This gives us different colors and the color is determined by the gaps in the energy band.

### TECHNOLOGIES USED IN SMART TRAFFIC CONTROL SYSTEM

**RFID labels:** The traffic executive's frameworks that are created utilizing the RFID framework is equipped for giving critical traffic related data which would help in lessening the movement time for workers. It tends to be helpful for different purposes like following stolen autos, vehicles that avoid traffic flags or tickets, tolls and so forth. This innovation encourages the framework to gather required information and determined the normal speed of vehicles on the streets of the city. The procured information, for example



the normal speed determined at different intersections is then transmitted to the focal calculation server which at that point computes the time taken by a vehicle to go in a specific street [8]. Accordingly, the server makes a guide of briefest time ways of the entire city. This information would then be able to be gotten to by clients through an interface module put in their vehicles.

**Sensors and smaller scale controllers:** Utilizing IR sensors alongside miniaturized scale controllers and Drove's, a model of a traffic control framework can be made which can demonstrate worth for constant utilization of controlling traffic signals dependent on the thickness of the traffic. A 4-side intersection is viewed as where the traffic stream on each side is just a single way [9]. There are 3 parts of the framework:

- Display Unit: Comprises of 3 Drove's: Red, Golden and Green on each side of the intersection making an aggregate of 12 LED's.
- Detector Unit: Comprises of a course of action of photodiode and IR Drove at every intersection which identifies the nearness of vehicle by recognizing an adjustment in opposition.
- Controller Unit: Comprises of a smaller scale controller which gets the IR sensor yield and appropriately controls the gleaming of LED's.

**Actuator nodes:** A WSAN (Wireless Sensor and Actuator Node) is a group of sensors that gather information about the environment and actuators around them such as motors that interact with them. The communication between the elements is wireless [10]; the interactions are either autonomous or controlled by humans. WSAN's are built of approximately thousands of nodes where each node is connected to one or more sensors with sensor hubs as well as individual actuators or actors. These are used in locations like traffic control system or scientific development, where exact measurement and control of an environment is necessary.

**VANET:** VANET (Vehicular ad hoc networks) are created using the principles of MANET's (Mobile ad hoc Networks). It is a creation for vehicle to vehicle (V2V) data exchange. These vehicles to vehicle or vehicle to roadside communications architectures that co-exist in VANET's can help in providing road safety, navigation and other road-side services. VANET's are an important part of the ITS (Intelligent Traffic System) framework and are sometimes referred as Intelligent Transportation Networks [11].

## COMPARISON OF TRADITIONAL/CONVENTIONAL TRAFFIC CONTROL SYSTEM TO SMART TRAFFIC CONTROL SYSTEM.

The comparison of traditional traffic control system with the IoT based smart traffic lightning system has been shown in below Table 1.

Table 1: COMPARISON OF TRADITIONAL/CONVENTIONAL TRAFFIC CONTROL SYSTEM TO SMART TRAFFIC CONTROL SYSTEM.

S.NO	PARAMETERS	TRADITIONAL/CONVENTIONAL TRAFFI C CONTROL SYSTEM	SMART TRAFFIC CONTROL SYSTEM
1.	Excessive Time Delay	It uses a fixed time delay for different traffic directions and follows a particular cycle while switching between signals. As a result, this creates unwanted congestion during the peak hours and loss of man-hours. Also here, the junction timings are fixed so the vehicles have to wait at road crossing even though there is little or no traffic at all[12].	It uses Microcontroller interfaced with sensors which helps in changing the signal timing automatically based on the traffic density at the junction. This also helps in avoiding unnecessary waiting time at the junction.
2.	Traffic congestion	It creates unnecessary traffic jam. Also there are problems like Ambulance getting caught up by red traffic signal and wasting valuable time.	It reduces the traffic congestion. It is controlled by algorithm and it not only takes into consideration all complex road intersections in a city but also adds type of vehicles leading to accurate predictions of traffic flow.

3.	Aggressive driving	As a result of excessive delay and improper functioning of traffic lights drivers can get impatient and aggressive while driving which may lead to accidents, congestion, air and noise pollution.	This won't be the scenario here as it will improve travel time reliability by progressively moving vehicles through intersections. It will also provide city planners with accurate predictions of pollution and emission levels as well as estimation of best fuel efficiency for various types of vehicles in the city.
4.	Gathering Traffic data	Conventional systems cannot gather traffic data. It cannot measure the number and type of vehicles using a particular road.	Smart traffic control systems can effectively gather traffic data. It can measure the number and type of vehicles using a particular road or visiting a particular part of the city, also monitor peak traffic times, journey[13][14], length and other data.
5.	Cost of Traffic signals	The cost of installing and maintaining the traditional traffic signals was much more cheaper because of the lack of smart devices starting from \$100,000 and will go on up depending upon quality of the material.	The cost of installing and maintaining the latest traffic signals is costlier than the traditional system because of the additions such as RFID labels, sensors and small scale controllers and actuator nodes starting from \$250,000 and increasing depending on the quality of the material[15][16].

### REAL LIFE EXAMPLE OF SMART TRAFFIC LIGHT CONTROL SYSTEM IN BHUBANESWAR

In India, the concept of intelligent traffic control is still fairly new. It has been implemented and Bhubaneswar with varying degrees of success, while it is still in the process of implemented in Delhi. Here we will discuss the smart traffic control system adopted in Bhubaneswar, its working, its components, the advantages it has, the drawbacks and the methods in which we can try to overcome these drawbacks.

In recent times, Bhubaneswar has emerged as one of the fast-growing, important trading and a commercial hub in the state of Odisha and Eastern India. This fact-paced development in the city has put adverse pressure on the ease of commuting in the city. Traffic Management has been identified as an important key for enhancing mobility of citizens in the city. For enhancing the efficiency of the signalized intersections, the city has given a proposal to have a coordinated traffic signal control system. This led to the installation of Adaptive Traffic Signal Control System at signalized intersections in the city. Thus, Bhubaneswar has recently procured the requisite technology of traffic engineering named the Composite Signal Control Strategy (CoSiCoSt) developed by C-DAC (Centre for Development of Advanced Computing) which is a research and development organization under the Department of Electronics and Information Technology, Government of India. CoSiCoSt technology is an advanced control system which is capable of synchronizing traffic signals according to the real time traffic conditions. The system gets its input from the sensors embedded in the roads and the synchronize the group of traffic signals accordingly. This type of signaling system runs on solar power and it is being planned to be upgraded with automatic number plate recognition, variable message signs and surveillance cameras for real-time emergency and incident management system. The system shall be integrated with other smart city modules in the Central Command Centre and provide real-time decision support. The Adaptive Traffic Signal Control System is a part of the Intelligent City Operations and Management Centre which falls under the Pan City Proposal. The key outputs/outcomes implementation for pilot intersection is currently underway. The Adaptive Traffic Signal Control System is being planned to be installed at 58 traffic signals, 14 pelican crossings and blinkers at five locations in the city. The project is leading to the distribution of green phase (traffic signal) time equitably and faster response to traffic conditions and emergencies. The system also predicts traffic volumes and accordingly adjusts signal timings. The project will also travel time reliability, reduce

congestion and related Green House Gas (GHG) emissions. The project is funded through Smart City Funds with a finance of 14.7 crores. The agency which is implementing the project is Bhubaneswar Smart City Limited (BSCL).

## CONCLUSION

In this paper we have seen that the IOT is having a vast amount of applications where it can be used. An example include usage in Smart cities, Healthcare and in other modern infrastructure has changed the things in a drastic manner. By studying in detail, we have compared the traffic signal system of traditional manner with the smart traffic-based mechanism based on IoT. Being a traditional system, we found that it was having various drawbacks such as it was unable to gather the real time data traffic light, time delay of red/green/yellow lights was fixed ir-respective of any amount of traffic in either of the 4 sides of road. As a result of the excessive delay in lights the drivers also become impatient due to more waiting hence all these things may lead to traffic jam as well as an accident. So, for avoiding all these things in the traditional lightning system a new mechanism called as the smart traffic lightning mechanism was proposed which uses the concept of IoT and the various components such as the Sensors, RFID signals and other devices. Although costing gets increased in later system but the time delay has been adjusted among the road side having more/less amount of traffic. The delay will get reduce if traffic is higher than expected and vice versa. In India, the concept of intelligent traffic control is still fairly new. It has been implemented and Bhubaneswar with varying degrees of success, while it is still in the process of implemented in Delhi. Here we will discuss the smart traffic control system adopted in Bhubaneswar, its working, its components, the advantages it has, the drawbacks and the methods in which we can try to overcome these drawbacks.

### CONFLICT OF INTEREST

There is no conflict of interest.

### ACKNOWLEDGEMENTS

None.

### FINANCIAL DISCLOSURE

None.

## REFERENCES

- [1] Ghazal B, et al. [2016] Smart traffic light control system. 2016 third international conference on electrical, electronics, computer engineering and their applications (EECEA). IEEE, doi: 10.1109/EECEA.2016.7470780
- [2] Tapashetti A, et al. [2016] IoT-enabled air quality monitoring device: A low cost smart health solution, 2016 IEEE Global Humanitarian Technology Conference (GHTC). doi: 10.1109/GHTC.2016.7857352
- [3] Geetha S, Gouthami S. [2016] Internet of things enabled real time water quality monitoring system. Smart Water 2.1 doi: 10.1186/s40713-017-0005-y
- [4] Prasad AV. Et al [2017] Exploring the Convergence of Big Data and the Internet of Things. IGI Global.
- [5] Andrea Z, et al. [2014] Internet of things for smart cities. IEEE Internet of Things journal 1 (1): 22-32.
- [6] Luigi A, et al. [2010] The internet of things: A survey. Computer networks 54(15): 2787-2805.
- [7] Schaffers H, et al. [2011] Smart cities and the future internet: Towards cooperation frameworks for open innovation, The Future Internet Lect. Notes Comput Sci. 6656:431- 446.
- [8] Mischa D, et al. [2011] Smart cities: An action plan. Proc. Barcelona Smart Cities Congress, Barcelona, Spain.
- [9] Patan R, et al. [2016] Real-time smart traffic management system for smart cities by using Internet of Things and big data. 2016 international conference on emerging technological trends (ICETT). IEEE, 2016.
- [10] Chao KH, Chen PY. [2014] An intelligent traffic flow control system based on radio frequency identification and wireless sensor networks. International journal of distributed sensor networks 10 (5): 694545.
- [11] Hasan MM, et al. [2014] Smart traffic control system with application of image processing techniques." 2014 International Conference on Informatics, Electronics & Vision (ICIEV). IEEE, 2014.
- [12] Arasteh H, et al. [2016] IoT-based smart cities: a survey. 2016 IEEE 16th International Conference on Environment and Electrical Engineering (EEEIC). IEEE, 2016.
- [13] Cheng B, et al. [2015] Building a big data platform for smart cities: Experience and lessons from Santander. 2015 IEEE International Congress on Big Data. IEEE.
- [14] Choosri N, et al. [2015] IoT-RFID testbed for supporting traffic light control. International Journal of Information and Electronics Engineering 5.2: 102.
- [15] Volodymyr M, Hahanov V. [2014] Smart traffic light in terms of the cognitive road traffic management system (CTMS) based on the Internet of Things." Proceedings of IEEE East-West Design & Test Symposium (EWDTS 2014). IEEE, 2014.
- [16] <https://timesofindia.indiatimes.com/city/bhubaneswar/adaptive-traffic-signal-system-inaugurated-in-bhubaneswar/articleshow/64921486.cms>

## ARTICLE

## WIND ENERGY CONVERSION SYSTEMS: A REVIEW

Deepak Solanki<sup>1</sup>, Aditi Arora<sup>1</sup>, Nishant Raghav<sup>1</sup>, Aditya Sharma<sup>1</sup>, Ashish Grover<sup>1</sup>, Mohit Verma<sup>1,2\*</sup><sup>1</sup>Department of Electrical and Electronics Engineering, Manav Rachna International Institute of Research and Studies, Faridabad, Haryana, INDIA<sup>2</sup>Accendere CL Educate, New Delhi, INDIA

## ABSTRACT

Among all the recent technologies, one of the rapid evolving techniques used for the generation of energy is wind power. This is a non-renewable source of energy i.e. it will be continuing useful for the production of power for several coming years. Nowadays, it is becoming a trend to install or establish a system to generate wind power across all over the appropriate places of the world with high or low wind force. The wind energy proves itself as one of the leading components in the electrical power generation sector, and will definitely play a prime role in the renewable energy sector. Every city looking for the development is highly reliant on electricity for their growth. Relative analysis will be very important element for the selection of any renewable energy system. . With the help of life cycle Cost Benefits analysis, unit cost of energy can be calculated .In Wind Energy systems the main component of generation is turbine and generator. Conventional power generation turbines are very much comparable to modern wind turbines as their life span is of about 20-25 years. These turbines are of two types -Horizontal Axis Wind Turbine (HAWT) and Vertical Axis Wind Turbine (VAWT). The inconsistent wind velocity is a major problem, which leads the voltage/frequency fluctuations, in turns the stability in WECS. In this paper, wind energy is reviewed and we have discussed the stochastic structure of wind, Offshore and Onshore wind farms which mainly focuses on Aerodynamics, Mechanical and Electrical aspects.

## INTRODUCTION

The useful form of wind energy converted in electrical energy with the help of rotor, sails, and blades. The site selection for Wind Energy Conversion System (WECS) depends upon the availability of the wind [1]. The WECS has many components like wind turbine, control system, generator, interconnection apparatus. There are two types of Wind turbines:

- Horizontal Axis Wind Turbine (HAWT)
- Vertical Axis Wind Turbine (VAWT)

Contemporary wind turbine used HAWT with 2 or 3 blades and activate either downward or upward configuration. The PMSG work with very high torque at low speed with less noise and need no external excitation. DFIG have winding on both stationary and rotating part where major power transfer between shaft and grid. The doubly fed induction generator (DFIG) or PMSG type is the most commonly used generator for wind energy conversion system. Fed Induction Generator (DFIG) or PMSG type [2]. Majority of wind turbine manufacturer make use of DFIG for their WECS as they have advantage in terms of cost, weight and size. This reduction of weight and size is due to the use of multi bridge in the system which includes several components in one housing such as main shaft, shaft bearing, gearbox, etc. The efficiency of generator with multi blades concept is reduced but it becomes cheaper and more reliable than that of the standard one.

Different control strategies like Field Oriented Control (FOC), Direct Torque Control (DTC) [3] are implemented to achieve high efficient energy conversion on these drives. The electrical and mechanical part of wind turbine are mostly linear and there modeling will be easier.

## WIND TECHNOLOGIES

Recently the private organizations such as Vestas, Siemens Gamesa are also involve with the wind energy technological office for enhancing the efficiency of next generation wind turbine at low cost. These collaborative research/studies have impact effectively to lowering the cost. Now a day the average cost of wind energy in the UNITED STATE is 3¢ per KWH, which is 55¢ in 1980. Though there is a miles to go and several wind industry has been continuously working to ensure the future growth of this technology [4]. Further to improve reliability, increase capacity factor, and cost reduction building should be done on earlier successes. Before 1998, the average capacity factor was 22% for wind turbine which increased to an average of nearly 35% today, up from 30% in 2000 with the help of these collaborative efforts.

## WIND ENERGY CONVERSION SYSTEM

Wind energy conversion system consists of following main parts as shown in [Fig. 1]:

1. Wind Turbine
2. Gear system and coupling
3. Generator
4. Controller

## KEY WORDS

Wind Turbine, Wind Mill,  
Wind Farm, Onshore,  
Offshore.

Received: 28 Mar 2019  
Accepted: 10 May 2019  
Published: 19 May 2019

## \*Corresponding Author

Email:  
mohit.verma@accendere.co.in

These are mainly the generating unit which converts the wind energy into electrical energy and the generating energy sent to the power grid for electrical loads.

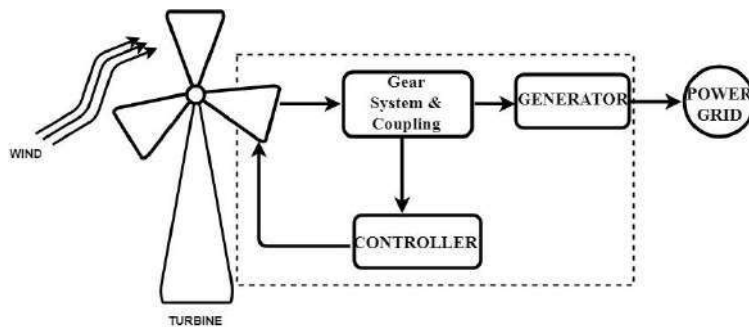


Fig. 1: Block diagram of wind energy conversion system [5].

## WIND TURBINE

This device is used to produce the electrical energy from kinetic energy of wind. In the present trends the wind mill are also known as wind turbine. The maximum 6MW power can be generated by the largest wind turbine [6]. As compare to fossil fuel, it generates quite less power. The fossil fuel power plant can be produce in the range of 500MW to 1300MW. But it also have major drawback like limited and when fossil fuel burns, it produce harmful pollutants which directly affect the nature. So that's why the WECS now in more trend because it is a renewable source of energy and cannot affect the nature. They are of two types: Vertical and Horizontal.

## HORIZONTAL AXIS WIND TURBINE (HAWT)

In this type of wind turbine, the electrical generator along with the main rotor shaft is placed at the top of the tower. The blades of the turbine are arranged in such a manner so that the wind can exert maximum of its force to rotate the turbine. This rotational energy is used to drive an electrical generator to produce the current. There are two types of HAWT- with gear and gear less [7].

In geared wind turbine a gearbox is attached in between the turbine and electrical generator. This gearbox is used to speed up the rotation of the blade. This high speed rotation is appropriate to drive an electric generator. The slow rotation of the blade is transformed to a faster rotation by the gear box which is more suitable to drive an electric generator. In gearless turbines a permanent magnetic generator is used which is directly drive by the blades. As downwind machines do not require an additional mechanism for keeping them in line with the wind [8] so they have been built. For day time visibility by aircraft the blades are generally colored white and its range is from 20-80 meters.

## VERTICAL AXIS WIND TURBINE (VAWT)

They have main rotor shaft which is arranged vertically. It is inherently less steerable so it becomes an advantage when the turbine is integrated into a building. The major drawback of VAWT is that less energy is produced by their design averaged over time, which is. The buildings often redirect wind over the roof which cans double the speed of the wind turbine when the turbine is mounted on a rooftop. When wind speed within the built environment is much lower than at exposed rural site, the concern subtypes of the VAWT may be noise [9].

## NEW OFFSHORE TECHNOLOGY TO GROW WIND TURBINE

According to DOE (Department of Energy) the united states has significant offshore wind resources. Offshore wind could provide almost twice the total electricity generation that US needed in 2025. Development of these resources is also on the rise, largely financed by the private sector. The first planned offshore wind project in the US was THE CAPE WIND PROJECT, a 131 turbines offshore wind farm to be located in the Nantucket sound.

## BENEFITS

The most significant benefits of offshore wind are of course they cleaner energy and overall improvement in environmental impact. Other benefits may depend on projects and sites; include lower cost of energy and economic benefits for the area.



## LIMITATIONS

### Underwater noise and electro-magnetic fields

An environmental impact of great concern that come with the installation and operation of an offshore wind facility is increased noise. Installing turbines requires pile-driving, drilling and dredging, all very loud operations. In addition, the turbines will continue to generate disruptive underwater noise and vibrations once they are functioning and will emit EM waves.

### VESSEL TRAFFIC

During the exploratory stages of the project and when the turbines and the cables are being installed, heavy boat traffic is expected in a concentrated area. This is expected to decrease as a result of shipping routes being altered to avoid the turbines. A decrease in boat traffic is not the only long term benefits that wind farm may bring to marine wild life.

## WIND BELT- LOW COST ENERGY PRODUCTION USING FLUTTERING WIND BELT

It is a device which works on the theory of aero elastic flutter and on mutual induction method between the magnet and the coil. The magnet is arranged on the ribbon in this device which on passing wind, start fluttering on the based on aero elastic flutter theory [10]. As a result of fluttering, the magnet between the two coils which are arranged one above the other and having little space for the magnet between them also to reciprocate. Mutual induction takes place due to this movement of magnet between the coils by the flutter which leads to the induction of current and the voltage. The voltage produce is increased when the speed of the wind increases.

### MAGNETIC PROPERTIES OF WIND BELT

The magnets used in this device are permanent magnet or rear earth magnet which has high magnetic field intensity as compared to the ferrite magnet. The magnetic field of these magnets never weakens and they also have high resistance towards the corrosion.

### COIL PROPERTIES OF WIND BELT

The copper is used for making the coil of wind belt. Therefore the current induced in the coil largely depends on the rating of copper wire used. The copper turn and the total weight of the coil directly affect the output.

### LIMITATION OF WIND BELT

The diameter of the magnet used is 1mm, which restricts the fluttering of ribbon, in order to avoid this; we use the similar magnet of smaller size. These magnets are lightly weighted, same magnetic strength, better result and output voltage due to its low weight and area. As compared to the others devices of this range at low to medium wind velocity this device is very cheap and gives better output.

## ECONOMICAL TRENDS OF WIND ENERGY

### Past trends

The average capital cost of the electricity produced by wind energy has decline noticeably from the 1980's to the early 2000. This historical cost reduction is attributed to the dramatic enhancement in the performance of the turbine which resulted due to the advancement in turbine components. In the duration of year 2004 to 2009, the cost of the wind turbine increases due to the capital cost raise in the market. This cost raise is dedicated to various factors (in terms of wind turbine) such as turbine up scaling, raised in material prices, energy prices, manufacturer profitability, and labor cost [11].

### Present trends

After 2009, the cost of the wind turbine was started to declined but it is still little bit higher and hadn't touch the same rate of 1980's .However, the performance is continuously improving at the same pace [12].

## Future trends

On the basis of various observations and studies, it is predicted that the LCOE of wind energy will fall and continuing the same trend for the near future [13]. As per the data available this fall is now under lying in between the range of 20% to 80% and it is predicted that this range will become in between 20% to 30% with the reduction in LCOE. The estimated per year initial cost reduction ranges from 1% to 6%.

## Operators of future wind energy cost reduction

The major factors which effect the cost reduction are availability of better material, and real time control capability. These factors are also responsible for the enhancement of the reliability if wind turbine. Cost is expected to decline in the future- similar to those, which is observed in between 2004-2009. Manufacturing improvement and innovation in logistic challenge are also expected in reducing the cost of wind energy. Among manufacturers there is an increasing competition which drives down the LCOE of onshore wind energy to a greater extent than otherwise envisioned.

## CLASSIFICATIONS OF GENERATORS FOR WIND TURBINE

### Permanent magnet synchronous generator (PMSG)

This generator is used to enhance the reliability of variable speed wind turbine [14, 15]. It has self excitation property due to which it offers enhance efficiency and power factor. It is also helpful to extract the maximum power from the wind turbine in the condition of fluctuating wind [16].

### Induction generator as wind power generator

This generator is used for the efficient control on power and speed up of the turbine [17]. In turbine system this motor is directly attached to the grid. This motor controls the power with the help of hydraulic pitch system and starting current limiting circuitry. The entire system is simple and having robustness.

## CONTROL STRATEGY OF WECS

### Pitch adjustment

This is mainly the adjustment of angle of turbine blade in order to give maximum output. The blade can be adjusted through tilt angle (angle of attack). If the blade is tilted in such a manner that its flat side faces the force of wind then the angle of attack is increased. The decreasing situation of the angle of attack opens the edge of the blade to face the wind. Through of manner of generate the maximum power output.

### Yaw adjustment

In case of yaw adjustment tower/pole the entire wind turbine is rotated on its horizontal axis in order to give the maximum output.

## APPLICATIONS OF WIND ENERGY

The wind energy is used to produce electricity. The large turbine blade is rotated due to the power of wind [8]. This rotated motion of the turbine is then converted into the electrical current with the help of electrical generator. Some of the prominent applications which use wind energy are:

- Wind electric
- Wind pump
- Wind energy-water desalination
- Wind mill
- Wind turbine

## WIND FARMS

Arrangement of large wind turbines are known as wind farms. It is of two types:

- Offshore wind farms
- Onshore wind farms

On the basis of the location of the turbines which is on the land or in the sea. They are known as Onshore and Offshore respectively.

## OFFSHORE WIND FARMS

The wind farms which are situated in the sea and the height of the turbine is high and the transmission cables are used to transmit energy from generating stations to substations [18]. The undersea cables are used for the transmission of the power from turbine to grid.

### Advantages:

- The size and the height of the wind mill installed in this category are large, which allow collecting more energy.
- Again, due to its position in the sea (far from the seashore), hence it doesn't interfere with the land available at the seashore which can be used in any other valuable purpose.
- Generally the wind flow out at the sea with large wind force as compare to the other. Due to this huge wind force, the higher amount of energy is produce in much higher in volume.
- As the wind farm impact negatively to the environment. Therefore it is prefer to build these farms in remote areas or where the environment condition is not too delicate.
- The wind flow can not to effect by the physical restriction such as building or hills, etc.

### Disadvantages:

- Cost is the biggest disadvantage oh the offshore wind farm. These farms are highly expensive as compare to the fossil fuel generator and the nuclear plant. This is reported 91% and 51% respectively, while these are built for the support only. Also, the cables used for them are costlier, as they need to cover a long distance to reach to onshore battery [15].
- Further the cable runs more power is lost due to voltage drop in long cable.

## ONSHORE WIND FARMS

It is situated on the land area so it is known as onshore wind farms. The height of the wind turbine is 20 meter and distance between two turbines is 200 meter [3].

### Advantages:

- Onshore wind farm is used as mass firms due to its cost effectiveness.
- As the distance between the end consumer and the wind mill is less which in term effectively reduces the amount of voltage drop.
- The installations of these wind mills are easy and it consumes less time to install.

### Disadvantages:

- The major drawbacks of these farms are that they seem to be obstacle to observe the beauty of the landscape/ nature.
- These farms are not capable to produce the energy all over the year due to the physical hurdles/obstacle such as buildings or hills and especially due to the lower speed of wind.
- The noise produce by these farms are huge that it affects the nearby community as noise pollution.

## GEOGRAPHICAL WIND ENERGY PRODUCTION

According to the Global wind energy council; China is the largest wind energy generating country producing 19660 MW in 2017 which makes up the 37% of world wide wind energy production. India has the 5th rank in the wind electricity generation producing 4148 MW of energy, which is 8% of the world wide generation [19].

In India, top most wind energy generating states are Tamil Nadu, Maharashtra, Gujrat, Rajasthan and Karnataka. These states together, generate 93% of total wind energy produced in India. The table 1 shown below represents the percentage of wind energy production in India.

**Table 1:** State wise wind energy production in India [20]

Sl. No.	State	% Generation
1	Tamil Nadu	33
2	Maharashtra	19
3	Gujrat	16
4	Rajasthan	14
5	Karnataka	11
6	Others	7

## CONCLUSION AND FUTURE WORKS

It is concluded in this paper that wind farm power generation individually has high capital cost, but the clean energy source may be used in Hybrid power generation. The LCOE of wind energy will continue to fall on a long term international basis and in fixed wind resource classes this is suggested by variety of factors. The most complicated cost modeling along with more advanced component, turbine, project level design and cost tools give greater power inside into possible future cost which is based on changes in material used and design architecture. The capital cost reduction and performance improvement has led to decrease in the cost of wind energy appreciably. Together all these efforts are enhance to be able to understand future cost, prioritize and the impact of incentives is understood in future.

### CONFLICT OF INTEREST

There is no conflict of interest.

### ACKNOWLEDGEMENTS

Authors would like to express the gratitude to the Research Mentors of Accendere Knowledge Management Services Pvt. Ltd. for their comments on an earlier version of the manuscript. Although any errors are our own and should not tarnish the reputations of these esteemed persons.

### FINANCIAL DISCLOSURE

None.

## REFERENCES

- [1] Mohamed MB, Jemli M, Gossa M, Jemli K. [2004] Doubly fed induction generator (DFIG) in wind turbine modeling and power flow control. In 2004 IEEE International Conference on Industrial Technology, 2004. IEEE ICIT'04. 2:580-584. IEEE.
- [2] Verde A, Lastres O, Hernández G, Ibañez G, Vereá L, Sebastian PJ. [2018] A new method for characterization of small capacity wind turbines with permanent magnet synchronous generator: An experimental study. *Heliyon*. 4(8): e00732.
- [3] Cardell JB, Connors SR. [1998] Wind power in New England: modeling and analysis of non-dispatchable renewable energy technologies. *IEEE Transactions on Power Systems*. 13(2): 710-715.
- [4] Wizelius T. [2015] Developing wind power projects: theory and practice. Routledge.
- [5] Pandey S, Islam S, Bakhsh FI. [2012] Application of Matrix Converter to Enhance the Performance of Wind Turbine Driven Asynchronous Generator: A Review. *energy conversion*, 3(4):1-6.
- [6] Wang CN, Lin WC, Le XK. [2014] Modelling of a PMSG wind turbine with autonomous control. *Mathematical Problems in Engineering*. doi: 10.1155/2014/856173
- [7] El-Kasmi A, Masson C. [2008] An extended k-ε model for turbulent flow through horizontal-axis wind turbines. *Journal of Wind Engineering and Industrial Aerodynamics*. 96(1):103-122.
- [8] Sharma A, Kar SK. (Eds.). [2015] *Energy sustainability through green energy*. Springer.
- [9] Buchner AJ, Lohry MW, Martinelli L., Soria J, Smits AJ. [2015] Dynamic stall in vertical axis wind turbines: comparing experiments and computations. *Journal of Wind Engineering and Industrial Aerodynamics*. 146:163-171.
- [10] Bhagat MRD, Lande MS. [2014] Small Scale Generation by Harnessing the Wind Energy. *IJRET: International Journal of Research in Engineering and Technology*. 3(2):149-156.
- [11] Goldemberg J. [2006] The promise of clean energy. *Energy policy*. 34(15):2185-2190.
- [12] Mitigation CC. [2011] IPCC special report on renewable energy sources and climate change mitigation. [<https://www.ipcc.ch/report/renewable-energy-sources-and-climate-change-mitigation/>]
- [13] Scenario S N L. [2013] A shift in perspective for a world in transition. Shell International BV, The Hague.
- [14] Tsai MF, Hsu WC, Wu TW, Wang JK. [2009] Design and implementation of an FPGA-based digital control IC of maximum-power-point-tracking charger for vertical-axis wind turbine generators. In 2009 IEEE International Conference on Power Electronics and Drive Systems (PEDS). 764-769.
- [15] Musial W, Ram B. [2010] Large-scale offshore wind power in the United States: Assessment of opportunities and barriers (No. NREL/TP-500-40745). National Renewable Energy Lab.(NREL), Golden, CO (United States).
- [16] Brahma J, Krichen L, Ouali A. [2009] A comparative study between three sensorless control strategies for PMSG in wind energy conversion system. *Applied energy*. 86(9):1565-1573.
- [17] Zhang X, Wang Y. [2014] Robust fuzzy control for doubly fed wind power systems with variable speed based on variable structure control technique. *Mathematical Problems in Engineering*. doi: 10.1155/2014/750101
- [18] Rock M, Parsons L. [2010] *Offshore Wind Energy*. Fact Sheet, Environmental and Energy Study Institute.
- [19] Top 10 Largest Wind Energy Producing Countries in the World [2018]. Energy and Fules. [<https://www.bizvibe.com/blog/top-10-wind-energy-producing-countries-world>]
- [20] Top five states in India with highest wind electricity generation. Energy Tagged India. [<http://greencleanguide.com/top-five-states-in-india-with-highest-wind-electricity-generation/>]

# ARTICLE

## NOVEL 2-BIT FULL ADDER DESIGN IN QUANTUM DOT CELLULAR AUTOMATA TECHNIQUE

Pranali Nile, Sayli Mohite, Sankit Kassa\*

Usha Mittal Institute of Technology, Mumbai, INDIA

### ABSTRACT

**Back ground:** Quantum dot Cellular Automata (QCA) consists of a cell which includes two electrons logically interacting in the four quantum dot cell. QCA helps the design for faster speed, smaller size, and low power consumption. QCA is the new form of nanotechnology for many electronic circuits in VLSI paradigm. **Methods:** In this manuscript, QCA Designer 2.0.3 tool has been utilized for verifying the output of the circuit. **Results:** In this paper, the designs of 1-bit and 2-bit full adder are proposed which reduce the total number of QCA gates and its particular area and power consumption compared to previous well known designs. **Conclusions:** The proposed QCA full adder circuit saves up to 50% Cell counts and 67% Area composed to the previously reported designs.

### INTRODUCTION

QCA is a technology which stands for Quantum Dot and Cellular Automata. QCA is an advanced version in VLSI arena to implement IC designing than CMOS (Complementary Metal Oxide Semiconductor). CMOS was measured on micro-scale that was consisting of high density and had low power Very Large Scale Integration (VLSI) circuit [1-4]. The drawbacks of CMOS technology have high leakage current, power dissipation and limitation of speed in GHz range. Therefore, CMOS technology has been overtaken by QCA technology. In digital logics, adders are basic circuits. Adder circuits in conventional transistors required many wires; therefore the earlier adder circuit's speed was much less because of so many wires. Hence such circuit's implementations were difficult. A Quantum dot Cellular Automata is used as a software program. Hence, in this software, the design of QCA has been implemented.

This paper consists of: Basics of QCA, proposed designs of 1-bit and 2-bit Full Adder, simulation result, discussion and conclusion.

### MATERIALS AND METHODS

QCA design consists of some basic key points.

#### QCA cell consisting of four dots

In QCA cell, it consists of quantum dots that are basically four dots in one square. From these four dots, only two dots are having electrons which are arranged diagonally to each other. The two electrons are not able to leave a cell; else they will be able to tunnel in between the dots as shown in [Fig. 1][5-8].

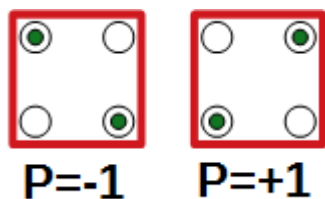


Fig. 1: Four dots of QCA cell.

Only two electrons are allowed to place in a cell, if two or more electrons are present in a cell, then Coulomb repulsion will come in contact and repulsion will take place. Hence, there are two polarization states that are  $P=-1$  for logic 0 and  $P=+1$  for logic 1.

#### Components of QCA

In a QCA inverter gate, the input is shown as A and output as A' which is shown in [Fig. 2]. To make the input A strong, same types of two cells are connected with each other and at 45 degree angle, the next cell is placed, which gives the output. Therefore, when A has the logic as logic 0 the output A' gives the logic as 1 and vice-versa.

3 input QCA majority gate is depicted in [Fig. 2]. A, B, C are given as the 3 inputs [9-11]. Suppose the input for A is logic 0 and input for B is logic 0 then C is considered as AND or OR gate respectively depending on

\*Corresponding Author  
Email:  
rel1356@mnnit.ac.in



the polarization of either logic 0 or logic 1. The output is obtained from majority input from all the 3 inputs. If all the majority inputs are given as logic 0, so the output will become logic 0.

Wire of QCA cell-The wire of QCA cell can have the same polarization up to 10 cells for logic 0 or 1; after that logic will be different that is either logic 0 or 1. As the cells are connected to each other, therefore the long interconnection of wires is not needed.

Crossover Gate- When two QCA wires come in contact and if they don't form a majority gate [12-14]. The crossover gate is represented by clock 1 as horizontal wire and clock 3 as vertical wire. In any crossover gate there are two combinations of clocks, clock 0 with clock 2 and clock 1 with clock 3.

QCA Component	Symbol	Actual Symbol
QCA Inverter Gate		
3 Input QCA Majority Gate		
Wire of QCA cell		
Crossover Gate		

Fig. 2: Components of QCA symbols.

### QCA clocks

In QCA clocks, it basically gives the direction of cells to control the flow of data. QCA includes four clocks: Switch, hold, release and relax. So the cells are given the direction of flow as per the clocks as 0,1,2,3 as shown in [Fig. 3]. In clock 0 the phase is to start, in clock 1 it will hold the cells, then in 2 clock the cells will be released and finally in the last clock that is clock 3 the cells will be relax and again start from clock 0 [15-20].

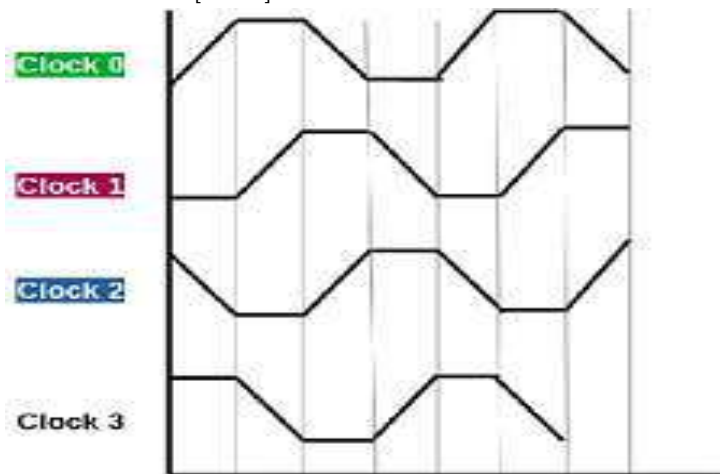


Fig. 3: Clocks in QCA.

## RESULTS AND DISCUSSION

### Proposed design of 1-bit full adder

In the full adder circuit, there are three inputs namely A, B, Cin and output as Sum(S) and Carry (Cout). The truth table of 1-bit Full Adder is given in [Table 1].

**Table 1:** Truth table of 1-bit full adder

A	B	Cin	Sum (S)	Carry (Cout)
0	0	0	0	0
0	0	1	1	0
0	1	0	1	0
0	1	1	0	1
1	0	0	1	0
1	0	1	0	1
1	1	0	0	1
1	1	1	1	1

The equation of Sum(S) and Carry (Cout) is given as:

$$\text{Sum} = A'BCin' + A'B'Cin + AB'Cin' + ABCin$$

$$\text{Cout} = AB + BCin + CinA$$

### Simulation result of 1-bit full adder

A, B, Cin are the inputs, Sum and Carry are the outputs for the given 1-bit full adder design as shown in [Fig. 4].

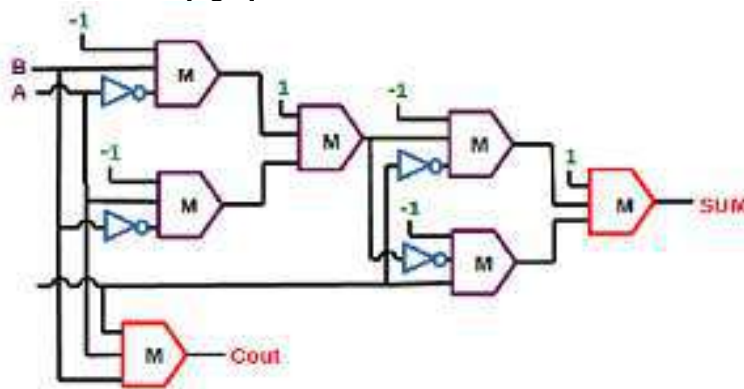


**Fig. 4:** Block diagram of 1-bit full adder using QCA gates.

In the 1-bit full adder design implementation as shown in [Fig. 5], the clocks are used depending upon the gates. The majority gate uses a separate clock cycle. If for AND operation Clock 1 is used then the same clock might be used for other AND operation also. If OR operation is used then Clock 3 is used to get the final output.

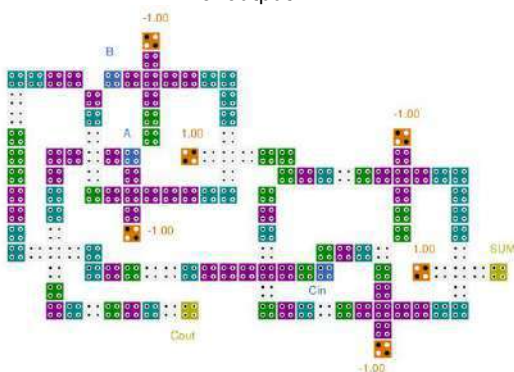


**Fig. 5:** Implementation of 1-bit full adder using QCA designer 2.0.3.

Fig. 6 shows the simulation of 1-bit full adder having Sum and Carry (Cout) as an output.

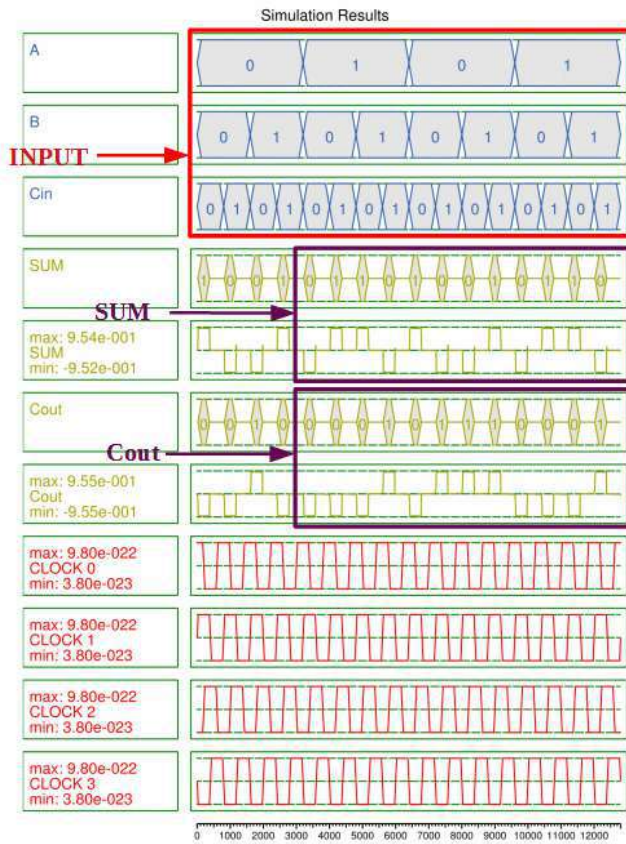


Fig. 6: Simulation of 1-bit full adder using QCA designer 2.0.3.

Proposed design of 2-bit full adder

The 2-bit Full adder comprises of five inputs namely A0,B0,A1,B1,Cin and three outputs namely S0,S1,Cout. The truth table for 2-bit Full Adder is given in [Table 2].

Table 2: Truth table of 2-bit full adder

A0	A1	B0	B1	Cin	S0	S1	Cout
0	0	0	0	0	0	0	0
0	0	0	1	0	0	1	0
0	0	1	0	0	1	0	0
0	0	1	1	0	1	1	0
0	1	0	0	0	0	1	0
0	1	0	1	1	1	1	0
0	1	1	0	0	1	1	0
0	1	1	1	1	0	1	1
1	0	0	0	0	1	0	0
1	0	0	1	0	1	1	0
1	0	1	0	0	0	0	1
1	0	1	1	0	0	1	1
1	1	0	0	0	1	1	0
1	1	0	1	1	0	1	1
1	1	1	0	0	0	1	1
1	1	1	1	1	1	1	1

Simulation result of 2-bit full adder

A0, B0, A1, B1, Cin are the inputs and S0, S1, Cout are the outputs for the proposed 2-bit full adder design as shown in [Fig. 7].

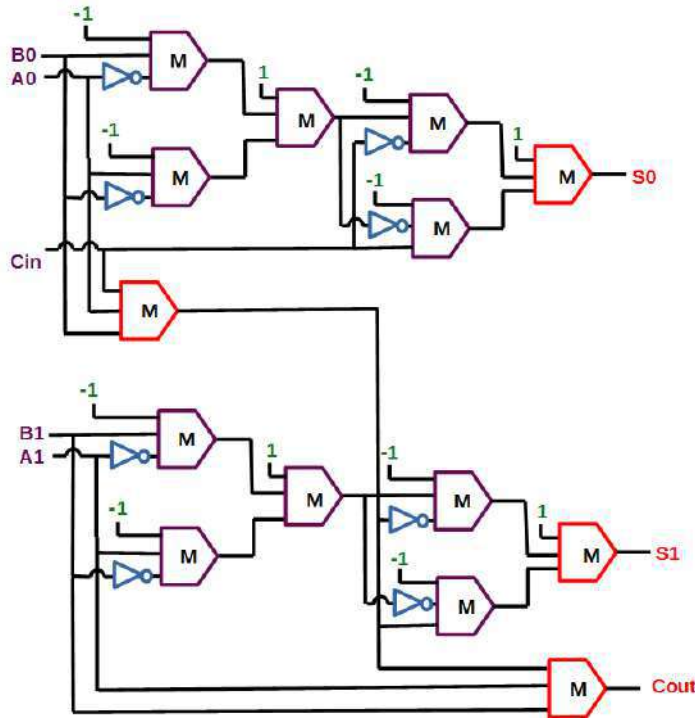


Fig. 7: Block diagram of 2-bit full adder using QCA gates.

In [Fig. 8], the implementation of 2-bit full adder design is shown.

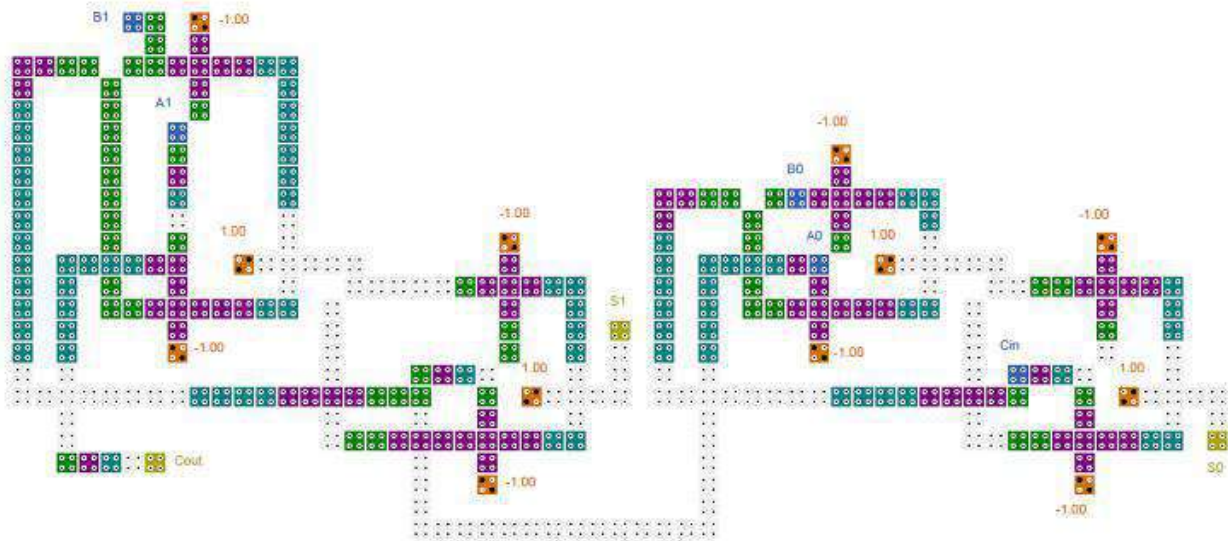


Fig. 8: Implementation of 2-bit full adder using QCA designer 2.0.3.

The simulation of 2-bit full adder is shown in [Fig. 9], which has Sum and Carry (Cout) as the output.

The proposed 2-bit full adder design saves up to 65 % of area and up to 50 % of total cell counts compared to the most recent available full adder design, shown in [Table 3].

The proposed mechanism and style of designing a Full Adder (FA) circuits are novel. The proposed FA uses crossover approach in its design which is best suited for designing any new circuit in QCA technology with minimum number of cells and area. Crossover approach gives a freedom to design the circuit in single layer only compared to multilayer approach, which requires more number of cells, latency and area. The proposed FA circuits are robust and accurate in acquiring its output.



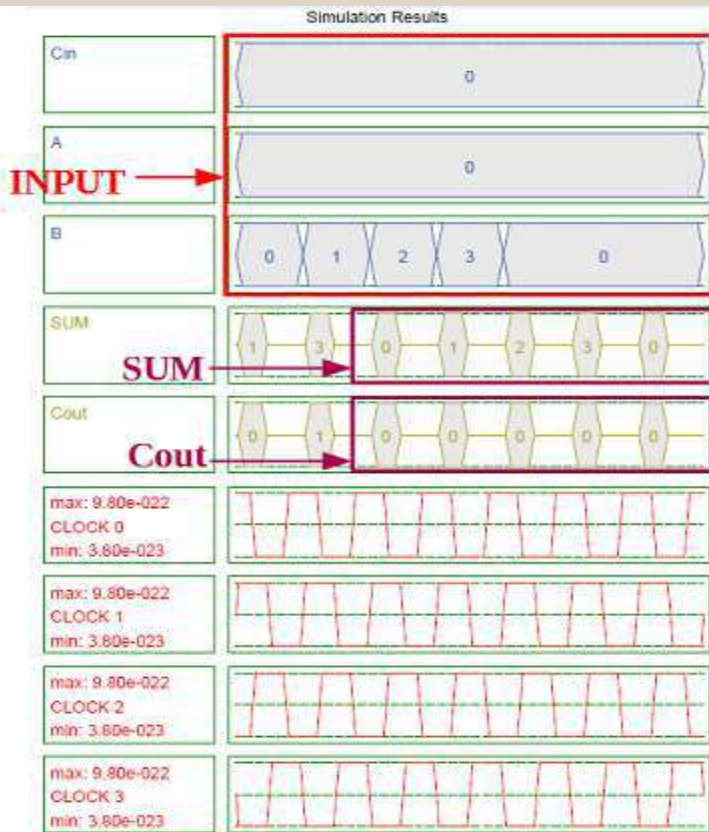


Fig. 9: Simulation of 2-bit full adder using QCA designer 2.0.3.

## CONCLUSION

In these paper basics of QCA, wire of QCA cells, types of gates and QCA clocks have been discussed. The paper comprises of single layer input design on 1-bit full adder as shown in [Fig. 5] and 2-bit full adder as shown in [Fig. 8]. Full adder is a basic circuit in ALU and Microprocessor circuits, which needs to be design very carefully. The proposed 2-bit Full adder design uses 314 numbers of QCA cells, 2 clock latency and area of 0.53  $\mu\text{m}^2$ . In the proposed 2-bit Full adder, the total number of QCA cells is 45% less with almost 33% less area, compared to the previous latest designs. Therefore, the proposed QCA design circuits have fast speed, small size and power consumption is less. The proposed FA designs have the potential to be a basic reference designs for larger designs at digital VLSI technology.

### CONFLICT OF INTEREST

There is no conflict of interest.

### ACKNOWLEDGEMENTS

We would like to thank our Principal Dr. Sanjay Pawar and HOD Dr. Shikha Nema to encourage us for writing this paper. It is our great pleasure to express our gratitude to all those who have contributed and motivated us for completing this work in time.

### FINANCIAL DISCLOSURE

None

## REFERENCES

- [1] Vetteth A, Walus K, Jullien GA, Dimitrov V, Jullien V. [2002] Quantum Dot Cellular Automata Carry-Look-Ahead Adder and Barrel Shifter. In: Proceed. IEEE Emerging Telecommun. Technol. Dallas TX.2-I-4.
- [2] Kim K, Wu K, Karri R. [2007] The Robust QCA Adder Designs Using Composable QCA Building Blocks. IEEE Trans. CAD Integr. Circuits Syst., 26: 176-183.
- [3] AmmarSafavi, A. and Mohammad Mosleh, B. [2013] An Overview of Full Adders in QCA Technology. International Journal of Computer Science and Network Solutions.
- [4] Santra S, Roy U. [2014] Design and Implementation of Quantum Cellular Automata Based Novel Adder Circuits. World Academy of Science, Engineering, and Technology. International Journal of Computer, Information Science and Engineering, 8(1): 178-183.
- [5] Orlov A, Amlani I, Bernstein G, Lent C, Sinder G. [1997] Realization of Functional Cell for Quantum Dot Cellular Automata, Science, 277 (5328): 928-930
- [6] Lent C, Tougaw P, Porod W, Bernstein G. [1993] Quantum cellular automata, Nanotechnology, 4(1): 4957-4963.
- [7] Venkataramani P, Srivastava S, Bhanja S. [2008] Sequential Circuit Design in Quantum Dot Cellular Automata. 8th IEEE Conf. on Nanotechnology, 534-537
- [8] Kassa S, Nagaria R, Karthik R. [2018] Energy efficient neoteric de-sign of 3-input Majority Gate with its



- implementation and physical proof in Quantum dot Cellular Automata, *Nano Communication Networks*, 15(1): 28–40.
- [9] Chaudhary A, Chen D, Hu X, Niemier M, Ravichandran R, Whitton K. [2007] Fabricatable interconnect and molecular QCA circuits, *IEEE Trans. Comput.-Aided Design Integr. Circuits Syst.*, 26(11): 1978-1991.
- [10] Kassa S, Nagaria R. [2016] A novel design of quantum dot cellular automata 5-input majority gate with some physical proofs, *Journal of Computational Electronics*, Springer Publication, 15(1): 324-334.
- [11] Zhang R, Walus K, Wang W, Jullien G. [2004] The Method of Majority Logic Reduction of Quantum Cellular Automata, *IEEE Trans on Nanotechnology*, 3(4): 443-450.
- [12] Amlani I, Orlov A, Kummamuru R, Bernstein G, Lent C, Snider G. [2000] Experimental demonstration for the lead less quantum dot cellular automata cell, *Appl. Phys. Lett.*, 77(2000): 738-740.
- [13] Karthik R, Kassa S. [2018] Implementation of flip flops using QCA tool, *Journal of Fundamental and Applied Sciences*, 10(6S): 2332-2341.
- [14] Rumi Z, Walus K, Wang W, Jullien G. [2004] A method of majority logic reduction for quantum cellular automata, *IEEE Trans. Nanotechnol.*, 3(4): 443-450.
- [15] Cho H. [2007] Adder Designs and Analyses for Quantum Dot Cellular Automata, *IEEE Transactions on Nanotechnology*, 6(3): 374-383.
- [16] Kassa S, Nagaria R. [2017] A Novel Design for 4-Bit Code Converters in Quantum Dot Cellular Automata, *Journal of Low Power Electronics*, 13(3): 482-489.
- [17] Jagarlamudi H, Saha M, Jagarlamudi P. [2011] Quantum Dot Cellular Automata Based Effective Design for Combinational and Sequential Logical Structures, *International Scholarly and Scientific Research & Innovation*, 5(12): 1529-1533.
- [18] Cho H, Swartzlander E. [2007] Adder designs and analyses of quantum dot cellular automata, *IEEE Trans. Nanotechnol.*, 6(3): 374-383.
- [19] Townsend W, Abraham J. [2004] Complex Gate Implementations of Quantum Dot Cellular Automata, 4th IEEE Conference on Nanotechnology, 625-627.
- [20] Kassa S, Nagaria R. [2016] An innovative low power Full Adder design in Nano Technology based Quantum Dot Cellular Automata, *Journal of Low Power Electronics*, 12(2): 107-111.

## ARTICLE

# RENEWABLE ENERGY ON THE SOCIAL AND ECONOMIC GROWTH OF INDIA

Mudit Mishra\*, Shaurya Sindhu

Department of Civil Engineering, Manav Rachna International Institute of Research & Studies, Faridabad, INDIA

## ABSTRACT

India is a vast country and has second largest population in the world. In recent years, India has become a very fast growing economy in the world. To fulfill the human and infrastructural requirements a huge amount of energy will be required in near future. Presently the major source of energy in India is through thermal power plants. It is the approximately 65% of total energy generated. Rest of energy is being generated from hydro, wind, solar and nuclear sources. However, the production of energy from these sources is quite low so far. In thermal power plants coal is used as a fuel and burning of coal creates a lot of environmental and health problems. Also efficiency of thermal power plants is less and it produces a larger quantity of waste material such as fly ash. The disposal of these materials is a matter of serious concern. Further the reserve of coal is limited. Hence to produce clean and green energy, the focus has come on the renewable energy. The renewable energy may be derived from natural resources like water, wind, sun and plants as mentioned before, conserving the natural resources at the same time. Also, it contributes in welfare and growth of the society and country. The present paper summarizes the discussion on different sources of renewable energy and their effect on the social and economic growth of India

## INTRODUCTION

In the modern world, India is being emerged as the fastest growing economy. To meet the human and infrastructural requirements a lot of energy is needed in future decades. The main source of energy in India is coal based thermal power plants. It generates power more than 65% of the total production. The reserve of coal in India is limited and till 2050 more than 90% of its reserve will be consumed. The coal based thermal power plants generate huge amount of pollutants and solid waste. The effective disposal of generated pollutants and wastes a matter of serious concern. Also, it releases the huge amount of hot gases into the atmosphere which increases the global warming. To avoid this situation, one can switch to alternate or renewable energy sources. Renewable energy comes directly from the natural sources and is very less hazardous. Based on the birth sources, it can be classified in different categories like solar energy, wind energy, hydro energy, geothermal energy and fusion nuclear energy. Unfortunately, the production of the energy from these sources is quite low. The main advantage of the renewable energy is that it uses the natural sources which are available at free of cost. Further, no harmful pollutants are emitted during the production. It conserves the degradation of natural resources and produce green energy. The social impact of renewable energy is very high and it can be contributed towards the growth of the economy. In the present paper the social and economic growth of the renewable energy are summarized [1].

### KEY WORDS

Renewable energy,  
Economic growth, Social  
impact

Received: 28 Mar 2019  
Accepted: 21 May 2019  
Published: 29 June 2019

## DIFFERENT SOURCES OF ENERGY

### Solar energy

Sun is a major source of energy and its energy available throughout the year. Solar energy comes from the sun in the form of solar radiation. By using solar panels and photovoltaic cells the radiation is converted in electricity. Solar energy can be generated in any part of the earth and it reaches at remotely located places, where other sources of energy are not feasible. The initial cost of installation of solar panels is comparatively high but the maintenance cost is low. For individual installation, no grid formation is required [2].

### Hydropower energy

Hydropower comes from energy of water and now-a-days becomes the major source of energy after the thermal power. By constructing dams over the rivers, the power of water can be utilized. A hydro power plant consists of a dam, a reservoir and a production unit. The construction of hydropower plants is a tedious and challenging job and it requires a lot of technical expertise. Its social impact is too high as compared to others sources of energy [3].

### Geothermal energy

Geothermal energy is generated from the earth's crust, which has a lot of potential. It found deep below the surface of the earth. Hot molten magma produces a lot of heat, which are converted to electrical

\*Corresponding Author

Email:  
mudit.mishra2607@gmail.com  
Tel.: +919971898822

energy. However, it is not available at all over the earth but can be found at certain places. It is a clean and renewable form of energy because it does not contribute to any greenhouse emission [4].

**Wind energy**

Wind energy is also a source of renewable energy. The power of wind is extracted to produce green and clean energy. Air current flowing across the earth's surface is utilized and using wind turbines, kinetic energy of the wind is converted to electric energy. Generally individual wind turbines are small in capacity, but as a whole it can produce huge amount of energy [1].

**Nuclear energy**

Nuclear energy is produced by the fission or fusion process of the material. However, a fusion process can be treated as a source of renewable energy because it comes from the Hydrogen. Compared to fission reactors, fusion reactors are more environmentally friendly. It produces a lot of energy by using few amount of hydrogen fuel. It can be a major source of energy in future if utilized properly [1].

A comparison of different types of renewable energy resources is presented in [Table 1].

**Table 1:** Comparison of different Renewable Energy Sources

Description	Solar Energy	Hydro Energy	Geothermal Energy	Wind Energy	Nuclear (Fusion)
Source	Sun	Water	Hot magma present in the earth crust	Wind	Hydrogen
Environmental Effect	Pollution free, no emission of pollutants	Pollution free, no emission of pollutants	Pollution free, very less amount of pollutants emission	Pollution free, no emission of pollutants	Pollution free, very less amount of pollutants emission in the operation phase
Waste Generation	No waste is generated	No waste is generated	No waste is generated	No waste is generated	No waste is generated
Fuel requirement	No	No	No	No	Yes
Storage	Can be stored through batteries	No storage	No storage	No storage	No storage
Initial Installation Cost	High for individual installation, Medium for power plant installation	Very High	Medium	Low	Very High
Maintenance Cost	Low	Medium	Low	Low	High
Coverage Area	Medium	Very Large	Medium	Low	Very Large
Special Technology Requirement	No	No	Yes	No	Yes
Safety and Security Requirement	Low	High	Low	Low	Very High
Major Advantage	Can be reached at remotely located places, where other sources of energy is not feasible	Multipurpose utility, power generation , irrigation, storage of water	Requires very less maintains and releases the pressure of earth, reduces the chance of unwanted volcanic eruption	Requires very less installation and maintenance cost and no special arrangement are required, best suitable in coastal areas	Provides massive amount of energy using small amount of fuel
Major Disadvantage	Depends upon the	Construction cost and	Not available at	Depends upon the	Highly specialized

THE IIOAB3 JOURNAL

	availability of sun light, not useful in area where the availability of sun light is rare	time is too large, also heavy machinery and manpower are required	all the places, available only at its potential locations	speed and availability of wind, not available at locations where wind power is low	techniques are required for construction and operation of fusion reactors, research is still going on
--	---	---	---	--	---

**Social and Economic impact**

India is a fast growing economy and has the 2nd largest population in the world. To fulfil the infrastructural and human requirements the energy requirement is mandatory. The social and economic impact of renewable energy resources is different and depends upon the situation and locations. Presently in India total power generation is approximately 1, 11, 901 MW, in which only 18.2% comes from the renewable energy sources which is low [Table 2]. The most power comes from thermal power plants which are about 66%. However, the reserve of coal is limited and till 2050 most of it reserve will be consumed. So that focus must be on the production of energy through renewable energy [1].

As discussed renewable energy comes from natural sources and generates clean and green energy. Due to thermal power plants a large amount of pollutants diffuses into the atmosphere which is harmful for human life. Generation of hot air by the thermal power plants, also increase the temperature of the earth and contributed in greenhouse emission. Huge amount of waste is generated by the burning of coal and its disposal is a matter of serious concern. Gases released from the thermal plants cause several diseases. It influenced the growth of the human being which indirectly affects the growth and economy of the country. If due to diseases, or health concern people are not efficient, the overall growth of the country will be affected badly. Hence, to avoid such situations the focuses should be on 'increase the energy generation by renewable energy sources' [1].

**Table 2:** Total installed capacity in India (Up to December 2017)  
(Source: Ministry of Power, Government of India, [1])

Type of Plant	Total generation in MW	Percent of total Production (%)
Thermal	2,18,960	66.2%
Hydro	44,963	13.6%
Nuclear	6,780	2.0%
Other renewable energy sources (Small Hydro, Solar, Wind etc.)	60,158	18.2%
Total	1,11,901	

The impacts of different types of renewable energy sources are different. It depends upon the following factors

- i. Requirement
- ii. Social impact
- iii. Investment cost
- iv. Benefits
- v. Safely and Security.

For production of energy 'requirement' is must. To fulfil the requirement feasibility study is carried out to understand whether it is feasible or not. The study consists social and environmental factors, benefits, cost and safety issues. However, in these factors requirement and social impact has the most impact. For implementation of a renewable energy project there are two sides one is social impact and other is economical effect. Social impact can be termed as the influence of the project on the life of the mankind. It covers the following points

**a. Routine life of public:** Energy plays a vital role in every human life. Hence, impact of energy on its daily life is crucial. Also, pollutants from thermal power plants cause health issues. Hence he has full right to take clean and green energy. Renewable energy is environmental friendly and hence it is best suitable as per health concern. Except hydro and nuclear energy all the other sources are best suited to daily life of public in India [1].

**b. Total influenced area:** For generation of large amounts of power, a power plant and grid is required. For installation of it a large area will be required and it evacuated some populated areas. Installation of hydro and nuclear plants wants a wider area. Also, the area around it should be covered in

'population free zone' due to proper operation, maintenance and security reasons. Wind, solar and geothermal plants are comparatively small in nature and generally installed in the non-populated areas. The impact of hydro and nuclear power on the social life is higher because it involves the shifting of population, which is very difficult to achieve in Indian situation. India is the second largest pollution in the world and shifting of small amount of people is a tedious job due to political and economic reasons [1].

**c. Safety and securities:** All the renewable energy plant should be safe against failure and must have higher degree of securities. Due to improvement in research and technology, it can be achieved and implemented. Hydro and nuclear power plants require extra safety feature because if they meet any accident larger casualties will be happening. In geothermal plants, sometimes eruption of magma is occurred due to large pressure and temperature. It causes the adverse effect on the environment and the health of human. Hence extra safety features should be enabled to protect the human life [1].

Similarly, social impact & economic impacts can be defined. However, economical aspect is the most dominating factor in India. India has high potential of renewable energy sources, but unfortunately due to lack political willpower and unawareness the resources are not fully utilized. Because of this dependency increases on the thermal power plant which is costlier than renewable energy resources. Per unit cost of power production of thermal power plants is higher as compared to renewable energy sources. Hence, by using renewable energy resources a lot of money can be saved which will be utilized in other constructive works. In India most of the power plants are running on coal. Extraction of coal from mine also causes health issues. Further, during the production of energy a lot of gases and waste is generated. It causes the lot of health issues and huge amount of money is required for treatment. A lot of money also spends on the disposal of waste produced by the thermal power plants. If the amount of money spend on these problems are saved, the economy will be boosted up. Use of renewable energy sources can reduce this problem and hence contributes to the growth of the economy [1].

The installation cost of the some of the renewable energy plants i.e. hydropower and nuclear power is higher, but if we see at growth point of view it contributed higher in economy. It provides us the power at cheaper rates. Special technology is required for geothermal and nuclear (fusion) power plant which is achievable. All the renewable energy has different impacts. Some of them has higher impact and some of have low impact. In [Table 3], impacts of different renewable energy on social and economic growth are listed.

Solar energy has low social impact because it requires less resources, area and mobilization. Similar to this wind and geothermal energy has low social impact. Hydro and nuclear energy have high impact due to larger mobilization of people, consummation of larger area and utilization of higher resources. However, they contribute higher in the economic growth. Wind energy has least impact on social and economic growth because it requires very less mobilization and generates small amount of energy compared to others. Geothermal energy requires very less mobilization because it's available at remote location which is far away from the populated area. All the available renewable energy sources contribute in their own way and their little contribution; also boost up the economy of the country. For the growth of the country, it is necessary that the renewable energy resources are fully utilized. Potential of renewable energy resources should be identified and feasibility study must be carried out. This leads our step towards the green and clean India [1].

**Table 3:** Impact of different renewable energy on Economy and Social Growth of India

Type of Renewable Energy	Social Impact	Economical Impact
Solar Energy	Low	Medium
Hydro Energy	High	High
Geothermal Energy	Low	Medium
Wind Energy	Low	Low
Nuclear (Fusion)	High	High

## CONCLUSION

Renewable energy has significant social and economic effects. If the potential of renewable energy resources is identified and fully utilized, it will boost up the economy and social growth of the India. It provides clear and green energy and can fulfill the future energy requirements. Due to this, global warming and relative health issues will be diminished. Also, dependency on the thermal power plants will be substantially reduced, which help us to conserve the natural resources.

### CONFLICT OF INTEREST

There is no conflict of interest.

### ACKNOWLEDGEMENTS

The authors express their deepest gratitude towards the help of Accendere Knowledge Management Services, New Delhi, India for giving the valuable suggestions for preparing the manuscript.



FINANCIAL DISCLOSURE

None.

REFERENCES

- [1] Annual Report [2017], Ministry of Power, Government of India.
- [2] [https://en.wikipedia.org/wiki/Solar\\_power\\_in\\_India](https://en.wikipedia.org/wiki/Solar_power_in_India)
- [3] <https://www.studentenergy.org/topics/hydro-power>.
- [4] <https://www.renewableenergyworld.com/geothermal-energy/tech.html>

## ARTICLE

## VISUAL DATA REPRESENTATION SYSTEM FOR ICE TESTING

Lenar A. Galiullin\*, Rustam A. Valiev

*Naberezhnye Chelny Institute, Kazan Federal University, 68/19 Mira Ave., Naberezhnye Chelny, RUSSIA*

## ABSTRACT

Leading engine manufacturers carry on investigations and R&D work to improve reliability and durability of internal combustion engines (ICE), particularly, diesel engines. Diesel engine examination and testing are the main methods, allowing to verify manufacturing quality of parts and assembly components, units and engine in whole, accuracy of assembling, correspondence of main diesel engine characteristics to the requirements of technical specifications. The types of diesel engine test procedures are regulated by the state standards (GOST) and international standards (ISO), which define the procedures for engine commissioning and requirements to engine performance standards. Manufacturers continue to improve the construction of engines and performance indicators even after their commissioning and installation. Current diesel engine test procedure is complex and time-consuming process that can be compared with experimental studies. For this reason, automation systems for engine testing (AST) are created. The need for constant improvement of performance standards of diesel engines raise the costs with respect to test procedures in the course of development of new engine prototypes. In particular, high costs are associated with a mismatch between a level of automation of manufacturing and R&D works. Therefore, automation of test procedures is one of the main goals to be achieved in order to improve the level of technology at production and quality of manufactured diesel engines.

## INTRODUCTION

## KEY WORDS

engine; decomposition;  
automation; test; diesel;  
simulation.

Effective interaction facilities used by product engineer and ECM play an important role in automation systems for engine testing (AST) development [1]. As a rule, internal data is represented in the computer systems in a specific format that cannot be understood by a common user.

In order to solve the problem with effective interaction of human and ECM it is necessary to use a working language that should be close to natural language (NL). NL interaction can be developed with the help of cognitive graphics [2].

For a long time, tasks and task-solving procedures were divided into formal-logical and graphical-intuitive. However, this approach does not meet current requirements any more. Effective solution even of a perfectly formalized task requires graphical-intuitive reasoning to be applied both at the stage of hypothesis generation and at all consequent stages, including the stage of decision making. This fact is stipulated both by the necessity of complete data representation that cannot be achieved with formal-logical tools, and by much higher pass-through rate of visual analyzer in case of integral-graphic representation of information in comparison with serial-character representation, for example, textual. In human-computer systems designed to solve such tasks, taking into account specific capabilities of ECM and human with regard to data processing, the computer may play such a role that would allow to transform input data within the framework of formal-logical description in a way that makes it possible to reveal a pattern contained in it by representing such data in a form that is convenient to a specialist.

If to consider graphics as a modeling tool, firstly, it is necessary to note that a model should fit the represented phenomenon adequately. In other words, not every type of graphical representation suits every specific phenomenon [3]. Secondly, like every model, graphical representation of a phenomenon is not a detailed representation. Besides, a model may require (in most cases implicitly) an assumption concerning the character of phenomenon to be fulfilled. For example, representation in the form of surface assumes a continuous character of the phenomenon. For this reason, it is desirable to have a possibility both to observe a model, and to rebuild it dynamically by changing information content (a set of variables and their multiple values) and modifying the parameters: scale, appearance of components, consistency between values of displayed attributes and visual variables, representing them [4].

## MATERIALS AND METHODS

Decomposition of test procedure should be implemented to create graphic structures, describing test process. The paper [5] offers decomposition principle, allowing to split the procedure into units, blocs, modes, modules, and elementary operations. Elementary operations represent indivisible procedural components, like switch actuation, signal pick-up from a specific device, etc. In our situation this principle doesn't work, as graphic structures of high information capacity will be used in technology language [6]. For this reason, they cannot be used as elementary operations. We will decompose enlarged structures. Let's represent the procedure in the form of control operations. Let's define the following levels of a control operation:

- Engine crankshaft speed control;
- Brake assembly control;
- Oil, fuel, cooling fluid temperature control;
- Environmental simulation (for example, imitation of weather conditions).

## \*Corresponding Author

Email:  
galilenar@yandex.ru  
Tel.: 8-906-124-53-18

Received: 8 Aug 2019  
Accepted: 26 Sept 2019  
Published: 30 Sept 2019

In its turn, each control operation should be also decomposed [7]. As we are going to deal with characteristic curves, consisting of specific segments (for example, in case of engine crankshaft speed control process a user will use rotation speed/time curve with specific segments: drive, brake, constant speed), it is necessary to carry out decomposition by those segments [8]. As a result, we obtain the elementary components, i.e. the components, which constitute the whole engine test procedure, allowing to display the task with the help of graphical representations, to control the procedure [9].

Hence, we obtain four levels of detailization and concretization of general test tasks, when using adopted principle of decomposition:

- General procedure (P),
- Control operation (CO),
- Control operation for a specific device (COj),
- Elementary control operation (ECOi).

Control operations allow to manage test modes [10]. Besides, they are functionally dependent from ECO. Other levels represent the bunch of underlying components.

Elementary control operations and measurements represent the complex groups, consisting of uniform sub-programs used to fulfill a specific task [11].

Hence, it is possible to represent random test procedure P as a function of control operation C:

$$P = [C_{ij}]_{mn}$$

where

$[C_{ij}]_{mn}$  – is a set of unified i-th parametrically customized technological control operations of j-th functional type;

m – is a number of elementary operations with regard to a specific control operation implemented on different types of control devices;

n – is a number of functional types of control operations.

Let's represent a random unified parametrically customized technological control operation  $y_{ij}$  as follows:

$$y_{ij} = \{d'_{ij}; W_{ij}(d'_{ij} | w_{ij}); d_{ij}\}$$

where

$d'_{ij}$  is an input data vector for a control operation,

$d_{ij}$  – is an output data vector for a control operation,

$W_{ij}$  – is an algorithm of transformation of input data into output data,

$w_{ij}$  – is a vector parameter for control operation adjustment.

Functional types of technological operations follow the adopted principle of decomposition and generalized cycle of test operations [12]. This type of operations includes engine mode control operation, load device control operation, etc.

Let's assume that engine crankshaft speed control operation is the control operation of the first functional type and  $j=1$ , then we will obtain the following random elementary engine shaft speed control operation:

$$y_{i1} = \{d'_{i1}; W_{i1}(d'_{i1} | w_{i1}); d_{i1}\}$$

Consequently, test procedure can be represented as a matrix with a number of elementary control operations [13]. Matrix columns are the elementary control operations of a specific functional type. This decomposition was carried out in order to apply graphical representations in AST. For this reason, it is necessary to decompose graphical test language in accordance with the decomposition principle suggested above by specifying typical linguistic tools for elementary control operations of corresponding functional type [14].

Decomposition of engine test language means language representation in the form of its possibly intersecting fragments with specified purposes, which, being taken together, allow to describe random automatic test procedures [15].

Possibility to decompose AST language on the basis of graphic elements results from earlier mentioned decomposition principle used with regard to test procedure. Hence, we obtain the following equation by analogy with:

$$L = [L'_{ij}]_{mn}$$

where

$[L'ij]_{mn}$  – is multiple fragments of AST language, which is the language of  $i$ -th technological control operations of  $j$ -th functional type.

As unified parametrically customized technological operation is the basic concept of test procedure, it is necessary to take the following unified linguistic description of the operations as a basis for language unification  $L'ij$  ( $i=1\dots m, j = 1\dots n$ ):

$$l'ij = \{t'ij; G'ij(t'ij)\}, i=1\dots m, j = 1\dots n$$

where

$t'ij$  – is a graphical representation of input data for  $i$ -th control operation of  $j$ -th functional type,  
 $G'ij$  – are the grammatical forms of algorithm descriptions with regard to control operation.

The grammatical form is the most rational tool for language representation of technological operations [16].

Equation results, taking into account the specific character of graphical representation of technological operations [17]. We have no input data here, as it does not make sense to represent it in graphical form [18]. It is supposed that setting data contains data-intensive graphical elements of input data.

Grammatical form uses essential notions and definitions of automated test domain [19].

If  $j=1$ , we obtain a linguistic description of the operations of the first functional type, i.e. control operations (i.e. engine crankshaft speed control operation mentioned above) [20]:

$$l'i1 = \{t'i1; G'i1(t'i1)\}$$

Hence, linguistic support consists of a matrix that contains the components of technology control language [21], in which the matrix columns contain linguistic description of elementary control operations of a specific functional type [22].

Taking into account condition-action rules it is possible to represent the system as follows [23]:

$$GE_{aij} = W_{aij}$$

where

$GE_{aij}$  and  $A_{aij}$  – are condition (graphical element) and action of  $a$ -th production ( $a=1\dots a$ ) respectively;

$a$  – is a number of variants of execution of technological control operation  $y_{ij}$  ( $i=1\dots m, j=1\dots n$ ).

Hence, variants of execution of control and measurement operations are explicitly bind to graphic elements, defining them [24].

## RESULTS AND DISCUSSION

The following unified conditions necessary to launch and complete component execution, and transition conditions for sequential execution of components are used [25]:

- Expiration of predefined time period [26];
- Arrival of specified triggering signal [27];
- Band fault (alert condition) [28].

Hence, the unification of composition fragments  $L'ij$  ( $i = 1\dots m, j = 1\dots n$ ) of engine test system language is provided by [29]:

- Unified linguistic description of technological control operations with six functional types of basic control operations [Table 1];
- Unified linguistic description of variants of execution of technological control operations in the form of condition-action rules.

System analysis of automatic engine test procedures described above and suggested principles of formalization of their linguistic description allow to proceed with modeling of characters for graphical test language, and then with modeling of its grammar rules.

Representation of operations in the form of condition-action rules is the most suitable form of representation of test procedures used by a test engineer. This was demonstrated by psychological investigations of human decision-making process: when reasoning, an individual uses “condition-action” rules, i.e. the rules, which are similar to the productions. Besides, the productions are the most important components of the production systems, which are used as a basis for the development of the major part of intelligence systems, particularly, for the development of expert systems. Moreover, a test engineer uses task-oriented graphical representations by setting the conditions for execution of technological operations,

which significantly simplify his work, as the appearance of representation allows to assess the final result – the representation is identical to control operation. Consequently, the application of graphical representations and production representation of technological operations promotes the development of automation systems for engine testing with the involvement of intelligence systems.

## CONCLUSIONS

The process of test procedure development with the help of graphical language comes down to the creation of desirable technological parameters-time dependency graphs from the graphical representations of elementary operations.

### CONFLICT OF INTEREST

There is no conflict of interest.

### ACKNOWLEDGEMENTS

The work is performed according to the Russian Government Program of Competitive Growth of Kazan Federal University.

### FINANCIAL DISCLOSURE

None.

## REFERENCES

- [1] Galiullin LA, Valiev RA. [2016] Modeling of internal combustion engines test conditions based on neural network. *International Journal of Pharmacy and Technology*. 8(3):14902-14910.
- [2] Guihang L, Jian W, Qiang W, Jingui S. [2011] Application for diesel engine in fault diagnose based on fuzzy neural network and information fusion. 2011 IEEE 3rd International Conference on Communication Software and Networks, ICCSN 2011. art. no. 6014398. 102 - 105.
- [3] Galiullin LA, Valiev RA. [2018] An automated diagnostic system for ICE. *Journal of Advanced Research in Dynamical and Control Systems*. 10 (10):1767-1772.
- [4] Shah M, Gaikwad V, Lokhande S, Borhade S. [2011] Fault identification for I.C. engines using artificial neural network. *Proceedings of 2011 International Conference on Process Automation, Control and Computing, PACC*. art. no. 5978891.
- [5] Yu Y, Yang J. [2011] The development of fault diagnosis system for diesel engine based on fuzzy logic. *Proceedings. 8th International Conference on Fuzzy Systems and Knowledge Discovery, FSKD*. 1. art. no. 6019556.472 - 475.
- [6] Wei D. [2011] Design of Web based expert system of electronic control engine fault diagnosis. *BMEI- Proceedings. International Conference on Business Management and Electronic Information*. 1. art. no. 5916978. 482 - 485.
- [7] Galiullin LA, Valiev RA. [2018] Method for neuro-fuzzy inference system learning for ICE tests. *Journal of Advanced Research in Dynamical and Control Systems*. 10(10):1773-1779.
- [8] Galiullin LA, Valiev RA. [2018] Modeling of internal combustion engines by adaptive network-based fuzzy inference system, *Journal of Advanced Research in Dynamical and Control Systems*. 10 (10):1759-1766.
- [9] Ahmed R, El Sayed M, Gadsden SA, Tjong J, Habibi S. [2015] Automotive internal-combustion-engine fault detection and classification using artificial neural network techniques. *IEEE Transactions on Vehicular Technology*. 64(1):21-33.
- [10] Galiullin LA, Valiev RA. [2018] Optimization of the parameters of an internal combustion engine using a neural network. *Journal of Advanced Research in Dynamical and Control Systems*. 10 (10):1754-1758.
- [11] Chen J, Randall R, Feng N, Peeters B, Van Der Auweraer H. [2013] Automated diagnosis system for mechanical faults in IC engines. 10th International Conference on Condition Monitoring and Machinery Failure Prevention Technologies, CM 2013 and MFPT. 2:892-903. doi: 10.1533/9780857094537.10.679
- [12] Chen J, Randall R, Peeters B, Desmet W, Van Der Auweraer H. [2012] Neural network based diagnosis of mechanical faults in IC engines. *Institution of Mechanical Engineers - 10th International Conference on Vibrations in Rotating Machinery*. 679-690. doi: 10.1533/9780857094537.10.679
- [13] Randall RB. [2009] The application of fault simulation to machine diagnostics and prognostics. 16th International Congress on Sound and Vibration, ICSV. 8:5042-5055. doi: 10.20855/ijav.2009.14.2240.
- [14] Galiullin LA, Valiev RA, Lejsan Mingaleeva B. [2018] Development of a Neuro-Fuzzy Diagnostic System Mathematical Model for Internal Combustion Engines. *HELIX*. 8(1):2535-2540.
- [15] Wu JD, Huang CK, Chang YW, Shiao YJ. [2010] Fault diagnosis for internal combustion engines using intake manifold pressure and artificial neural network. *Expert Systems with Applications*. 37(2):949-958.
- [16] Galiullin LA, Valiev RA. [2017] Mathematical modelling of diesel engine testing and diagnostic regimes. *Turkish Online Journal of Design Art and Communication*. 7:1864-1871.
- [17] Danfeng D, Yan M, Xiurong G. [2009] Application of PNN to fault diagnosis of IC engine. 2nd International Conference on Intelligent Computing Technology and Automation, ICICTA. 2(5287738):495-498.
- [18] McDowell N, McCullough G, Wang X, Kruger U, Irwin GW. [2008] Application of auto-associative neural networks to transient fault detection in an IC engine. *Proceedings of the 2007 Fall Technical Conference of the ASME Internal Combustion Engine Division*. 555-562. doi: 10.1115/ICEF2007-1728.
- [19] Galiullin LA, Valiev RA. [2017] Diagnostics Technological Process Modeling for Internal Combustion Engines. *International Conference on Industrial Engineering, Applications and Manufacturing (ICIEAM)*. doi: 10.1109/ICIEAM.2017.8076124.
- [20] Galiullin LA, Valiev RA. [2017] Diagnosis System of Internal Combustion Engine Development. *Revista Publicando*. 4(13):128-137.
- [21] Galiullin LA, Valiev RA, Mingaleeva LB. [2017] Method of internal combustion engines testing on the basis of the graphic language. *Journal of Fundamental and Applied Sciences*. 9(1):1524-1533.
- [22] Galiullin LA. [2016] Development of Automated Test System for Diesel Engines Based on Fuzzy Logic. *IEEE 2016 2ND International Conference on Industrial Engineering, Applications and Manufacturing (ICIEAM)*. doi: 10.1109/ICIEAM.2016.7911582.
- [23] Li X, Yu F, Jin H, Liu J, Li Z, Zhang X. [2011] Simulation platform design for diesel engine fault. *International Conference on Electrical and Control Engineering, ICECE 2011 - Proceedings*. art. no. 6057562. 4963 - 4967.
- [24] Isermann R. [2005] Model-based fault-detection and diagnosis - Status and applications. *Annual Reviews in Control*. 29(1):71-85.
- [25] Valiev RA, Khairullin AKh, Shibakov VG. [2015] Automated Design Systems for Manufacturing Processes. *Russian Engineering Research*. 35(9):662 - 665.
- [26] Galiullin LA, Valiev RA. [2018] Control vector for ice automated test and diagnostic system. *dilemas contemporaneos-educacion politica y valores*. 6:95.



- [27] Galiullin LA, Valiev RA, Khairullin Haliullovi A. [2018] Method for modeling the parameters of the internal combustion engine. IIOAB JOURNAL. 9:83-90. <https://doi.org/10.1016/j.protcy.2012.03.027>.
- [28] Galiullin LA, Valiev RA. [2018] Internal combustion engine fault simulation method. IIOAB OURNAL. 9:91-96. doi: 10.1088/1757-899X/421/2/022042.
- [29] Galiullin LA, Valiev RA. [2016] Automation of Diesel Engine Test Procedure. IEEE 2016 2ND International Conference on Industrial Engineering, Applications and Manufacturing (ICIEAM). doi: 10.1109/ICIEAM.2016.7910938.

# ARTICLE

## NEURAL NETWORK FOR INTERNAL COMBUSTION ENGINES TESTING

Lenar A. Galiullin\*, Rustam A. Valiev

Naberezhnye Chelny Institute, Kazan Federal University, 68/19 Mira Ave., Naberezhnye Chelny, RUSSIA

### ABSTRACT

In the present world the problems of the fuel and energy resources' optimization consumption belong to challenging issues. Transport consumes more than 30% of the produced hydrocarbons, and the fuel costs account for about 20% of the product cost. More highly charged is the environmental contamination, and more than half of the emissions can be attributed to the share of internal combustion engines (ICE). Production of the internal combustion engines is enhanced towards improving the engine's environmental, economic and operational parameters. This involves the use of electronic control units - ignition control and fuel injection systems. It allows to greatly reducing the ICE energy consumption and emission toxicity. During the vehicle operation corresponding units and knots always wear and age. This leads to deterioration of economic, environmental and effective parameters of a vehicle. Therefore, in order to maintain an ICE in the optimum condition and to early detect any changes in the parameters that lead to deterioration of the environmental, economic and effective parameters of its operation, the main aspect includes the maintenance and repair system, its scientific validity and perfection. In such case the technical diagnostics is of paramount importance.

### INTRODUCTION

Enhanced production of cars, tractors and their increasing role in meeting the modern society's needs lead to a continuous improvement of the machinery power units - internal combustion engines (ICE) [1]. Declared ICE power, cost effectiveness, toxicity and other estimates, as well as its reliability and durability are set by the tests in the bench and in operation conditions [2]. Currently, all newly created, modernized and serial car and tractor engines are subject to various kinds of tests, which nature, scope and content are determined by their purpose and specified in the GOST [3]. The tests constitute the final stage of the complex process of creating and improving the internal combustion engines [4]. In this regard, all newly created, modernized and serial internal combustion engines are tested in a different way [5]. The tests allow to estimate the engine's quality and to compare its performance with that of other engines [6]. The test process specifies engine's traction and dynamic, economic, environmental, and other indicators and establishes compliance of these indicators to the standards and specifications [7]. The tests reveal the engine's characteristics and the comparison of test results of different types of engines allows to estimate the effectiveness of their design features, workmanship and technical condition.

At present, the ICE tests represent a complicated and time-consuming process, which little different from the experimental study [8]. Therefore, ICE automated inspection systems (ICE AIS) are created.

When studying an ICE and designing its mathematical model, a problem of obtaining the object operation law as a whole or some parts thereof usually arises [9]. Such model cannot most often be designed based on the known regularities, and a type of the object operation law is unknown. In such cases, solution to this problem can be reduced to allocating any significant input and output characteristics of the object and conducting a series of experiments in order to obtain any object operation data in particular cases.

In order to solve this problem, the hybrid neural networks are proposed to be used to adjust the fuzzy systems.

### MATERIALS AND METHODS

A fuzzy hybrid neural network represents a clear neural network, which is based on a multi-layer perceptron [Fig. 1].

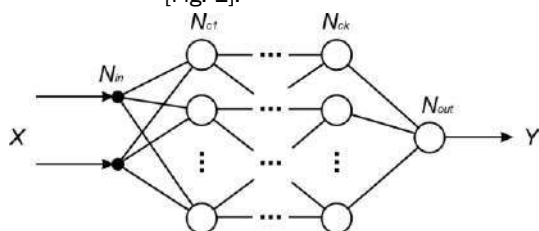


Fig. 1: Multilayer structure of hybrid network.

#### KEY WORDS

Tests, neural network, automatization, system, engine.

Received: 16 Aug 2019  
Accepted: 30 Sep 2019  
Published: 3 Oct 2019

\*Corresponding Author

Email:  
galilenar@yandex.ru

where

X means a vector of input parameters;  
Y means a vector of output parameters;  
Nin, Nout means an input and output layer;  
Nc1, Nck means hidden layers.

The hybrid network for the adjustment of fuzzy system, as opposed to a multi-layer perceptron, includes an adaptive layer of membership functions; logical AND-, OR-neurons (logical neurons modelling logical connectives) [10].

The network visualizes an input vector to an output one  $X \rightarrow Y$ :

$$y = \sum_{i=1}^M \frac{w_i}{\sum_{j=1}^N w_j} \left( p_{i0} + \sum_{j=1}^N p_{ij} x_j \right)$$

which can be expressed as

$$y(x) = \frac{1}{\sum_{k=1}^M w_k} \sum_{k=1}^M w_k y_k(x)$$

where ;

$$y_k(x) = p_{k0} + \sum_{j=1}^N p_{kj} x_j$$

N means a number of input variables;  
wk means weights of various neuronal links;  
p0, p1, ..., pN means digital weights selected in the adaptation (learning) of a network.

The weights wk present in this expression are interpreted as a significance of the components  $\mu_A^{(k)}(x)$  (degree of membership of a specific numerical value to a fuzzy mark A) [11]. Under this condition, the formula can be compared to the multilayer network structure.

If  $y_i(x)=c_i$ , then:

$$y(x) = \frac{\sum_{i=1}^M c_i w_i}{\sum_{i=1}^M w_i} = \frac{\sum_{i=1}^M c_i \cdot \prod_{j=1}^N \mu_{ij}(x_j)}{\sum_{i=1}^M \prod_{j=1}^N \mu_{ij}(x_j)}$$

where ci means a weight ratio (in terms of fuzzy systems, this is the membership function centre of the right part of fuzzy rules);

$\mu_{ij}()$  means the Gaussian function in exponential form with parameters of the centre  $c_{ij}$ , width  $\sigma_{ij}$  and shape  $b_{ij}$ . From the point of the fuzzy systems,  $\mu_{ij}()$  means a membership function to a fuzzy set. The engine operation during the tests is represented as vector X of a desired variation in time of the ICE input parameters [12]. The engine operation time with the specified parameters depends on a type of tests and it is specified in the test program.

$x_1 = \{603; 73,4; 18,6\}$  – for a moment of 15 minutes;  
 $x_2 = \{825; 99; 23,1\}$  – for a moment of 30 minutes;  
 $x_n = \{2458; 110; 59,3\}$  – for a moment of 180 minutes.

The crankshaft speed n, rpm; load torque to motor shaft  $M_H, N_m$ ; hourly fuel consumption  $G_t, kg/h$ , respectively [13], are selected as input parameters.

In order to generate a control action as a vector of the rack motion values of the high-pressure fuel pump (HPFP) for a diesel engine, the hybrid network should consist of three layers.

## RESULTS AND DISCUSSION

Layer 1 is represented by the radial basis neurons, and it simulates membership functions of the fuzzy output system.

In [14] demonstrated a possibility to control an ICE during the tests using the fuzzy logic methods.

The parameterized shape function (Gaussian curve with parameters  $c$ ,  $\sigma$ ,  $b$ ) is chosen as a membership function; its parameters are configured using a hybrid network. When designing a hybrid network, the condition of fuzzy rules IF ( $x_i \in A_i$ ) is implemented via the russification function, which is represented by the generalized Gaussian function separately for each variable  $x_i$ :

$$\mu_{A_i}(x_i) = \frac{1}{1 + \left( \frac{x_i - c_i}{\sigma_i} \right)^{2b}}$$

where

$\mu_{A_i}(x_i)$  means the degree of membership of an explicit value  $x_i$  to a fuzzy mark  $A_i$ .

The generalized Gaussian function at an appropriate choice of the exponent  $b$  may be degenerated both in the standard Gaussian function ( $b = 1$ ), triangular ( $b = 0.6$ ) or trapezoidal function.

Fuzzy sets [15] should be determined for given input parameters of the engine operation. The greater number of fuzzy sets of a parameter increases the accuracy of the resulting control action; however, it is computer-intensive [16]. Three fuzzy sets should be defined for the engine speed, two fuzzy sets - for the load torque and four fuzzy sets - for the hourly fuel consumption.

The first layer's task is to calculate the input data degree of membership to the respective fuzzy sets. For this purpose the numerical values of the parameters are subject to normalization:

$x_1 = \{0.24; 0.58; 0.31\}$  - for a moment of 15 minutes;

$x_2 = \{0.38; 0.80; 0.39\}$  - for a moment of 30 minutes;

$x_n = \{1; 0.81; 1\}$  - for a moment of 180 minutes.

Degree of membership of the normalized values of the input parameters to the fuzzy marks:

$\mu(x_1) = \{(0,84; 0,1; 0,06); (0,42; 0,48); (0,78; 0,1; 0,1; 0,02)\};$

$\mu(x_2) = \{(0,62; 0,2; 0,18); (0,23; 0,77); (0,25; 0,40; 0,2; 0,05)\};$

$\mu(x_n) = \{(0,1; 0,12; 0,78); (0,25; 0,75); (0,1; 0,2; 0,15; 0,65)\}.$

This parametric layer with parameters  $c_j^{(k)}$ ,  $\sigma_j^{(k)}$ ,  $b_j^{(k)}$  subject to adaptation during learning.

Layer 2 - the layer consists of AND-neurons [17], which model a logical connective AND using the following formula [18]:

$$w_i = \mu_{A_i}(x_1) \cdot \mu_{B_i}(x_2)$$

Links with the previous layer are set so as to obtain all possible combinations of the membership functions of two input signals [19].

Assume that the input space is evenly divided with  $N_1$  membership functions for signal  $x_1$  and, respectively, with  $N_2$  membership functions for signal  $x_2$  [20].

In other words,  $N_1$  of fuzzy sets for the first input signal should be defined [21]:  $A_1^1, \dots, A_1^{N_1}$  and  $N_2$   $A_2^1, \dots, A_2^{N_2}$ , - for the second signal. It will result in  $N_1 \times N_2$  rules of the following form [22]:

$R(k): \text{IF } (x_1 \in A_1^k \text{ AND } \dots \text{ AND } x_n \in A_n^k) \text{ THEN } y = c(k)$

For

$k=1, \dots, N$ , where  $R(k)$  means the fuzzy  $k$ -th rule [23],

$x_1, \dots, x_n$  means input parameters of the engine operation [24];

$A_1^k, \dots, A_n^k$ , means fuzzy sets from components of conditions [25];

$c(k)$  means constant [26];

$N$  means a number of rules [27].

This layer determines the extent, to which the input signal values correspond to the conditions of the rules [28]. The input and output relationship is as follows [29]:

$$\tau_k = \prod_{i=1, \dots, n} \mu_{A_i^k}(\bar{x}_i)$$

$$\hat{\tau}_k = \prod_{i=1, \dots, n} \mu_{A_i^k}(\bar{x}_i) \stackrel{def}{=} \frac{\tau_k}{\sum_{i=1}^N \tau_i}$$

where

$\mu_{A_i^k}(\bar{x}_i)$  means a degree of compliance of the input data with the conditions of the rules,

$\tau_k$  means a degree of the activity of the k-th rule,

$\hat{\tau}_k$  means normalized value  $\tau_k$

The outputs of this layer represent normalized degrees of activity of the rules.

$$\begin{aligned} \tau_k(x1) &= 0,84 \cdot 0,42 \cdot 0,78 = 0,28; & (x1) &= 0,28/(0,84+0,42+0,78)=0,14; \\ \tau_k(x2) &= 0,62 \cdot 0,77 \cdot 0,40 = 0,19; & (x1) &= 0,19/(0,62+0,77+0,40)=0,11; \\ \tau_k(xn) &= 0,78 \cdot 0,75 \cdot 0,65 = 0,38; & (x1) &= 0,38/(0,78+0,75+0,65)=0,17. \end{aligned}$$

Layer 3 represents a function generator that calculates the values  $y_k(x) = p_{k0} + \sum_{j=1}^N p_{kj} x_j$ . In this layer

the signals  $y_k(x)$  are multiplied by the values  $w_k$  generated in the previous layer. This is a parametric layer, in which linear weights  $p_{kj}$  are to be adapted for  $k = 1, 2, \dots, M$  and  $j = 1, 2, \dots, N$ .

This layer implements the defuzzification method. At its output the signal represents a sum of products of weights and normalized activity degrees of the rules  $\hat{\tau}_k$ .

$$\begin{aligned} y(x1) &= (x1) \cdot (x1) = 0 \cdot 0,14 = 0; \\ y(x2) &= (x2) \cdot (x2) = 0 \cdot 0,11 = 0; \\ y(xn) &= (xn) \cdot (xn) = 0 \cdot 0,17 = 0 \end{aligned}$$

The weights of links marked with the symbol correspond to the constant  $c(k)$  in the rules. They should have zero initial values, which reflects the lack of conclusions before the start of the network's learning. Therefore, it can be argued that the modification of these weights during learning leads to the rules building. After the process of learning of the hybrid network the parameters  $(x_n)$  will be changed, so that the output will result in a normalized rack motion value of HPFP  $h$ .

The first layer comprises three M·N nonlinear parameters of the Gaussian function (M - number of received rules, N - total number of fuzzy sets for the input vector), and the third - M linear parameters  $c_i$ .

## CONCLUSIONS

The hybrid network for each vector of the input of parameters generates an engine's control action. For diesel the motion of HPFP rack -  $h$ , mm can represent the control action.

For a given input vector the hybrid network received the control vector:

$$h = \{0; 1,35; 3,21; 4,62; 15; 17,3; 24,1; 27,6; 38,8; 42,4; 49,3\}$$

The resulting deviations of the calculation indices from the experimental ones was due to the appropriate selection of the learning sample, which was used during the hybrid network's learning.

The advantages of the model based on the fuzzy neural network include a possibility to obtain new information in the form of a certain forecast. For example, forecast for the test control vector of unknown ICE model.

In order to create the knowledge base in the form of fuzzy control rules, the hybrid network based on the multilayer perceptron is selected; it allows to approximate the ICE operation mode parameters in the whole range of their values.

The hybrid network contains only two parametric layers (first and third), which parameters are specified in the learning process. The errors of 4% correspond to GOST 15995-80, and they are caused by the non-linearity of the crankshaft speed in the range of 800-1500 rpm.



**CONFLICT OF INTEREST**

There is no conflict of interest.

**ACKNOWLEDGEMENTS**

The work is performed according to the Russian Government Program of Competitive Growth of Kazan Federal University.

**FINANCIAL DISCLOSURE**

None.

**REFERENCES**

- [1] Yu Y, Yang J. [2011] The development of fault diagnosis system for diesel engine based on fuzzy logic. Proceedings - 2011 8th International Conference on Fuzzy Systems and Knowledge Discovery, FSKD. 1. Art no. 6019556. 472 - 475.
- [2] Shah M, Gaikwad V, Lokhande S, Borhade S. [2011] Fault identification for I.C. engines using artificial neural network. Proceedings of 2011 International Conference on Process Automation, Control and Computing, PACC. art. no. 5978891.
- [3] Galiullin LA, Valiev RA. [2016] Modeling of internal combustion engines test conditions based on neural network. International Journal of Pharmacy and Technology. 8(3):14902-14910.
- [4] Wei D. [2011] Design of Web based expert system of electronic control engine fault diagnosis. BMEI 2011 - Proceedings 2011 International Conference on Business Management and Electronic Information. 1. art. no. 5916978. 482 - 485.
- [5] Galiullin LA, Valiev RA. [2018] An automated diagnostic system for ICE. Journal of Advanced Research in Dynamical and Control Systems. 10 (10):1767-1772.
- [6] Guihang L, Jian W, Qiang W, Jingui S. [2011] Application for diesel engine in fault diagnose based on fuzzy neural network and information fusion. IEEE 3rd International Conference on Communication Software and Networks, ICCSN. art. no. 6014398. 102 - 105.
- [7] Galiullin LA, Valiev RA. [2018] Optimization of the parameters of an internal combustion engine using a neural network. Journal of Advanced Research in Dynamical and Control Systems. 10 (10):1754-1758.
- [8] Galiullin LA, Valiev RA. [2018] Method for neuro-fuzzy inference system learning for ICE tests. Journal of Advanced Research in Dynamical and Control Systems. 10 (10):1773-1779.
- [9] Ahmed R, Sayed MEI, Gadsden SA, Tjong J, Habibi S. [2015] Automotive internal-combustion-engine fault detection and classification using artificial neural network techniques. IEEE Transactions on Vehicular Technology. 64 (1): 21-33.
- [10] Galiullin LA, Valiev RA. [2018] Modeling of internal combustion engines by adaptive network-based fuzzy inference system. Journal of Advanced Research in Dynamical and Control Systems. 10(10):1759-1766.
- [11] Chen J, Randall R, Feng N, Peeters B, Van Der Auweraer H. [2013] Automated diagnosis system for mechanical faults in IC engines. 10th International Conference on Condition Monitoring and Machinery Failure Prevention Technologies, CM and MFPT. 2:892-903.
- [12] Isermann R. [2005] Model-based fault-detection and diagnosis - Status and applications. Annual Reviews in Control. 29(1):71-85.
- [13] Chen J, Randall R, Peeters B, Desmet W, Van Der Auweraer H. [2012] Neural network based diagnosis of mechanical faults in IC engines. Institution of Mechanical Engineers - 10th International Conference on Vibrations in Rotating Machinery. 679-690. doi: 10.1533/9780857094537.10.679.
- [14] Galiullin LA, Valiev RA, Lejsan B, Mingaleeva. [2018] Development of a Neuro-Fuzzy Diagnostic System Mathematical Model for Internal Combustion Engines. HELIX. 8(1):2535-2540.
- [15] Wu JD, Huang CK, Chang YW, Shiao YJ. [2010] Fault diagnosis for internal combustion engines using intake manifold pressure and artificial neural network. Expert Systems with Applications. 37(2):949-958.
- [16] Galiullin LA, Valiev RA. [2017] Mathematical modelling of diesel engine testing and diagnostic regimes. Turkish Online Journal of Design Art and Communication. 7:1864-1871. doi: 10.4271/2004-01-0423.
- [17] Li X, Yu F, Jin H, Liu J, Li Z, Zhang X. [2011] Simulation platform design for diesel engine fault. International Conference on Electrical and Control Engineering, ICECE Proceedings. Art no. 6057562. 4963 - 4967.
- [18] Danfeng D, Yan M, Xiurong G. [2009] Application of PNN to fault diagnosis of IC engine. 2009 2nd International Conference on Intelligent Computing Technology and Automation, ICICTA. 2:495-498. Art № 5287738.
- [19] Galiullin LA, Valiev RA. [2017] Diagnosis System of Internal Combustion Engine Development. Revista Publicando. 4(13):128-137.
- [20] Randall RB. [2009] The application of fault simulation to machine diagnostics and prognostics. 16th International Congress on Sound and Vibration, ICSV. 14(2):81-89.
- [21] Galiullin LA, Valiev RA. [2017] Diagnostics Technological Process Modeling for Internal Combustion Engines. International Conference on Industrial Engineering, Applications and Manufacturing (ICIEAM). doi: 10.1109/ICIEAM.2017.8076124.
- [22] McDowell N, McCullough G, Wang X, Kruger U, Irwin GW. [2008] Application of auto-associative neural networks to transient fault detection in an IC engine. Proceedings of the 2007 Fall Technical Conference of the ASME Internal Combustion Engine Division. 555-562. <https://doi.org/10.1115/ICEF2007-1728>
- [23] Galiullin LA, Valiev RA, Mingaleeva LB. [2017] Method of internal combustion engines testing on the basis of the graphic language. Journal of Fundamental and Applied Sciences. 9(1):1524-1533.
- [24] Galiullin LA, Valiev RA. [2018] Control vector for ice automated test and diagnostic system. Dilemas contemporaneos-educacion politica y valores. 6. article № 95.
- [25] Galiullin LA, Valiev RA. [2016] Automation of Diesel Engine Test Procedure. IEEE 2016 2ND International Conference on Industrial Engineering, Applications and Manufacturing (ICIEAM). doi: 10.1109/ICIEAM.2016.7910938.
- [26] Valiev RA, Khairullin AKH, Shibakov VG. [2015] Automated Design Systems for Manufacturing Processes. Russian Engineering Research. 35(9):662-665.
- [27] Galiullin LA, Valiev RA, Khairullin A, Haliulloovich. [2018] Method for modeling the parameters of the internal combustion engine. IIOAB JOURNAL. 9:83-90. <https://doi.org/10.1016/j.protcy.2012.03.027>.
- [28] Galiullin LA, Valiev RA. [2018] Internal combustion engine fault simulation method. IIOAB JOURNAL. 9(1):91-96.
- [29] Galiullin LA. [2016] Development of Automated Test System for Diesel Engines Based on Fuzzy Logic. IEEE 2016 2ND International Conference on Industrial Engineering, Applications and Manufacturing (ICIEAM). doi: 10.1109/ICIEAM.2016.7911582.